

Durability of rubber products



Twente University **Press**

Publisher: Twente University Press,
P.O. Box 217, 7500 AE Enschede, The Netherlands,
www.tup.utwente.nl
Print: Océ Facility Services, Enschede, The Netherlands

Cover design: by Jos Peters

© N.M. Huntink, Zutphen, 2003.

No part of this work may be reproduced by print, photocopy, or other means without the permission in writing from the publisher.

ISBN 90 365 1946 2

DURABILITY OF RUBBER PRODUCTS

**DEVELOPMENT OF NEW ANTIDEGRADANTS
FOR LONG-TERM PROTECTION**

PROEFSCHRIFT

ter verkrijging van
de graad van doctor aan de Universiteit Twente,
op gezag van de rector magnificus,
prof. dr. F.A. van Vught,
volgens besluit van het College voor Promoties
in het openbaar te verdedigen
op vrijdag 7 november 2003 om 15:00 uur

door

Nicolaas Maria Huntink

geboren op 8 mei 1963
te Doetinchem

Dit proefschrift is goedgekeurd door:

Promotor: prof. dr. ir. J.W.M. Noordermeer
Assistent-promotor: dr. R.N. Datta

Voorwoord

Tijdens de laatste jaren van mijn loopbaan bij Flexsys B.V. in Deventer heb ik gewerkt aan een promotieonderzoek, uitgevoerd binnen de ‘New Products Group’, in samenwerking met de onderzoeksgroep “Rubbertechnologie” van de Universiteit Twente. Dit onderzoek is nu ten einde gekomen. Veel personen hebben door hun aanwezigheid en hulp bijgedragen aan het tot stand komen van dit proefschrift. Ik wil graag gebruik maken van de mogelijkheid om deze personen te bedanken. Als eerste wil ik mijn promotor, professor Noordermeer, bedanken voor de gelegenheid die hij mij gegeven heeft om in zijn groep te werken aan mijn promotieonderzoek. Door de goede begeleiding en kritische beoordeling van mijn werk heb ik veel geleerd.

Veel dank ben ik verschuldigd aan mijn assistent-promotor, Rabin Datta, die mij heeft geadviseerd en gemotiveerd dit promotieonderzoek uit te voeren. Zijn enthousiaste en doortastende manier van begeleiden zal ik niet gauw vergeten, net zoals zijn vriendschap en de vele anekdotes uit India. De dagen die we samen op kantoor of tijdens een dienstreis hebben doorgebracht waren altijd gezellig en vaak zeer leerzaam. Auke Talma wil ik ook graag bedanken voor al zijn ideeën en hulp bij de ontwikkeling en synthese van de verschillende antidegradanten die beschreven staan in dit proefschrift. Auke was mede verantwoordelijk voor de goede sfeer binnen de ‘New Products Group’. Bertus Oldehanter wil ik graag bedanken voor de vele syntheses die hij voor mij heeft uitgevoerd. Zijn kennis van computers is ook regelmatig van pas gekomen. Sumana Datta wil ik graag bedanken voor de analytische ondersteuning en hulp bij de verschillende modelonderzoeken. De vele discussies die we hebben gevoerd hebben een grote bijdrage geleverd aan dit proefschrift. Wasil Maslow wil ik graag bedanken voor het DOSY ¹H-NMR werk. Zijn expertise was zeer waardevol voor het ophelderen van het werkingsmechanisme van PPD-C18. I would like to thank the students Olivier Courier and Geraline van ‘t Slot for their help with the ozonolysis experiments described in Chapter 6.

Johan Baaij, Gerard Hogeboom, Martin Hondeveld, Andre Roolvink, Remco Meijer en Rene Willemsen wil ik graag bedanken voor hun hulp in het rubberlab en voor de plezierige tijd die ik daar heb doorgebracht. Johan was altijd aanwezig en bereid om de meest uiteenlopende problemen op te lossen. Gerard, bedankt dat je, nadat Flexsys besloten had om de ‘New Products Group’ op te heffen, toch nog bereid was om de vele rubbermengsels voor mij te testen. De samenwerking met het rubberlab was altijd goed en plezierig. I would like to thank Leona Baclowski and Horn-Jau Lin for their help with the DSC-measurements described in Chapter 8.

Henk Schreurs, Arie de Hoog, Hans Hofstraat, Enno Klop, Rob van Puijenbroek, Brenda Rossenaar en Minie Janssen-Mulders wil ik graag bedanken voor hun hulp en inzet bij het onderzoek naar het effect van antidegradanten op de thermische stabiliteit van onoplosbaar zwavel, beschreven in hoofdstuk 9. De projectbesprekingen eens in de zes tot acht weken waren altijd zeer interessant en leerzaam.

I would like to thank the colleagues of the RBT group at the University Twente for their hospitality and the fun we had, especially during the study trips to London and Limburg. Richard en Joost, bedankt dat jullie mijn paranimfen willen zijn. Gerda, bedankt voor je hulp bij allerlei administratieve zaken.

Mijn familie wil ik graag bedanken voor alles wat ze voor mij hebben gedaan en de interesse voor mijn werk. Marion, bedankt dat je de laatste maanden wat vaker alleen hebt klaar gestaan voor Luc en Mart, zodat ik ongestoord aan mijn proefschrift kon werken. Luc en Mart, bedankt dat jullie de meeste nachten lekker hebben doorgeslapen.

Contents

| | | |
|---------------------------------------|--|-----|
| Chapter 1 | General introduction | 1 |
| Chapter 2 | Durability of rubber compounds | 12 |
| Chapter 3 | Synthesis and characterization of potential long-lasting antidegradants | 53 |
| Chapter 4 | Development of test protocols for screening potential slow-migrating antidegradants | 77 |
| Chapter 5 | Evaluation of slow release antidegradants in typical passenger and truck tire sidewall compounds | 93 |
| Chapter 6 | Ozonolysis of model olefins - Efficiency of antiozonants - | 115 |
| Chapter 7 | Quinonediimine as bound antioxidant in silica compounds with the possibility to reduce the level of silane coupling agent | 137 |
| Chapter 8 | Ranking of several antidegradants for their effectiveness to protect rubber against oxidation using differential scanning calorimetry and by accelerated aging of steelcord skim compounds | 159 |
| Chapter 9 | The interaction of antidegradants with sulfur vulcanization agents | 175 |
| Main symbols and abbreviations | | 195 |
| Summary | | 199 |
| Samenvatting | | 203 |

Chapter 1

General introduction

1.1 Introduction

The first people using rubber were the natives of Haiti. They played a ball game, the balls being made from the sap, a white milky fluid, of a tree.¹ Natural rubber (NR) or caoutchouc is the product condensed from this sap (latex). The name caoutchouc was derived from the Indian word “caa-o-chu”, meaning “weeping tree”. In 1770 the Englishman, Joseph Priestley, recommended the material for use as an eraser, or rubber, the latter term being adopted by the English-speaking world as a generic term for materials of high reversible elasticity.² In those days, Europeans were rubbing out pencil marks with small cubes of rubber. The rubber however was not an easy substance to work with because it deteriorated very easily.

There are hundreds of latex-producing plants, belonging to different botanical families, and they are predominantly found in tropical climates. Not all caoutchouc-producing plants are harvested for industrial purposes, because the yield is either too small, the caoutchouc content in the latex too low, or the caoutchouc contains too many resinous impurities. Early plantation economies used *Ficus elastica*, *Funtumia*, *de Castilloa*, and *Manihot* plants, but they were soon replaced by the *Hevea brasiliensis*, because the latter gives a much higher yield of a superior caoutchouc.³

The invention of useful rubber is commonly attributed to Charles Goodyear.⁴ Natural or India rubber, as it was then known, had little uses. Rubber products melted in hot weather, froze and cracked in cold, and adhered to everything they touched. In 1830 Goodyear began experimenting with raw rubber to turn it into a useable product. In 1839 he managed to harden it by mixing the rubber with sulfur, white lead and oil of turpentine and drying it near a hot stove. The pieces, which had come into direct contact with the stove, had changed into an elastic, non-sticky product. The process known as vulcanization had been born. The term vulcanization was named after Vulcan, the Roman god of fire.

In 1906, Bayer started a research program to produce synthetic rubber because Germany was resentful of the dominance that the UK and Holland held over supplies of natural rubber.⁵ The first synthetic rubber suitable for industrial scale production, methyl rubber (polydimethylbutadiene), was developed in 1910. It was very susceptible to oxidative break-down.⁶

Early users of vulcanized natural rubber soon became aware of the sensitivity of the material to deterioration under a variety of conditions and in a number of ways. These included the change to a sticky mass on general aging, the formation of deep

cracks in a direction perpendicular to the application of a stress (now associated with ozone attack), deterioration in contact with copper wire (a serious problem when natural rubber was widely used as an electrical insulator) and the surface hardening that could be observed after exposure to light.

At the beginning of the 1920's passenger car tires rarely survived 5.000 km of use for reasons other than oxygen attack.⁷ However, car manufactures and the public started demanding longer life of tires and other rubber products. Application of reinforcing carbon blacks resulted in a significantly increased tread life. At the same time the degrading effects of oxygen came to the foreground and research was started to find means that would prevent oxygen and related compounds from destroying rubber products, especially tires. Rubber history credits three chemists with being the first people to develop commercially successful antioxidants: Herbert Winkelman and Harold Gray at B.F. Goodrich and, independently, Sidney Cadwell at US Rubber. All three served later as American Chemical Society Rubber Division chairmen, and Cadwell (1956) and Winkelman (1961) became Charles Goodyear Medal winners, at least in part for their pioneering work on these substances.⁷ Their two non-accelerating antioxidants differed in chemical detail, but both were condensation products of an aromatic amine and an aliphatic aldehyde. Commercial exploitation of antidegradants started after World War I. The American army, still suffering from the chemical-warfare horrors of World War I, wanted to make and store for long term hundreds of thousands of gas masks. Aware that the kinds of rubber products, with which they were then familiar, deteriorated rather rapidly in air, the first plan was to store the masks in some inert atmosphere like nitrogen, a plan entailing some difficulties. Cadwell was able to convince the military organization that there was a simpler measure and that he could guarantee it would work. He proved that masks compounded from a rubber containing his antioxidant remained serviceable for a long time, even if simply stored in air, given a reasonable degree of shelter from sunlight and heat. The American army ordered a huge number of masks made of rubber containing Cadwell's antioxidant. In the decades since, hundreds of new antioxidants have been developed, falling in the class of staining or non-staining products. The staining antioxidants are members of the huge family of amino compounds. Because they discolor rubber, these antioxidants are used primarily in black rubbers. The non-staining antioxidants are commonly designated as phenolics and phosphites.

The history of protection against ozone attack is somewhat shorter. Until the mid-1950s, wax was the only available antiozonant. The waxes with their low solubility in rubber gradually migrate to the air-exposed product surfaces and form a layer of bloom, through which ozone cannot penetrate. These waxes gave only protection against ozone attack in static applications but not in dynamic applications. In 1954 three chemists working at the Rock Island Arsenal: R.F. Shaw, Z.T. Ossefort and W.J. Touhey, discovered that the addition of dialkyl-phenylene diamines and/or alkyl-aryl-phenylene diamines to the waxes provided also protection against ozone in dynamic applications.^{7,8} The combination of wax and diamine is still the most widely used package of antidegradants today.

Today, it is recognized that most of the degradation encountered with natural and synthetic rubbers is due either to oxygen or to ozone. Although the latter is only encountered in tiny quantities, about 10 parts per thousand million in clean air, its effects can be devastating, particularly for dynamically loaded rubbers. The result is early appearance of cracks across the direction of stress. The rate of crack growth increases with the tension and varies from one kind of rubber to another. In every case the rate of crack growth will be fast enough to render the rubber useless. Some synthetic rubbers containing few or no unsaturated carbon-carbon bonds are resistant to ozone. However, by far most rubbers need special protection against ozone attack.

Although a lot of research has already been done to improve the lifetime of rubber goods, there is a need for antidegradants that last longer in rubber compounds and provide longer-term protection. Nowadays, truck tires need improved protection of the sidewall, because they are retreaded more and more times. And in Japan for example, there is a recent requirement defined for modulus (hardness) stabilization of passenger tire tread compounds in order to keep their grip performance constant upon aging.

1.2 Aim of this thesis

The aim of the investigations presented in this thesis is to develop new long-lasting antidegradants and to gain a better insight in the protection mechanism of these products. A better understanding of the mechanism can help to pave the way for new developments, providing longer-term protection of rubber compounds.

Long-lasting antioxidants are expected to remain longer active in rubber compounds compared to conventional antioxidants, both during processing and service. Developments in this field are based on high molecular weight and polymer bound antioxidants. Long-lasting antiozonants are meant to migrate slower to the surface of rubber compounds compared to conventional antiozonants. Developments in this field are based on high molecular weight products.

In the next paragraph the concept of the thesis is described. Different approaches are used to study the most important characteristics of conventional and 28 newly synthesized antidegradants, in order to develop new products and to prove their long-lasting performance.

1.3 Concept of this thesis

The research described in this thesis comprises the synthesis, screening and selection of potential long-lasting antidegradants, the determination of their migration behavior, the determination of their efficiency as antioxidant and/or antiozonant and their effect on other compounding ingredients. The thesis is divided into 9 chapters as outlined:

Chapter 2 provides an overview of available antidegradants and their mechanistic aspects. Most developments with emphasis on long-term antioxidant as well as antiozonant protection are summarized.

Chapter 3 covers the synthesis and characterization of the antidegradants, which are evaluated and studied as long lasting antidegradant. The potential long lasting antiozonants and long lasting antioxidants are all based on 4-ADPA (4-amino-diphenylamine) and/or 6PPD (N-(1,3-dimethylbutyl)-N'-phenyl-p-phenylene-diamine).

Chapter 4 deals with the migration behavior of antiozonants. This chapter outlines the development of a test protocol for screening potential slow migrating antiozonants.

Chapter 5 deals with the evaluation of a variety of potential long lasting antidegradants. Dynamic and mechanical properties of several compounded antidegradants are determined before and after different aging procedures. Furthermore, the mechanism of PPD-C18, the most promising antidegradant of all the tested molecules, is elucidated using different techniques.

Chapter 6 focuses on the efficiency of chemical antiozonants. The reactivity of potential long lasting antiozonants with ozone in the presence of model rubbers is estimated and compared to that of conventional antiozonants.

Chapter 7 focuses on N-1,3-dimethylbutyl-N'-phenyl quinonediimine (6QDI) as polymer bound antioxidant. The effect of QDI as bound antioxidant in silica compounds with a possibility to reduce the level of silane coupling agent is investigated. The mechanism of polymer bounding is investigated using squalene as a model substrate.

Chapter 8 focuses on the oxidation induction time (OIT) of potential long lasting antioxidants. The OIT is determined by DSC measurements. Several potential antidegradants are also studied in a steelcord adhesion compound by determination of the dynamic mechanical properties before and after hot air aging.

Chapter 9 discusses the effect of antidegradants on other compounding ingredients. Special attention is paid to the interaction of antidegradants with a polymeric form of sulfur, which is used in tires where high sulfur loadings are required to meet high performance demands.

1.4 References

1. Natuurrubber, **20**, (2000), 4.
2. J.A. Brydson, "Rubbery Materials and their Compounds", Elsevier Science Publishers Ltd., Essex (1988).
3. W. Hofmann, "Rubber Technology Handbook", Hanser Publishers, Munich (1994).
4. D.G. Lloyd, Lecture presented at the AGM of the Manchester Polymers Group in May 1994.
5. W. Hofmann, "Vulcanisation and Vulcanising Agents", Maclaren and Sons, London (1967).
6. M. Bögemann, *Angew. Chem.*, **51**, (1938), 113.
7. L. Sebrell, *European Rubber Journal*, (Jan. 1985), 23.
8. G.J. Lake, *Rubber Chem. Technol.*, **43** (1970), 1230.

Chapter 2

Durability of rubber compounds[#]

The developments on long-term protection of rubber against aerobic aging are reviewed. Although conventional antidegradants such as N-isopropyl-N'-phenyl-p-phenylenediamine (IPPD) and N-(1,3-dimethylbutyl)-N'-phenyl-p-phenylenediamine (6PPD) are still the most widely used antidegradants in rubber, there is a trend and demand for longer-lasting and non-staining products. The relatively low molecular weight (MW) antioxidants have undergone an evolutionary change towards higher molecular weight products with the objective to achieve permanence in the rubber matrix, without loss of antioxidant activity. In the last two decades, several approaches have been evaluated in order to achieve this objective: attachment of hydrocarbon chains to conventional antioxidants in order to increase the MW and compatibility with the rubber matrix; oligomeric or polymeric antioxidants; and polymer bound or covulcanizable antioxidants. The disadvantage of polymer bound antioxidants was overcome by grafting antioxidants on low MW polysiloxanes, which are compatible with many polymers. New developments on antiozonants have focused on non-staining and slow migrating products, which last longer in rubber compounds. Several new types of non-staining antiozonants have been developed, but none of them appeared to be as efficient as the chemically substituted p-phenylenediamines. The most prevalent approach to achieve non-staining ozone protection of rubber compounds is to use an inherently ozone-resistant, saturated backbone polymer in blends with a diene rubber. The disadvantage of this approach however, is the complicated mixing procedure needed to ensure that the required small polymer domain size is achieved.

The present chapter gives an overview of the various antioxidants and antiozonants in use today for rubber purposes.

2.1. Introduction

Rubber compounds can be degraded by reactions with oxygen, ozone, light, metal ions and heat. Antidegradants protect rubber against aerobic aging (oxygen) and ozone attack. They are of prime importance and play a vital role in rubber products to maintain the properties at service conditions. Protection of rubbers or stabilization of crosslinked networks against anaerobic aging can be achieved via other approaches:

[#] This chapter has been accepted for publication in Rubber Chemistry and Technology as a review article (Rubber Chem. and Technol., Vol. 77 (3) Rubber Reviews, July/August 2004)

e.g. employing an EV-curing system, application of 1,3-Bis(citraconimidomethyl)-benzene, Hexamethylene-1,6-bis(thiosulphate) disodium salt dihydrate, Hexamethylene-1,6-bis(dibenzylthiuram disulfide) and Zn-soaps.¹

Degradation by oxygen and ozone proceeds via different chemical mechanisms²⁻¹³ and results in different effects on physical properties of rubber. Ozone degradation results in discoloration and eventual cracking of samples. Ozone degradation is primarily a surface phenomenon. Oxygen degradation results in hardening or softening (depending on the base polymer) throughout the rubber article. For example, vulcanizates that are based on natural rubber (NR), polyisoprene rubber (IR) and butyl rubber (IIR) preferably undergo cleavage reactions during the oxidation process; they generally become softer. During progressive aging, a crosslinking mechanism starts to dominate again: completely oxidized NR is usually hard and brittle. On the other hand, vulcanizates obtained from styrene-butadiene-rubber (SBR), nitrile butadiene rubber (NBR), chloroprene rubber (CR), ethylene propylene diene rubber (EPDM), etc. undergo cyclization and crosslinking reactions that lead to hardening of the aged part. When completely oxidized, these vulcanizates are turned into hard and brittle products. Rubbers that do not contain C=C unsaturation, such as acrylic rubber (ACM), chlorinated polyethylene (CM), chlorosulfonated polyethylene (CSM), polychloromethyloxiran (CO), ethylene-ethyl acrylate copolymer (EAM), epichlorohydrin rubber (ECO), ethylene propylene rubber (EPM), ethylene-vinylacetate copolymer (EVM), rubbers with fluoro and fluoralkyl or fluoralkoxy substituent groups on the polymer chain (FKM), silicone rubber (Q), and others are much less sensitive to oxidation than diene rubbers.

Although conventional antidegradants such as 6PPD (N-1,3-Dimethylbutyl)-N'-phenyl-p-phenylenediamine) and IPPD (N-isopropyl-N'-phenyl-p-phenylenediamine) provide protection against oxidation and ozonation, the protection lasts only short term. Longer-term protection requires a different class of antidegradants. Long-lasting antioxidants must be polymer bound or must have a lower volatility and leachability than conventional antioxidants, whereas long-lasting antiozonants must have a lower migration rate than the conventional antiozonants.

The purpose of this chapter is to review the developments on long term protection of rubbers against aerobic aging, especially on long-term protection against ozone. Although numerous reviews of antioxidants and antiozonants aspects have been published,²⁻¹³ in most cases they only cover one element (e.g. fracture and fatigue in SBR and BR vulcanizates;⁵ the black sidewall surface discoloration and non-staining technology;⁶ ozonolysis of natural rubber;¹¹ etc.), bound antioxidants, migration of the total field. In this review attempts will be made to summarize most developments with emphasis on long-term antioxidant as well as antiozonant protection.

2.2. Oxidation and antioxidant chemistry

2.2.1 Introduction

The changes in properties observed on oxidative aging of different elastomers and their vulcanizates, and of many other polymeric materials, are well known. Antiozonants and antioxidants are employed to limit these changes. However, the most effective antioxidant for one material may be ineffective, or even harmful in another material or under different conditions. A rubber compounder must be aware of the effect of oxygen attack on rubber and should know how to compound for oxygen resistance.

This chapter is intended as an introduction to the phenomena of oxidation of rubber and the protection against these with antioxidants.

2.2.2. Mechanism of rubber oxidation

The oxidation of polymers is most commonly depicted in terms of the kinetic scheme developed by Bolland and coworkers.¹⁴ The scheme is summarized in figure 2.1. The key to the process is the initial formation of a free-radical species. At high temperatures and at large shear forces, it is likely that free radical formation takes place by cleavage of carbon-carbon and carbon-hydrogen bonds.

Many elastomers are already observed to oxidize at moderate temperatures (below 60°C), where the energetics would not favor cleavage of carbon-carbon and carbon-hydrogen bonds. Thus, several studies have been conducted to determine whether trace impurities present in the polymer systems could account for the relative ease of oxidation. Two separate studies concluded that traces of peroxide were present in the polymer and that initiation occurred at low temperatures due to the relatively easy homolysis of these peroxides into free radicals.^{15,16} Due to the high reactivity of free radicals, only trace amounts of these peroxides need to be present to provide initiation of the oxidative chain process. On the other hand, mechanical shear during processing and bale compaction and localized heat during the drying and packaging of the raw polymer are the most important causes of carbon-carbon and carbon-hydrogen bond cleavage. The resultant free radicals react with oxygen to form the peroxides responsible for degradation.

The oxidation of hydrocarbon polymers resembles the oxidation of low molecular weight hydrocarbons, with the polymer having its own internal source of peroxide initiators present. By making the assumption that peroxides are present in even the most carefully prepared raw rubber, the ease of oxidation of rubber at low to moderate temperatures can be understood. Therefore, it is extremely important to compound rubber for extended oxidation resistance through the use of protective additives and to be aware of pro-oxidant impurities present in the rubber or the rubber compound.

Probably an important pro-oxidant for all rubbers is ultraviolet light. Blake and Bruce¹⁷ performed a study of the oxygen absorption rates of unvulcanized NR rubbers under exposure to UV-light. It was observed that exposure to light caused dramatic increases in the oxygen absorption rate of NR. They studied the oxygen absorption rates of NR with various compounding additives. A summary of their results is given in Table 2.1. This table shows that phenyl- β -naphthylamine, an additive previously used for prevention of rubber oxidation (hardly used anymore because of toxicity reasons) can operate as a pro-oxidant under exposure to UV-light. Fillers like zinc oxide, titanium dioxide, whiting and specially carbon black, lowered the rate of oxygen absorption of NR with exposure to UV-light. This was attributed to the ability to make the compound opaque, thus limiting the penetration of UV-light into the test films of NR. In the case of benzidine and hydroquinone, the effects were attributed to the ability of these materials to preferentially absorb the harmful UV-light. Thus, it is very important to consider the pro-oxidant behavior of UV-light when compounding rubbers for extended life.

Table 2.1: Oxidation of NR Pale Crepe at 46°C Accelerated by UV-Light.¹⁷

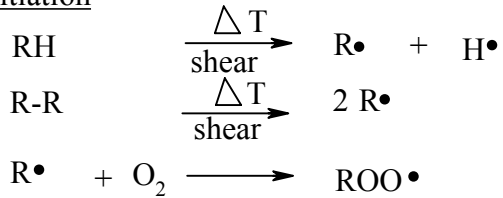
| Additive | Absorption of O ₂ [cm ³ /h] |
|-----------------------------------|--|
| None | 0.067 |
| 2% Sulfur | 0.028 |
| 2% Benzidine | 0.014 |
| 2% Hydroquinone | 0.014 |
| 2% Phenyl- β -naphthylamine | 0.076 |
| 5% Zinc oxide | 0.010 |
| 1% P-33 Carbon black*) | 0.018 |

*) P-33 is a fine thermal black, ASTM nomenclature N880.

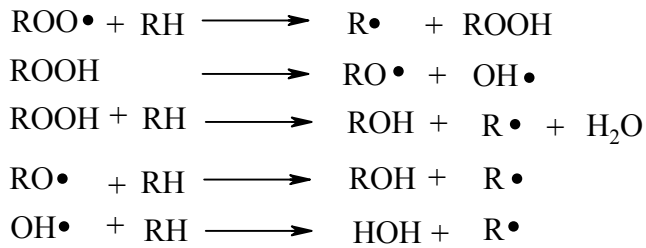
The rate of peroxide decomposition and the resultant rate of oxidation is markedly increased by the presence of ions of metals such as iron, copper, manganese, and cobalt.¹³ This catalytic decomposition is based on a redox mechanism, as in figure 2.2. Consequently, it is important to control and limit the amounts of metal impurities in raw rubber. The influence of antioxidants against these rubber poisons depends at least partially on a complex formation (chelation) of the damaging ion. In favor of this theory is the fact that simple chelating agents that have no aging protective activity, like ethylene diamine tetraacetic acid (EDTA), act as copper protectors.

The rather simple sequence of reactions described in figure 2.1 is complicated by other reactions, when oxidizable impurities or compounding ingredients are present. There are also the secondary processes whereby peroxides and free radicals undergo reactions leading to chain scission as well as crosslinking reactions. These reactions are closely related to the primary oxidation process, so that for a given type of polymer or vulcanizate the degree of deterioration of physical properties is generally proportional to the extent of oxidation.

Initiation



Propagation



Termination

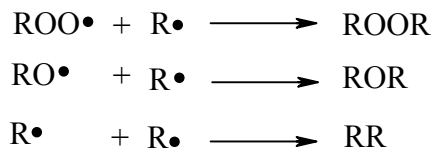


Fig. 2.1: Bolland oxidation mechanism (RH = rubber hydrocarbon).¹⁴

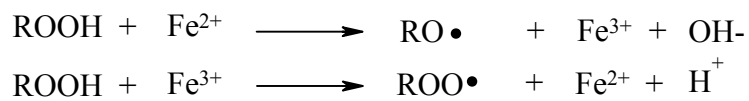


Fig 2.2: Decomposition of peroxides by ions of metals (Redox mechanism).

2.2.3. Stabilization mechanism of antioxidants

Complete inhibition of oxidation is seldom obtained in elastomers by addition of antioxidants or stabilizers. What is usually observed is an extended period of retarded oxidation in the presence of the antioxidant. It has been demonstrated that during this period the rate of oxidation decreases with inhibitor concentration until the optimum concentration is reached and then increases again. The rate of the retarded reaction is affected by changes in oxygen concentration¹⁸, in contrast to the uninhibited reaction, which proceeds at the same rate in oxygen or in air. These and other differences observed in the presence of oxidation inhibitors reflect significant changes in initiation and propagation, as well as in termination reactions.

It is important to recognize that different types of inhibitors often function by different mechanisms, and that a given antioxidant may react in more than one way. Thus a material that acts as an antioxidant under one set of conditions may become a pro-oxidant in another situation. The search for possible synergistic combinations of antioxidants can be conducted more logically and efficiently if we seek to combine the effects of different modes of action. Five general modes of oxidation inhibition are commonly recognized:

1. *Metal deactivators* - Organic compounds capable of forming coordination complexes with metals are known to be useful in inhibiting metal-activated oxidation. These compounds have multiple coordination sites and are capable of forming cyclic structures, which “cage” the pro-oxidant metal ions. EDTA and its various salts are examples of this type of metal chelating compounds.
2. *Light absorbers* – These chemicals protect from photo-oxidation by absorbing the ultraviolet light energy, which would otherwise initiate oxidation, either by decomposing a peroxide or by sensitizing the oxidizable material to oxygen attack. The absorbed energy must be disposed of by processes, which do not produce activated sites or free radicals. Fillers which impart opacity to the compound (e.g. carbon black, zinc oxide) tend to stabilize rubbers against UV catalyzed oxidation.
3. *Peroxide decomposers* – These function by reacting with the initiating peroxides to form nonradical products. Presumably mercaptans, thiophenols, and other organic sulfur compounds function in this way.¹⁹ It has been suggested that zinc dialkyldithiocarbamates function as peroxide decomposers, thus giving rubber compounds good initial oxidative stability.
4. *Free radical chain stoppers* – These chemicals interact with chain propagating $RO_2\bullet$ radicals to form inactive products.
5. *Inhibitor regenerators* - These react with intermediates or products formed in the chain-stopping reaction so as to regenerate the original inhibitor or form another product capable of functioning as an antioxidant.

Termination of propagating radicals during the oxidative chain reaction is believed to be the dominant mechanism by which amine and phenolic antioxidants

operate. The mechanism proposed to account for this behavior is given in figures 2.3 and 2.4. The deactivation of $R\bullet$ via chain braking electron acceptors (CBA) is demonstrated for a hindered amine light stabilizer (HALS). The mechanism involves reaction of the HALS with a hydroperoxide, resulting in the formation of a stable nitroxyl radical, which traps a hydrocarbon radical or abstracts a labile hydrogen from a hydrocarbon radical under formation of stable products. The hydroxylamine (CB-AH) formed via this mechanism can be used for the stabilization of peroxide radicals.

$R\bullet$ that is not fully deactivated via the mechanism described in figure 2.3 reacts with oxygen resulting in a peroxide radical. These peroxy radicals abstract a labile hydrogen from primary stabilizers like hindered phenols or secondary amines, resulting in less active hydroperoxides and preventing hydrogen abstraction from the polymer chain. The resulting antioxidant radical is more stable than the initial peroxy radical and terminates by reaction with another radical in the system. This mechanism was proposed by Shelton²⁰, who demonstrated that replacement of the reactive hydrogen in aromatic amine antioxidants by deuterium results in a slower abstraction of deuterium by peroxy radicals and therefore in a less effective antioxidant. It has also been proposed that aromatic compounds such as phenols and aromatic amines can form π -electron complexes with peroxy radicals, which terminate to form stable products¹⁵. It appears that direct hydrogen absorption, π -electron complex formation or both, describe the antioxidant action of most amine and phenolic antioxidants. It is important that the level of antioxidant be kept at the optimum, since excess antioxidant can result in a pro-oxidant effect ($A-H + O_2 \rightarrow AOOH$).

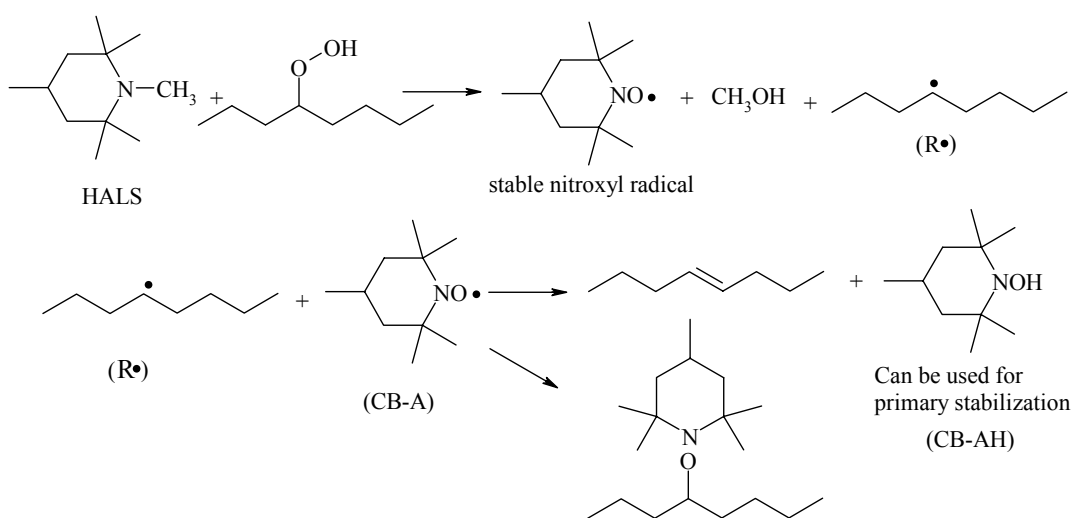


Fig. 2.3: Deactivation of $R\bullet$ via chain braking electron acceptors (CB-A).

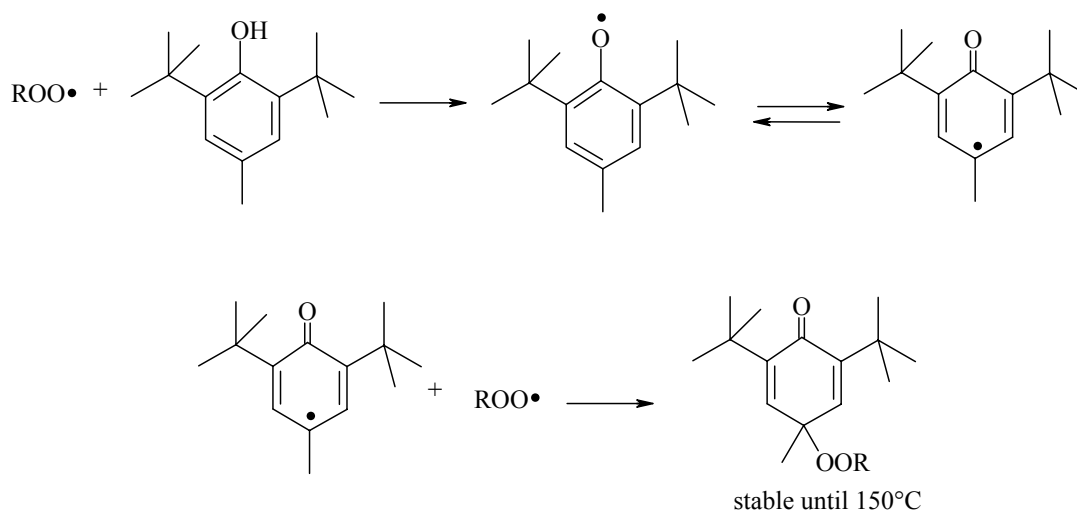


Fig. 2.4: Primary stabilization via radical scavenging by hindered phenolics.

The mechanism of secondary stabilization by antioxidants is demonstrated in figure 2.5. Tris-nonylphenyl phosphites, derived from PCl_3 and various alcohols, and thio-compounds are active as a secondary stabilizer.²¹ They are used to decompose peroxides into non-free-radical products, presumably by a polar mechanism. The secondary antioxidant is reacting with the hydroperoxide resulting in an oxidized antioxidant and an alcohol. The thio-compounds can react with two hydroperoxide molecules.

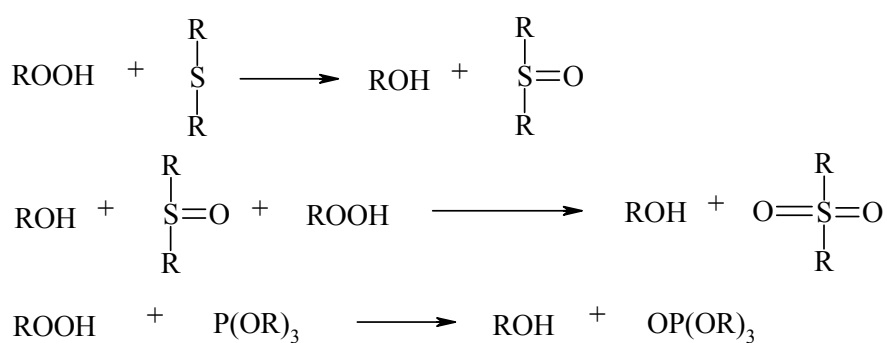


Fig. 2.5: Secondary stabilization by phosphites and thio-compounds.

2.2.4 Methods of studying the oxidation resistance of rubber

The most common test used to study the oxidation resistance of rubber compounds involves the accelerated aging of tensile dumbbell samples in an oxygen containing atmospheres. Brown, Forrest and Soulagnet²² recently reviewed long-term and accelerated aging test procedures. The ASTM practices (D 454 (09.01); D 865 (09.01); D 2000 (09.01, 09.02); D3137 (09.01); D 572 (09.01); D 3676 (09.02); D 380 (09.02)) for these tests clearly state that these are accelerated tests and should be used for relative comparisons of various compounds and that these tests may not correlate to actual long-term aging behavior. However, these tests are useful in evaluating aging-resistant compounds and various antioxidant packages. The resistance of a compound to oxidation is generally measured by the percentage change in the various physical properties (e.g. tensile strength, elongation at break, hardness, modulus). For an elastomer which reacts with oxygen, resulting in crosslinking (generally butadiene-based elastomers such as BR, SBR, NBR), the accelerated tests result in increases in tensile modulus and hardness with a corresponding decrease in ultimate elongation. For an elastomer which reacts with oxygen resulting in chain scission (generally isoprene-based elastomers such as NR and IR), the accelerated aging tests result in decreases in tensile modulus and hardness with either increasing or decreasing ultimate elongation, depending on the extent of degradation.²³ The most effective antioxidant package for a given elastomer compound gives the smallest changes in physical properties during an accelerated aging test.

Thermoanalytical techniques such as DSC and TGA have also been widely used to study rubber oxidation.²⁴⁻²⁷ The oxidative stability of rubbers and the effectiveness of various antioxidants can be evaluated with DSC based on the heat change (oxidation exotherm) during oxidation, the activation energy of oxidation, the isothermal induction time, the onset temperature of oxidation, and the oxidation peak temperature.

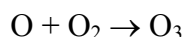
Spectroscopic techniques as ¹³C-NMR,²⁸ ESR,²⁹ pyrolysis-GC/MS and pyrolysis-FTIR,³⁰ X-ray diffraction³¹ and SEM³² techniques are also used to study rubber oxidation.

2.3. Ozone and Antiozonant Chemistry

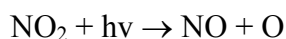
2.3.1 Introduction

Layer and Lattimer⁷ and Bailey³³ gave the historical background regarding protection of rubber against ozone. As early as 1885 Thomson observed that stretched rubber cracked on aging.³⁴ In the early 1920's, a number of investigators studied this phenomenon in more detail. They found that cracks occurred only in stretched rubber, formed in a direction perpendicular to the elongation, and grew most rapidly at an elongation of about 10%.^{35,36} Fabry and Buisson observed crack formation in the presence of ozone, but questioned the influence of this ozone. Ozone was believed to be present only in the upper atmosphere and not at those places where rubber is commonly used.³⁷ By 1935, analytical techniques had developed sufficiently to be able to measure that trace amounts of ozone, parts per hundred million (pphm), were present in the troposphere.³⁸ Even so, these trace amounts were felt to be too insignificant to be the cause of severe damage. Therefore, other factors responsible for cracking were sought. Sunlight seemed to be an indispensable factor; hence names like "suncracking" and "sunchecking" were frequently used to describe this phenomenon. Direct sunlight, however, was not necessary, since cracking occurred equally well on the shady side as well as on the sunny side of the rubber.³⁹ Also dust was thought to be responsible for cracking. Dust, once settled on the rubber and activated by sunlight, would give off oxidizing moieties and crack the rubber.^{39,40} Today, we know that only a few pphm of ozone in our atmosphere can cause severe cracking of rubber and that sunlight is responsible for its formation.

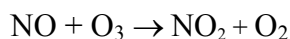
Ozone in the atmosphere is formed by the chemical reaction of atomic and molecular oxygen:



At high altitudes, the oxygen atoms are generated by the photolysis of molecular oxygen by the far ultraviolet light of the sun. In the troposphere, where only longer wavelength ultraviolet light exists, photolysis of nitrogen dioxide is the major source of oxygen atoms:⁴¹



The nitric oxide produced in this reaction reacts with ozone to regenerate oxygen and nitrogen dioxide:



An equilibrium is established which gives rise to a so-called photostationary-state relation, which depends on the relative rates of the above reactions:

$$[\text{O}_3] = j[\text{NO}_2] / k[\text{NO}]$$

j = reaction rate of the formation of O_3

k = reaction rate of the decomposition of O_3

Based solely on this relationship, it has been predicted that the ozone concentration should be about 2 ppm at solar noon in the U.S.⁷ Indeed, in unpolluted environments, ozone concentrations usually are in the range of 2 to 5 ppm. However, in polluted urban areas, ozone concentrations can be as high as 50 ppm. Peroxy radicals formed from hydrocarbon emissions cause this enhanced ozone concentration. These radicals oxidize nitric oxide to nitrogen dioxide, thereby shifting the above steady state relationship to higher ozone levels.

Since ozone is generated by photolytic reactions, anything that affects available sunlight will affect the ozone concentration. Consequently, ozone levels are the highest in the summer months, when the days are longer and the sun is more intense.⁴² Similarly, ozone levels are highest near midday and decrease almost to zero at night.⁴³ Temperature has little effect on ozone formation.

The ozone-cracking problem was first taken seriously by the United States Government in the early 1950's. On reactivating military vehicles, moth-balled since World War II, it was found that tires were severely cracked and useless. Government-sponsored research projects rapidly led to the discovery of *p*-phenylenediamine antiozonants. Since then, these original antiozonants have been displaced by longer lasting *p*-phenylenediamine derivatives.

2.3.2. Mechanism of ozone attack on elastomers

Ozone cracking is an electrophilic reaction and starts with the attack of ozone at a location where the electron density is high.⁴⁴ In this respect unsaturated organic compounds are highly reactive with ozone. The reaction of ozone is a bimolecular reaction where one molecule of ozone reacts with one double bond of the rubber, as can be seen in figure 2.6. The first step is a direct 1,3-dipolar addition of the ozone to the double bond to form a primary ozonide (I), or molozinide, which is only detectable at very low temperatures. At room temperature, these ozonides cleave as soon as they are formed to give an aldehyde or ketone and a zwitterion (carbonyl oxide). Cleavage occurs in the direction, which favors the formation of the most stable zwitterion (II). Thus, electron donating groups, such as the methyl group in natural rubber, are predominately attached to the zwitterion, while electron-withdrawing groups, such as the chlorine in chloroprene rubber, are found on the aldehyde.⁴⁵ Normally, in solution, the aldehyde and zwitterion fragments recombine to form an ozonide, but higher molecular weight polymeric peroxides (III) can also be formed by combination of zwitterions. The presence of water increases the rate of chain cleavage, which is probably related to the formation of hydroperoxides. The same chemistry occurs on ozonation of rubber, in solution and in the solid state.⁴⁶

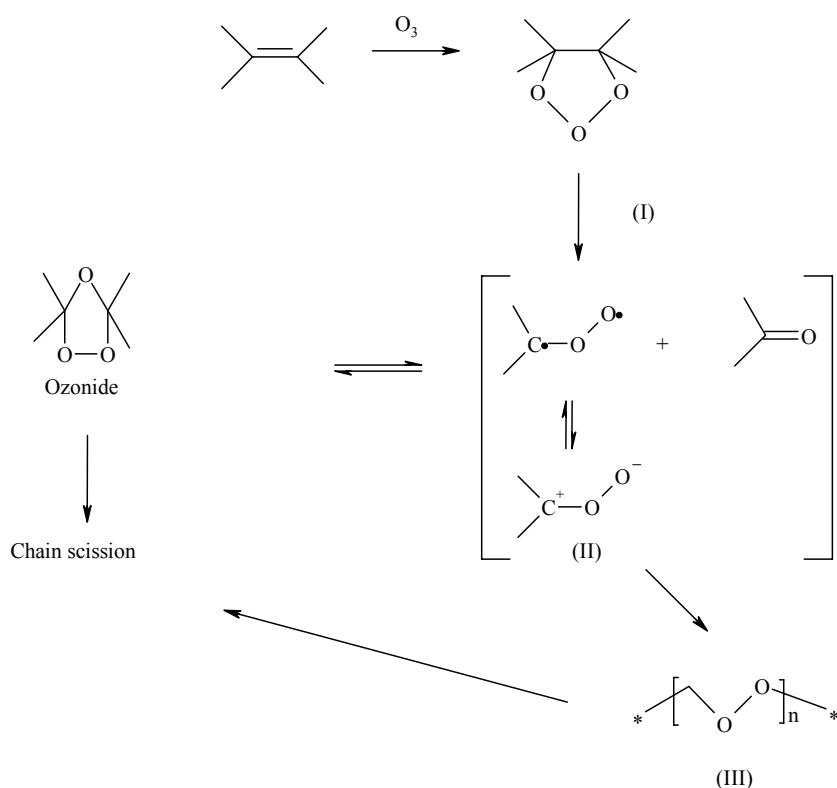


Fig. 2.6: Ozone attack on double bonds.

Due to the retractive forces in stretched rubber, the aldehyde and zwitterion fragments are separated at the molecular-relaxation rate. Therefore, the ozonides and peroxides form at sites remote from the initial cleavage, and underlying rubber chains are exposed to ozone. These unstable ozonides and polymeric peroxides cleave to a variety of oxygenated products, such as acids, esters, ketones, and aldehydes, and also expose new rubber chains to the effects of ozone. The net result is that when rubber chains are cleaved, they retract in the direction of the stress and expose underlying unsaturation. Continuation of this process results in the formation of the characteristic ozone cracks. It should be noted that in the case of butadiene rubbers a small amount of crosslinking occurs during ozonation. This is considered to be due to the reaction between the biradical of the carbonyl oxide and the double bonds of the butadiene rubber.⁴⁷

The reaction of ozone with olefinic compounds is very rapid. Substituents on the double bond, which donate electrons, increase the rate of reaction, while electron-withdrawing substituents slow the reaction down. Thus the rate of reaction with ozone decreases as follows: polyisoprene > polybutadiene > polychloroprene.⁴⁸ The effect of substituents on the double bond is clearly demonstrated in Tables 2.2 and 2.3. Rubbers that contain only pendant double bonds such as EPDM, do not cleave since the double bond is not in the polymer backbone.

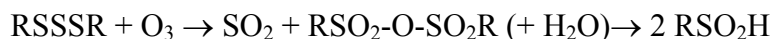
Table 2.2: Relative second-order rate constants for ozonations of selected olefins in CCl₄ at room temperature⁴⁴

| Olefins | Reaction rate K _{rel} [l/mole.s ⁻¹] |
|------------------------------------|---|
| Cl ₂ C=CCl ₂ | 1.0 |
| ClH=CCl ₂ | 3.6 |
| H ₂ C=CCl ₂ | 22.1 |
| cis-ClCH=CHCl | 35.7 |
| trans-ClCH=CHCl | 591 |
| H ₂ C=CHCl | 1180 |
| H ₂ C=CH ₂ | 25000 |
| H ₂ C=CHPr | 81000 |
| H ₂ C=CMe ₂ | 97000 |
| cis-MeCH=CHMe | 163000 |
| Me ₂ C=CHMe | 167000 |
| Me ₂ C=CMe ₂ | 200000 |
| 1,3-Butadiene | 74000 |
| Styrene | 103000 |

Table 2.3: Relative second-order rate constants for ozonations of different unsaturated rubbers in CCl₄ at room temperature^{7,33,48}

| Rubbers | Reaction rate K _{rel} [l/mole.s ⁻¹] |
|---------|---|
| CR | 1.0 |
| BR | 1.5 |
| SBR | 1.5 |
| IR | 3.5 |

Although the cracking of rubbers is related to the reaction of ozone on the double bond, it must be mentioned that ozone reacts also with sulfur crosslinks. These reactions however are much slower. The reaction of ozone with di- and polysulfides is at least 50 times slower than the corresponding reaction with olefins.⁴⁹



Unstretched rubber reacts with ozone until all of the surface double bonds are consumed, and then the reaction stops.⁵⁰ The reaction is fast in the beginning, the rate progressively decreases while the available unsaturation is depleted and ultimately the reaction stops. During this reaction, a gray film, or frosting, forms on the surface of the rubber, but no cracks are noticed. The thickness of this film of ozonized rubber is estimated to be 10 to 40 molecular layers (60 to 240 Å) thick, based on the measurements of the ozone absorbed by unstretched rubber.^{51,52} Disrupting this film by stretching brings new unsaturation to the surface and allows more ozone to be absorbed.

Cracks are only observed when the rubber is stretched above a critical elongation. Two factors determine cracking under static conditions: the critical stress necessary for cracks to form and the rate of crack growth. It was established that all rubbers require the same critical stored energy for cracking to occur.⁵³ This energy is thought to be the energy necessary to separate the two surfaces of a growing crack. Thus depending on the stiffness of the polymer, cracks are formed above a certain elongation. Cracks will only form and grow if the ozonized surface products are moved aside to expose underlying unsaturation. Energy of some form is required to accomplish this. Under static conditions, this is equal to the critical stored energy. Under dynamic conditions, flexing by itself supplies the energy to disturb the surface and no critical energy is required.

The rate of crack growth depends on the polymer and is directly proportional to the ozone concentration. The rate of crack growth is independent of the applied stress as long as it exceeds the critical value. The rate of crack growth also depends on the mobility of the underlying chain segments of rubber, which is necessary to untangle and position double bonds for further attack by ozone. Consequently, anything that will increase the mobility of the rubber chains will increase the rate of crack growth. For example, the slow crack growth rate in IIR becomes equal to that of NR and SBR when sufficient plasticizer is added or when the temperature is raised.⁵⁴ Conversely, decreasing chain mobility diminishes the crack growth rate. For this reason, increasing the crosslinking density in some cases decreases mobility and reduces the rate of crack growth.

2.3.3 Mechanism of antiozonants

Rubbers can be protected against ozone by use of chemical antiozonants and via several physical methods. The chemical antiozonants protect rubber under both static and dynamic conditions, whereas the physical methods are more related towards protection under static conditions.

2.3.3.1 Protection against ozone under static conditions

There are several physical methods that can be used to protect rubber against ozone. They are wrapping, covering, or coating the rubber surface.⁵⁵ This can be accomplished by adding waxes to the rubber and/or adding an ozone resistant polymer that increases the critical stress. Waxes are the most important in this respect. Two types of waxes are used to protect rubber against ozone, paraffinic and microcrystalline. Paraffinic waxes are predominantly straight chain hydrocarbons of relatively low molecular weight of about 350 to 420. They are highly crystalline due to their linear structure and form large crystals having a melting range from 38 to 74°C. Microcrystalline waxes are obtained from higher molecular petroleum residuals and have higher molecular weights than the paraffinic waxes, ranging from 490 to

800. In contrast to the paraffinic waxes, microcrystalline waxes are predominantly branched, and therefore form smaller, more irregular crystals that melt from about 57 to 100°C. Waxes exert their protection by blooming to the surface to form a film of hydrocarbons that is impermeable to ozone. Protection is only obtained when the film is thick enough to provide a barrier to the ozone. Thus the thicker the film, the better the protection. The obtained thickness of the bloom layer depends both on the solubility and the diffusion rate of the wax, which depend on the temperature. Bloom occurs whenever the solubility of the wax in the rubber is exceeded. Therefore, at temperatures lower than 40°C, the smaller and more soluble paraffinic waxes provide the best protection. Lowering the temperature reduces the solubility of the paraffinic waxes and increases the thickness of their bloom. Yet, their small size allows them to migrate rapidly to the surface, in spite of lower temperatures. Conversely, as the temperature increases, the high solubility of the paraffinic waxes becomes a disadvantage. They become too soluble in the rubber and do not form a thick enough protective bloom. Microcrystalline waxes perform better at higher temperatures, since higher temperatures increase their rate of migration to the surface and this allows more wax to be incorporated into the rubber. Therefore, blends of paraffinic and microcrystalline waxes are commonly used to guarantee protection over the widest possible temperature range.⁵⁶ Combinations of waxes and chemical antiozonants show synergistic improvement in ozone resistance.⁵⁷ Presence of the antiozonant results in a thicker bloom layer.

Another way to protect rubber against ozone is to add an ozone-resistant polymer (i.e. EPM, EPDM, halobutyl, polyethylene, polyvinyl acetate, etc.) to the rubber. Microscopic studies of these mixtures show that the added polymer exists as a separate, dispersed phase.⁵⁸ Consequently, as a crack grows in the rubber, it encounters a domain of the added polymer, which reduces the stress at the crack tip. This raises the critical stress required for cracking to occur, and crack growth ceases. Under dynamic conditions, where almost no critical stress is required, these polymer blends do not completely prevent cracking. In this case they function by reducing the segmental mobility of the rubber chains and this slows the rate of crack growth. This method is effective when the polymer is added at a level between 20 and 50%. Higher levels do not result in further improvement of the ozone resistance.⁵⁹ At lower levels, propagation cracks circumvent the stress-relieving domains or will not reduce segmental mobility sufficiently. This method of protecting rubber against ozone is used on a limited basis, since vulcanizates of these blended rubbers frequently exhibit poorer properties. However, it is the only effective nondiscoloring method of protecting rubber under dynamic conditions.

2.3.3.2 Protection against ozone under dynamic conditions

Under dynamic conditions, i.e. under cyclic deformations (stretching and compression) the physical methods to protect against ozone are no longer valid.

Chemical antiozonants have been developed to protect rubber against ozone under such dynamic conditions. Several mechanisms have been proposed to explain how chemical antiozonants protect rubber. The scavenging mechanism, the protective film mechanism or a combination of both are nowadays the most accepted mechanisms.

The scavenging mechanism states that antiozonants function by migrating towards the surface of the rubber and, due to their exceptional reactivity towards ozone, scavenge the ozone before it can react with the rubber.⁶⁰ The scavenging mechanism is based on the facts that all antiozonants react much more rapidly with ozone than do the double bonds of the rubber molecules. This fact distinguishes antiozonants from antioxidants.

Studies of the reaction rates of various substituted paraphenylene diamines (PPDA's) towards ozone show that their reactivities are directly related to the electron density on the nitrogens due to the different substituents. Reactivity decreases in the following order: N,N,N',N'-tetraalkyl- > N,N,N'-trialkyl- > N,N'-dialkyl- > N-alkyl-N'-aryl- > N,N'-diaryl.⁶¹ It should be noted, that their ease of oxidation decreases in the same order. As expected, PPDA's (para phenylene diamines) substituted by normal, secondary, and tertiary alkyl groups all exhibit essentially the same reaction rates. Only the initial reaction of the antiozonant with the ozone is rapid; the resulting ozonized products always react much more slowly. Thus the number of moles of ozone absorbed by a compound is not necessarily an indication of its effectiveness. It is only the rate of reaction that is important.

By itself, the scavenging mechanism suffers from a number of shortcomings. According to this mechanism, the antiozonant must rapidly migrate to the surface of the rubber in order to scavenge the ozone. However, calculations show that the rate of diffusion of antiozonants to the rubber surface is too slow to scavenge all the available ozone.⁶² Many compounds, which react very rapidly with ozone and therefore should be excellent scavengers, are not effective. A good example is the poor activity of N,N'-di-n-octyl-PPDA (DnOPPD) compared to the excellent activity of its sec-octyl isomer, DOPPD.¹³ Since these isomers have the same reactivity towards ozone, the same solubility in rubber, the same molecular weight (and diffusion rates) and melting points (both are liquids), the difference in their antiozonant activities must reside in the nature of their ozonized products.

The protective film mechanism states that the rapid reaction of ozone with the antiozonant produces a film on the surface of the rubber, which prevents attack on the rubber, like waxes are doing.⁶³ This mechanism is based on the fact that the ozone uptake of elongated rubber containing a substituted p-phenylene diamine type of antiozonant is very fast initially and then decreases rather rapidly with time and eventually stops almost completely. The film has been studied spectroscopically and shown to consist of unreacted antiozonant and its ozonized products, but no ozonized rubber is involved.⁶⁴ Since these ozonized products are polar, they have poor solubility in the rubber and accumulate on the surface.

Currently, the most accepted mechanism of antiozonant action is a combination of the scavenging and the protective film formation. Based on this

mechanism, one concludes that the higher critical elongation exhibited by DOPPD is due to the nature of the protective film that forms while scavenging ozone. The only way a film or coating can increase critical stress is, if it completely prevents ozone from reaching the surface. Only a continuous flexible film can do this. For example, wax forms such a protective but non-flexible film and increases the critical elongation.⁶⁵ A continuous flexible film also explains why DOPPD does not increase the critical elongation under dynamic conditions. In this case, flexing would disrupt the continuity of the film and destroy its ability to completely coat the rubber surface, just as flexing destroys the effectiveness of waxes. It also explains why DOPPD does not increase the critical elongation in NBR.⁶⁶ In NBR very little DOPPD is found on the surface. Consequently, any film, which forms on the surface, is too thin to be effective. The difference in the amount of DOPPD on the surface of NBR compared to SBR is attributed to the higher solubility of DOPPD in NBR.

The effect of ozone and DOPPD concentrations on critical stress can be explained by considering the factors involved in film formation and destruction. At a fixed ozone concentration, increasing the concentration of DOPPD will increase the critical elongation because the equilibrium concentration of DOPPD on the surface of the rubber increases with loading. This results in the formation of a thicker, more durable and flexible film. The higher equilibrium surface concentration of DOPPD, lying just below the film, also guarantees that any of the film destroyed by ozone will be efficiently repaired before cracks can form. On the other hand, increasing the ozone concentration at a fixed DOPPD level decreases the critical stress because the film reacts and is too rapidly destroyed by ozone, to be repaired. Thus, the critical elongation will be that point, where the ozone concentration destroys the film more quickly than that it can be repaired. At very high ozone levels, this barrier is so quickly destroyed that the critical stress is the same as the value for an unprotected stock. Since N-isopropyl-N'-phenyl-p-phenylenediamine (IPPD) does not increase critical elongation, its reaction products with ozone must form a barrier which contains many flaws. Indeed, IPPD is known to give a powdery bloom. However, combining IPPD with waxes results in a dramatic increase in the critical stress. This has been attributed to the ability of IPPD to facilitate wax migration and increase the thickness and continuity of the wax bloom.⁶⁷

2.3.3.3 Protection against ozone by substituted PPD's

The most effective antiozonants are the substituted PPD's. Their mechanism of protection against ozone is based on the 'scavenger-protective film' mechanism.⁶⁸⁻
⁷⁰ The reaction of ozone with the antiozonant is much faster than the reaction with the carbon-carbon double bonds of the rubber on the rubber surface.⁵⁶ The rubber is protected from the ozone attack till the surface antiozonant is depleted. As the antiozonant is continuously consumed through its reaction with ozone at the rubber surface, diffusion of the antiozonant from the inner parts to the surface replenishes the surface concentration to provide the continuous protection against ozone. A thin

flexible film developed from the antiozonant/ozone reaction products on the rubber surface also offers protection.

In a PPD molecule, the aryl alkyl-substituted NH group is more reactive towards ozone than the bisaryl-substituted NH group owing to the higher charge density on the N-atom of the aryl alkyl-substitute.⁷¹ This correlates very well with the literature report that aryl alkyl-PPD (e.g., 6PPD) produced nitron, while the bisalkyl-PPD such as 77PD [N,N'-Bis(1,4-dimethylpentyl)-p-phenylenediamine] produced dinitron instead.^{68,69} Apparently, the stabilizing effect of the N-aryl group on the nitron retards further reaction of the nitron with ozone. A simplified reaction mechanism for the aryl-alkyl PPD's such as 6PPD is depicted in figure 2.7.

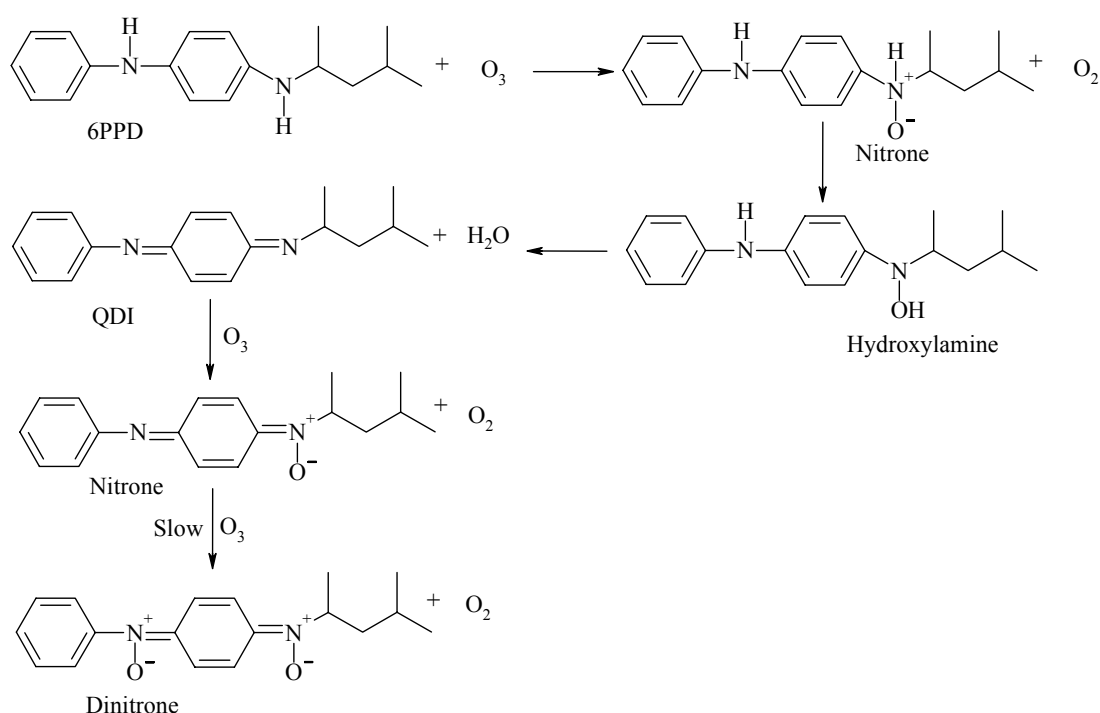


Fig. 2.7: Ozonation mechanism for aryl-alkyl-PPD's.⁷⁰

2.3.4 Methods of studying the ozone resistance of rubber

Since ozone attack on rubber is essentially a surface phenomenon, the test methods involve exposure of the rubber samples under static and/or dynamic strain, in a closed chamber at a constant temperature, to an atmosphere containing a given concentration of ozone. Curing test, test pieces are examined periodically for cracking. The length and amount of cracks is assessed according to the Bayer method.^{72, 73} The ISO standard ozone test conditions involve a test temperature of $40 \pm 1^\circ C$ and an ozone level of 50 ± 5 pphm (parts per hundred million), with a test duration of 72

hours. Testing is done under static⁷² and/or dynamic strain.⁷³ These are accelerated tests and should be used for the relative comparison of compounds, rather than for the prediction of long-term service life. The method is rather complicated and demands a long duration of ozone exposure. Therefore, in some cases the rate constants of the antiozonants reaction with ozone in solution are used instead to evaluate the efficiency of different antiozonants.⁷⁴

The loss of antiozonants, either in a chemical or physical manner, appears to be the limiting factor in providing long-term protection of rubber products. That is why for new antiozonants not only the efficiency of the antiozonants must be evaluated, but one also has to watch other properties that influence their protective functions in an indifferent manner. E.g. the molecule's mobility, their ability to migrate, is one of the parameters determining the efficiency of antiozonant action. Determination of the mobility kinetics of antiozonants can be done with a gravimetric method elaborated by Kavun.⁷⁵ This method was used to determine the diffusion coefficient of several substituted PPD's, in different rubbers and at different temperatures.⁷⁶ The diffusion coefficients were calculated using the classical diffusion theory: Table 2.4. The diffusion coefficients increase with increasing temperature and with decreased compatibility with the rubber. The lower diffusion coefficient observed for SPPD (N-(1-phenylethyl)-N'-phenyl-p-phenylenediamine) compared to that of IPPD and 6PPD was explained by an increased molecular weight and/or increased compatibility with the rubbers.

Table 2.4: Diffusion coefficients for IPPD, 6PPD and SPPD (see figure 2.14), in different rubbers and at different temperatures⁷⁶

| Rubber | Temperature | D [cm ² /s] | | |
|---------|-------------|------------------------|---------|---------|
| | | IPPD | 6PPD | SPPD |
| NR/BR | 10°C | 1.16E-8 | 7.82E-9 | 6.56E-9 |
| | 25°C | 2.99E-8 | 1.92E-8 | 1.54E-8 |
| | 38°C | 6.89E-8 | 4.55E-8 | 3.58E-8 |
| | 62°C | 1.88E-7 | 1.47E-7 | 1.20E-7 |
| | 85°C | 3.51E-7 | 2.79E-7 | 2.17E-7 |
| NR | 10°C | 3.40E-9 | 1.70E-9 | 1.30E-9 |
| | 38°C | 2.56E-8 | 1.39E-8 | 1.11E-8 |
| | 62°C | 1.19E-7 | 7.05E-8 | 6.05E-8 |
| | 85°C | 3.11E-7 | 2.34E-7 | 1.66E-7 |
| SBR1500 | 38°C | 1.03E-8 | 6.13E-9 | 4.62E-9 |
| | 62°C | 4.28E-8 | 3.05E-8 | 2.47E-8 |
| | 85°C | 1.36E-7 | 9.72E-8 | 6.02E-8 |
| BR | 38°C | 1.32E-7 | 8.56E-8 | 6.79E-8 |
| | 62°C | 2.71E-7 | 1.99E-7 | 1.64E-7 |

2.4 Mechanism of protection against Flex Cracking

Flex cracking, the occurrence and growth of cracks in the surface of rubber when repeatedly submitted to a deformation cycle, is determined by fatigue testing. Fatiguing of rubbers at room temperature is a degradation process caused by repeated mechanical stress under limited access of oxygen. The mechanical deformation stress is believed to generate macroalkyl radicals ($R\bullet$). A small fraction of the macroalkyl radicals reacts with oxygen to form alkylperoxy radicals, still leaving a high concentration of the macroalkyl radicals. Consequently, removal of the macroalkyl radicals in a catalytic process constitutes a prevailing anti-fatigue process.⁹ On the other hand, the macroalkyl radicals are rapidly converted to the alkylperoxy radicals under air-oven heat aging. The auto-oxidation propagated by the alkylperoxy radicals thus dominates the degradation process. Therefore, removal of the alkylperoxy radicals becomes the primary function of an antioxidant.

It has been shown that diarylamines are good anti-fatigue agents and that diarylamine nitroxyl radicals are even more effective than the parent amines. The anti-fatigue mechanism of the amine anti-degradants, shown in figure 2.8, has been proposed where the formation of the intermediate nitroxyl radicals plays an active role.⁷⁷ Generation of nitroxyl radicals from the free amines is first depicted in figure 2.8. In the fatigue process, macroalkyl radicals are generated and subsequently removed by reaction with these nitroxyl radicals. The resulting hydroxylamine can be re-oxidized by alkylperoxy radicals to re-generate the nitroxyl radicals in an auto-oxidation chain-breaking process.

The nitroxyl radicals can be partially converted back to the free diarylamine during vulcanization through the reductive action of thiyl radicals of thiols. The free diarylamine thus regenerated, would repeat the reaction described in figure 2.8 to form more nitroxyl radicals.

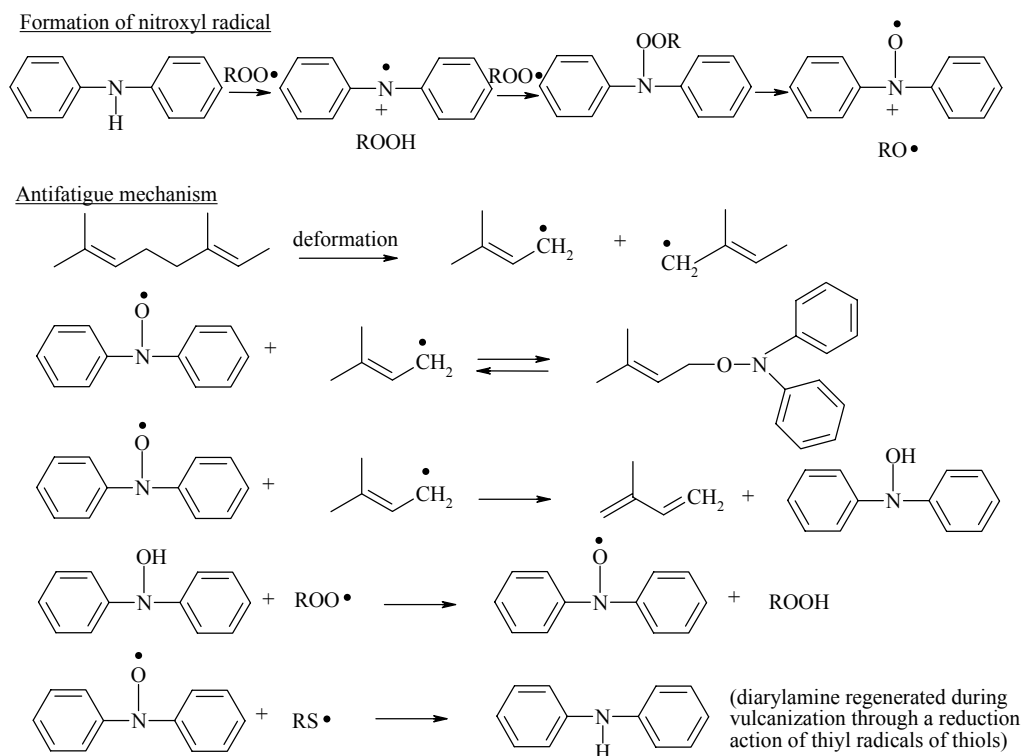


Fig. 2.8: Anti-fatigue mechanism of diaryl amines.

2.5 Trends towards long-lasting antidegradants

2.5.1 Introduction

Antidegradants are very important compounding additives in their role to economically maintain rubber properties at service conditions. Although conventional antidegradants such as 6PPD and IPPD provide protection against oxygen and ozone, this protection is of short duration. Producers of rubber chemicals are focussing on new developments, addressing longer and better protection of rubber products.⁷⁸ Therefore, several new types of long-lasting antioxidants and long-lasting antiozonants have been developed over the last two decades.

2.5.2 Long-lasting antioxidants

To limit the thermal oxidative deterioration of elastomers and their vulcanizates during storage, processing, and use, different systems of antioxidants are used. The activity of the antioxidants depends on their ability to trap peroxy and

hydroperoxy radicals and their catalytic action in hydroperoxide decomposition. Their compatibility with the polymers also plays a major role. Moreover, it is very important to limit antioxidant loss by extraction (leaching) or by volatilization. Food packaging and medical devices are areas in which additive migration or extraction is of major concern. Contact with oils or fats could conceivably lead to ingestion of mobile polymer stabilizers. In an effort to address this concern, the US Food and Drug Administration (FDA) has set a code of regulations governing the use of additives in food contact applications.⁷⁹ These regulations contain a list of acceptable polymer additives and dose limits for polymers, which may be used for specific food contact. Inclusion of a particular compound in this list depends both on specific extractability and toxicological factors. Obviously, polymer bound stabilizers cannot be extracted and would therefore prevent inadvertent food contamination. An additional consideration is the effect of additive migration on surface properties. As additives migrate or bloom to the polymer surface, the ability to seal or coat the surface may deteriorate. This affects coating adhesion and lamination peel strength.

The above-described issues are the reasons for an increased interest in the synthesis of new antioxidants with the possibility to graft to the polymer backbone or to form polymeric or oligomeric antidegradants. In the last two decades, several approaches have been evaluated in order to develop such new antioxidants:

- Attachment of hydrocarbon chains to conventional antioxidants in order to increase the MW and compatibility with polymers;⁸⁰
- Polymeric or oligomeric antioxidants;⁸¹
- Polymer bound or covulcanizable antioxidants;⁸²⁻⁸⁴
- Binding of several functional groups onto a single platform.⁸⁵

Examination of the history of antioxidants such as hindered phenols and amines shows a move from low molecular weight products to higher molecular weight products. Specifically, polymer industries have abandoned the use of e.g. butylated hydroxy toluene (BHT) in favor of tetrakis(3,5-di-*t*-butyl-4-hydroxyhydrocinnamyl)methane (see figure 2.9). Likewise, polymeric HALS, like poly-methylpropyl-3-oxy-[4(2,2,6,6-tetramethyl)piperidinyl] siloxane, replaced the low molecular weight hindered amine Lowilite 77 (see fig. 2.10). The next obvious step was to produce a new class of stabilizers, which are chemically bound to the polymer chain. This approach has had varying degrees of success. While the extraction resistance of the bound stabilizers was significantly improved, performance suffered greatly. Because degradation processes may occur in localized portions of the bulk of the polymer, mobility of the stabilizer plays a key role in antioxidant activity.

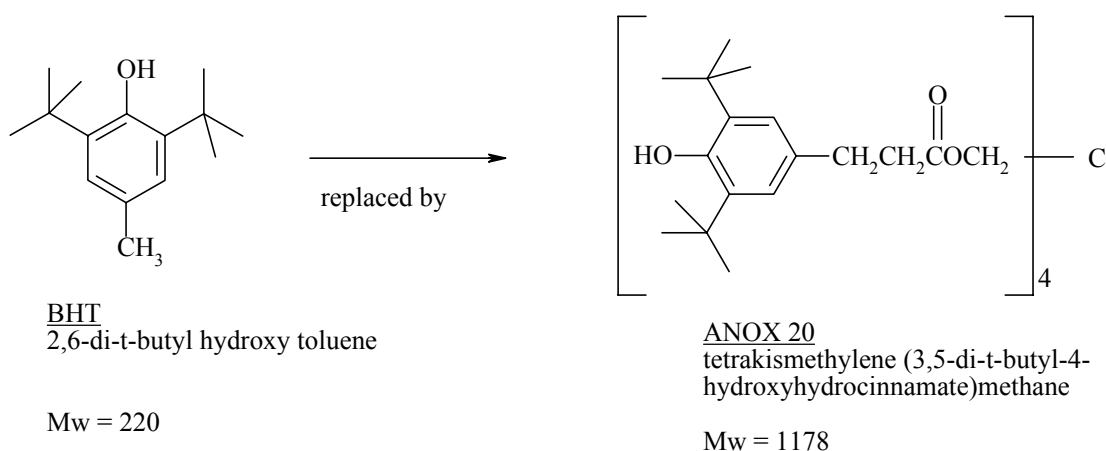


Fig. 2.9: Replacement of low MW phenolic AOx by high MW product.

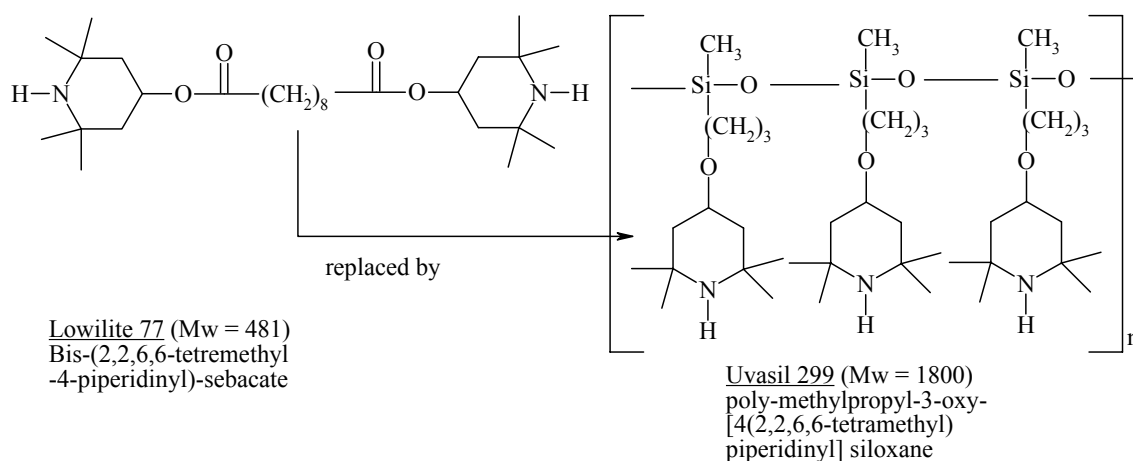


Fig. 2.10: Replacement of low MW HALS by high MW product.

The antioxidative activities of polymeric antioxidants prepared from Verona oil and the conventional phenolic antioxidant 3-(3,5-di-*tert*-butyl-4-hydroxyphenyl)propionic acid (DTBH), chemically grafted to polystyrene and polyurethanes, is similar and in some cases even better than that of the corresponding low molecular weight phenolic antioxidants.⁸¹

Several ways of obtaining polymer-bound antioxidants have been described. Roos and D'Amico^{86,87} reported polymerizable *p*-phenylene diamine antioxidants. Cain et al. reported the 'ene' addition of nitrosophenols or aniline derivatives to produce polymer bound stabilizers.⁸⁸ The most versatile method of preparation of bound antioxidant is by the direct reaction of a conventional antioxidant with a

polymer. Scott et al. have demonstrated that simple hindered phenols, which contain a methyl group in the o- or p-position, can react with natural rubber in presence of oxidizing free radicals to yield polymer bound antioxidants.⁸⁹ The antioxidants like styrenated phenol, diphenylamine etc. bound to hydroxyl terminated liquid natural rubber by modified Friedel-Craft's reactions were found to be effective in improving the aging resistance.⁹⁰ PPD's bound to natural rubber showed improved aging resistance compared to conventional PPD's, but as expected a worse ozone resistance because the bounded antidegradants cannot migrate to the surface.⁸² Quinone diimines (QDI) have been reported as bound antioxidant and diffusible antiozonant. During vulcanization, part of the QDI is grafted to the polymer backbone and acts as bound antioxidant, whereas the other part is reduced to PPD and is active as diffusible antiozonant.⁸³

The protection efficiency of antioxidant couples consisting of a classical compound (disubstituted p-phenylenediamines and dihydroquinoline derivatives) and compounds with a disulfide bridge, resulting from diamine and phenolic structures, was reported by Meghea and Giurginca.⁸⁴ Antioxidants containing a disulfide bridge are able to graft onto the elastomer chain during processing and curing, leading to a level of protection superior to the classical antidegradants.

One of the latest developments in stabilizers are the polysiloxanes, which provide flexible, versatile backbones for a variety of classes of polymer stabilizers. The siloxanes appear to be good backbones, because they are rather inexpensive, easily functionalized, have a high level of functionalizable sites, good compatibility with many polymers and excellent thermo and photolytic stability.⁸⁵ Hindered amines, hindered phenolics and metal deactivators have been grafted onto the polysiloxanes. The low extractability of siloxane based additives was further enhanced by the inclusion of graftable pendant groups onto the polysiloxane backbone.⁹¹ The grafted stabilizers maintain their activity due to the flexible siloxane platform. This was seen as a limitation of monomeric stabilizers, which have been grafted onto the polymer matrix and thus are not mobile at all. Sulekha et al. used low molecular weight chlorinated polyisobutylene and chlorinated paraffin wax as a platform to graft paraphenylene diamine.^{92,93} These oligomer-bound antioxidants impart improved ozone and flex resistance and chemical properties to vulcanizates of NR, SBR, IIR and NBR and to blends of NR/BR and NR/SBR, in comparison with those containing conventional antioxidants.⁹⁴ The presence of liquid polymer bound paraphenylene diamine reduces the amount of plasticizer required for compounding.⁹⁵

2.5.3 Long-lasting antiozonants

There is a clear demand for long-lasting antiozonants (two or three times longer-lasting than conventional antiozonants as IPPD and 6PPD) and for non-staining and non-discoloring antiozonants for better appearance products such as tire sidewalls. The functional classes of antiozonants include substituted monophenols, hindered bisphenols and thiobisphenols, substituted hydroquinones, organic

phosphites, and thioesters.² Triphenyl phosphine, substituted thioureas and isothiureas, thiosemicarbazides, esters of dithiocarbamates, lactams, and olefinic and enamine compounds are reported as non-staining antiozonants.^{96,97} Approaches to completely replace the PPD's with a non-discoloring antiozonant have had only limited success, leading to the development of new classes of non-staining antiozonants.

Warrach and Tsou¹¹⁹ reported that bis-(1,2,3,6-tetrahydrobenzaldehyde)-pentaerythrityl acetal provides superior ozone protection for polychloroprene, butyl rubber, chlorobutyl and bromobutyl rubbers relative to p-phenylenediamine antiozonants, without discoloring the rubber or staining white-painted steel test panels. However, the ozone resistance of diene elastomers (natural rubber, polyisoprene, styrene-butadiene rubber, polybutadiene, nitrile rubber) or inherently ozone-resistant elastomers (ethylene-propylene copolymers, ethylene-propylene-diene terpolymers, chlorosulfonated polyethylene, ethylene vinylacetate) is not improved by this compound.

Rollick, Gillick and Kuczkowski^{96,98} reported a new class of antiozonants for rubber that do not discolor upon exposure to oxygen, ozone or ultraviolet light, namely triazinethiones. Only changes in substitution on the nitrogen adjacent to the thiocarbonyl group affected their antiozonant efficiency. Accelerated weatherometer aging of a titanium dioxide/treated-clay filled styrene-butadiene rubber compound showed their non-discoloring nature. Use of 4 phr tetrahydro-1,3,5-tri-n-butyl-(S)-triazinethione (see figure 2.11) resulted essentially in no change in color, whereas use of only 1phr of N-(1,3-dimethylbutyl)-N'-phenyl-para-phenylenediamine significantly discolored the rubber compared to the control, see Table 2.5. The triazinethiones provided a significant degree of ozone protection to a natural rubber / butadiene rubber black sidewall compound. They are reported as particularly valuable for use in light-colored stocks.

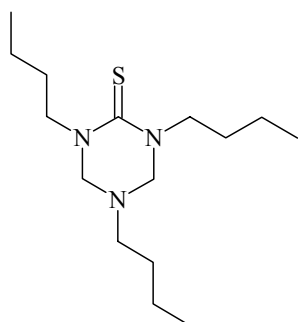


Fig. 2.11: Tetrahydro-1,3,5-tri-n-butyl-(S)-triazinethione.

Table 2.5: Weatherometer induced discoloration of 6PPD and TBTT containing SBR.⁹⁶

| Antiozonant ^A | Hours | L | A | b | ΔE^B |
|--------------------------|-------|-------|-------|-------|--------------|
| None | 24 | 89.89 | 0 | 7.78 | |
| | 48 | 89.61 | -0.10 | 10.19 | |
| | 96 | 89.72 | -0.10 | 11.90 | |
| 1phr 6PPD ^C | 24 | 34.21 | 3.69 | 8.21 | 55.80 |
| | 48 | 40.25 | 2.47 | 7.93 | 49.48 |
| | 96 | 45.93 | 1.86 | 8.40 | 43.97 |
| 4phr TBTT ^D | 24 | 86.66 | 0.80 | 10.28 | 4.09 |
| | 48 | 87.81 | 0.81 | 10.99 | 2.17 |
| | 96 | 87.52 | 1.01 | 11.49 | 2.50 |

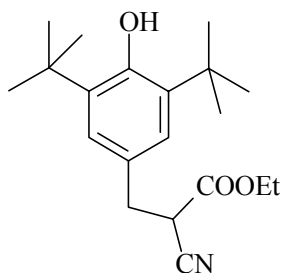
^A Formulation: 100phr SBR 1502, 30phr titanium dioxide, 30phr mercaptosilinated clay, 10phr ZnO, 5phr naphthenic oil, 2phr stearic acid, 2phr sulfur, 0.25phr TMTD (tetramethyl thiuram disulfide)

^B $\Delta E = \sqrt{((\Delta L)^2 + (\Delta a)^2 + (\Delta b)^2)}$ = change in whiteness (ΔL), hue (Δa) and chroma (Δb) upon aging

^C N-(1,3-Dimethylbutyl)-N'-phenyl-para-phenylenediamine

^D Tetrahydro-1,3,5-tri-(n)-butyl-(S)-triazinethione

Ivan, Giurginca and Herdan⁹⁹ reported that 3,5-di-tert-butyl-4-hydroxybenzylcyanoacetate is a non-staining antiozonant that affords similar protection to natural rubber and to cis-polyisoprene compounds as N-isopropyl-N'-phenyl-para-phenylenediamine does (see figure 2.12). This product last longer than conventional non-staining antiozonants, like the styrenated phenols.

**Fig. 2.12:** 3,5-di-tert-butyl-4-hydroxybenzyl cyanoacetate.

Wheeler¹⁰⁰ described a new class of non-staining antiozonants, namely the tris-N-substituted-triazines.

2,4,6-Tris-(N-1,4-dimethylpentyl-para-phenylenediamino)-1,3,5-triazine (see figure 2.13), gave excellent ozone resistance in a natural rubber / butadiene rubber compound when compared to N-(1,3-dimethylbutyl)-N'-phenyl-para-phenylenediamine, but without contact, migration or diffusion staining (see Table 2.6). Hong¹⁰¹ reported equal dynamic ozone performance of this triazine antiozonant to the PPD's in both natural rubber and butadiene rubber compounds. Birdsall, Hong and Hajdasz¹⁰² described that the triazine antiozonant formed a discoloring bloom on a

natural rubber / butadiene rubber compound, but that the bloom was minimal when compounded at two phr or lower levels. When used in combination with a PPD, better ozone protection is obtained compared to using the triazine antiozonant alone, at the same total level of antiozonant. The combination PPD and triazine antiozonant provides longer-term protection.¹⁰³

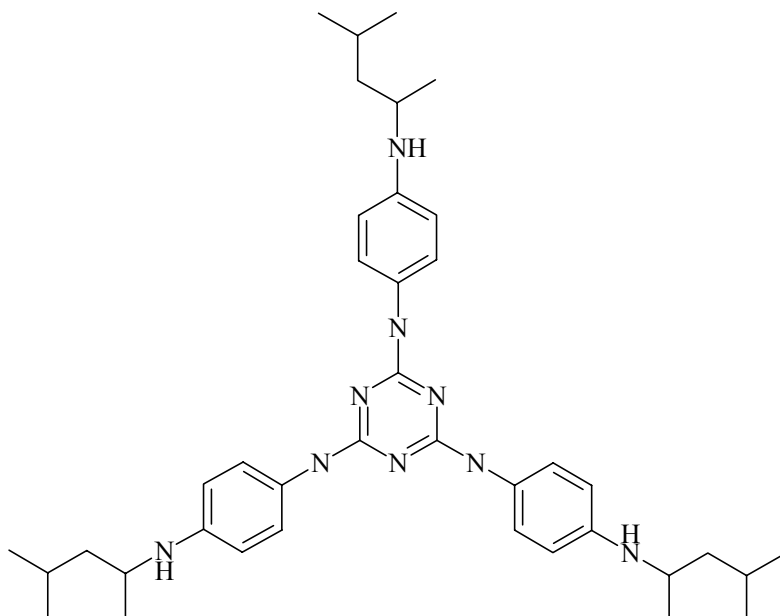


Fig. 2.13: 2,4,6-Tris-(N-1,4-dimethylpentyl-para-phenylenediamino)-1,3,5-triazine (TAPDT).

Table 2.6: Staining experiments^a of the triazine antiozonant.¹⁰⁰

| Method | Antiozonant | L |
|--|--------------------|-------|
| A. Contact stain After 96 hours | Blank | 87.10 |
| | TAPDT ^B | 83.77 |
| | HPPD ^C | 65.59 |
| B. Migration stain After 96 hours | Blank | 86.89 |
| | TAPDT ^B | 87.53 |
| | HPPD ^C | 77.79 |
| C. Diffusion stain, exposed to sunlamp 4 hours at 328°K | Blank | 88.10 |
| | TAPDT ^B | 82.42 |
| | HPPD ^C | 32.65 |

^A Tests were carried out as designated in ASTM Method D-925-83 related to staining of surfaces by contact, migration, or by diffusion. Hunter color values were measured on the L-scale. On this scale 100 is white and 0 is black.

^B Tris-(N-1,4-Dimethylpentyl-para-phenylenediamino)-1,3,5-triazine

^C N-(1,3-Dimethylbutyl)-N'-phenyl-para-phenylenediamine

Lehocky, Syrový and Kavun⁷⁶ reported the migration rates of IPPD, 6PPD and SPPD (see figure 2.14), determined in different polymers and at different temperatures. SPPD showed the lowest migration rate and is therefore expected to last longest in rubber compounds, see Table 2.4. However, the importance of the migration rate should not be overestimated, as the value is not sufficient to determine the effect and the efficiency of the antiozonant.

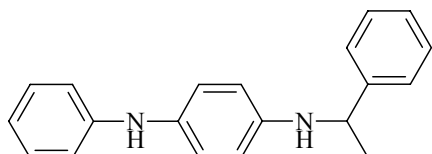


Fig. 2.14: Structure of (N-(1-phenylethyl)-N'-phenyl-p-phenylenediamine) (SPPD).

The most prevalent approach to achieve long-lasting and non-staining ozone protection of rubber compounds is to use an inherently ozone-resistant, saturated-backbone polymer in blends with a diene rubber. The ozone-resistant polymer must be used in sufficient concentration (minimum 25 phr) and must also be sufficiently dispersed to form domains that effectively block the continuous propagation of an ozone-initiated crack through the diene rubber phase within the compound. Elastomers such as ethylene-propylene-diene terpolymers, halogenated butyl rubbers, or brominated isobutylene-co-para-methylstyrene elastomers have been proposed in combination with natural rubber and / or butadiene rubber.

Ogawa, Shiomura and Takizawa^{104,105} reported the use of various EPDM polymers in blends with natural rubber in black sidewall formulations. Laboratory testing showed improved resistance to crack growth and thermal aging.

Hong¹⁰⁶ reported that a polymer blend of 60 phr of natural rubber and 40 phr of EPDM rubber afforded the best protection of a black sidewall compound to ozone attack. Use of a higher molecular weight EPDM rubber gave good flex fatigue-to-failure and adhesion to both carcass and tread compounds. TAPDT mixed with the natural rubber to form a masterbatch followed by blending with the EPDM rubber and other ingredients, afforded the most effective processing in order to protect the natural rubber phase. Compounds containing this natural rubber/EPDM rubber blend (60/40) with 2.4 phr of the triazine antiozonant passed all requirements for the tire black sidewall.

Sumner and Fries¹⁰⁷ reported that ozone resistance depended on the level of the EPDM rubber. When using 40phr of EPDM rubber in the compound there is no cracking throughout the life of the black sidewall. Ozone resistance also depends on proper mixing of the EPDM rubber with natural rubber in order to achieve a polymer domain size of less than one micron. Otherwise cracking can be severe. The combination of high molecular weight and high ethylidene norbornene (ENB) content afforded good adhesion to highly unsaturated polymers. The adhesion mechanism involves the creation of radicals when long chains of EPDM rubber and natural rubber

are broken down by shearing and mechanical work. Grafting between the two elastomers is believed to occur. The graft polymer is thought to act as compatibilizer. The natural rubber/EPDM rubber compound does not rely on migration of antidegradants to achieve ozone resistance and therefore does not stain the sidewall. Appearance is excellent throughout the service life of the tire. However, at the current stage of development, natural rubber/EPDM rubber sidewall compounds are difficult to mix, too expensive, result in an increased rolling resistance and have a reduced tack compared to natural rubber/butadiene rubber sidewall compounds. Related work carried out by Polysar in this field is described in detail.¹⁰⁸⁻¹¹⁸

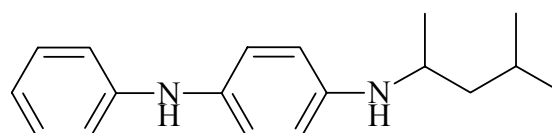
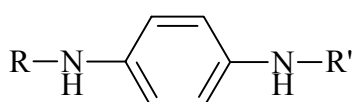
2.6 Classes of Antidegradants

The most commonly used antidegradants for general-purpose rubbers are listed in this section. Antidegradants are divided into staining and non-staining products, with or without fatigue, ozone and oxygen protection.

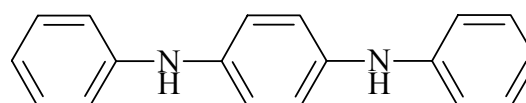
2.6.1 Staining antidegradants

2.6.1.1 Antioxidants with fatigue and ozone protection (antiozonants)

P-PHENYLENEDIAMINE-DERIVATIVES (STRONGLY DISCOLORING)



6PPD



DPPD

N-Isopropyl-N'-phenyl-p-phenylenediamine (IPPD)

N-(1,3-Dimethylbutyl)-N'-phenyl-p-phenylenediamine (6PPD)

N-N'-Bis-(1,4-dimethylpentyl)-p-phenylenediamine (77PD)

N,N'-Bis-(1-ethyl-3-methylpentyl)-p-phenylenediamine (DOPD)

N,N'-Diphenyl-p-phenylenediamine (DPPD)

N,N'-Ditolyl-p-phenylenediamine (DTPD)

N,N'-Di-β-naphthyl-p-phenylenediamine (DNPD)

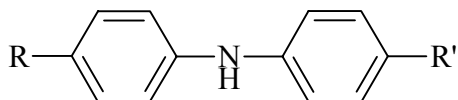
N,N'-Bis(1-methylheptyl)-p-phenylenediamine
N,N'-Di-sec-butyl-p-phenylenediamine (44PD)
N-Phenyl-N'-cyclohexyl-p-phenylenediamine
N-Phenyl-N'-1-methylheptyl-p-phenylenediamine

Notes:

- The most effective compounds for ozone- and fatigue protection under static and dynamic conditions;
- They increase the critical energy necessary to form ozone cracks under static and dynamic conditions (crack formation at higher extensions);
- They reduce the crack growth under static and dynamic conditions;
- The effectiveness depends on the type and size of the nitrogen substituents;
- Less effective in NBR due to good solubility;
- DNPD is the best antioxidant but a worse antiozonant due to a low migration rate.

2.6.1.2 Antioxidants with fatigue but without ozone protection

DIPHENYLAMINE-DERIVATIVES (STRONGLY DISCOLORING)

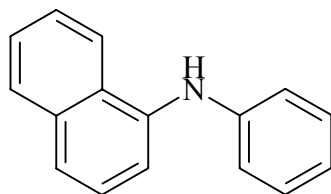


Octylated diphenylamine (ODPA)
Styrenated diphenylamine (SDPA)
Acetone/diphenylamine condensation product (ADPA)
4,4'-Bis(α,α -dimethylbenzyl) diphenylamine
4,4-Dicumyl-diphenylamine

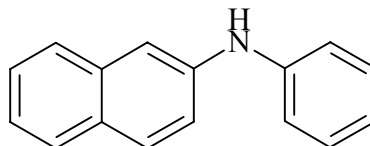
Notes:

- Good antioxidant- and heat protection activity;
- Roughly equally effective to each other in general purpose rubbers;
- ODPA is an exceptionally good heat protector in CR;
- Limited amount of fatigue protection in NR and IR (not as good as PAN or PBN);
- Fatigue protection in SBR and BR is very small.

NAPHTHYLAMINE-DERIVATIVES (STRONGLY DISCOLORING)



PAN



PBN

Phenyl- α -naphthylamine (PAN)

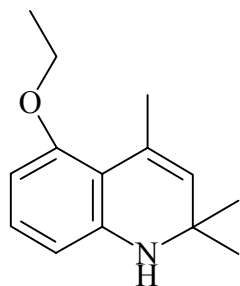
Phenyl- β -naphthylamine (PBN)

Notes:

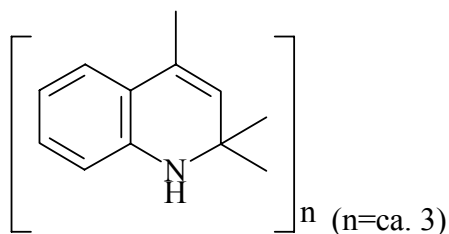
- PAN and PBN are active in NR as fatigue protectors, less active in SBR and BR;
- PAN and PBN are highly effective antioxidants, but have become much less important because of toxicological considerations.

2.6.1.3 Antioxidants with little or no fatigue protection

DIHYDROQUINOLINE-DERIVATIVES (STRONGLY DISCOLORING)



ETMQ



TMQ

6-Ethoxy-2,2,4-trimethyl-1,2-dihydroquinoline (ETMQ)

2,2,4-Trimethyl-1,2-dihydroquinoline, polymerized (TMQ)

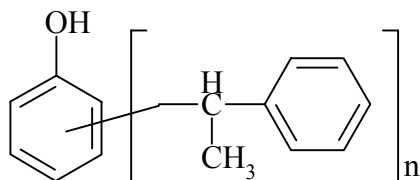
Notes:

- ETMQ is effective as both antifatigue agent and antioxidant;
- TMQ is an excellent antioxidant and long lasting heat stabilizer (low volatility).

2.6.2 Non-staining antidegradants

2.6.2.1 Antioxidants with fatigue and ozone protection

MONOPHENOL DERIVATIVES (NON-DISCOLORING)



Styrenated phenol (SPH)

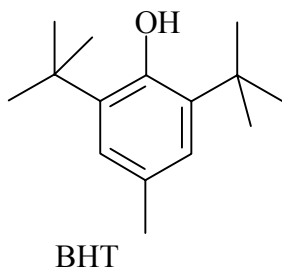
Styrenated and alkylated phenol (SAPH)

Notes:

- SPH has roughly the same fatigue protection as ODPA, much less effective than p-phenylenediamines.

2.6.2.2 Antioxidants without fatigue and ozone protection

MONOPHENOL DERIVATIVES (NON-DISCOLORING)



2,6-Di-t-butyl hydroxy toluene (BHT)

2,6-Di-t-butyl-4-nonylphenol

3-(3,5-Di-t-butyl-4-hydroxyphenyl) propionic methyl ester

2,6-Di-t-butyl-4-ethyl phenol

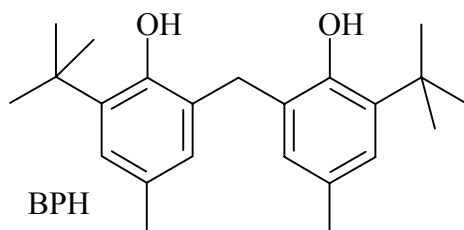
Octadecyl 3,5-di-t-butyl-4-hydroxyhydrocinnamate

4-Nonylphenol

Notes:

- BHT is frequently used, but because of its high volatility due to the low MW only active at low temperatures.

BIPHENOL-DERIVATIVES (NON-DISCOLORING)



- 2,2'-Methylene-bis-(4-methyl-6-tert.butylphenol) (BPH)
- 2,2'-Methylene-bis-(4-methyl-6-cyclohexylphenol)
- 2,2'-Isobutylidene-bis-(4-methyl-6-tert.butylphenol)
- 2,2'-Dicyclopentyl-bis-(4-methyl-6-tert.butyl-phenol)
- Triethyleneglycol-bis(3-t-butyl-4-hydroxy-5-methylphenyl)-propionate

Notes:

- Excellent protection against oxygen;
- After prolonged light exposure, a certain amount of pink discoloration occurs due to the formation of chromophoric structures, which is very small with IBPH.

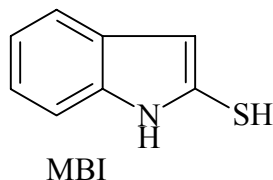
TRIPHENOL-DERIVATIVES (NON-DISCOLORING)

- Tris-1,1,3-(2'-methyl-4'-hydroxy-5-tert.butyl-phenyl)-butane
- 1,3,5-Trimethyl-2,4,6-tris(3',5'-di-tert.butyl-4'-hydroxy-benzyl)-benzene
- Tris(3,5-di-t-butyl-4-hydroxy benzyl)isocyanurate

Notes:

- Have a very low volatility and are therefore used for rubber that is processed at higher temperatures.

BENZIMIDAZOLE-DERIVATIVES (NON-DISCOLORING)

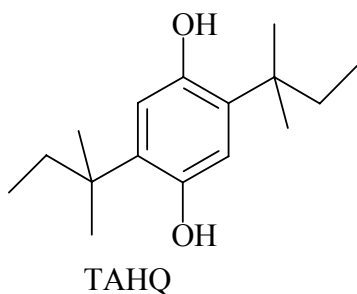


- | | |
|--------------------------------|-------|
| 2-Mercaptobenzimidazole | MBI |
| Zinc-2-mercaptobenzimidazole | ZMBI |
| Methyl-2-mercaptobenzimidazole | MMBI |
| Zinc-2-methylmercaptoimidazole | ZMMBI |

Notes:

- Heterocyclic mercaptans are moderately active, non-discoloring aging protectors (less active than the hindered phenols);
- Very active synergistically with other antioxidants, seldomly used alone.

HYDROQUINONES (NON-DISCOLORING)

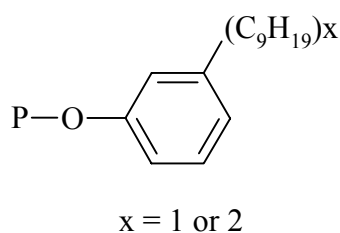


- 2,5-Di-t-butyl hydroquinone (TBHQ)
- 2,5-Di(tert-amyl)hydroquinone (TAHQ)
- Hydroquinone (HQ)
- p-Methoxy-phenol
- Toluhydroquinone (THQ)

Notes:

- Not very reactive towards oxygen, act as radical trap;
- Used as stabilizer in uncured rubber.

PHOSPHITES



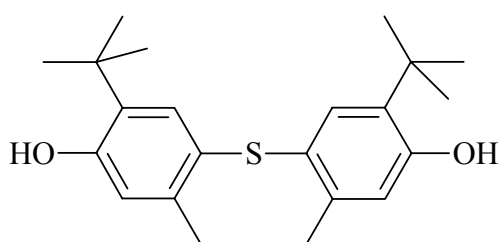
TNPP

- | | |
|---|------|
| Tris(mixed mono- and di-nonylphenyl)phosphite | TNPP |
| Diphenyl isodecyl phosphite | DIDP |
| Diphenyl isooctyl phosphite | DIOP |
| Distearyl pentaerythritol diphosphite | DPDP |

Notes:

- Phosphites (derived from PCl_3 and various phenols) function as peroxide decomposer;
- They are hydrolyzed especially in the presence of acidic materials;
- They are destroyed during sulfur vulcanization, therefore used for stabilization of synthetic rubber during processing and manufacturing (sometimes with non-sulfur cure systems).

THIOBISPHENOLS



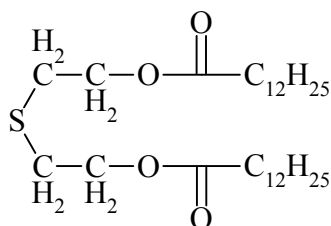
TBMC

4,4'-Thiobis-6-(t-butyl-m-cresol) (TBMC)
2,4-Bis[(octylthio)methyl]-o-cresol

Notes:

- Moderate to excellent antioxidants;
- Only slightly volatile, therefore good long-term antioxidants;
- Slightly activating sulfur cure systems, due to the sulfur bridge.

Thioesters



DLTDP

Dilauryl thiodipropionate (DLTDP)
Dimyristyl thiodipropionate
Distearyl dithiodipropionate
Distearyl thiopropionate

Ditridecyl thiodipropionate
Octadecyl 3-mercaptopropionate
Pentaerythrityl tetrakis (β -laurylthiopropionate)
2,2'-Thiodiethylbis-(3',5'-di-t-butyl-4-hydroxyphenol)-propionate
Thiodipropionate polyester

Notes:

- Peroxide decomposers like the phosphites;
- Synergistic with antioxidants that work via free radical mechanism.

2.6.2.3 Antiozonants without antioxidant protection

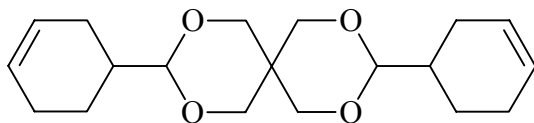
(A) PARAFFINIC WAX

Mainly straight chain hydrocarbons, low MW (350-420).
Highly crystalline due to their linear structure, they form large crystals (melting at 38-74°C).
Maximum film thickness at $\approx 20^\circ\text{C}$; at lower temperatures reduced solubility, but also reduced migration rate; at high temperatures solubility too good to bloom out.

(B) MICROCRYSTALLINE WAX

Obtained from higher MW petroleum residuals (MW 490-800).
Molecules are predominantly branched and hence form smaller, more irregular crystals (melting from about 57 to 100°C).
Maximum film thickness at $\approx 50\text{-}60^\circ\text{C}$; at lower temperatures mobility is too low to get blooming, due to the branching of the molecules.

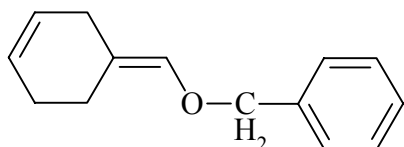
(C) UNSATURATED ACETALS



Bis-(1,2,3,6-tetrahydrobenzaldehyde)-pentaerythrityl acetal (AFS)

Antiozonant for light colored products, less effective than PPD's (Unsaturated Acetals, for EPDM and halobutyl).

(D) ENOLETHER



4-(Benzyloxymethylene)cyclohexene (AFD)

Antiozonant for light colored products, has roughly the same fatigue protection as ODPA; less effective than PPD's.

2.6.3 Long-lasting antidegradants

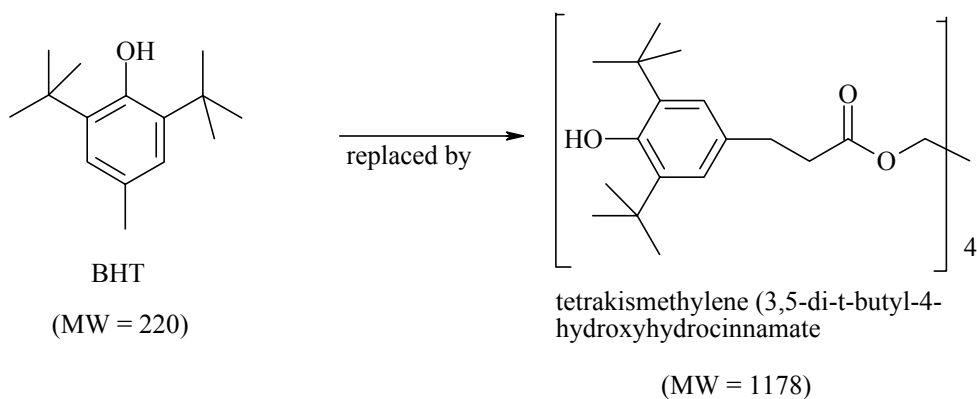
2.6.3.1 Long-lasting antioxidants

(A) HIGH MW ANTIOXIDANTS

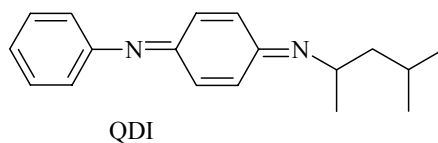
Tetrakismethylene(3,5-di-t-butyl-4-hydroxyhydrocinnamate)methane
Polymeric and oligomeric AOx.

Notes:

- Polymer industries have abandoned products like butylated hydroxytoluene (BHT, MW = 220) for those like tetrakismethylene(3,5-di-t-butyl-4-hydroxyhydrocinnamate)methane (MW = 1178).¹²



(B) POLYMER BOUND AO'S OR COVULCANIZABLE AO'S SUCH AS:



Nitrosophenols

Quinone diimines (QDI)

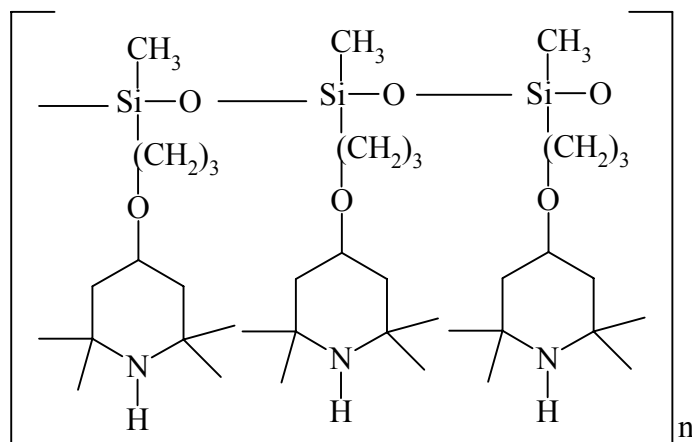
Nonylphenol disulfide oligomer

Verona oil reacted with 3-(3,5-di-tert-butyl-4-hydroxyphenyl)propionic acid

Notes:

- QDI can be applied in all type of diene rubbers. Approximately 20 - 60% of this product is grafted (and thus not extractable) to the polymer backbone, depending on the applied mixing conditions.^{83,120,121}
- Nonylphenol disulfided oligomers can be used in all type of diene rubbers. The antioxidant is grafted to the polymer backbone during vulcanization, via a sulfur bridge. The grafted antioxidant is not extractable.⁸⁴
- Conventional antidegradants are grafted to Verona oil and subsequently copolymerized during polymer synthesis. Antioxidants are completely covalent bounded to the polymer and thus not extractable. Can be applied during polystyrene and polyurethane synthesis.⁸¹

(C) BOUNDED FUNCTIONAL GROUPS TO A SINGLE PLATFORM (I.E. POLYSILOXANES)



Poly-methylpropyl-3-oxy-[4(2,2,6,6-tetramethyl)piperidinyl] siloxane

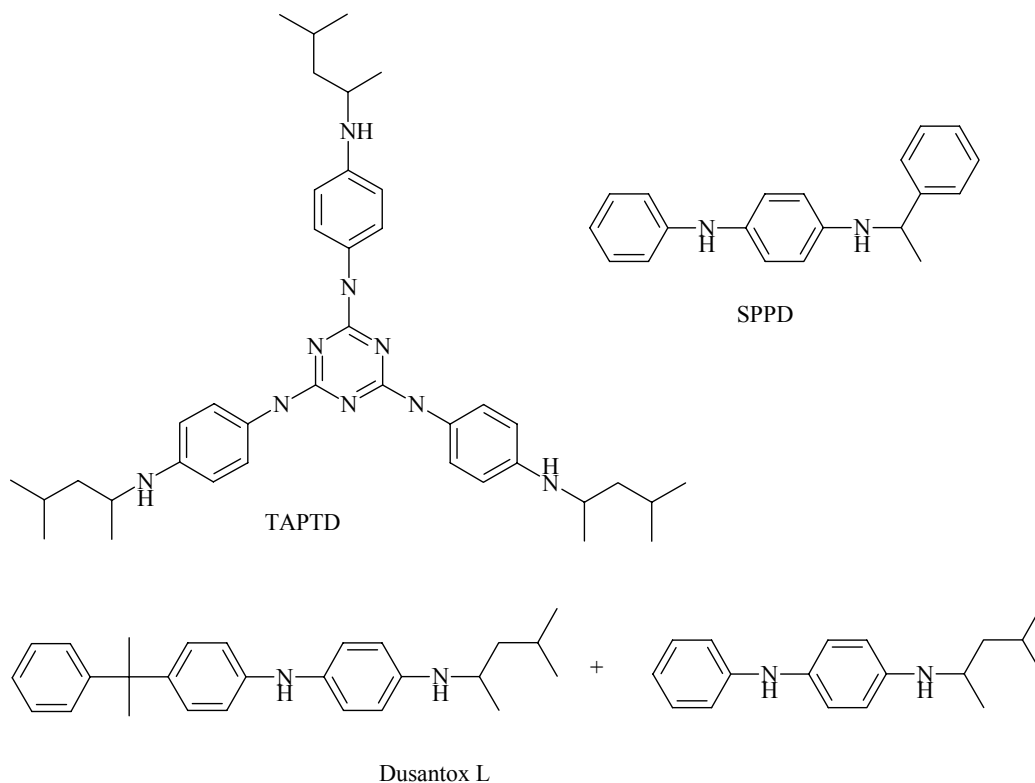
Paraphenylenediamine grafted to chlorinated paraffin wax

Paraphenylenediamine grafted to chlorinated polyisobutylene

Note:

- There are theoretically unlimited possibilities of tailoring MW, functionality and structural characteristics of the polysiloxanes.^{12,85} Therefore, applicable in almost all rubbers and plastics.

2.6.3.2 Long-lasting antiozonants



N-(1-phenylethyl)-N'-phenyl-p-phenylenediamine (SPPD)

Mixture of 6PPD and N-(1,3-dimethylbutyl)-N'-(4-cumylphenyl)-p-phenylenediamine (Dusantox L)

2,4,6-Tris-(N-1,4-dimethylpentyl-p-phenylenediamino)-1,3,5-triazine (TAPTD)

Stearic acid salt of 6PPD (PPD-C18)

Notes:

- SPPD and Dusantox L are development products. These products migrate slower than 6PPD. Can be used in the same polymers as 6PPD.⁷⁶
- PPD-C18 is also a development product. This product migrates slower and is less staining than 6PPD. Can be used in the same polymers as 6PPD.^{122,123}
- TAPDT is not being used extensively in the rubber industry because of its limited solubility in synthetic polymers and its high cost. It is soluble in NR, has fair solubility in CR, BIIR, CIIR, IR, EPDM and NBR, but has limited solubility in BR and SBR. It is a non-staining product.^{70,78}

2.6.4 Miscellaneous

Polycarbodiimide (PCD)

Benzofurane derivative (BD)

Nickel dimethyldithiocarbamate (NiDMC)

Ethylene diamine tetracetic acid (EDTA)

N-Alkyl thioureas (dibutyl thiourea) (DBTU)

Notes:

- As an anti-oxidant, BD is superior to styrenated phenol (SPH);
- BD less volatile than SPH and therefore effective at higher temperatures;
- BD acts as ozone protector in light colored vulcanizates;
- NiDMC acts as rubber-poison protector (via complex formation);
- EDTA acts as a copper protector;
- PCD protects the polymers against hydrolysis;
- DBTU provides some protection against ozone. Seldomly used as antidegradants, because their bloom is water soluble and because they affect the sulfur cure.

2.7 Summary of the literature survey and objective of this thesis

In the present chapter, the developments on long-term protection of rubber vulcanizates against aerobic aging have been reviewed. Although conventional antidegradants such as IPPD and 6PPD are still the most widely used antidegradants in the rubber industry, there is a trend and demand for longer-lasting and non-staining products as compared to conventional antidegradants. The relatively low molecular weight (MW) antioxidants have undergone an evolutionary change towards higher molecular weight products, with the objective to achieve permanence in the rubber polymer, without loss of antioxidant activity. In the last two decades, several directions have been taken in order to achieve this objective: attachment of hydrocarbon chains to conventional antioxidants in order to increase the MW and compatibility with the rubber matrix; oligomeric or polymeric antioxidants; and polymer bound or covulcanizable antioxidants. The disadvantage of polymer bound antioxidants was solved by grafting antioxidants onto low MW polysiloxanes, which are compatible with many polymers, or by grafting of paraphenylene diamine on low MW chlorinated polyisobutylene or paraffinic wax. New developments on antiozonants have focused on non-staining and slow migrating products, which last longer than conventional antidegradants in rubber compounds. Several new types of non-staining antiozonants have been developed, but none of them appeared to be as efficient as the chemically substituted p-phenylenediamines. The most prevalent approach to achieve non-staining ozone protection of rubber compounds is to use an inherently ozone-resistant, saturated backbone polymer in blends with a diene rubber. The disadvantage of this approach however, is the complicated mixing procedure needed to ensure that the required small polymer domain size is achieved. Additionally, inhomogeneous filler and curative distribution restrict this approach for practical use.

Based on the above described conclusions and on the fact that conventional antidegradants like IPPD and 6PPD are still the most widely used antidegradants today, it can be concluded that there is still a need for new antidegradants providing longer-term protection of rubber compounds as compared to conventional antidegradants. Furthermore, environmental issues and changes in legislation require improvement and maintenance of the physical properties of rubber vulcanizates during service.

The research described in this thesis focuses on the synthesis, screening and selection of potential long-lasting antidegradants, the determination of their migration behavior, the determination of their efficiency as antioxidant and/or antiozonant and their effect on other compounding ingredients. Evaluation is done in some typical passenger tire sidewall compounds and steelcord adhesion compounds. Long-term protection against ozone is vital for sidewall compounds and long-term protection against oxygen for steelcord adhesion skim compounds.

2.8 References

1. R.N. Datta, N.M. Huntink, RubberChem'01, Brussels, paper 5 (April 3-4, 2001).
2. J.R. Davies, *Plastics and Rubber International*, **11**, (1986), 16.
3. R.W. Keller, *Rubber Chem. Technol.*, **58**, (1985), 637.
4. B.L. Stuck, Technical Report, Sovereign Chemical Company, (Sept. 17, 1995).
5. J. Zhao, G.N. Ghebremeskel, *Rubber Chem. Technol.*, **74**, (2001), 409.
6. W.H. Waddel, *Rubber Chem. Technol.*, **71**, (1998), 590.
7. R.W. Layer, R.P. Lattimer, *Rubber Chem. Technol.*, **63**, (1990), 426.
8. D. Erhardt, *Int. Polym. Sci. Technol.*, **25**, (1998), 11.
9. S.K. Rakovski, D.R. Cherneva, *Int. J. Polym. Mater.*, **14**, (1990), 21.
10. G. Scott, *Rubber Chem. Technol.*, **58**, (1985), 269.
11. S.S. Solanky and R.P. Singh, *Prog. Rubber Plast. Technol.*, **17**, (2001), 13.
12. R.L. Gray, R.E. Lee, *Chem. Technol. Polym. Addit.*, (1999), 21.
13. J. C. Ambelang, R.H. Kline, O.M. Lorenz, C.R. Parks and C. Wadelin, *Rubber Chem. Technol.*, **36**, (1963), 1497.
14. J.L. Bolland, *Quart. Rev., Chem. Soc.*, **3**, (1949), 1.
15. J.R. Shelton and D.N. Vincent, *J. Am. Chem. Soc.*, **85**, (1963), 2433.
16. L. Bateman, M. Cain, T. Colclough, and J.I. Cunneen, *J. Chem. Soc.*, (1962), 3570.
17. J.T. Blake and P.L. Bruce, *Ind. Eng. Chem.*, **33**, (1941), 1198.
18. J.R. Shelton, *Rubber Chem. Technol.*, **30**, (1957), 1270
19. W.L. Hawkins and M.A. Worthington, *J. Polym. Sci., part A, Polym. Chem.*, **1**, (1963), 3489.
20. J.R. Shelton, *J. Appl. Polym. Sci.*, **2**, (1959), 345.
21. J.S. Dick, "Rubber Technology: compounding and testing for performance", Hanser Publishers, (2001), 453.
22. R.P. Brown, M.J. Forrest and G. Soulagnet, *Rapra Review Reports*, **10**, No. 2 (2000).
23. A.N. Gent, *J. Appl. Polym. Sci.*, **6**, (1962), 497.
24. D.J. Burlett, *Rubber Chem. Technol.*, **72**, (1999), 165.
25. N.C. Billingham, D.C. Bott and A.S. Manke, Applied Science Publishers, London, (1981), chap. 3.
26. D.I. Marshall, E. George, J.M. Turnipseed and J.L. Glenn, *Polym. Eng. Sci.*, **13**, (1973), 415.
27. H.E. Bair, *Polym. Eng. Sci.*, **13**, (1973), 435.
28. D.D. Parker, J.L. Koenig, ACS, *Poly. Mat. Sci and Eng.*, **76**, Conference proceedings, (1997), 193.
29. K. Kaluder, M. Andreis, T. Marinovic, Z. Veksli, *J. Elastomers Plast.*, **29**, No.4, (1997), 270.
30. G.N. Ghebremeskel, J.K. Sekinger, J.L. Hoffpaur, C. Hendrix, *Rubber Chem. Technol.* **69**, (1996), 874.

31. H. Lavabratt, E. Ostman, S. Persson, B. Stenberg, A.B. Skega, *J. Appl. Polym. Sci.*, **44**, No.1, (1992), 83.
32. D.K. Setua, *Polym. Degrad. Stab.*, **12**, No.2, (1985), 169.
33. P.S. Bailey, "Ozonation in organic chemistry", Volume 39.1, (1978), 3.
34. Thomson, *J. Soc. Chem. Ind.*, **4**, (1885), 710.
35. N.A. Shepard, S. Krall, H.L. Morris, *Ind. Eng. Chem.*, **18**, (1926), 615.
36. I. Williams, *Ind. Eng. Chem.*, **18**, (1926), 367.
37. C. Fabry, H. Buisson, *J. Phys. Radium*, **2**, No. 6, (1921), 197.
38. C. Fabry, H. Buisson, *Comptes Rendus Hebdomadaires des Séances de L'académie des Sciences*, **192**, (1931), 457.
39. A. van Rossem, H.W. Talen, *Kautschuk*, **7**, (1931), 115.
40. C. Dufraisse, *Rubber Chem. Technol.*, **6**, (1933), 157.
41. J.H. Seinfeld, *Science*, **243**, (1989), 745.
42. D. Bruck, *Kautsch. Gummi. Kunstst.*, **42**, No. 9, (1989), 76.
43. A.J. Haagen-Smit, M.F. Brunelle, and J.W. Haagen-Smit, *Rubber Chem. Technol.*, **32**, (1959), 1134.
44. Y. Saito, *Int. Polym. Sci. Technol.*, **22**, (1995), 47.
45. D. Bruck, H. Konigshofen, and L. Ruetz, *Rubber Chem. Technol.*, **58**, (1985), 728.
46. P.S. Bailey, "Ozonation in organic chemistry", Volume 39.1, (1978), 25.
47. K.W. Ho, *J. Polym. Sci.*, **24**, (1986), 2467.
48. S.D. Razumovskii, V.V. Podmasteriev, G.E. Zaikov, *Polym. Degrad. Stab.*, **20**, (1988), 37.
49. D. Barnard, *J. Chem. Soc.*, (1957), 4547.
50. F.R. Erickson, R.A. Berntsen, E.L. Hill, and P. Kusy, *Rubber Chem. Technol.*, **32**, (1959), 1062.
51. E.H. Andrews, M. Braden, *J. Polym. Sci.*, **55**, (1961), 787.
52. J.H. Gilbert, in "Proc. Rubber Technol. 4th Conf.", T.H. Messenger, Ed., *Instit. Rubber Ind.*, London, (1963), 696.
53. M. Braden, A.N. Gent, *J. Appl. Polym. Sci.*, **3**, (1960), 90.
54. M. Braden, A.N. Gent, *Rubber Chem. Technol.*, **35**, (1962), 200.
55. A. Cottin, G. Peyron, WO 200123464-A1, Michelin, (2001).
56. F. Cataldo, *Polym. Degrad. Stab.*, **72**, (2001), 287.
57. D.A. Lederer, M. Fath, *Rubber Chem. Technol.*, **54**, (1981), 415.
58. E.H. Andrews, *J. Appl. Polym. Sci.*, **10**, (1966), 47.
59. E.Z. Levit, T.E. Ognevskaya, B.N. Dedusenko, D.B. Boguslovskii, *Kauch. Rezina*, **5**, (1979), 14.
60. S.D. Razumovskii, L.S. Batashova, *Rubber Chem. Technol.* **43**, (1970), 1340.
61. M. Braden, *J. Appl. Polym. Sci.*, **6**, (1962), 86.
62. H.W. Engels, H. Hammer, D. Brück, W. Redetzky, *Rubber Chem. Technol.*, **62**, (1989), 609.
63. W. Hofmann, "Rubber Technology Handbook", Hanser Publishers, (1989), 273.

64. J.C. Andries, C.K. Rhee, R.W. Smith, D.B. Ross, H.E. Diem, *Rubber Chem. Technol.*, **52**, (1979), 823.
65. P.M. Lewes, *Polym. Degrad. Stab.*, **15**, (1986), 33.
66. E.H. Andrews and M. Braden, *J. Appl. Polym. Sci.*, **7**, (1963), 1003.
67. P.M. Mavrina, L.G. Angert, I.G. Anisimov, A.V. Melikova, *Soviet Rubber Technology* **31**, No. 12, (1972), 18.
68. R.P. Latimer, E.R. Hooser, R.W. Layer, C.K. Rhee, *Rubber Chem. Technol.*, **53**, (1980), 1170.
69. R.P. Latimer, E.R. Hooser, R.W. Layer, C.K. Rhee, *Rubber Chem. Technol.*, **56**, (1983), 431.
70. S.W. Hong, C-Y. Lin, *Rubber World*, (August 2000), 36.
71. S.W. Hong, P.K. Greene, C-Y. Lin, ACS Rubber Division 155th Conference, Chicago, IL, paper 65, (April 13-16, 1999).
72. ISO 1431-1 '89, Resistance to ozone under static strain, (1989).
73. ISO 1431-2 '82, Resistance to ozone under dynamic strain, (1982).
74. M.P. Anachkov, S.K. Rakovsky, S.D. Razumovskii, *Int. J. Polym. Mater.*, **14**, (1990), 79.
75. S.M. Kavun, Yu.M. Genkina, V.S. Filippov, *Kauch. Rezina*, **6**, (1995), 10.
76. P. Lehocky, L. Syrovy, S.M. Kavun, *RubberChem'01*, Brussels, paper 18, (April 3-4, 2001).
77. H.S. Dweik and G. Scott, *Rubber Chem. Technol.*, **57**, (1984), 735.
78. S.W. Hong, *Elastomer*, **34**, No. 2, (1999), 156.
79. US Food and Drug Administration, Code of Federal Regulations, **21**, (1995).
80. G. Scott, ACS Symposium Series, 280 (P. Klemschuk, ed.), ACS Rubber Div. Meeting, Washington DC, (1985), 173.
81. R.K. Kimwomi, G. Kossmehl, E.B. Zeinalov, P.M. Gitu, B.P. Bhatt, *Macromol. Chem. Phys.*, **202**, No. 13, (2001), 2790.
82. S. Avirah, M.I. Geetha, R. J. Cochin, Kottayam, *Kautsch. Gummi Kunstst.*, **49**, No. 12, (1996), 831.
83. F. Ignatz-Hoover, O. Maender, R. Lohr, *Rubber world*, **218**, No. 2, (1998), 38.
84. A. Meghea, M. Giurginca, *Polym. Degrad. Stab.*, **73**, (2001), 481.
85. R.L. Gray, R.E. Lee, C. Neri, *Polyolefins X*, Int. Conf., Houston, (Feb. 23-26, 1997), 599.
86. E. Roos (To Bayer AG), U.S. 3,211,793 (1965).
87. J.J. D'Amico and S.T. Webster (to Monsanto Co.), U.S. 3,668,245 (1972).
88. M.E. Cain, G.T. Knight, P.M. Lewis, B. Saville, *J. Rubber Res. Inst. Malaysia*, **22**, (1969), 289.
89. K.W. Sirimevan Kularatne, G. Scott, *Eur. Poly. J.*, **4**, (1978), 835.
90. S. Avirah, R. Joseph, *Angew. Makromol. Chem.*, **1**, (1991), 193.
91. F. Gratani, *Polypropylene '93: MBS conference*, Zurich, (Oct. 26-27, 1993).
92. P.B. Sulekha, R. Joseph, K.E. George, *Polym. Degrad. Stab.*, **63**, (1999), 225.
93. P.B. Sulekha, R. Joseph, S. Prathapan, *J. Appl. Polym. Sci.*, **81**, (2001), 2183.
94. P.B. Sulekha, R. Joseph, K.N. Madhusoodanan, K.T. Thomas, *Polym. Degrad. Stab.*, **77**, (2002), 403.

95. P.B. Sulekha, R. Joseph, *Plastics, Rubber and Composites*, **31**, (2002), 1.
96. K.L. Rollick, J.G. Gillick, J.L. Bush, J.A. Kuczkowski, paper 52, ACS Rubber Div. Meeting, Cincinnati, Ohio (Oct. 18-21, 1988).
97. K. Fujiwara and T. Ueno, *Int. Polym. Sci. Technol.*, **18**, (1991), 36.
98. K.L. Rollick, J.G. Gillick, J.A. Kuczkowski (to The Goodyear Tire & Rubber Co.), U.S. 5,019,611 (May 28, 1991).
99. G. Ivan, M. Giurginca, J.M. Herdan, *Int. J. Polym. Mater.*, **18**, (1992), 87.
100. E.L. Wheeler, paper 73, ACS Rubber Div. Meeting, Detroit, Michigan, (Oct. 17-20, 1989).
101. S.W. Hong, paper 72, ACS Rubber Div. Meeting, Detroit, Michigan, (Oct. 17-20, 1989).
102. D.A. Birdsall, S.W. Hong, D.j. Hajdasz, Tyretech '91 Conf. Proc., Berlin, Germany, (Oct. 24-25, 1991), 108.
103. S.W. Hong, M.P. Ferrandio, ACS Rubber Div. Meeting, Cleveland Ohio, (Oct. 1997).
104. M. Ogawa, Y. Shiomura, T. Takizawa (to Bridgestone Corporation), U.S. 4,801,641 (Jan. 31, 1989).
105. M. Ogawa, Y. Shiomura, T. Takizawa (to Bridgestone Corporation), U.S. 4,886,850 (Dec. 12, 1989).
106. S.W. Hong, *Rubber Plast. News*, (December 25, 1989), 14.
107. A.J.M. Sumner, H. Fries, *Kautsch. Gummi Kunstst.*, **45**, (1992), 558.
108. G.W. Marwede, B. Stollfuss, A.J.M. Sumner, *Kautsch. Gummi Kunstst.*, **46**, (1993), 380.
109. G.W. Marwede, B. Stollfuss, A.J.M. Sumner, *Plastics and Rubber Weekly*, **1471**, (Feb. 1993), 10.
110. W. Hellens, paper 23, ACS Rubber Div. Meeting, Nashville, (Nov. 3-6, 1992).
111. A.J.M. Sumner, H. Fries, Tyretech '91, Berlin, (Oct. 24-25, 1991), 102.
112. A.J.M. Sumner, paper 37, ACS Rubber Div. Meeting, Detroit, Michigan, (Oct. 17-20, 1989).
113. W. Hellens, paper 40, ACS Rubber Div. Meeting, Detroit, Michigan, (Oct. 17-20, 1989).
114. W. Hellens, D.C. Edwards, Z.J. Lobos, *Rubber Plastic News*, (Oct., 1990), 61.
115. J.R. Dunn, D.C. Edwards, *Industria della Gomma*, **30**, No. 1, (Jan. 1986), 18.
116. W. Hellens, S.A.H. Mohammed, R. Hallman, to Polysar Ltd., US 4,645,793 (Feb. 24, 1987).
117. D.C. Edwards, J.A. Crossman, to Polysar Ltd., US 4,588,780 (May 13, 1986).
118. G.C. Blackshaw, I.M. Kristensen, *J. Elastomers Plast.*, **7**, No. 3, (1975), 215.
119. W. Warrach, D. Tsou, *Rubber Plast. News*, (June 4, 1984), 18.
120. R.N. Datta, F. Ignatz-Hoover, P. Ebell, *Kautschukchemikalien*, GAK 7/2000 – Jahrgang **53**.
121. F. Ignatz-Hoover, R.N. Datta, *Rubber World*, (August 2000), 43.
122. R.N. Datta, N.M. Huntink, A.G. Talma, paper #14A, presented at the ITEC'02, Akron Ohio, (Sept. 10-12, 2002).
123. R.N. Datta, A.G. Talma (to Flexsys), WO 01/68761 A1 (2001).

Chapter 3

Synthesis and characterization of potential long-lasting antidegradants

The outline of the synthesis of several potential long lasting antidegradants is described in the current chapter. Slow-diffusion (high molecular weight) antidegradants were prepared by addition of 4-amino-diphenylamine (4-ADPA) and/or N-(1,3-dimethylbutyl)-N'-phenyl-p-phenylenediamine (6PPD) onto different chemical groups by exploiting various kinds of chemistry: salt formation, Michael addition, Mannich reactions, nucleophilic substitution, amide formation and formation of disubstituted ureas. These expected slow-diffusion antidegradants were synthesized, because they were expected to last longer in rubber than conventional antidegradants like 6PPD and N-isopropyl-N'-phenyl-p-phenylenediamine (IPPD). The syntheses appeared to be straightforward. However, purification of the final products was complicated. Purification by distillation was not possible due to the relatively high molecular weight of the antidegradants. While purifying by washing, a relatively large amount of the synthesized antidegradants is lost due to the small difference in polarity between that of the raw materials and final product. No attempts were made to optimize the syntheses because only small amounts of sample were needed for evaluation in the context of this thesis.

The structures and purities of the products synthesized were confirmed by $^1\text{H-NMR}$ and $^{13}\text{C-NMR}$. Special attention was paid to the characterization of PPD-C18, the most promising antidegradant according to the results described later in Chapter 5. It was demonstrated by DOSY $^1\text{H-NMR}$ (diffusion ordered spectroscopy) that the salt prepared from 6PPD and stearic acid appears to be a complex, when analyzed in the melt. However, the salt seems to be a rather weak complex that decomposes into a mixture of 6PPD and stearic acid, when analyzed in a solvent.

3.1 Introduction

Although conventional antidegradants for rubbers such as 6PPD (N-(1,3-dimethylbutyl)-N'-phenyl-p-phenylenediamine) and IPPD (N-isopropyl-N'-phenyl-p-phenylenediamine) provide protection against oxygen and ozone, this protection is of short duration. As mentioned in Chapter 2, there is still a need for new antidegradants providing longer-term protection of rubber compounds as compared to conventional antidegradants.

Longer-term protection requires a different class of antidegradants. Long-lasting antioxidants must be polymer bound or must have a lower volatility and leachability than conventional antioxidants, whereas long-lasting antiozonants must have a lower migration rate than the conventional antiozonants. In order to pursue long-lasting antioxidants and antiozonants, several concepts were developed for high molecular weight antidegradants based on 4-ADPA and 6PPD as the original molecules. Since most of these chemicals were not commercially available, they had to be synthesized. The synthesis and characterization of these potential antidegradants, is described in the current chapter.

3.2 Experimental

3.2.1 Materials

For the syntheses the following chemicals were used: methanol (J.T. Baker, assay min. 99.8%; CAS nr. [67-56-1]); ethanol (J.T. Baker, assay min. 99.9%; CAS nr. [64-17-5]); toluene (J.T. Baker, assay min. 99.5%; CAS nr. [108-88-3]); chloroform (J.T. Baker, assay min. 99.8%; CAS nr. [67-66-3]); dichloromethane (J.T. Baker, assay min. 99.5%; CAS nr. [75-09-2]); tetrahydrofuran (Janssen, assay min. 99.5%; CAS nr. [109-99-9]); dimethyl formamide (Janssen, assay min. 99%; CAS nr. [68-12-2]); formaldehyde (Janssen; 37wt% solution in water; CAS nr. [50-00-0]); stearic acid (J.T. Baker; CAS nr. [57-11-4]); fumaric acid (Janssen, assay min. 99%; CAS nr. [110-17-8]); phthalic acid (Janssen, assay min. 99%; CAS nr. [88-99-3]); succinic acid (Janssen, assay min. 99%; CAS nr. [110-15-6]); tartaric acid (Janssen, assay min. 99%; CAS nr. [87-69-4]); acetic acid (Janssen, assay min. 99.5%; CAS nr. [64-19-7]); heptanoic acid (Janssen, assay min. 98%; CAS nr. [111-14-8]); benzoic acid (Janssen, assay min. 99%; CAS nr. [65-85-0]); methane sulfonic acid (Across, assay min. 99%; CAS nr. [75-75-2]); adipic acid (Janssen, assay min. 99%; CAS nr. [124-04-9]); maleic acid (Janssen, assay min. 99%; CAS nr. [110-16-7]); toluene diisocyanate (Aldrich, assay min. 96%; CAS nr. [584-84-9]); N-phenylmaleimid (Janssen, assay min. 97%; CAS nr. [941-69-5]); benzoin (Janssen, assay min. 98%; CAS nr. [579-44-2]); HCl (Janssen, assay min. 37%; CAS nr. [7647-01-0]); chalcone (Across, assay min. 97%; CAS nr. [94-41-7]); acrylic acid (Janssen, assay min. 99%; CAS nr. [79-10-7]); 1,4-Diazabicyclo[2,2,2]octane (DABCO; Across, assay min. 97%; CAS nr. [280-57-9]); 2,2'-dithiobenzoyl dichloride (Fluka, assay min. 98%; CAS nr. [19602-82-5]); (1-bromoethyl)benzene (Janssen, assay min. 97%; CAS nr. [585-71-7]); 3,3'-dithiopropionyl dichloride (Fluka, assay min. 98%; CAS nr. [1002-18-2]); sodium hydroxide (Janssen, assay min. 98%; CAS nr. [1310-73-2]); triethanol amine (TEA; Janssen, assay min. 97%; CAS nr. [102-71-6]); crotonic acid (Janssen, assay min. 98%; CAS nr. [3724-65-0]); thionylchloride (Janssen, assay min. 99.6%; CAS nr. [7719-09-7]); sodium borohydride (Baker, assay min. 99%; CAS nr. [16940-66-2]); ammoniumchloride (Janssen, assay min. 99%; CAS nr. [12125-02-9]);

ethylacetate (Janssen, assay min. 99.5%; CAS nr. [141-78-6]); phenoxy ethanol (Janssen, assay min. 99%; CAS nr. [122-99-6]); Aniline (Janssen, assay min. 99.8%; CAS nr. [62-53-3]); 2,5-hexane dione (Janssen, assay min. 97%; CAS nr. [110-13-4]); 3,5-di-*t*-butyl-4-hydroxy benzaldehyde (Janssen, assay min. 97%; CAS nr. [68-12-2]); 2,6-di-*t*-butylphenol (Janssen, assay min. 99%; CAS nr. [128-39-2]).

3.2.2 Characterization of the products

The characterization of the synthesized products was carried out by using the following techniques:

FTIR

FTIR-measurements were performed on a Perkin Elmer Spectrum 2000 equipped with a Golden Gate Diamond ATR (Attenuated Total Reflection) probe.

¹H-NMR and ¹³C-NMR spectroscopy

The antidegradants were dissolved in deuterated chloroform (Aldrich, 99.8 atom-% D; CAS nr. [865-49-6]) or in Dimethyl sulfoxide (DMSO) (Janssen, 99.96 atom-% D; CAS nr. [865-49-6]). ¹H-NMR and ¹³C-NMR measurements were performed on a Varian Inova – 400 MHz (Varian) model L 700 spectrometer.

DOSY ¹H-NMR spectroscopy¹

The existence of a complex between 6PPD and different carboxylic acids was determined by Diffusion Ordered Spectroscopy (DOSY) ¹H-NMR. This two-dimensional spectroscopic technique can differentiate between products having similar chemical shifts in a NMR spectrum but different molecular weights. This technique is based on differences in diffusion or mobility: see fig. 3.1. Lower molecular weight products are more mobile than those with a higher molecular weight and generate signals at higher values on the y-axis of the two-dimensional ¹H-NMR spectra. Samples were analyzed both in the melt and after dissolving in deuterated chloroform. Measurements were performed on a Varian Inova – 400 MHz (Varian) model L 700 spectrometer.

DSC-measurements

DSC measurements were performed on a Mettler DSC 820.

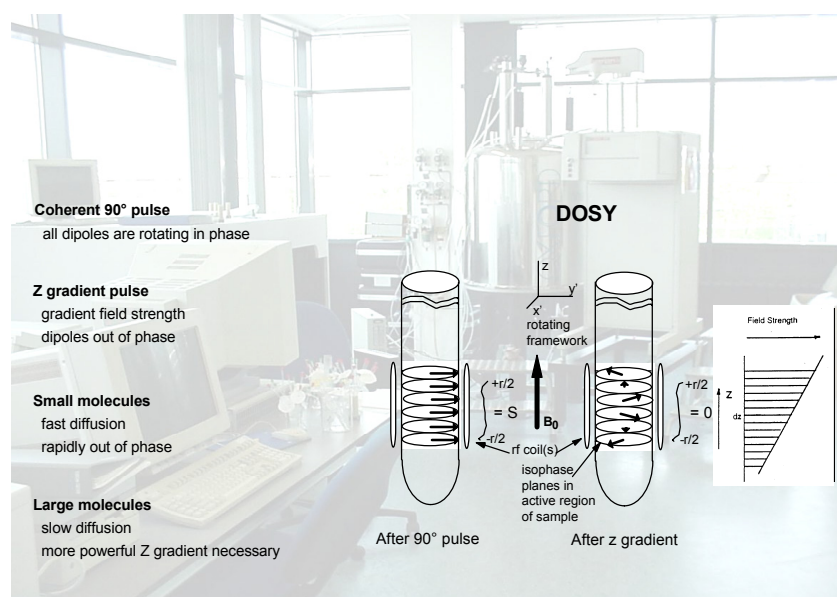


Fig. 3.1: Principle of Diffusion Ordered Spectroscopy (DOSY).
(S = spin; r = region; B₀ = applied magnetic field)

3.3 Synthesis and characterization of antidegradants

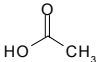
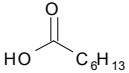
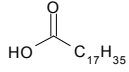
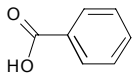
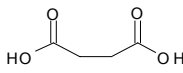
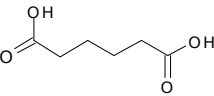
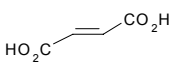
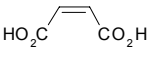
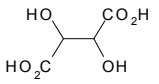
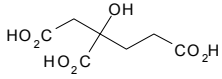
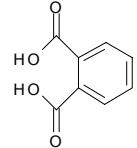
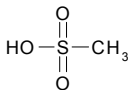
Salts of 6PPD and carboxylic acids:

PPD-C18 (stearic acid), PPD-FA (fumaric acid), PPD-PA (phthalic acid), PPD-SA (succinic acid), PPD-TA (tartaric acid), PPD-AA (acetic acid), PPD-HA (heptanoic acid), PPD-BA (benzoic acid), PPD-MSA (methyl sulfonic acid) and PPD-ADA (adipic acid) were synthesized by melting PPD and an equimolar amount of the corresponding acid under continuously stirring for 120 min. or by refluxing in methanol for two hours. Crystallization of the reaction products resulted in a yield between 95 and 100%. Identification was done by DSC. The presence of only one melting peak indicated that the salts were completely formed.

Special attention was paid to the characterization of PPD-C18, the most promising antidegradant according to the results described later in Chapter 5. This product was identified by FTIR: disappearance of the NH vibration between 3370 and 3390cm⁻¹; see fig. 3.2; and by DOSY ¹H-NMR. It is clear from the spectra plotted in fig. 3.3 that the proton signals for both the stearic acid part (1.2-2.6 ppm) and the 6PPD part (7.0-7.6 ppm) of PPD-C18 are located at approximately the same level on the y-axis of the DOSY ¹H-NMR spectra. The proton signals of the methylester of stearic acid are positioned at a higher level, at lower molecular weight on the y-axis. These facts indicate that PPD-C18 is present as a complex rather than as a mixture of 6PPD and stearic acid. However, the salt seems to be a rather weak complex, that easily decomposes into a mixture of 6PPD and stearic acid when analyzed in a solvent.

Salts were prepared from carboxylic acids having different pKa values in order to find out if this has an effect on the stability and migration characteristics of the complexes. The structures and the pKa values of the different acids used in these syntheses are listed in Table 3.1.

Table 3.1: Structure and pKa values of different acids used for the synthesis of the 6PPD-salts.²

| Abbrev. | Chemical name | Structure | pKa |
|---------|-----------------------|---|--------------------|
| AA | Acetic acid |  | 4.75 |
| HA | Heptanoic acid |  | 4.89 |
| C18 | Stearic acid |  | 5.00 |
| BA | Benzoic acid |  | 4.19 |
| SA | Succinic acid |  | 4.16 - 5.61 |
| ADA | Adipic acid |  | 4.43 - 4.41 |
| FA | Fumaric acid |  | 3.03 - 4.44 |
| MA | Maleic acid |  | 1.83 - 6.07 |
| TA | Tartaric acid |  | 2.98 - 4.34 |
| CA | Citric acid |  | 3.14 - 5.95 - 6.39 |
| PA | Phtalic acid |  | 2.89 - 5.51 |
| MSA | Methane sulfonic acid |  | -2.00 |

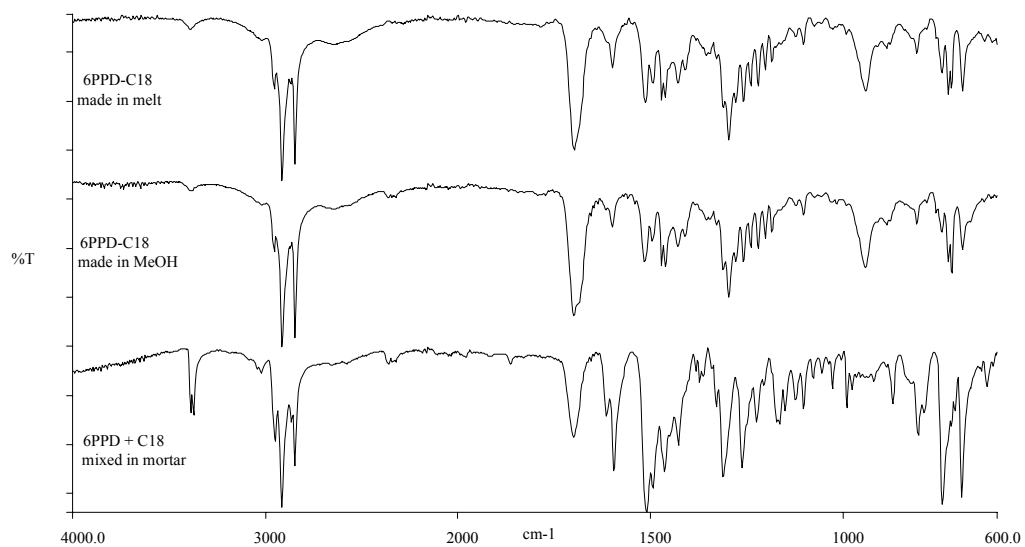


Fig. 3.2: FTIR spectrum of PPD-C18 prepared in different ways.

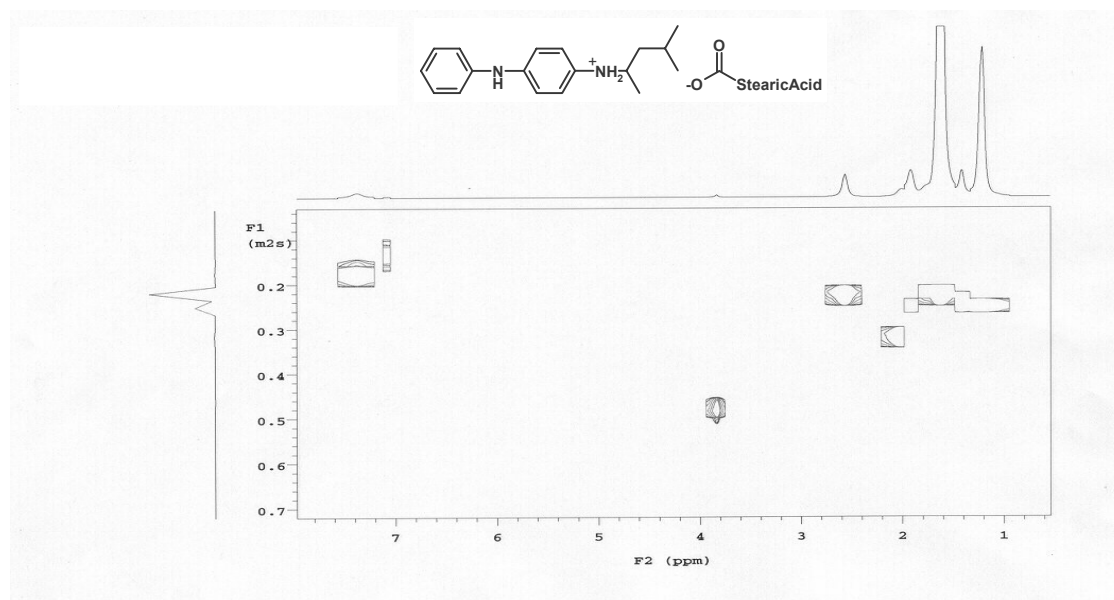


Fig. 3.3: DOSY-¹H-NMR spectrum of PPD-C18 determined in the melt.

4Asi-Ph (1-Phenyl-3-(4-(phenylamino)phenylamino)pyrrolidine-2,5-dione):

4Asi-Ph was synthesized by reaction of 4-phenylamino diphenylamine (4-ADPA) and N-phenylmaleimid. 30.6g 4-ADPA, 34.6g N-phenylmaleimid and 100ml toluene were refluxed for 1 hour. The reaction product was filtered and washed two times with 50ml toluene. The filtrate was dried overnight in a vacuum oven at 50°C. The yield was 32%. The purity of >98% was estimated by ¹H-NMR: see fig. 3.4.

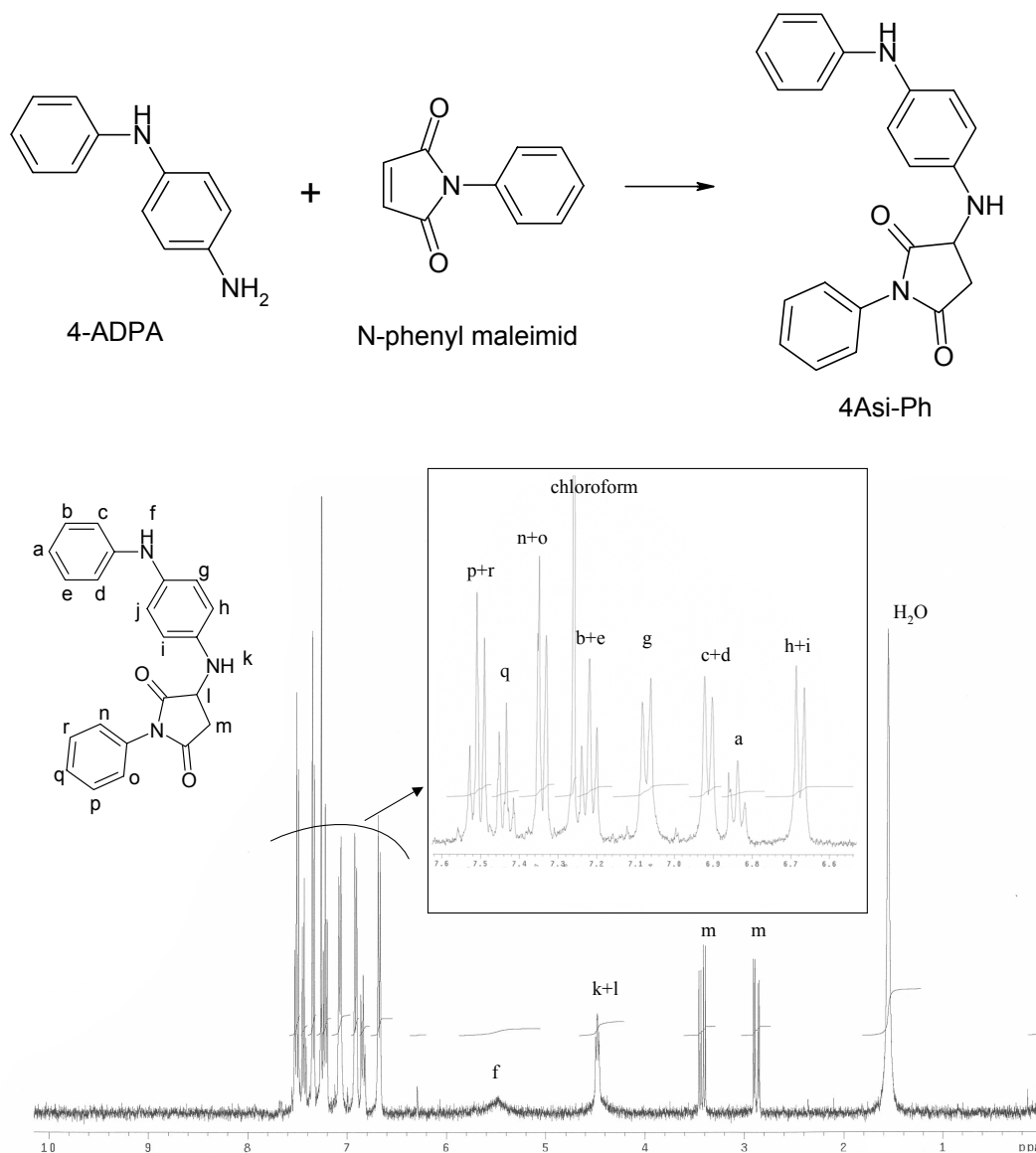


Fig. 3.4: ¹H-NMR spectrum of 4Asi-Ph determined in deuterated chloroform.
 δ : 2.88 + 3.43 (m); 4.49 (k + l); 5.48 (f); 6.68 (h + i); 6.84 (a);
 6.92 (c + d); 7.07 (g); 7.23 (b + e); 7.35 (n + o); 7.44 (q); 7.51 (p + r).

ADPA-B (N, N Phenyl benzoyl-N-Phenyl paraphenylenediamine):

ADPA-B was synthesized by condensation of 4-ADPA and benzoin. 20g 4-ADPA, 23g benzoin, 0.5g concentrated HCl and 200ml toluene were refluxed overnight using a 500ml round bottom flask equipped with a Dean Stark framework. The toluene was evaporated using a rotavapor. The reaction product was recrystallized in methanol, filtered after standing overnight and subsequently dried using a rotavapor. The yield was 65%. The reaction product was analyzed by $^1\text{H-NMR}$ and DSC (melting point 110°C , no decomposition below 220°C). The purity of 96% was estimated by $^1\text{H-NMR}$: see fig. 3.5.

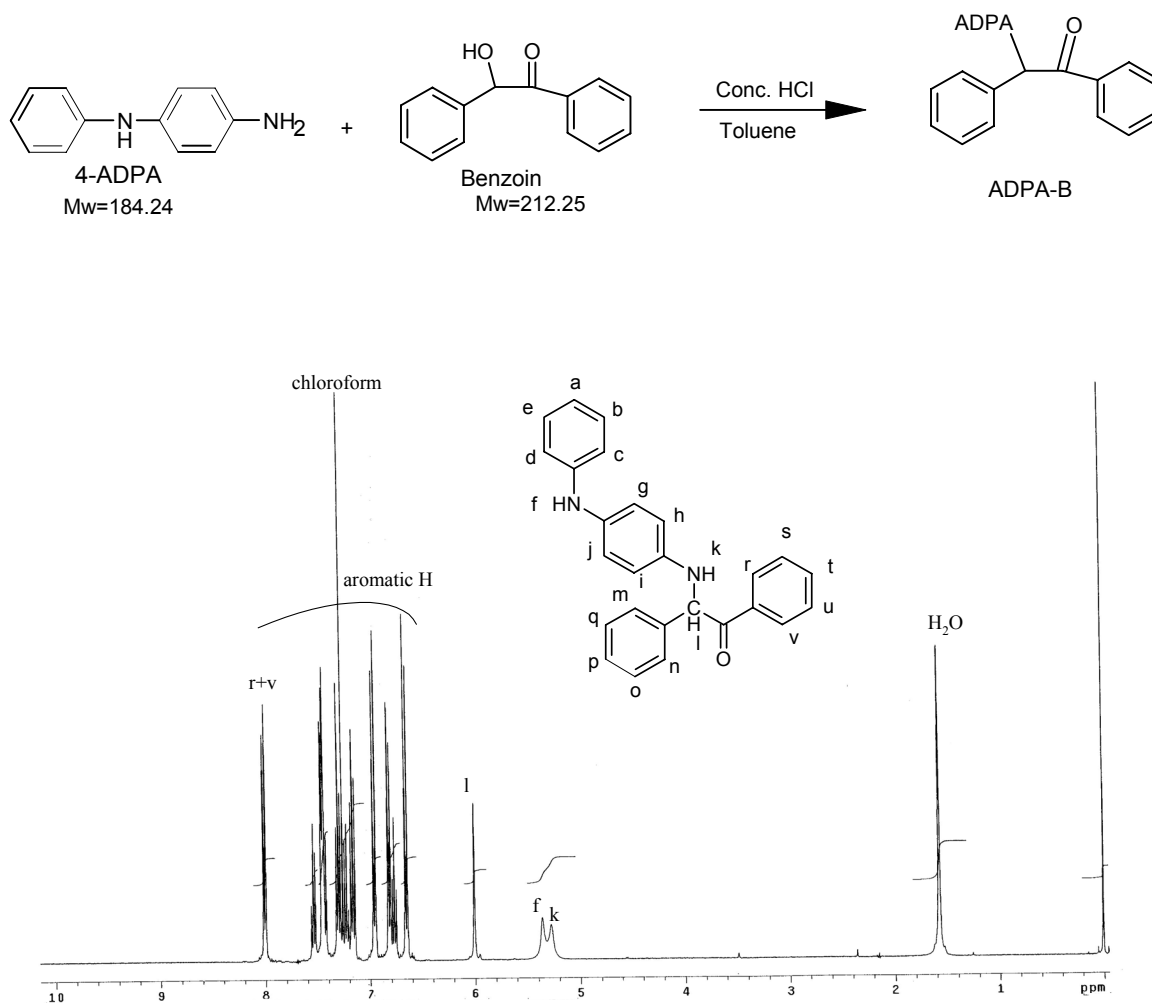


Fig. 3.5: $^1\text{H-NMR}$ spectrum of ADPA-B determined in deuterated chloroform.
 δ : 5.29 (k); 5.38 (f); 6.01 (f); 6.62 – 8.02 (aromatic H); 8.02 (r + v).

ADPA-C (N, N Phenyl methylene benzoyl-N-Phenyl paraphenylenediamine):

ADPA-C was synthesized via a Michael addition³ of 4-ADPA and Chalcone in methanol, with 1,4-diazabicyclo [2,2,2] octane DABCO as a catalyst.⁴ 5g, 0.0271 Mole 4-ADPA, 5.65g, 0.0271 mole Chalcone and 200mg DABCO were dissolved in 25ml methanol using a 100ml three-necked flask and stirred for 48 hours at room temperature. The reaction product was washed with methanol and dried on a rotavapor. The yield was 80%. The reaction product was analyzed by NMR, DSC and FTIR. The purity of 95% was estimated by ¹H-NMR: see fig. 3.6.

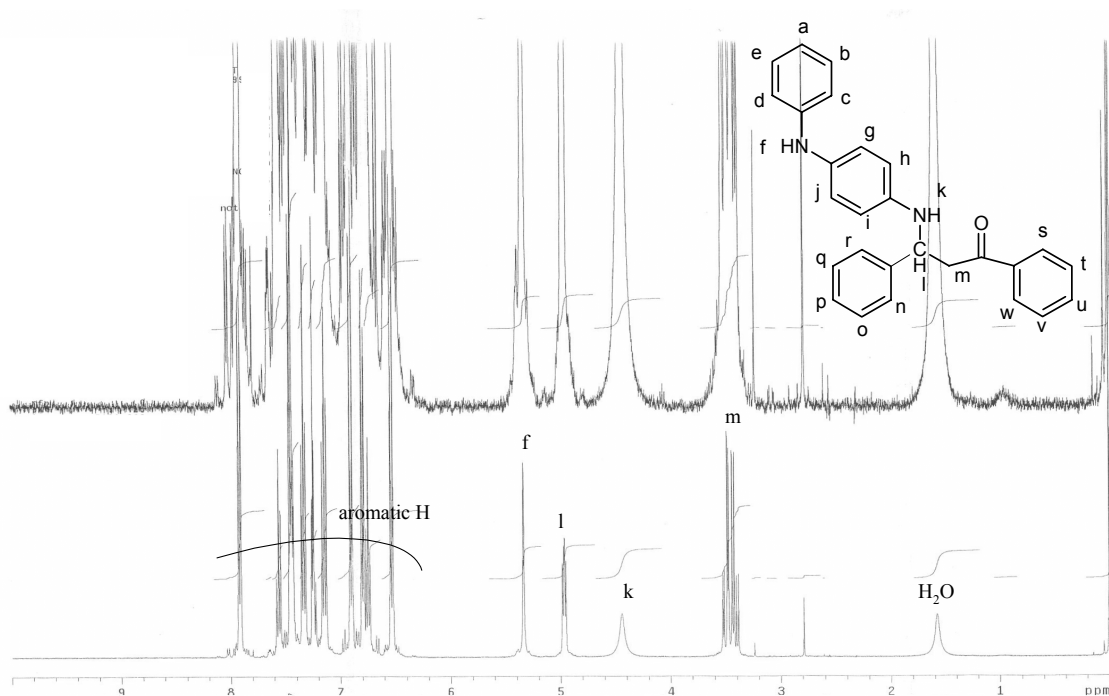
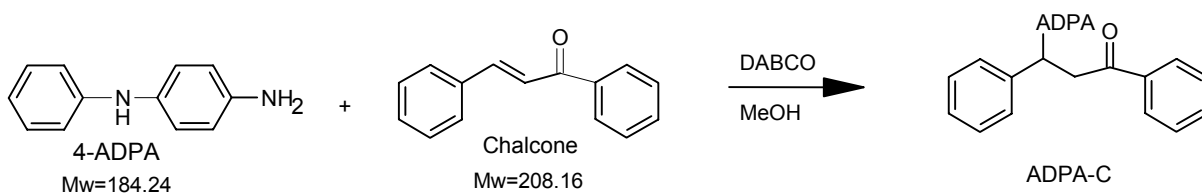


Fig. 3.6: ¹H-NMR spectrum of ADPA-C determined in deuterated chloroform.
 δ : 3.49 (m); 4.43 (k); 4.98 (l); 5.38 (f); 6.48 – 8.05 (aromatic H).

SPPD (N-Phenyl-N'-(1-phenylethyl)-1,4-benzenediamine):

SPPD was synthesized by reaction of 4-ADPA and (1-Bromoethyl)benzene, using TEA (triethanolamine) as a catalyst. 25g, 0.1357 Mole 4-ADPA, 25.11g, 0.1357 mole (1-Bromoethyl)benzene, 15g, 0.073 mole TEA and 200ml toluene were refluxed for 7 hours in a three-necked flask. The reaction product was filtered after standing overnight at room temperature. The filtrate was analyzed by GC, showing approximately 70% SPPD and 10% ADPA. The filtrate was dried and subsequently dissolved in dichloromethane, washed with water and dried on a rotavapor. The filtrate was purified on a silica column using toluene (100%) as the mobile phase. This resulted in a yield of 43%. The purity of 97% was estimated by $^1\text{H-NMR}$: see fig. 3.7.

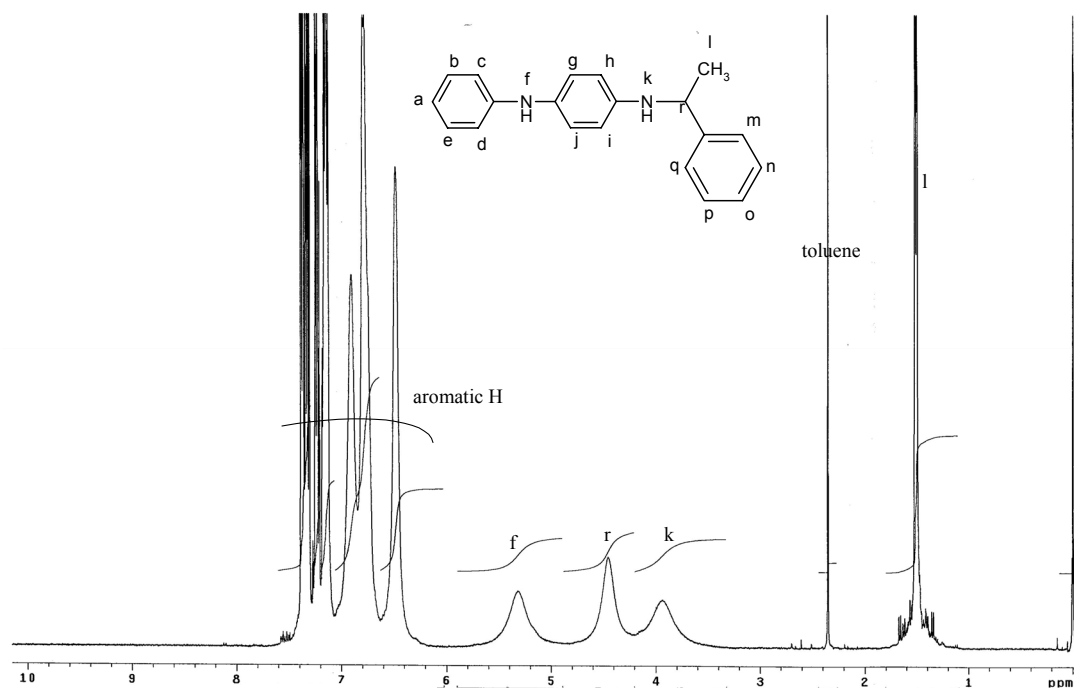
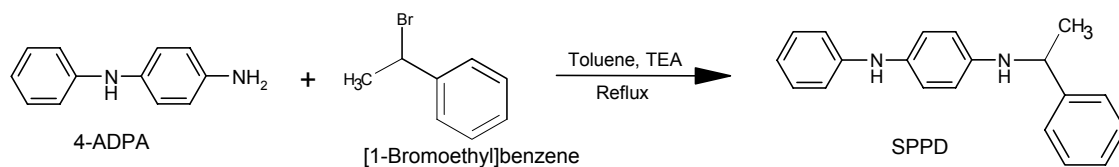
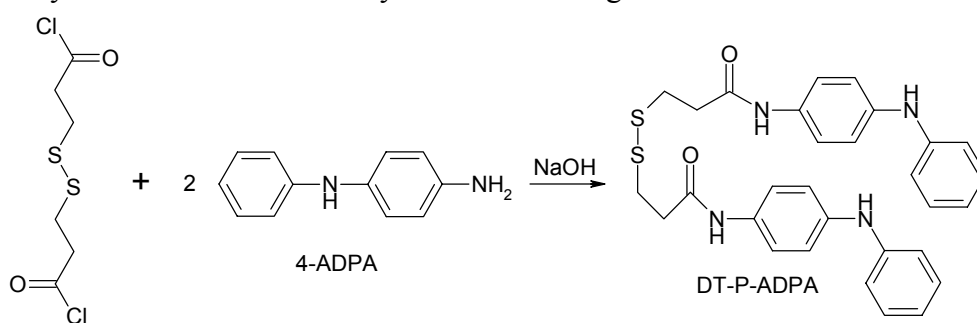


Fig. 3.7: $^1\text{H-NMR}$ spectrum of SPPD determined in deuterated chloroform.
 δ : 1.51 (l); 3.97 (k); 4.48 (r); 5.37 (f); 6.25 – 7.59 (aromatic H).

DT-P-ADPA (3,3'-Dithiobis(4-phenylaminophenyl)propanamide):

DT-P-ADPA was synthesized by reaction of 3,3'-dithiopropionyl dichloride and 4-ADPA to give the aminoamide HCl-salt, which was neutralized by sodium hydroxide to give the desired compound. 50.13g, 0.2 Mole 3,3'-dithiopropionyl dichloride was dissolved in 400ml methylene chloride. 73.69g, 0.4 mole 4-ADPA in 80 ml methylene chloride was added in 40 minutes at a temperature of 40°C. The mixture was stirred for 30 minutes at 40°C. 53.3g, 0.4 Mole NaOH and 50ml water were added in order to neutralize the salt. The filtrate was washed three times with 40ml water and subsequently dried under vacuum at 17mm Hg and 50°C. The yield was 78%. The reaction product was analyzed by FTIR, ¹H-NMR and ¹³C-NMR. The purity of 94% was estimated by ¹H-NMR: see fig. 3.8.



3,3'-Dithiodipropionyl dichloride

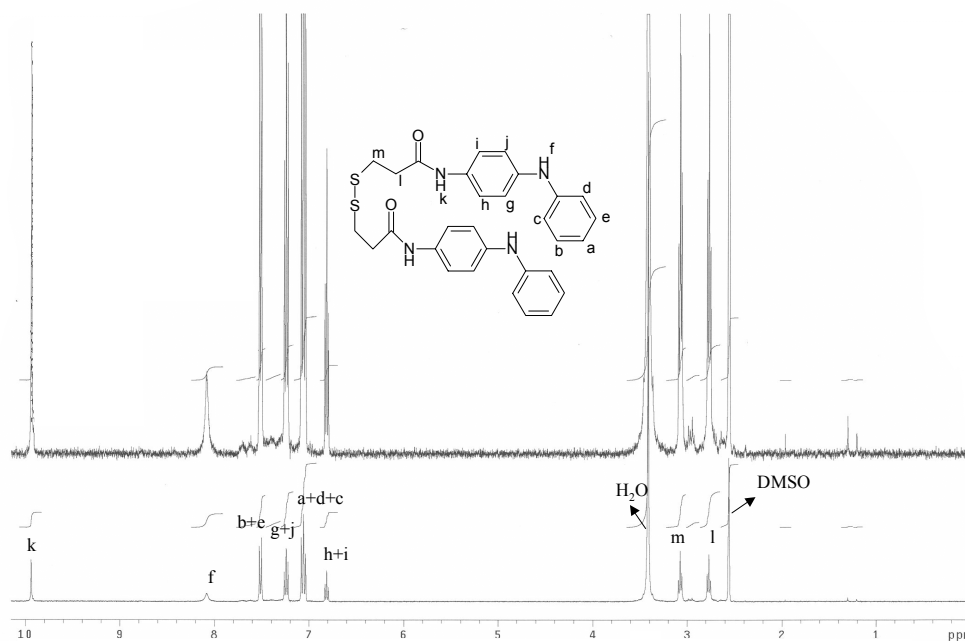


Fig. 3.8: ¹H-NMR spectrum of DT-P-ADPA determined in DMSO.
 δ : 2.77 (l); 3.08 (m); 6.81 (h + i); 7.05 (a + d + c); 7.26 (g + j);
 7.54 (b + e); 8.09 (f); 9.92 (k).

DT-S-ADPA (2,2'-Dithiobis(phenylaminophenyl)benzamide):

DT-S-ADPA was synthesized by reaction of 2,2'-dithiobenzoyl dichloride and 4-ADPA to give the aminoamide HCl-salt, which was neutralized by sodium hydroxide to produce the desired substance. 69.33g, 0.2 Mole 2,2'-dithiobenzoyl dichloride was dissolved in 400ml methylene chloride. 73.69g, 0.4 Mole 4-ADPA in 80 ml methylene chloride was added in 40 minutes at a temperature of 40°C. The mixture was stirred for 30 minutes at 40°C. 53.3g, 0.4 Mole NaOH and 50ml water were added in order to neutralize the salt. The filtrate was washed three times with 40ml water and subsequently dried under vacuum at 17mm Hg and 50°C. The yield was 73%. The reaction product was analyzed by FTIR, ¹H-NMR and ¹³C-NMR. The purity of 95% was estimated by ¹H-NMR: see fig. 3.9.

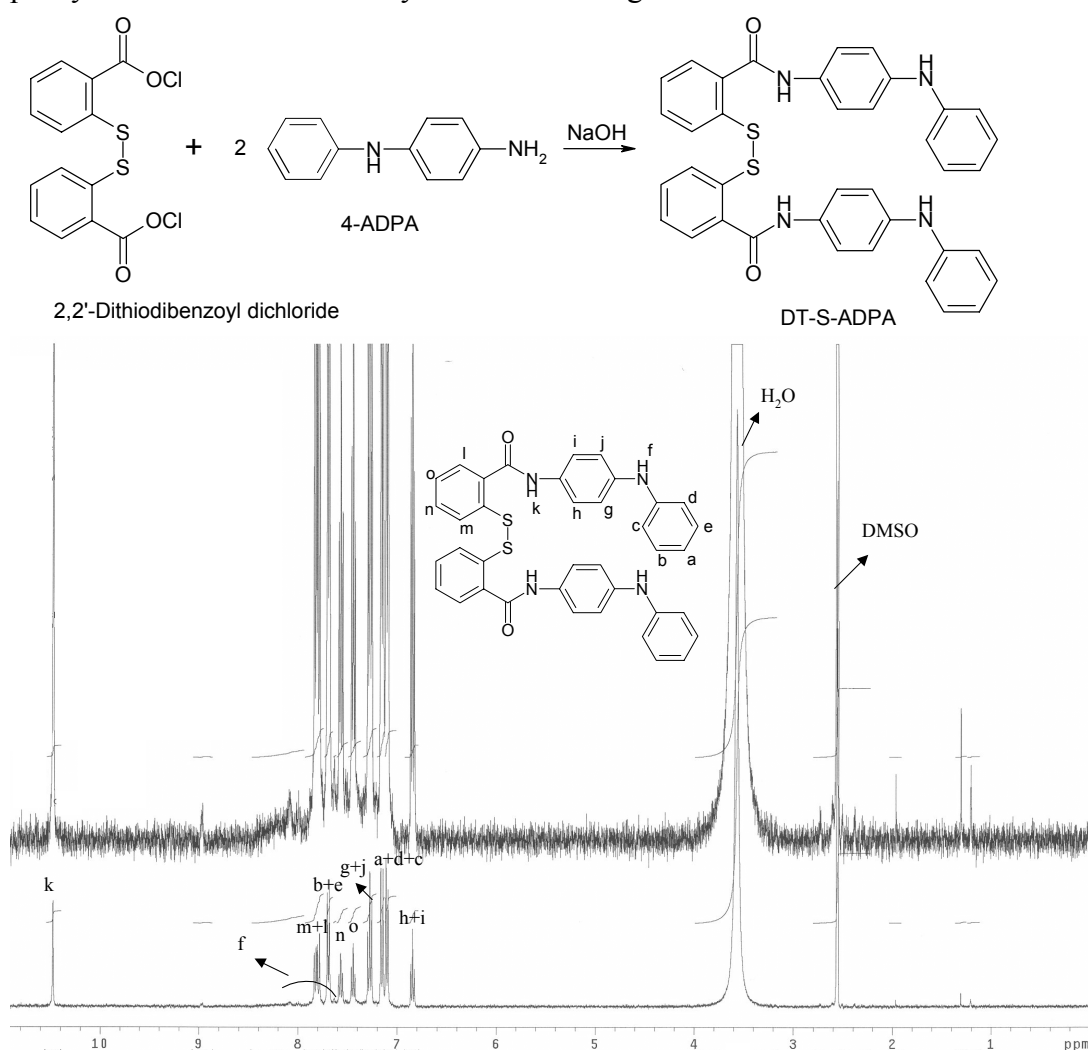
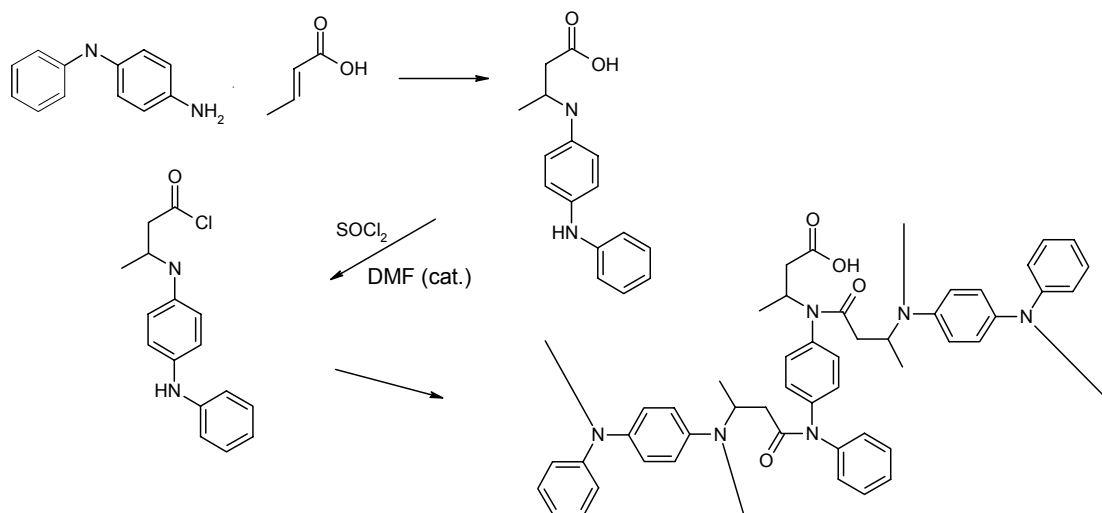


Fig. 3.9: ¹H-NMR spectrum of DT-S-ADPA determined in DMSO.
 δ : 6.83 (h + i); 7.14 (a + d + c); 7.28 (g + j); 7.44 (o); 7.59 (n);
 7.70 (b + e); 7.79 (m + l); 7.60 – 8.20 (f); 10.49 (k).

ADPA-pol (3-(4-Phenylamino)phenylamino butanoic acid, polymer):

ADPA-pol was synthesized by the chlorination of 3-((4-phenylamino)phenylamino)butanoic acid. 10g, 0.0542 Mole 4-ADPA, 4.66g, 0.0542 mole crotonic acid and 400mg DABCO were dissolved in 50ml methanol using a 250ml three-necked flask and stirred for 48 hours at room temperature (Michael addition reaction).⁵ The reaction product, which was formed via the Michael addition reaction was washed with methanol and dried on a rotavapor. 12.90g, 0.0476 Mole of the reaction product 3-((4-phenylamino)phenylamino)butanoic acid and 5 drops dimethylformamide (DMF) were dissolved in 150 ml thionylchloride and refluxed for 2 hours using a 500 ml round bottom flask. Some gas formation was observed in the beginning of the reaction, which disappeared after 15 to 30 minutes. The reaction product was washed with THF and dried on a rotavapor. The acid chloride, which was formed during the reaction of the acid with thionylchloride, reacted immediately with the amines present in the system to form the described polymer. The yield was 81%. Unfortunately, ADPA-pol was not soluble in any deuterated solvent and could therefore not be analyzed by ¹H-NMR.



ADPA-Bred (1,2-Diphenyl-2-(4-(phenylamino)phenylamino)ethanol):

ADPA-Bred was synthesized by reduction of ADPA-B with sodium borohydride (NaBH_4).⁶ 15g, 0.0396 Mole ADPA-B was dissolved in 250ml ethanol. 1.5g, 0.0396 Mole NaBH_4 was added at room temperature in 10 minutes. A clear brown solution was obtained after stirring for one hour. The mixture was stirred for another hour. Next, ammoniumchloride dissolved in water was added. The organic layer was separated, dissolved in dichloromethane, washed with water and dried on a rotavapor. The yield was 99% of a yellow to brown solid. The reaction product was purified on a silica column, using toluene/ethylacetate (95/5) as the mobile phase. The final yield was 42%. The product was analyzed by DSC, FTIR and $^1\text{H-NMR}$. The purity of 92% was estimated by $^1\text{H-NMR}$: see fig. 3.10.

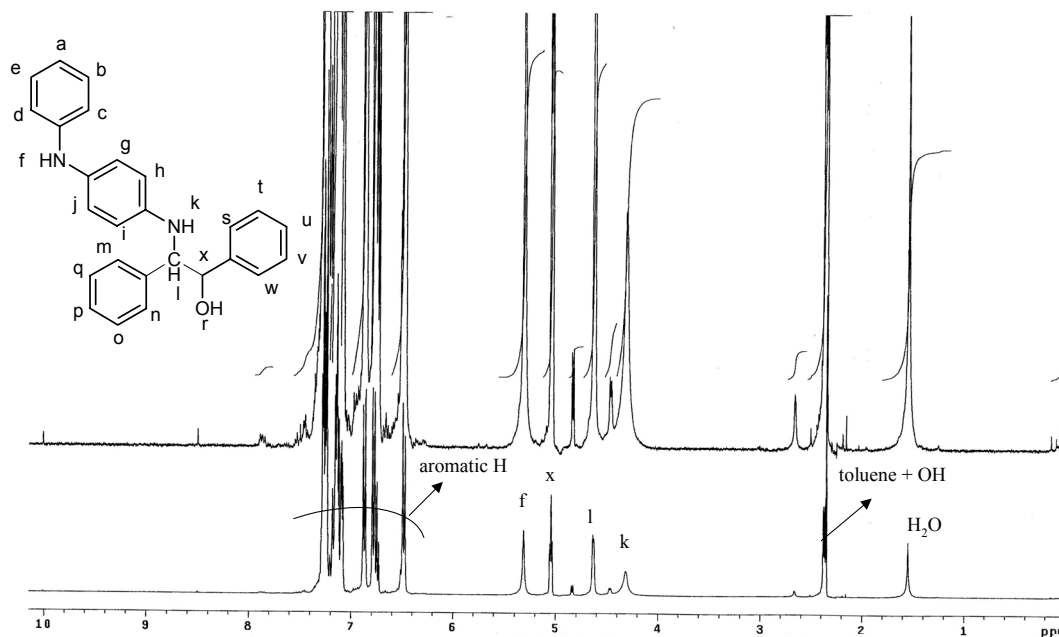
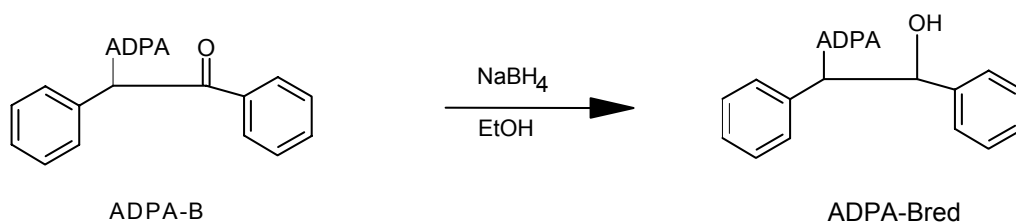


Fig. 3.10: $^1\text{H-NMR}$ spectrum of ADPA-Bred determined in deuterated chloroform.
 δ : 2.39 (r, OH); 4.34 (k); 4.63 (l); 5.04 (x); 5.33 (f);
 6.45 – 7.38 (aromatic H).

ADPA-DTBF (2,6-Di-tert-butyl-4-(4-(phenylamino)phenyliminomethyl)phenol):

ADPA-DTBF was synthesized by reaction of 3,5-di-tert-butyl-4-hydroxybenzaldehyde and 4-ADPA.⁷ 10.08g, 54.7 mMole 4-ADPA, 3,5-di-tert-butyl-4-hydroxybenzaldehyde and 75 ml methanol were refluxed for 1 hour in a 250ml round bottom flask. The reaction product was cooled overnight to room temperature and dried on a rotavapor. The yield was 72%. The product was analyzed by ¹H-NMR and DSC (sharp melting point at 149°C, whereas the aldehyde melts at 188°C). The purity of 98% was estimated by ¹H-NMR: see fig. 3.11.

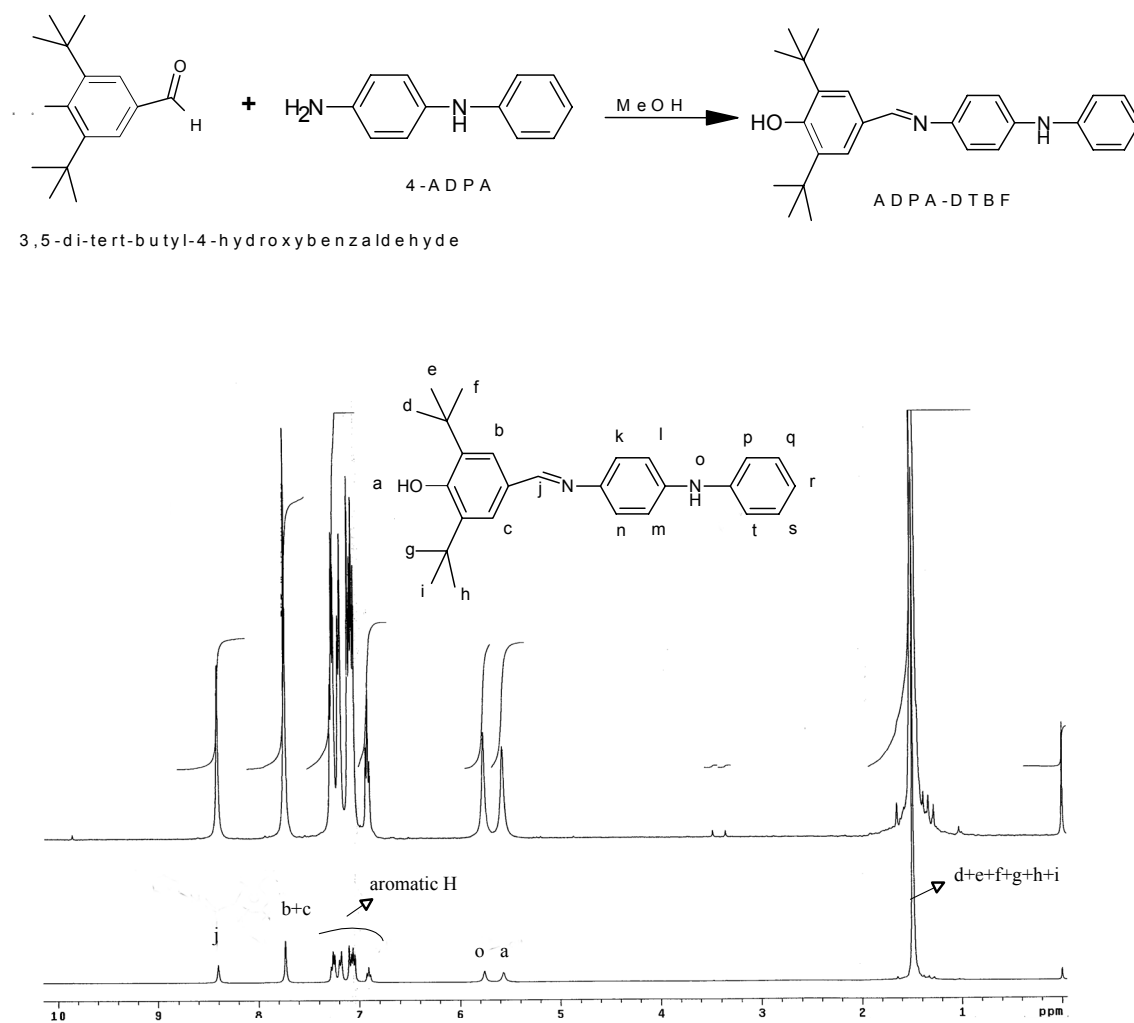


Fig. 3.11: ¹H-NMR spectrum of ADPA-DTBF determined in deuterated chloroform.
 δ : 1.49 (d + e + f + g + h + i); 5.58 (a, OH); 5.77 (o);
 6.88 – 7.30 (aromatic H); 7.75 (b + c); 8.41 (j).

ADPAT (2,4,6-Tris(4-(phenylamino)phenyl)-1,3,5-triazine):

ADPAT was synthesized by a reaction of 4-ADPA and formaldehyde in ethanol. 15.51g, 84.2 mMole 4-ADPA and 0.5g, 2.4 mmole of the catalyst 2,6-di-tert-butylphenol were dissolved in 75ml ethanol using a 250ml round bottom flask. The reaction mixture was heated till 70°C. 6.83g, 84.2 mMole formaline 37% was added to the reaction mixture in 20 minutes. The temperature was increased till reflux temperature (90-95°C). Mixture was refluxed for 1 hour and cooled to room temperature over night. The reaction product was filtered and dried on a rotavapor. The dried product was dissolved in dichloromethane and washed with water. The organic layer was dried on a rotavapor. The yield was 78%. The reaction product was characterized by ¹H-NMR. The purity of 94% was estimated by ¹H-NMR: see fig. 3.12.

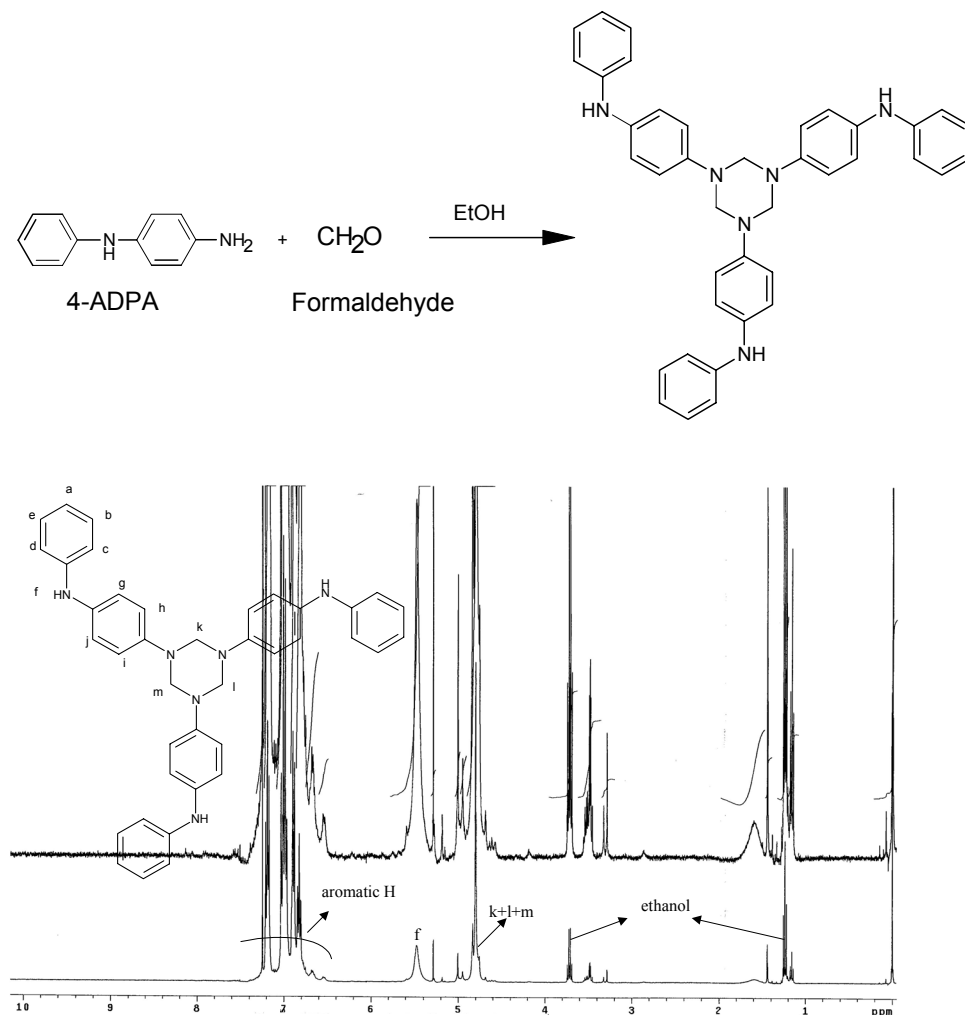


Fig. 3.12: ¹H-NMR spectrum of ADPAT determined in deuterated chloroform
 δ : 5.79 (k + l + m); 5.48 (f); 6.52 – 7.43 (aromatic H).

HTT (hexahydro-1,3,5-triphenyl-1,3,5-triazine):

HTT was synthesized by reaction of aniline and formaldehyde. 31.2g, 335.2 mMole aniline and 1g, 4.8 mmole of the catalyst 2,6-di-tert-butylphenol were dissolved in 100 ml ethanol using a 250ml round bottom flask. The reaction mixture was heated till 75°C. 27.2g, 335.2 mMole formaline 37% was added to the reaction mixture in 30 minutes. The reaction mixture was stirred for another 30 minutes and cooled down to room temperature over night. The reaction product (a white powder) was filtered and washed with ethanol and finally dried on a rotavapor. The yield was 78%. The purity of 95% was estimated by ¹H-NMR: see fig. 3.13.

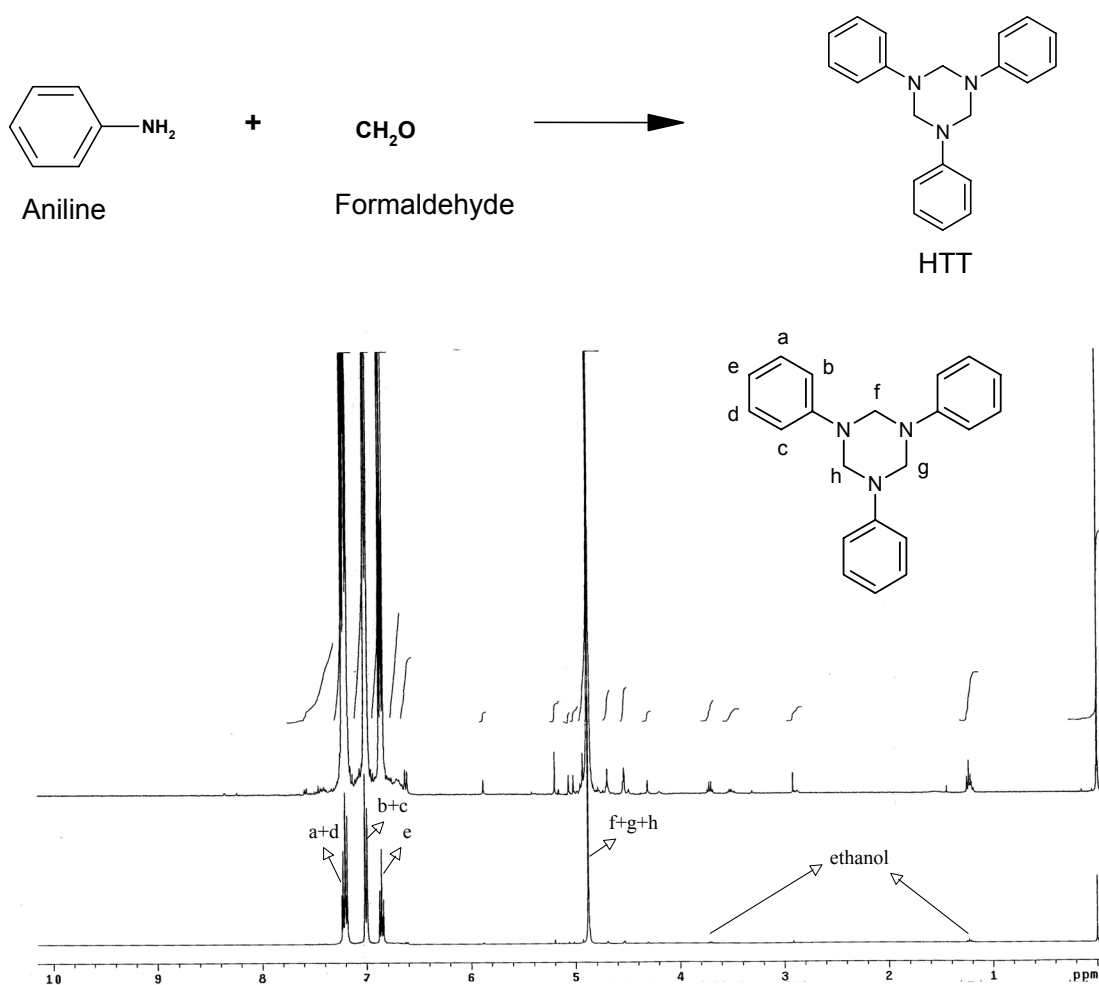


Fig. 3.13: ¹H-NMR spectrum of HTT determined in deuterated chloroform.
 δ : 4.88 (f + g + h); 6.86 (e); 7.01 (b + c); 7.21 (a + d).

PDPA (4-pyrrole-diphenylamine):

PDPA was synthesized by reaction of 2,5-hexanedione and 4-ADPA, using p-toluene sulfonic acid as a catalyst. 25g, 0.219 Mole 2,5-hexanedione, 40.5g, 0.219 mole 4-ADPA, 0.2g p-toluene sulfonic acid and 250ml toluene were refluxed in a 1000ml three-necked flask equipped with a Dean Stark framework. The reaction product was dried on a rotavapor. The dried product was dissolved in chloromethane and washed with water. The organic layer was dried on a rotavapor. The yield was 66%. The product was characterized by $^1\text{H-NMR}$ and IR spectroscopy. The purity of >99% was estimated by $^1\text{H-NMR}$: see fig. 3.14.

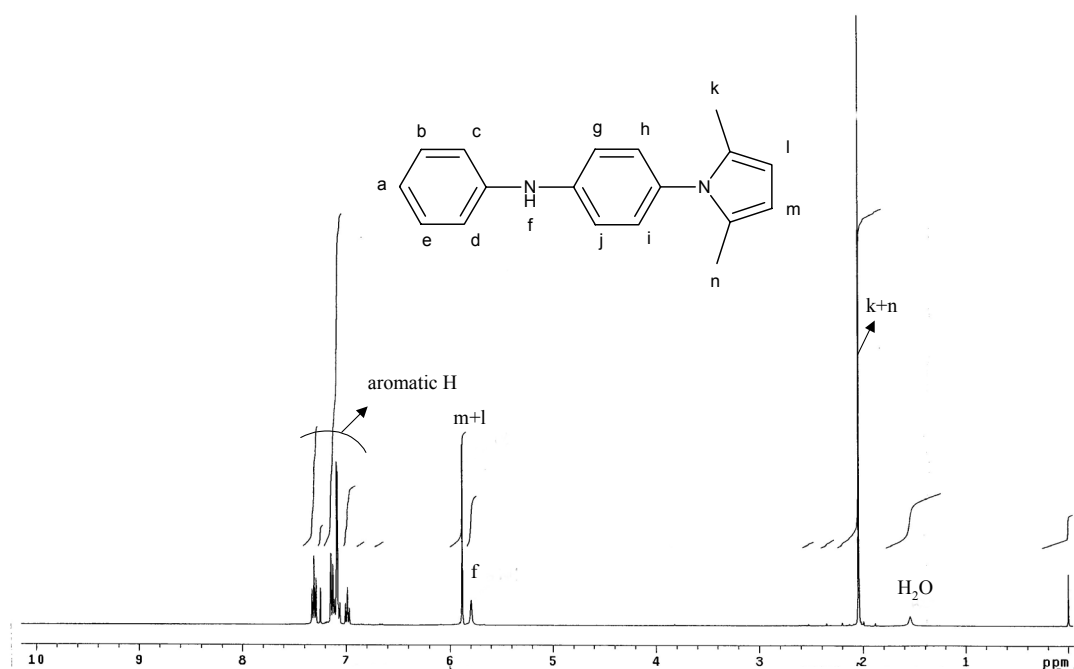
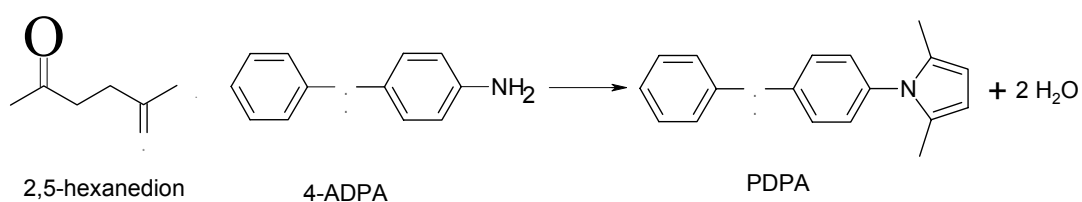
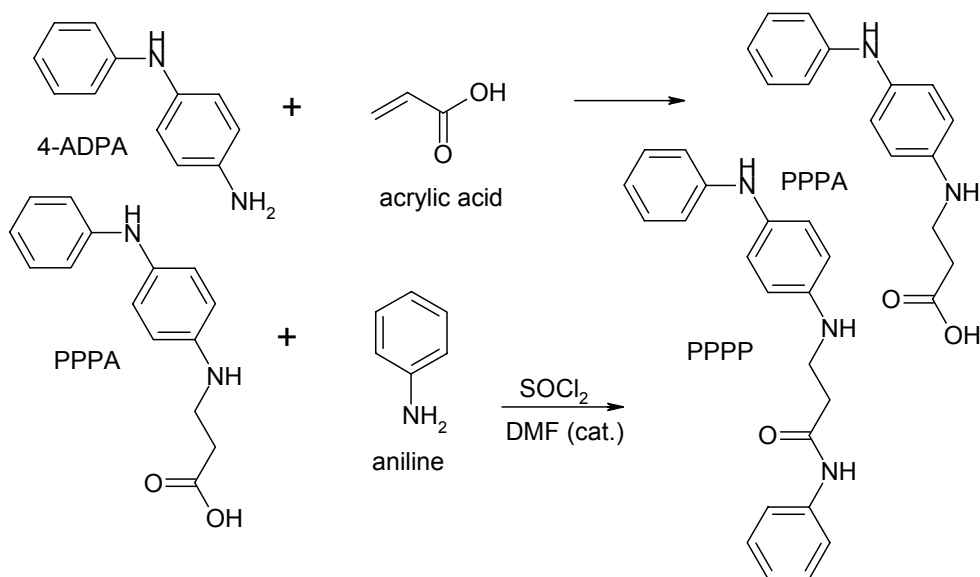


Fig 3.14: $^1\text{H-NMR}$ spectrum of PDPA determined in deuterated chloroform.
 δ : 2.04 (k + n); 5.80 (f); 6.89 (m + l); 6.98 – 7.38 (aromatic H).

PPPP (N-Phenyl-3-(4-(phenylamino)phenylamino)propanoate):

PPPP was synthesized by addition of 4-ADPA to acrylic acid and subsequently coupling with aniline. 10g, 0.0542 Mole 4-ADPA, 3.906g, 0.0542 mole acrylic acid and 400 mg 1,4-diazabicyclo[2,2,2]octane (DABCO) were dissolved in 50ml methanol using a 250ml three-necked flask and stirred for 48 hours at room temperature. The reaction product, which is formed via the Michael addition reaction was washed with methanol and dried on a rotavapor. 10.88g, 0.043 Mole 3-((4-Phenylamino)phenylamino) propanoic acid (PPPA), 4.00g, 0.043 mole aniline and 5 drops dimethyl formamide were dissolved in 150ml thionyl chloride and refluxed for two hours using a 500 ml round bottom flask. The reaction product was washed with THF and dried on a rotavapor. The acid chloride, which was formed during the reaction of the acid with thionyl chloride reacted immediately with aniline to form the amide. The yield was 84%. The product was analyzed by ¹H-NMR. The purity of 94% was estimated by ¹H-NMR: see fig. 3.15.



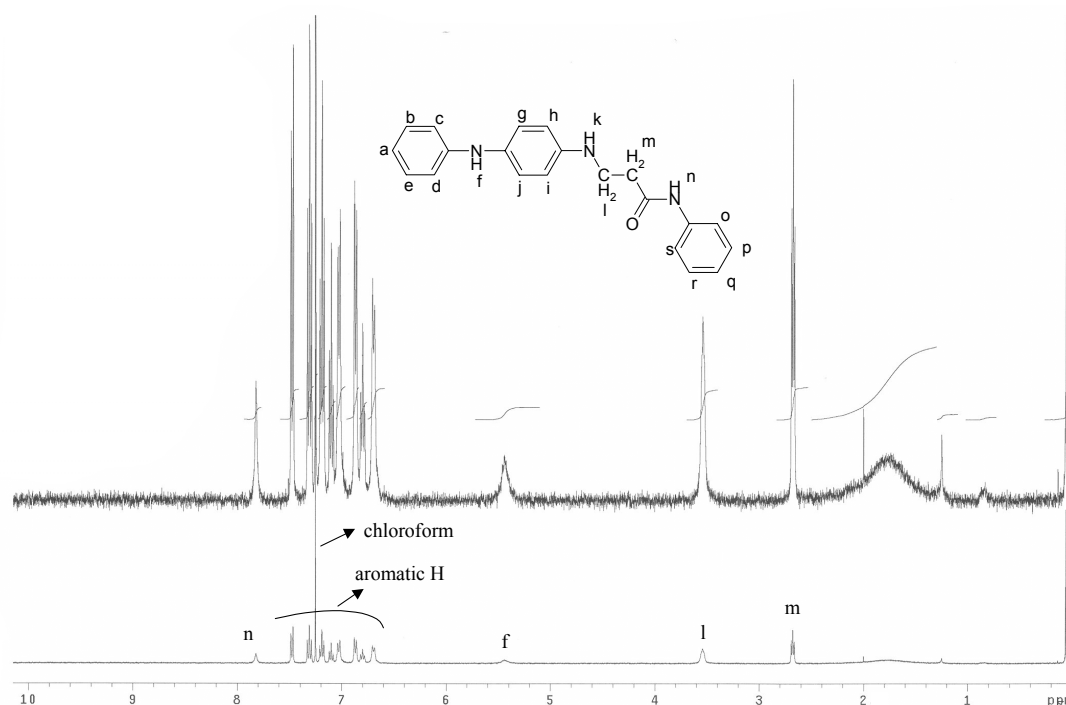


Fig 3.15: ¹H-NMR spectrum of PPPP determined in deuterated chloroform.
 δ : 2.68 (m); 3.57 (l); 5.43 (f); 6.63 – 7.51 (aromatic H); 7.82 (n).

PEPPP (2-Phenoxyethyl-3-(4-phenylamino)phenylamino)propanoate):

PEPPP was synthesized by addition of 4-ADPA to phenoxy-ethyl acrylate. 12g, 0.087 Mole phenoxy ethanol, 8.091g, 0.087 mole acrylic acid, 0.5g conc. HCl and 200ml THF were refluxed overnight using a 500ml round bottom flask equipped with a Dean Stark frame work. The reaction product phenoxy-ethyl acrylate was dried on a rotavapor. 16g, 0.083 Mole phenoxy-ethyl acrylate, 15.289g, 0.083 mole 4-ADPA and 500mg DABCO were dissolved in 100ml THF using a 250ml three-necked flask and stirred for 48 hours at room temperature. The reaction product, which was formed via the Michael addition reaction was washed with THF and dried on a rotavapor. The yield was 78%. The product was analyzed by ¹H-NMR. The purity of 95% was estimated by ¹H-NMR: see fig. 3.16.

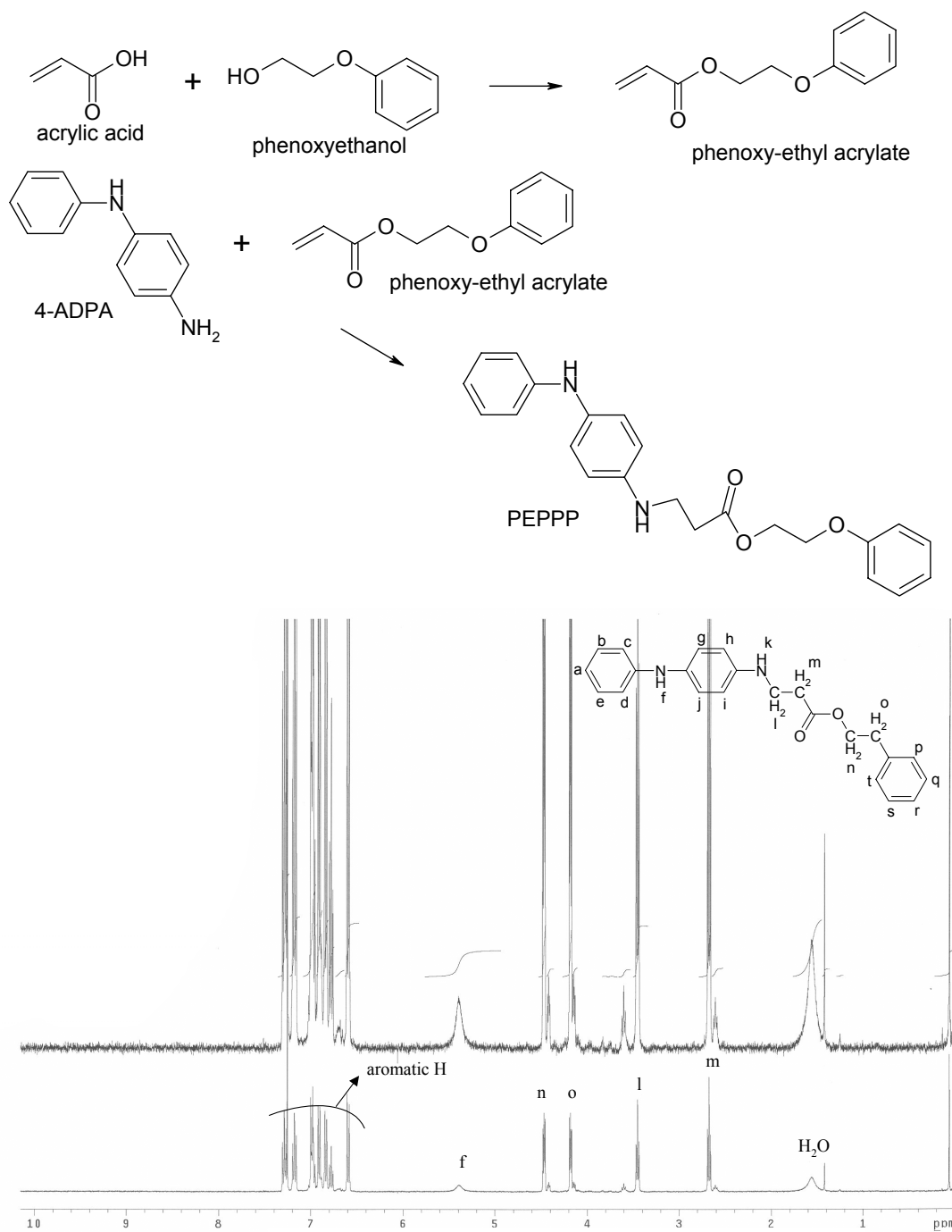
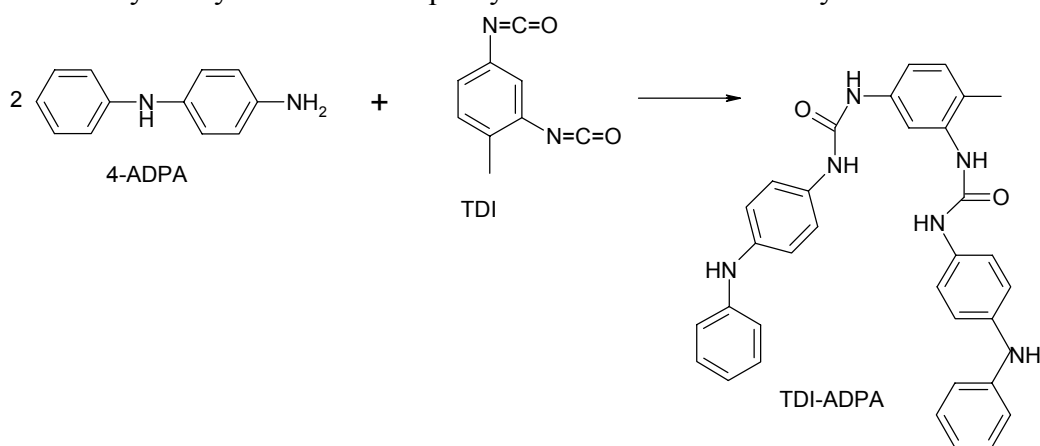


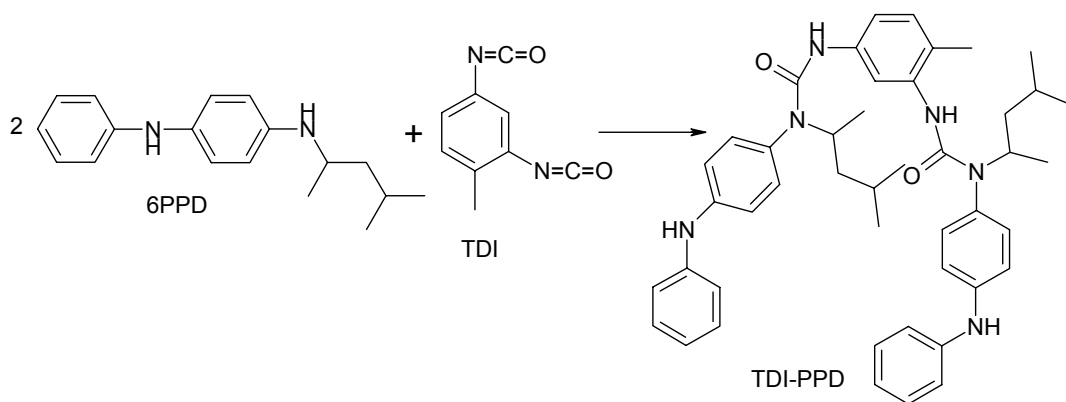
Fig 3.16: $^1\text{H-NMR}$ spectrum of PEPPP determined in deuterated chloroform.
 δ : 2.69 (m); 3.42 (l); 4.18 (o); 4.48 (n); 5.39 (f);
 6.58 – 7.32 (aromatic H).

TDI-ADPA (2,4-Bis(4-phenylamino)phenylureido toluene):

TDI-ADPA was synthesized by reaction of toluenediisocyanate (TDI) and 4-ADPA. 31.7g 4-ADPA was dissolved in 100ml toluene and heated at 25°C. To a solution of ADPA, 15g TDI dissolved in 100ml toluene was slowly added in 10 minutes. The reaction mixture was heated till 100°C and stirred for three hours. The reaction product (a very fine white powder) was filtered over a G4-filter, washed three times with 20ml toluene and dried overnight in air. The yield was 97%. The product was analyzed by ¹H-NMR. The purity of 95% was estimated by ¹H-NMR.

*TDI-PPD (2,4-Bis((N-4-phenylamino)phenyl)-N-(1,3-dimethylbutyl)ureido)toluene:*

TDI-PPD was synthesized by reaction of toluene diisocyanate (TDI) and 6PPD. 30.2g 6PPD was dissolved in 100ml toluene and heated at 25°C. 15.0g TDI dissolved in 100ml toluene was dosed in 10 minutes to the 6PPD solution. The reaction mixture was heated till 100°C and stirred for six hours. The reaction product (a very fine white powder) was filtered over a G4-filter, washed two times with 50ml toluene and dried overnight in air. The yield was 96%. The product was analyzed by ¹H-NMR. The purity of 95% was estimated by ¹H-NMR.



3.4 Conclusions

Several slow diffusion (high molecular weight) antidegradants were prepared by addition of 4-ADPA or 6PPD onto different functional groups by exploiting various kinds of chemistry: salt formation (PPD-AA, PPD-HA, PPD-C18, PPD-BA, PPD-SA, PPD-ADA, PPD-FA, PPD-MA, PPD-TA, PPD-CA, PPD-PA and PPD-MSA), Michael addition (4Asi-Ph, ADPA-C, ADPA-pol, PPPP and PEPPP), Mannich reactions (ADPA-DTBF, ADPAT, HTT and PDPA), condensation (ADPA-B and ADPA-Bred), nucleophilic substitution (SPPD), amide formation by reaction with acid chlorides (DT-P-ADPA and DT-S-ADPA) and formation of disubstituted ureas (TDI-ADPA and TDI-PPD).

The salts of 6PPD and different carboxylic acids were prepared by melting PPD and an equimolar amount of the corresponding acid under continuously stirring or by refluxing in methanol. The formation of the salt was confirmed by DSC measurements (only one melting peak). Special attention was paid to the characterization of PPD-C18, the most promising antidegradant according to the results described later in Chapter 5. It was demonstrated by DOSY ¹H-NMR that the salt prepared from 6PPD and stearic acid appears to be a complex, when analyzed in the melt. However, the salt seems to be a rather weak complex that decomposes into a mixture of 6PPD and stearic acid, when analyzed in a solvent.

4-Asi-Ph, ADPA-C, ADPA-pol, PPPP and PEPPP were prepared by Michael addition reactions onto 4-ADPA. It can be concluded from the obtained yield of these products that the reactivity between the phenylamino group of 4-ADPA and the double bond of the corresponding unsaturated compounds is very good. Side products formed during these reactions are mainly related to the reaction of 4-ADPA with the carbonyl group of the corresponding unsaturated compounds.

ADPA-DTBF, ADPAT, HTT and PDPA were prepared by Mannich reactions between 4-ADPA and aniline with 3,5-di-tert-butyl-4-hydroxybenzaldehyde, formaldehyde and 2,5-hexanedione. The obtained cyclic nitrogen compounds were easily formed.

TDI-ADPA and TDI-PPD were prepared by reaction of respectively 4-ADPA and 6PPD with toluene diisocyanate. The reactivity between the phenylamino group and isocyanates is very good. The reaction was performed in a water free atmosphere, because isocyanates are very reactive with water, forming carbamic acid that easily decomposes into an amine and carbon dioxide. The amine formed can react with isocyanates resulting in undesirable side products.

DT-P-ADPA and DT-S-ADPA were prepared by reaction of respectively 3,3'-dithiopropionyl dichloride and 2,2'-dithiobenzoyl dichloride with 4-ADPA. The reactivity between the phenylamino group of 4-ADPA and acid chloride was judged to be satisfactory.

ADPA-B was prepared by condensation of 4-ADPA with benzoin, using concentrated HCl as a catalyst. ADPA-Bred was prepared by reduction of ADPA-B with sodium borohydride. No problems were encountered during both the condensation as well as the reduction reaction.

SPPD was synthesized by reaction of 4-ADPA and bromoethylbenzene, using triethanolamine as a catalyst. The substitution of bromine with 4-ADPA appeared to be simple, with a low risk of formation of side products.

In general, it can be concluded that the above-described reactions were not complicated. However, purification of the final products was difficult. Most of the synthesized antidegradants have a relatively high molecular weight and thus can not be purified by distillation. Therefore, purification was mainly done by washing of the reaction product with different solvents and subsequent drying on a rotavapor. Unfortunately, part of the product was lost during this washing procedure because the polarity of both the raw materials and the corresponding antidegradants was quite similar, resulting in relatively low yields. No further attempts were made to optimize the above-described syntheses, because only small amounts of samples were needed for evaluation in the context of this research project.

3.5 References

1. P. Sänder, 2D & 3D HR-DOSY, Varian NMR applications laboratory, Darmstadt, Germany, (24 September 1998).
2. R.C. Weast, "Handbook of Chemistry and Physics", 51st edition, (1970-1971).
3. E.D. Bergmann, D. Ginsburg and R. Pappo, *Org. Reactions*, **10**, (1959), 179.
4. H. Hofman, U. Eggert, W. Poly, *Angew. Chem.*, **99**, (1987), 1047.
5. W.S. Johnson, E.L. Woroch, B.G. Buell, *J. Am. Chem. Soc.*, **61**, (June 16, 1949), 1901.
6. C.F. Nutaitis, J.E. Bernardo, *Synth. Commun.*, **20**, (1990), 487.
7. A.P. Bindra, J.A. Elix, *Tetrahedron letters*, **26**, (1970), 3749.

Chapter 4

Development of test protocols for screening potential slow-migrating antidegradants[#]

The migration behavior of antidegradants in rubber vulcanizates is influenced by the nature of the rubber and filler. Temperature plays a very important role too. Currently available antiozonants such as N-isopropyl-N'-phenyl-p-phenylene diamine (IPPD) and N-(1,3-dimethylbutyl)-N'-phenyl-p-phenylene diamine (6PPD) migrate and finally deplete, either during vulcanization or during service, thus affecting vital properties of rubber articles such as aging and fatigue resistance. Migration of antiozonants, on the other hand, is a prerequisite for ozone protection. Fast migration results in a too short-term protection; too slow migration suffers from inadequate initial protection.

In the present chapter a series of test protocols have been developed, for screening potential slow migrating antidegradants, providing long lasting antiozonant protection. A good correlation was found between outdoor aging and the dynamic heat aging test as developed in this chapter. Although both dynamic strain and temperature showed a large effect on the depletion of 6PPD, the effect of temperature was more pronounced.

4.1 Introduction

The migration of antidegradants (especially antiozonants) is an important feature in the protection of rubber formulations used in the tire industry and other industrial rubber products. There are numerous mechanisms outlined in literature describing ozone protection both under static and dynamic environments.^{1,2} To achieve sufficient ozone protection under static environments, waxes (paraffinic wax for temperatures below 40°C and microcrystalline wax for temperatures above 40°C) are the best choice. However, rubber articles face dynamic loadings and hence waxes alone cannot protect the article from ozone attack. Waxes function by migration to the surface of the rubber to provide a physical barrier against ozone attack under static conditions. Solubility and mobility govern the formation of wax layers (bloom) on the rubber surface as illustrated in fig. 4.1. Waxes do not offer any measurable protection

[#] A part of this work has been presented at the ITEC'02, September 10-12, in Akron (paper #14A) and published in *Kautsch. Gummi Kunstst.*, **55**, (2003), 310.

under dynamic conditions. This is probably due to inextensibility or poor adhesion of the protective film to the rubber.

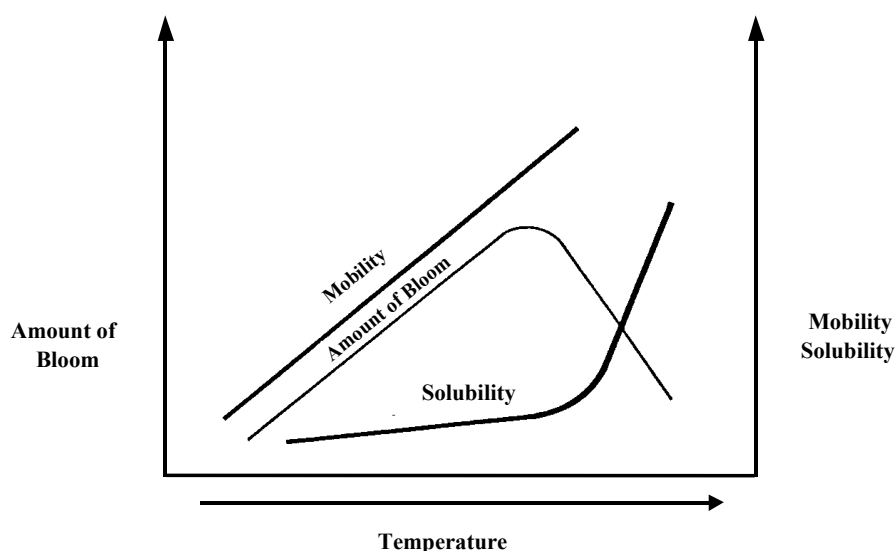


Fig. 4.1: Effects of solubility and mobility on wax bloom.³

For dynamic applications, the chemical antiozonants have been developed and are widely used today. The mechanism of protection is based on migration to the surface and reaction with ozone, keeping the rubber unreacted.⁴ The most widely used antidegradant system in rubber protection is a combination of wax and PPD's. The PPD's provide chemical protection against ozone attack under both static and dynamic conditions. They are not as effective as the waxes under static ozone exposure. Lederer et al. demonstrated the versatility of the wax/PPD systems to give a balance in both static and dynamic protection over a wide range of temperatures.⁵ This is shown in fig. 4.2.

The speed of migration of antiozonants plays a dominant role in protection against ozone. Several reports indicate however that diffusion is not the sole criteria.⁶ Also the products formed by reaction with ozone are excellent and effective antiozonants by themselves.

Currently, the most accepted mechanism of antiozonant action is a combination of scavenging and protective film formation.⁷⁻⁹ Therefore, it is obvious that the major characteristics required for antiozonant properties are fast migration to the surface of a rubber vulcanizate and reactivity towards ozone.

Migration behaviors of antidegradants in rubber vulcanizates are influenced by the matrices of rubber and filler.¹⁰ 2,6-Di-*t*-butyl-4-methyl phenol (BHT), *N*-phenyl-*N*'-isopropyl-*p*-phenylenediamine (IPPD), and *N*-phenyl-*N*'-(1,3-dimethylbutyl)-*p*-phenylenediamine (HPPD) migrate slower in SBR vulcanizates than in NR and BR

ones.¹⁰ Migration rates of antidegradants in silica-filled rubber vulcanizates are slower than those in carbon black-filled ones.¹¹ Migration rates of the antidegradants become slower and slower by increasing the filler content in the vulcanizates also. Intermolecular interactions between the antidegradants and the matrices in rubber vulcanizates affect the migration behaviors of the antidegradants. The stronger the intermolecular interactions of antidegradants with the matrices, the slower the migration rates. Migration of antidegradants throughout a rubber article can be explained by at least two mechanisms: bloom and diffusion.

Bloom occurs when a partly soluble antidegradant is used at a level in excess of its solubility at a given temperature.¹² For example, a material dissolved in the rubber mix at a high mixing temperature becomes supersaturated as the stock cools down. Crystallization of the component then occurs; crystallization is energetically more favorable at the surface of the rubber than in the bulk. As crystallization occurs at the surface, a concentration gradient occurs between the layer immediately beneath the surface (a saturated “solution”) and the bulk of the rubber (supersaturated). Because of this concentration gradient, further blooming will occur at the surface until the concentration of the component finally reaches the solubility limit throughout the rubber article. A component below its solubility limit will not bloom. The appearance of antiozonants at the surface of an article by a blooming mechanism is undesirable, since the antiozonant appears at the surface independent of the need (i.e. surface depletion of effective antiozonant). Appearance of excess antiozonant at the surface can lead to physical loss of the antiozonant. The solubility of antidegradants in the rubber matrix was studied by Luechen et al. in a NR/BR passenger tire sidewall compound (NR/BR), who demonstrated that 6PPD is soluble at 10 phr but starts to bloom at 20 phr.¹³

Diffusion can be defined as a movement of an antidegradant, which is extremely soluble in the rubber, prompted by a disruption in equilibrium. Solutions of compounds in rubber are known to behave similarly to solutions of low molecular weight products, and are characterized in the same way as ordinary solutions.^{14,15} When the concentration of a totally soluble component at the interface of a liquid is reduced the soluble component diffuses to the surface to re-establish concentration equilibrium. Diffusion, therefore, provides “as needed” protection at the surface of the rubber; i.e. the component does not bloom independent of need, but diffuses only when the surface concentration is depleted by chemical reaction or physical loss.

An antiozonant used at a level in excess of its solubility will, therefore, have two driving forces affecting its appearance at the surface of the vulcanizates: blooming and diffusion. An ideal antiozonant would be one, which is totally soluble and shows rapid migration to the surface when effective antiozonant protection at the surface is depleted. Thus, long-term protection with antidegradants depends upon a continued replenishment of active antiozonant at the surface of a rubber product.¹⁶

The speed of migration is a function of concentration gradient and diffusion coefficient. The concentration gradient originates from crystallization at the surface versus supersaturation in the matrix. The diffusion coefficient depends on several factors, such as molecular weight, temperature according to an Arrhenius like

relationship: $D = D_0 \exp [-E_a/RT]$, crosslink density, interactions with the matrix, etc.¹⁷

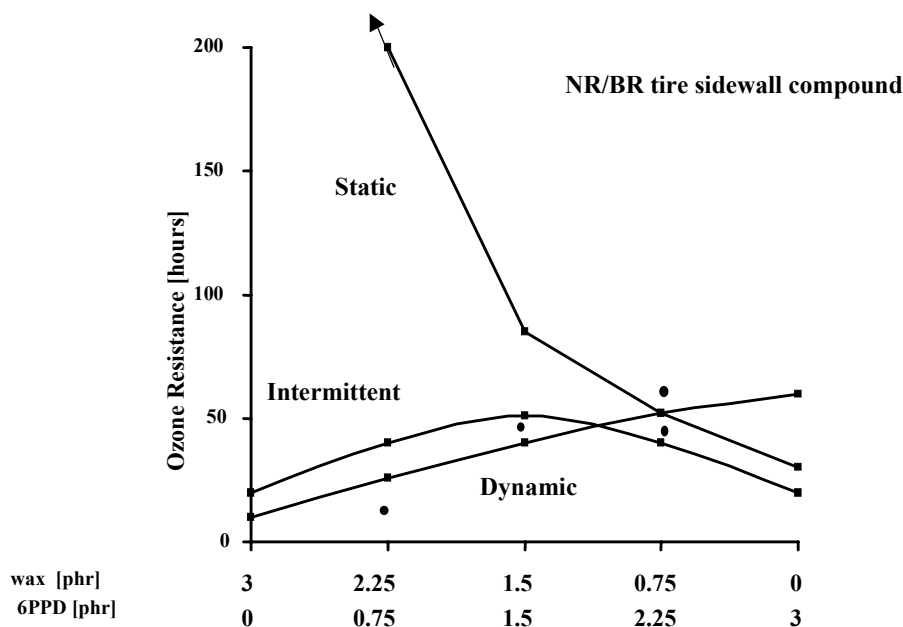


Fig. 4.2: Effects of wax/PPD mixtures on ozone protection.⁵

Although, conventional antidegradants like N-(1,3-dimethylbutyl)-N'-phenylphenylenediamine (6PPD, fig. 4.3) are still the most widely used in rubber, there is a trend and demand for longer-lasting and non-staining products.¹⁸ It has been a challenge to develop a slow diffusion antidegradant with the aim to protect rubber articles for longer duration and to provide longer lasting tire black sidewalls with better appearance.¹⁹ The research has resulted in the development of PPD-C18 (fig. 4.3), a salt of 6PPD and stearic acid as described in Chapter 3. In this chapter, methods will be developed and described for screening the antidegradants synthesized in Chapter 3, as slow migrating antidegradants providing long-term protection. Furthermore, a correlation is made between outdoor aging and the dynamic aging test protocol as developed in this chapter.

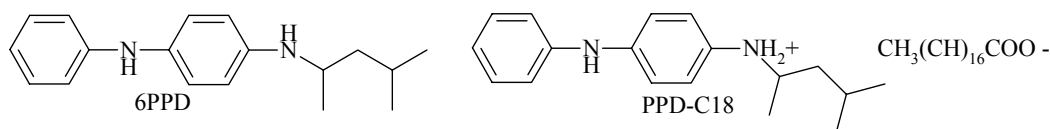


Fig. 4.3: Chemical structure of 6PPD and PPD-C18.

4.2 Experimental

4.2.1 Materials

The compounds for the experiments contained: NR SMR CV 60 (Natural Standard Malaysian Rubber with a constant viscosity ML(1+4) 100°C of 60±5, Wurfain & Co B.V.); BR Buna CB 10 (Butadiene Rubber with a cis-content of 95% and a vinyl content of 1%, Buna Werke Huels); carbon black N-550 (Cabot B.V.); naphthenic oil (Sunthene 4240, Sun Oil Co.); ZnO (Harzsiegel standard); stearic acid (J.T. Baker); Santoflex 6PPD (Flexsys); wax, blend of petroleum components (Sunolite 240, Witco S.A.); Santocure CBS (Flexsys); sulfur (J.T. Baker); Santoflex IPPD (Flexsys); PPD-C18 was synthesized by melting PPD and an equimolar amount of stearic acid under continuously stirring for 120 min., as described in Chapter 3.

4.2.2 Formulations, mixing and curing

The compound formulations are shown in Table 4.1. All the ingredients except sulfur and accelerators were mixed in a 1.6L internal mixer for 3 min. at 130°C. Sulfur and accelerator were mixed on a two-roll mill at 50-65°C according to standard laboratory mixing conditions. Cure data were determined on a Monsanto MDR 2000E at 150°C / 60 min., according to ISO 6502: 1991. Compounds were cured to optimum cure times (t_{90}) by compression molding at 150°C.

Table 4.1: Compound formulations tested in dynamic aging test protocol

| Ingredient / Mixes | 1 | 2 | 3 | 4 | 5 | 6 | 7 | 8 |
|--------------------|-------|-------|-------|-------|-------|-------|-------|-------|
| NR SMR CV 60 | 50.00 | 50.00 | 50.00 | 50.00 | 50.00 | 50.00 | 50.00 | 50.00 |
| BR Buna CB 10 | 50.00 | 50.00 | 50.00 | 50.00 | 50.00 | 50.00 | 50.00 | 50.00 |
| Carbon black N-550 | 50.00 | 50.00 | 50.00 | 50.00 | 50.00 | 50.00 | 50.00 | 50.00 |
| Na.oil Sunth. 4240 | 6.00 | 6.00 | 6.00 | 6.00 | 6.00 | 6.00 | 6.00 | 6.00 |
| Zinc oxide | 4.00 | 4.00 | 4.00 | 4.00 | 4.00 | 4.00 | 4.00 | 4.00 |
| Stearic acid | 2.50 | 2.50 | 2.50 | 2.50 | 2.50 | 2.50 | 2.50 | 2.50 |
| PPD-C18 | - | - | 5.00 | 3.00 | - | - | 5.00 | 3.00 |
| 6PPD | - | 2.50 | - | 1.00 | - | 2.50 | - | 1.00 |
| Wax Sunolite 240 | - | - | - | - | 1.50 | 1.50 | 1.50 | 1.50 |
| CBS | 0.80 | 0.80 | 0.80 | 0.80 | 0.80 | 0.80 | 0.80 | 0.80 |
| Sulfur | 2.00 | 2.00 | 2.00 | 2.00 | 2.00 | 2.00 | 2.00 | 2.00 |

4.2.3 Equipment used for various aging tests

Hot air ovens:

Test pieces were subjected to controlled deterioration by air at elevated temperatures: 70 ± 1 , 80 ± 1 and 90 ± 1 °C, and at atmospheric pressure. Test pieces were clamped in the oven, randomly distributed over the available clamps, so that test pieces are free from strain, freely exposed to air on all sides and not exposed to light.

Monsanto fatigue tester:

Test pieces were aged by subjecting to a dynamic strain, using a Monsanto fatigue tester at a frequency of 1.67 Hz, and at relatively low strains: 10 and 25% strain. Test pieces were mounted randomly in the grips of the fatigue tester.

Ozone cabinet :

Resistance to ozone cracking was measured in an Argentox ozone cabinet type 3MR-3R according to ISO 1431-1: 1989 (static ozone resistance test) and ISO 1431-2: 1989 (dynamic ozone resistance test). Measurements were performed at 40°C, 50pphm ozone, 25% dynamic or static strain, 0.6m/sec gasflow and 50% relative humidity. Test pieces were mounted randomly in the grips of the ozone cabinet and aged until break. Samples were observed at fixed time intervals. The time until break of the test specimen was recorded as a measure for resistance to ozone cracking.

4.2.4 Analytical techniques

GC/FIA-MS:

The amount of 6PPD present in the toluene and dichloromethane extractables of rubber vulcanizates was quantified using a capillary gas chromatograph equipped with a split injector and a flame ionization detector.

GC-conditions:

| | |
|------------------|--|
| Column | : fused silica column WCOT, 17m * 0.32 mm ID |
| Stationary phase | : Sil 5 CB, 100% polydimethylsiloxane, crosslinked |
| Film thickness | : 0.4 μ m |
| Injector | : Split, 250°C |
| Detector | : FID, 330°C |
| Temp. program | : 120°C (1 min.) $\xrightarrow{10^\circ\text{C}/\text{min}}$ 320°C (25 min.) |

Identification of the different peaks was done by FIA-MS using the Platform-II quadrupole ex Micromass. In positive ESI, components should give $[\text{MW} + \text{H}]^+$ or $[\text{MW} + \text{Na}]^+$ adducts, so m/z values of MW + 1 or MW + 23 are expected to be formed. Ionization was done by electrospray positive/negative (scan range 200-1500

Da; capillary voltage 3.50kV; HV lens 0.5V; skimmer 5V; Cone voltage 10/30 V/60V; source temperature 60°C). Methanol was used as a carrier solvent.

4.3 Development of test protocols for screening slow-migrating antidegradants

In this paragraph, the test protocol is described that was developed to screen antidegradants for long-term protection of rubber compounds, as described in Chapter 5. The effect of antidegradants on long-term protection of rubber networks is studied by determining the stress-strain properties, resistance against fatigue and ozone and distribution of crosslink types, before and after static and dynamic heat aging as described in this paragraph.

4.3.1 Static heat aging

Test pieces were aged in an air circulation oven for 7 and 14 days at 70 ± 1 , 80 ± 1 and 90 ± 1 °C. Samples were kept for 24 hours at room temperature before final mechanical testing. This aging procedure was used alone and also as part of the dynamic heat aging test described below.

4.3.2 Dynamic heat aging

Although, it is known that differences exist between accelerated aerobic aging tests (indoor) and long-term outdoor aging tests (i.e. influence of UV-light), an attempt was made to develop a laboratory dynamic aging test protocol that reflects long-term outdoor aging and migration characteristics. This is highly desirable, as it reduces cost and time involved in field tests.

A study was done to investigate the effect of time, temperature and dynamic strain on the migration rate of 6PPD in a typical passenger tire sidewall compound. The composition of the specific compound used for this study is described in Table 4.1: compound 2. Cured samples were subjected to a dynamic strain, using the Monsanto fatigue tester for 24 hours, at a frequency of 1.67Hz, and at relatively low strains: 10 and 25% strain. Afterwards, the remaining amount of 6PPD in the samples was analyzed by GC, according to the method described under 4.2.4. A low amount of remaining 6PPD in the compound after aging correlates with a higher migration rate and/or an increased depletion of 6PPD by chemical reaction or physical loss. The results are given in fig. 4.4. In this figure, the sample designated as “uncured” is unvulcanized compound. This was taken directly from the mixer, had not been subjected to the straining, but was taken along as a reference for the amount of 6PPD lost already during the mixing operation. Similar for the sample designated as

“cured”: it had not been strained, but acts as a reference for the amount of 6PPD lost by the curing process.

In another experimental set-up, the samples were aged in the air circulation oven under static conditions, between 70 and 90°C for periods of respectively 7 and 14 days. The results are given in fig. 4.5. The same applies to the samples designated as “uncured” and “cured”. Subsequently, the two experiments were combined into two series: one with dynamic straining at 10% strain and one with 25% strain. The static aging part of this combination was done for 7, respectively 14 days at 80°C. Results are depicted in figures 4.6 and 4.7 respectively.

It becomes clear from the results that during mixing in the internal mixer: designated as “uncured”, 8% of the 6PPD is already lost. After curing, another 5% of 6PPD is depleted: designated as “cured”. The decrease of 6PPD during curing is low, because curing is an anaerobic process, the samples being locked away from surrounding air in the curing press.

Figure 4.4 shows that the amount of remaining 6PPD decreases further when an increased dynamic strain is applied for 24 hours at room temperature. The amount of remaining 6PPD decreases also with static aging at increasing temperature, as seen in fig. 4.5. Comparing both temperature and strain effects, it can be concluded that temperature plays a larger role than dynamic straining under the conditions applied. It is interesting to note, that more than 50% of 6PPD is depleted after 7 days heating at 80°C. All of the 6PPD is depleted after heating for 14 days at 90°C. As expected, a combined dynamic straining and hot air aging results in an even faster depletion of 6PPD, than either of these procedures alone. This is demonstrated in figures 4.6 and 4.7. No clear differences could be observed when strain was increased from 10 to 25%.

Based on the results described above, it was decided to use the following dynamic heat aging test conditions for comparison of different antiozonants: rubber test pieces (2mm thick) were flexed on a Monsanto fatigue tester for 24 hours, at 23°C, 1.67Hz and 10% strain. After the flexing, bloom was removed with acetone (not extracted but wiped off with a tissue that was saturated with acetone). Finally, the test pieces were aged in an air circulation oven for 7 or 14 days at 70°C. This procedure was done once (designated as 1 cycle) or repeated several times (3 cycles, 4 cycles): ref. Table 4.2 and fig. 4.10, see later.

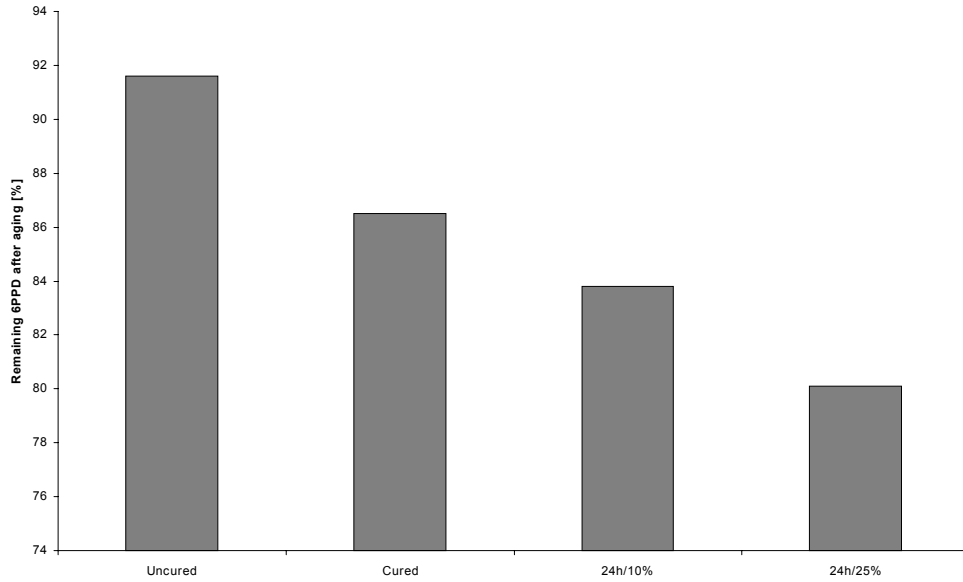


Fig. 4.4: Remaining amount of 6PPD after 24 hours testing in the Monsanto fatigue test equipment at 10 and 25% strain.

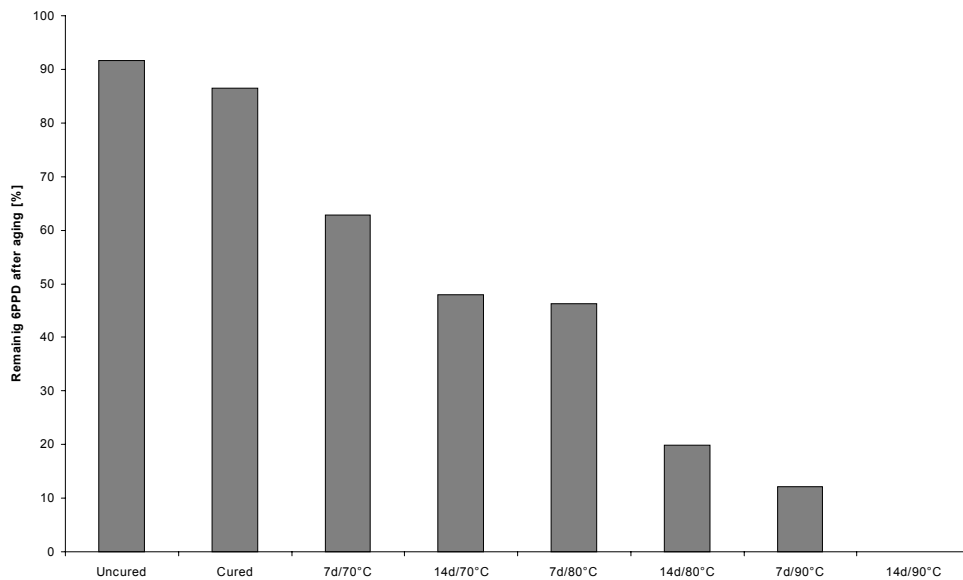


Fig. 4.5: Remaining amount of 6PPD after 7 resp. 14 days static aging at different temperatures: 70, 80 and 90°C.

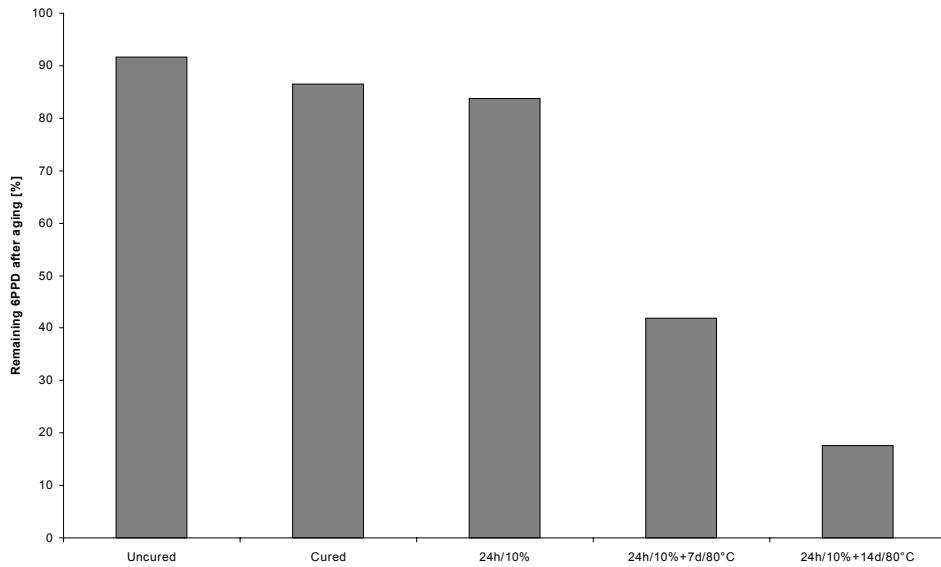


Fig. 4.6: Remaining amount of 6PPD after dynamic heat aging: 24 hours straining at 10% strain and subsequently 7 resp. 14 days static aging at 80°C.

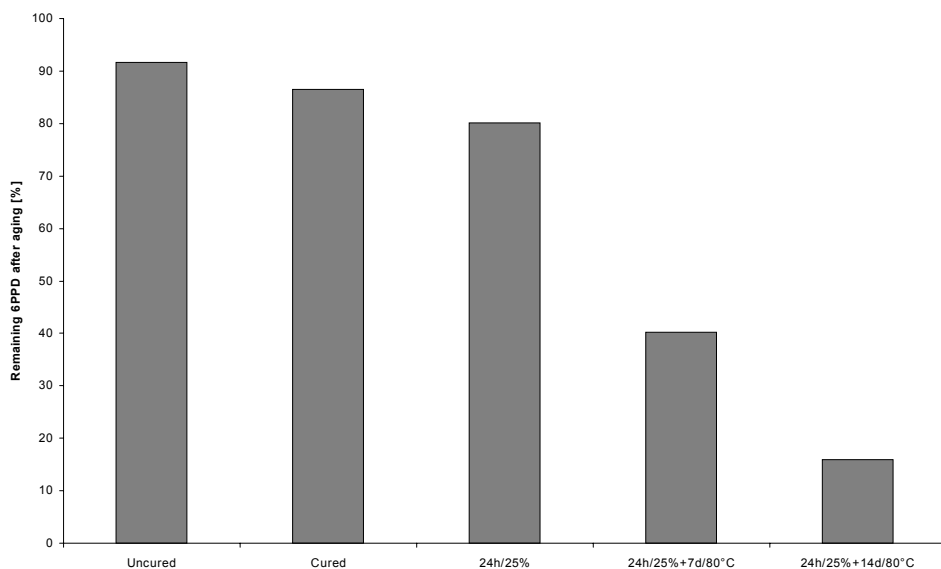


Fig. 4.7: Remaining amount of 6PPD after dynamic heat aging: 24 hours straining at 25% strain and subsequently 7 resp. 14 days static aging at 80°C.

4.3.3 Migration test

Migration characteristics of antidegradants were studied most directly by placing a plate of a control vulcanizate, without antiozonant, in-between two plates of vulcanizate containing the experimental antiozonant, as described by Kavun, Lehocky and Syrovy.^{20,21} The three plates were placed in a metal mold (see fig. 4.8), which was screwed hand tight in order to get a good contact between the surface of the outer and the inner plates, and subsequently put in an air circulation oven. The dimensions of the rubber plates are 100*100*10 mm (see fig. 4.8). Experiments were carried out at a constant temperature of 40°C. The amount of antiozonant that migrates to the center rubber plate was monitored by determination of the weight increase of the center plate; respectively, by analyzing the toluene and/or dichloromethane extractables of cryogenically ground rubber using GC and Flow Injection Analysis Mass Spectroscopy (FIA-MS). This was done after several fixed time intervals. An equilibrium was reached near the end of the experiment at the moment, that the central and the side plates reached constant weight.

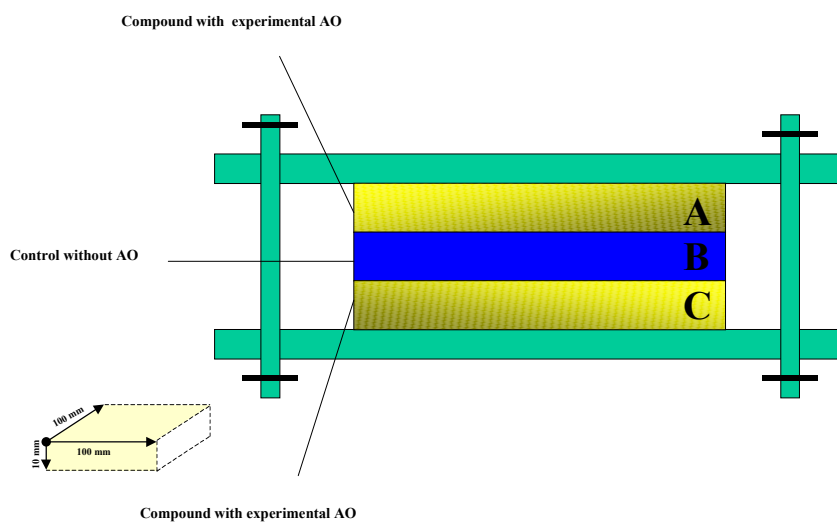


Fig. 4.8: Sample holder used for the migration tests, containing a plate of control vulcanizate (without antiozonant) in-between two plates of vulcanizate, containing the experimental antiozonant.

The dependence of the mass of the antidegradant in the central plate Δm_t [g] is plotted against the square root of the time $\Delta t^{1/2}$ [s^{1/2}]. An example of such a plot is given in fig. 4.9 for N-(1-phenylethyl)-N'-phenyl-p-phenylenediamine (SPPD). From such a plot the diffusion coefficient D [mm²/s] can be calculated according to the classical diffusion theory:

$$D = (\pi * l^2 / 16) * (tg^2 \alpha / \Delta m_{\infty}^2) \quad [\text{mm}^2/\text{s}] \quad (4.1)$$

l : vulcanizate plate thickness [mm];
 Δm_{∞}^2 : weight increase of the central plate at equilibrium;
 $tg \alpha$: $\Delta m_t / \Delta t^{1/2}$, determined from the slope of the curve.

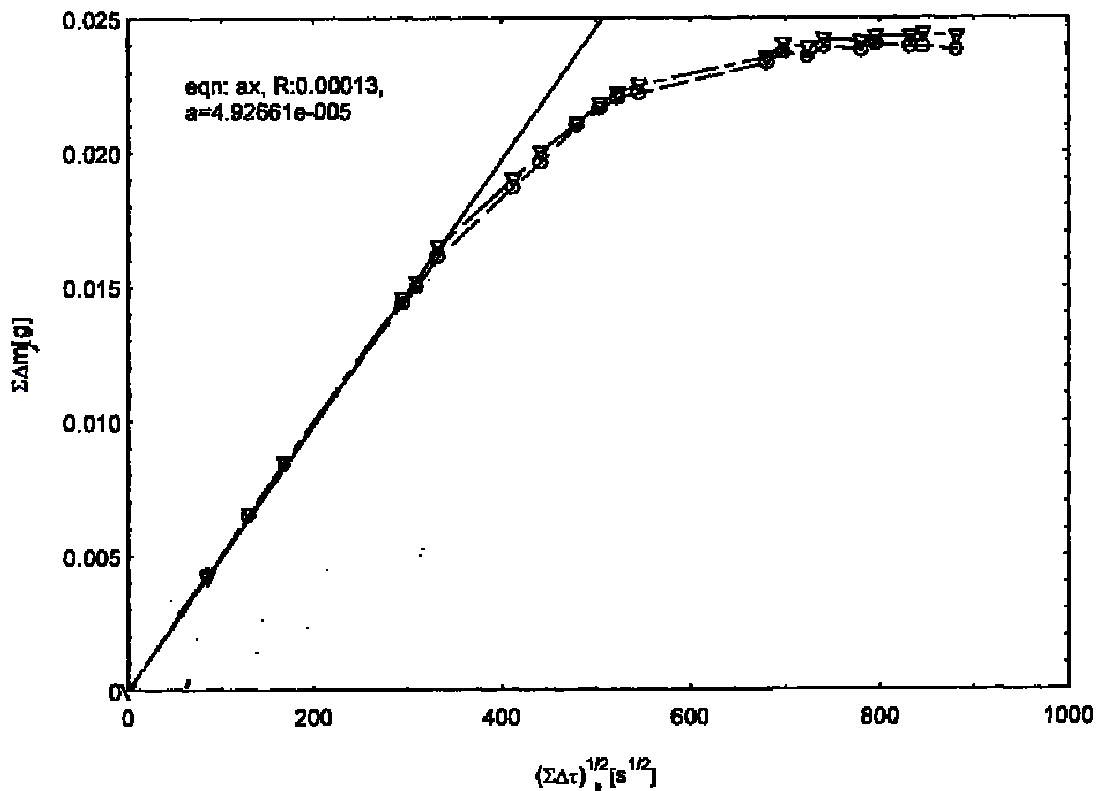


Fig. 4.9: Diffusion kinetics of SPPD in a NR/BR compound at 38°C.²¹

4.3.4 Ozone resistance

Resistance to ozone cracking was measured in an Argentox ozone cabinet type 3MR-3R according to ISO 1431-1: 1989 (static ozone resistance test) and ISO 1431-2: 1989 (dynamic ozone resistance test). Measurements were performed at a temperature of 40°C, 50pphm ozone, 25% static or dynamic strain, 0.6m/sec airflow and 50%RH (relative humidity). A constant strain of 25% was applied during the static ozone resistance test whereas a dynamic strain of 25% at a frequency of 0.1 Hz was applied during the dynamic ozone resistance test. The time until break of the test specimen was recorded as a measure for resistance to ozone cracking.

4.3.5 Aging of crosslink density distribution:

The effect of aging on the network structure was determined by equilibrium swelling in toluene using the method reported by Ellis and Welding.²³ The rubber volume fraction (V_r) obtained was converted into the Mooney-Rivlin elastic constant (C_1) and finally into the concentration of chemical crosslinks by using the Flory-Rehner equations as described in literature.^{24,25} The proportions of mono-, di-, and polysulfidic crosslinks in the vulcanizates were determined by equilibrium swelling in toluene before and after treatment with thiol amine chemical probes.²⁶ Details of the procedure have been reported by Datta et al.²⁷⁻²⁹ With the chemical probe reactions different sulfur cross-links can be selectively cleaved, leaving the more stable ones unaffected. Addition of a solution of propane-2-thiol and piperidine in n-heptane to the vulcanizates cleaves the polysulfidic cross-links in 2 hours at 20°C, leaving mono- and disulfidic cross-links as well as carbon-carbon cross-links unaffected. Addition of hexane-1-thiol in piperidine to the vulcanizates cleaves poly- and disulfidic cross-links in 48 hours at 20°C, leaving monosulfidic and carbon-carbon cross-links unaffected.

4.3.3 Correlation between outdoor- and lab-aging tests

In order to make a correlation between outdoor aging and migration by dynamic heat aging, a comparison was made between samples that were aged by several cycles of dynamic heat aging and samples that were aged on the roof top of the Flexsys laboratory in Deventer, the Netherlands. A cycle consisted of 24 hours flexing at 10% strain and subsequently hot air aging for 7 days at 70°C. The compound compositions of the tested samples are given in Table 4.1. It can be seen from fig. 4.10 and from the results given in Table 4.2 that a single dynamic heat aging cycle correlates well with 3 months outdoor aging. Furthermore, it seems that 12 months outdoor aging is more severe than 4 cycles dynamic heat aging.

Table 4.2: Remaining amount of 6PPD (% m/m) after aging at different conditions.

| Compound | 1 | 2 | 3 | 4 | 5 | 6 | 7 | 8 |
|--------------------|---------|---------------|---------------|-------------------|---------|---------------|---------------|-------------------|
| | Control | 6PPD | PPD-C18 | 6PPD / PPD-C18 | Control | 6PPD | PPD-C18 | 6PPD / PPD-C18 |
| | | | | | + wax | + wax | + wax | + wax |
| Mixed / Uncured | < 0.01 | 1.42 (95%) | 1.01 (69%) | 1.16 (78%) | < 0.01 | 1.41 (95%) | 0.99 (68%) | 1.10 (75%) |
| Cured | < 0.01 | 1.26 | 0.89 | 1.05 | < 0.01 | 1.24 | 0.90 | 1.02 |
| 1 cycle | < 0.01 | n.d. | n.d. | n.d. | < 0.01 | 0.94 | 0.78 | 0.81 |
| 3 cycles | < 0.01 | n.d. | n.d. | n.d. | < 0.01 | 0.61 | 0.66 | 0.69 |
| 4 cycles | < 0.01 | n.d. | n.d. | n.d. | < 0.01 | 0.48 | 0.57 | 0.52 |
| 3 months | < 0.01 | 0.82 | 0.69 | 0.77 | < 0.01 | 0.90 | 0.79 | 0.82 |
| 6 months | < 0.01 | 0.46 | 0.51 | 0.52 | < 0.01 | 0.67 | 0.71 | 0.69 |
| 12 months | < 0.01 | 0.13 | 0.24 | 0.22 | < 0.01 | 0.22 | 0.45 | 0.40 |

* n.d.: not determined

► Data within parentheses are the recovery values (= the amount of 6PPD remaining in the compound after aging, divided by the total amount of 6PPD that was mixed into the compound, times 100%; for these calculations, PPD-C18 is assumed to contain 50% m/m 6PPD).

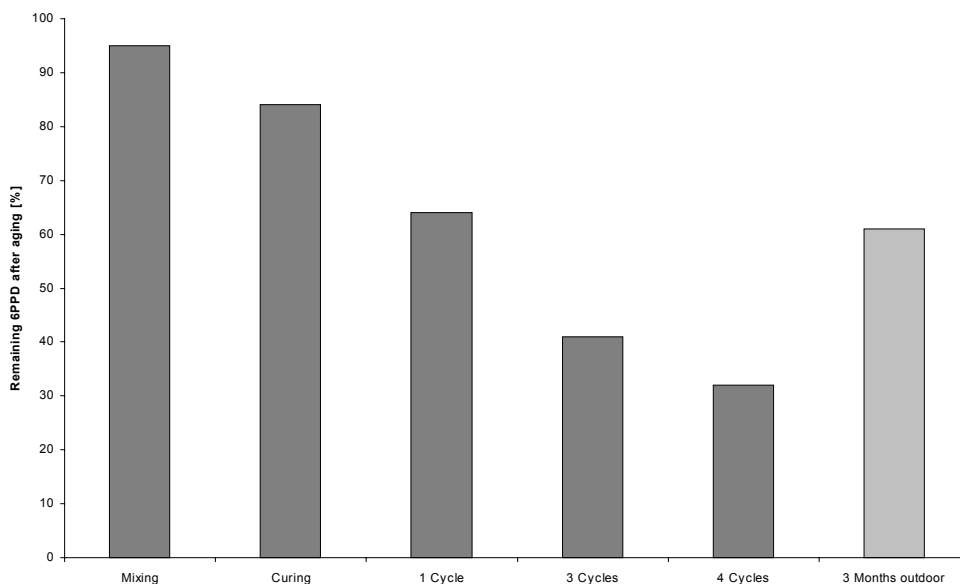


Fig. 4.10: Correlation between outdoor aging and dynamic heat aging.

4.4 Conclusions

The migration behavior of antidegradants in rubber vulcanizates is influenced by the nature of the rubber and filler. Temperature plays a very important role too. Currently available antiozonants such as N-isopropyl-N'-phenyl-p-phenylene diamine (IPPD) and N-(1,3-dimethylbutyl)-N'-phenyl-p-phenylene diamine (6PPD) migrate and finally deplete, either during vulcanization or during service, thus affecting vital properties of rubber articles such as aging and fatigue resistance. Migration of antiozonants is a prerequisite for ozone protection. Fast migration results in a too short-term protection; too slow migration suffers from inadequate initial protection.

In the present chapter a series of test protocols have been developed for screening potential slow migrating antidegradants, providing long lasting antiozonant protection. A good correlation was found between outdoor aging and dynamic heat aging. Although both strain and temperature showed a large effect on the depletion of 6PPD, the effect of temperature was more pronounced.

4.5 References

1. Cottin, G. Peyron, WO 200123464-A1, to Michelin, (2001).
2. F. Cataldo, *Polym. Degrad. Stab.* **72**, (2001), 287.
3. B.H. To, F. Ignatz-Hoover, G. Anthoine, *Rubber & Plastic News*, (October 15, 2001).
4. S.D. Razumovskii, L.S. Batashova, *Rubber Chem. Technol.* **43**, (1970), 1340.
5. D.S. Lederer, M.A. Fath, *Rubber Chem. Technol.*, **54**, (1981), 415.
6. H.W. Engels, H. Hammer, D. Brück, W. Redetzky, *Rubber Chem. Technol.* **62**, (1989), 609.
7. J. C. Ambelang, R.H. Kline, O.M. Lorenz, C.R. Parks and C. Wadelin, *Rubber Chem. Technol.* **36**, (1963), 1497.
8. W. Hofmann, "Rubber Technology Handbook", Hanser Publishers, Munich, (1989), 273.
9. J.C. Andries, C.K. Rhee, R.W. Smith, D.B. Ross, H.E. Diem, *Rubber Chem. Technol.* **52**, (1979), 823.
10. S.S. Choi, *J. Appl. Polym. Sci.*, **65**, (1997), 117.
11. S.S. Choi, *J. Appl. Polym. Sci.* **68**, (1998), 1821
12. E.H. Andrews and M. Braden, *J. Appl. Polym. Sci.*, **6**, (1962), 449.
13. J.J. Luechen, B.H. To, G.H. Kuhls, paper presented at a meeting of the Plastics and Rubber institute, Canberra, Australia, (October 1-4, 1980).
14. S.D. Razumovskii and L.S. Batashova, *Rubber Chem. Technol.*, **43**, (1970), 1340.
15. E.R. Erickson, R.A. Berntsen, E.L. Hill and P. Kusy, *Rubber Chem. Technol.*, **32**, (1959), 1062.
16. S.W. Hong, P.K. Greene, C.Y. Lin, *Tire Technol. Int.*, (2000), 59.
17. S.A. Pushpa, P. Goonetilleke, *Rubber Chem. Technol.*, **68**, (1995), 705.
18. S.W. Hong, *Elastomer* **34**, No. 2, (1999), 156.
19. R.N. Datta, A.G. Talma, WO 01/68761 A1, to Flexsys (2001).
20. S.M. Kavun, Yu.M. Genkina, V.S. Filipov, *Kauch. Rezina* **6**, (1995), 10.
21. P. Lehocky, L. Syrovy, S.M. Kavun, *RubberChem'01*, Brussels, paper 18 (April 3-4, 2001).
22. S.S. Choi, *J. Appl. Polym. Sci.*, **81**, (2001), 237.
23. Ellis and G. N. Welding, *Rubber Chem. Technol.*, **37**, (1964), 571.
24. P.J. Flory and J. Rehner, *J. Chem. Phys.*, **11**, (1943), 521.
25. Saville and A. A. Watson, *Rubber Chem. Technol.*, **40**, (1967), 100.
26. M. L. Selker and A.R. Kemp, *Ind. Eng. Chem.*, **36**, (1944), 20.
27. R.N. Datta and J.C. Wagenmakers, *J. Polym. Mat.*, **15**, (1998), 370.
28. R.N. Datta and F.A.A. Ingham, *Kautschuk Gummi Kunstst*, **52**, (1999), 758.
29. A.H.M. Schotman, P.J. C. van Haeren, A.J.M. Weber, F.G.H. van Wijk, J.W. Hofstraat, A.G. Talma, A. Steenbergen and R.N. Datta, *Rubber Chem. Technol.* **69**, (1996), 727.

Chapter 5

Evaluation of slow release antidegradants in typical passenger and truck tire sidewall compounds

Currently available antiozonants such as N-isopropyl-N'-phenyl-p-phenylene diamine (IPPD) and N-(1,3-dimethylbutyl)-N'-phenyl-p-phenylene diamine (6PPD) migrate either during vulcanization or during service, thus affecting vital properties such as aging protection and fatigue resistance. Migration is a prerequisite condition for ozone protection, but migration at high speed only provides short-term protection and gives insufficient long-term protection.

It has been a challenge to develop a slow migrating / diffusion antiozonant providing an extended antiozonant protection.

In this chapter a comparison has been made with regard to migration and protection against heat, ozone and flexing of antidegradants such as 6PPD, IPPD and 18 newly synthesized products in typical passenger tire sidewall compounds using the test protocols developed in Chapter 4. The combination of 6PPD and the stearic acid salt of 6PPD (PPD-C18) provides longer lasting and better appearance of tire black sidewalls. Physical and dynamic properties are better retained in the presence of this newly developed antidegradant.

PPD-C18 acts as a slow release compound for 6PPD, having a slower migration rate compared to 6PPD and IPPD. The corresponding protection mechanism against ozone of this antiozonant is therefore similar to that of 6PPD.

5.1 Introduction

There are numerous models outlined in literature describing ozone protection of rubber both under static and dynamic environments.^{1,2} To achieve sufficient ozone protection under static environments, waxes are preferred: paraffinic wax for temperatures below 40°C and microcrystalline wax for temperatures above 40°C. However, rubber articles face dynamic environments and hence waxes alone cannot protect the article from ozone attack. For dynamic applications, chemical antiozonants have been developed and are widely used today. The mechanism of protection is

A part of this work has been presented at the ITEC'02, September 10-12, in Akron (paper 14#A) and published in *Kautsch. Gummi Kunstst.*, **55**, (2003), 310.

migration to the surface and reaction with ozone and thereby keeping the rubber unattacked.³

The speed of migration of antiozonants plays a dominant role in protection against ozone. Several reports indicate however that diffusion is not the sole criterion.⁴ Also the products formed by reaction with ozone are excellent and effective antiozonants themselves. Currently, the most accepted mechanism of antiozonant action is a combination of scavenging and protective film formation.⁵⁻⁷ Therefore, it is obvious that the major characteristics required for antiozonant properties are migration to the surface of a rubber vulcanizate and reactivity towards ozone.

Although, conventional antidegradants as N-(1,3-dimethylbutyl)-N'-phenyl-phenylenediamine (6PPD) are still the most widely used antidegradants in rubber, there is a trend and demand for longer-lasting as well as non-staining products.⁸ The present research was therefore directed to develop slow diffusion antiozonants with the aim to protect rubber articles for longer duration and to provide longer lasting tire black sidewalls with better appearance.⁹ In Chapter 3 the development of high molecular weight products based on 4-amino-diphenylamine (4-ADPA) and 6PPD by exploiting various synthetic routes was described. The evaluation of these products is described in the present chapter. A comparison will be made with regard to migration and protection against heat, ozone and flexing by antidegradants such as 6PPD, IPPD and a number of the new materials in typical tire compounds using the test protocols developed in Chapter 4.

5.2 Experimental

5.2.1 Materials

The type and source of ingredients used in the rubber compounds are described below:

NR SMR CV 60 (natural rubber with a constant viscosity ML(1+4) 100°C of 60±5, Wurfain & Co B.V.); BR Buna CB 10 (Butadiene Rubber with a cis-content of 95% and a vinyl content of 1%, Buna Werk Huels); carbon black N-550 (Cabot B.V.); naphthenic oil (Sunthene 4240, Sun Oil Co.); ZnO (Harzsiegel standard); stearic acid (J.T. Baker); Flectol TMQ (Flexsys); Santoflex 6PPD (Flexsys); wax, blend of petroleum (Sunolite 240, Witco S.A.); Santocure CBS (Flexsys); Santocure TBBS (Flexsys); sulfur (J.T. Baker); Santoflex IPPD (Flexsys); Wingstay 100 (Goodyear); Q-Flex QDI (Flexsys); n-heptane (J.T. Baker); toluene (J.T. Baker); piperidine (Acros Organics); hexane-1-thiol (Acros Organics); propane-2-thiol (Acros Organics).

The chemical names, abbreviations and structures of all antidegradants tested are shown in Table 5.1. The synthesis and analysis of all antidegradants was described in Chapter 3.

Table 5.1: Antidegradants tested, variations on 4-ADPA and 6PPD.

| Abbrev. | Chemical name | Structure |
|--------------|---|-----------|
| QDI | Benzamine, N-(4-(1,3-dimethylbutyl)imino)-2,5-cyclohexadiene-1-ylidene) | |
| 6PPD | N-(1,3-dimethylbutyl)-N'-phenyl-p-phenylenediamine | |
| 77PD | N,N'-Bis(1,4-dimethylpentyl)-p-phenylenediamine | |
| IPPD | N-isopropyl-N'-phenyl-p-phenylenediamine | |
| Wingstay 100 | mixture of diaryl p-phenylene diamines | |
| TDI-6PPD | 2,4-bis(N'-(1,3-dimethylbutyl)-N"-deiphenylaminophenyl)ureido)toluene | |
| TDI-ADPA | 2,4-bis(N'-phenylaminophenyl)ureido)toluene | |
| 4Asi-Ph | ADPA-N-phenyl-citraconimid | |
| ADPA-B | N,N-Phenyl benzoyl-N-Phenyl p-phenylenediamine | |
| ADPA-C | N,N-Phenyl methylene benzoyl-N-Phenyl p-phenylenediamine | |
| SPPD | N-Phenyl-N'-(1-phenylethyl)-1,4-benzenediamine | |
| DT-P-ADPA | 3,3'-Dithiobis((4-phenylaminophenyl)propanamide | |

Table 5.1: Materials tested (continued).

| Abbrev. | Chemical name | Structure |
|-----------|--|-----------|
| DT-S-ADPA | 2,2'-Dithiobis((phenylamino)phenyl)benzamide | |
| ADPA-pol | 3-(4-(Phenylamino)phenylamino)butanoic acid, polymer | |
| ADPA-Bred | 1,2-Diphenyl-2-(4-(phenylamino)phenylamino)ethanol | |
| PPD-AA | PPD-salt of acetic acid | |
| PPD-HA | PPD-salt of heptanoic acid | |
| PPD-C18 | PPD-salt of stearic acid | |
| PPD-BA | PPD-salt of benzoic acid | |
| PPD-MSA | PPD-salt of methyl sulfonic acid | |
| PPD-SA | PPD-salt of succinic acid | |
| PPD-ADA | PPD-salt of adipic acid | |
| PPD-FA | PPD-salt of fumaric acid | |
| PPD-TA | PPD-salt of tartaric acid | |
| PPD-PA | PPD-salt of phthalic acid | |
| PPD-SA | PPD-salt of methyl sulfonic acid | |

5.2.2 Formulations, mixing and curing

The compound formulations are shown in Tables 5.2 to 5.4. The recipes in Tables 5.2 and 5.3 are based on a typical passenger tire sidewall formulation, the one in Table 5.4 on a typical truck tire sidewall formulation. There is a trend and demand for long lasting and non-staining antidegradants in both types of tires. The main difference between the two recipes is the blend of NR and BR for the passenger tire sidewalls, while for truck tire sidewalls pure NR is applied. It was considered useful to include both sorts of sidewalls in this study to somehow cover both applications. All the ingredients except sulfur and accelerators were mixed in a 1.6L internal mixer. Sulfur and accelerator were mixed in on a two-roll mill at 50-65°C according to standard laboratory mixing conditions. The compounds were cured to optimum cure by compression molding at 150°C/t₉₀.

Table 5.2: Passenger tire sidewall formulations mixed for the screening of different antidegradants.

| Ingredients / mixes | 1 Control | 2 6PPD | 3 IPPD 6PPD | 4 W100 6PPD | 5 PPD-C18 - | 6 TDI-PPD 6PPD | 7 TDI-ADPA 6PPD | 8 4Asi-Ph 6PPD | 9 ADPA-B 6PPD | 10 ADPA-C 6PPD |
|---------------------|--------------|-----------|-------------------|-------------------|-------------------|----------------------|-----------------------|----------------------|---------------------|----------------------|
| NR SMR CV | 50.00 | 50.00 | 50.00 | 50.00 | 50.00 | 50.00 | 50.00 | 50.00 | 50.00 | 50.00 |
| BR Buna CB 10 | 50.00 | 50.00 | 50.00 | 50.00 | 50.00 | 50.00 | 50.00 | 50.00 | 50.00 | 50.00 |
| Carbon black N-550 | 50.00 | 50.00 | 50.00 | 50.00 | 50.00 | 50.00 | 50.00 | 50.00 | 50.00 | 50.00 |
| Na.oil Sunth. 4240 | 6.00 | 6.00 | 6.00 | 6.00 | 6.00 | 6.00 | 6.00 | 6.00 | 6.00 | 6.00 |
| ZnO Harzsiegel St. | 4.00 | 4.00 | 4.00 | 4.00 | 4.00 | 4.00 | 4.00 | 4.00 | 4.00 | 4.00 |
| Stearic acid | 2.50 | 2.50 | 2.50 | 2.50 | - | 2.50 | 2.50 | 2.50 | 2.50 | 2.50 |
| Flectol TMQ-pst | 1.50 | 1.50 | 1.50 | 1.50 | 1.50 | 1.50 | 1.50 | 1.50 | 1.50 | 1.50 |
| Santoflex 6PPD-pst | - | 2.50 | 1.00 | 1.00 | - | 1.00 | 1.00 | 1.00 | 1.00 | 1.00 |
| Wax Sunolite 240 | 2.00 | 2.00 | 2.00 | 2.00 | 2.00 | 2.00 | 2.00 | 2.00 | 2.00 | 2.00 |
| S'cure CBS-grs-2mm | 1.00 | 1.00 | 1.00 | 1.00 | 1.00 | 1.00 | 1.00 | 1.00 | 1.00 | 1.00 |
| Sulfur | 1.20 | 1.20 | 1.20 | 1.20 | 1.20 | 1.20 | 1.20 | 1.20 | 1.20 | 1.20 |
| Santoflex IPPD | - | - | 1.50 | - | - | - | - | - | - | - |
| Wingstay 100 | - | - | - | 1.00 | - | - | - | - | - | - |
| PPD-C18 | - | - | - | - | 5.00 | - | - | - | - | - |
| TDI-6PPD | - | - | - | - | - | 1.50 | - | - | - | - |
| TDI-ADPA | - | - | - | - | - | - | 1.50 | - | - | - |
| 4Asi-Ph | - | - | - | - | - | - | - | 1.50 | - | - |
| ADPA-B | - | - | - | - | - | - | - | - | 1.50 | - |
| ADPA-C | - | - | - | - | - | - | - | - | - | 1.50 |

| Ingredients / mixes | 11 SPPD 6PPD | 12 DT-P-ADPA 6PPD | 13 DT-S-ADPA 6PPD | 14 ADPA-pol 6PPD | 15 ADPA-Bred 6PPD | 16 6QDI 6PPD | 17 PPD-FA 6PPD | 18 PPD-PA 6PPD | 19 PPD-SA 6PPD | 20 PPD-TA 6PPD |
|---------------------|--------------------|-------------------------|-------------------------|------------------------|-------------------------|--------------------|----------------------|----------------------|----------------------|----------------------|
| NR SMR CV | 50.00 | 50.00 | 50.00 | 50.00 | 50.00 | 50.00 | 50.00 | 50.00 | 50.00 | 50.00 |
| BR Buna CB 10 | 50.00 | 50.00 | 50.00 | 50.00 | 50.00 | 50.00 | 50.00 | 50.00 | 50.00 | 50.00 |
| Carbon black N-550 | 50.00 | 50.00 | 50.00 | 50.00 | 50.00 | 50.00 | 50.00 | 50.00 | 50.00 | 50.00 |
| Na.oil Sunth. 4240 | 6.00 | 6.00 | 6.00 | 6.00 | 6.00 | 6.00 | 6.00 | 6.00 | 6.00 | 6.00 |
| ZnO Harzsiegel St. | 4.00 | 4.00 | 4.00 | 4.00 | 4.00 | 4.00 | 4.00 | 4.00 | 4.00 | 4.00 |
| Stearic acid | 2.50 | 2.50 | 2.50 | 2.50 | 2.50 | 2.50 | 2.50 | 2.50 | 2.50 | 2.50 |
| Flectol TMQ-pst | 1.50 | 1.50 | 1.50 | 1.50 | 1.50 | 1.50 | 1.50 | 1.50 | 1.50 | 1.50 |
| Santoflex 6PPD-pst | 1.00 | 1.00 | 1.00 | 1.00 | 1.00 | 1.00 | 1.00 | 1.00 | 1.00 | 1.00 |
| Wax Sunolite 240 | 2.00 | 2.00 | 2.00 | 2.00 | 2.00 | 2.00 | 2.00 | 2.00 | 2.00 | 2.00 |
| S'cure CBS-grs-2mm | 1.00 | 1.00 | 1.00 | 1.00 | 1.00 | 1.00 | 1.00 | 1.00 | 1.00 | 1.00 |
| Sulfur | 1.20 | 1.20 | 1.20 | 1.20 | 1.20 | 1.20 | 1.20 | 1.20 | 1.20 | 1.20 |
| SPPD | 1.50 | - | - | - | - | - | - | - | - | - |
| DT-P-ADPA | - | 1.50 | - | - | - | - | - | - | - | - |
| DT-S-ADPA | - | - | 1.50 | - | - | - | - | - | - | - |
| ADPA-pol | - | - | - | 1.50 | - | - | - | - | - | - |
| ADPA-Bred | - | - | - | - | 1.50 | - | - | - | - | - |
| 6QDI | - | - | - | - | - | 1.50 | - | - | - | - |
| PPD-FA | - | - | - | - | - | - | 1.50 | - | - | - |
| PPD-PA | - | - | - | - | - | - | - | 1.50 | - | - |
| PPD-SA | - | - | - | - | - | - | - | - | 1.50 | - |
| PPD-TA | - | - | - | - | - | - | - | - | - | 1.50 |

| Ingredients / mixes | 21 | 22 | 23 | 24 | 25 | 26 |
|------------------------|----------------|----------------|----------------|-----------------|-----------------|-----------------|
| | PPD-AA 6PPD | PPD-HA 6PPD | PPD-BA 6PPD | PPD-MSA 6PPD | PPD-ADA 6PPD | PPD-C18 6PPD |
| NR SMR CV | 50.00 | 50.00 | 50.00 | 50.00 | 50.00 | 50.00 |
| BR Buna CB 10 | 50.00 | 50.00 | 50.00 | 50.00 | 50.00 | 50.00 |
| Carbon black N-550 | 50.00 | 50.00 | 50.00 | 50.00 | 50.00 | 50.00 |
| Na.oil Sunth. 4240 | 6.00 | 6.00 | 6.00 | 6.00 | 6.00 | 6.00 |
| ZnO Harzsiegel St. | 4.00 | 4.00 | 4.00 | 4.00 | 4.00 | 4.00 |
| Stearic acid | 2.50 | 2.50 | 2.50 | 2.50 | 2.50 | 2.50 |
| Flectol TMQ-pst | 1.50 | 1.50 | 1.50 | 1.50 | 1.50 | 1.50 |
| Santoflex 6PPD-pst | 1.00 | 1.00 | 1.00 | 1.00 | 1.00 | 1.00 |
| Wax Sunolite 240 | 2.00 | 2.00 | 2.00 | 2.00 | 2.00 | 2.00 |
| S'cure CBS-grs-2mm | 1.00 | 1.00 | 1.00 | 1.00 | 1.00 | 1.00 |
| Sulfur | 1.20 | 1.20 | 1.20 | 1.20 | 1.20 | 1.20 |
| PPD-AA | 1.50 | - | - | - | - | - |
| PPD-HA | - | 1.50 | - | - | - | - |
| PPD-BA | - | - | 1.50 | - | - | - |
| PPD-MSA | - | - | - | 1.50 | - | - |
| PPD-ADA | - | - | - | - | 1.50 | - |
| PPD-C18 | - | - | - | - | - | 1.50 |

Table 5.3: Passenger tire sidewall formulations mixed for determination of the migration characteristics of different antidegradants.

| Ingredients / mixes | 27 | 28 | 29 | 30 |
|------------------------|---------|-------|---------|-------|
| | Control | 6PPD | PPD-C18 | IPPD |
| NR SMR CV | 50.00 | 50.00 | 50.00 | 50.00 |
| BR Buna CB 10 | 50.00 | 50.00 | 50.00 | 50.00 |
| Carbon black N-550 | 50.00 | 50.00 | 50.00 | 50.00 |
| Na.oil Sunth. 4240 | 6.00 | 6.00 | 6.00 | 6.00 |
| Zinc oxide | 4.00 | 4.00 | 4.00 | 4.00 |
| Stearic acid | 2.50 | 2.50 | 2.50 | 2.50 |
| Santoflex 6PPD | - | 4.00 | - | - |
| Santoflex 6PPD/C18 | - | - | 7.80 | - |
| Santoflex IPPD | - | - | - | 3.40 |
| Santocure CBS | 0.80 | 0.80 | 0.80 | 0.80 |
| Sulfur | 2.00 | 2.00 | 2.00 | 2.00 |

Note: Compounds contain equimolar amounts of PPD.

Table 5.4: Truck tire sidewall formulations mixed for determination of the mechanical properties.

| Ingredients / Mixes | 31 Control | 32 6PPD | 33 6PPD/PPD-C18 |
|------------------------|---------------|------------|--------------------|
| NR SMR CV | 100.00 | 100.00 | 100.00 |
| Carbon black N-550 | 50.00 | 50.00 | 50.00 |
| Na.oil Synth. 4240 | 10.00 | 10.00 | 10.00 |
| Zinc oxide | 3.00 | 3.00 | 3.00 |
| Stearic acid | 2.00 | 2.00 | 2.00 |
| Wax Sunolite 240 | 1.00 | 1.00 | 1.00 |
| Santoflex PPD-C18 | - | - | 1.00 |
| Santoflex 6PPD | - | 2.00 | 1.00 |
| Santocure TBBS | 0.60 | 0.60 | 0.60 |
| Sulfur | 2.00 | 2.00 | 2.00 |

5.2.3 Aging of vulcanized compounds

Static heat aging:

Test pieces were aged in an air circulation oven for 14 days at 70°C. Samples were kept for 24 hours at room temperature before final measurements.

Dynamic heat aging:

Rubber test pieces (2mm thick) were flexed on a Monsanto fatigue tester for 24 hours, at 23°C, 1.67Hz and 10% strain. After the flexing, bloom was removed with acetone (not extracted but wiped off with a tissue that was saturated with acetone). Subsequently, the test pieces were aged in an air circulation oven for 14 days at 70°C. This procedure was developed in Chapter 4.

5.2.4. Migration

Migration of antidegradants was studied using the static migration test protocol described in Chapter 4.^{10,11}

5.2.5 Testing of mechanical properties

The effect of antidegradants on long-term protection of rubber networks was studied by determining the stress-strain properties, resistance against fatigue to failure and ozone, and distribution of crosslink types, before and after static and dynamic heat aging as described in Chapter 4.

5.2.6 Analytical techniques

GC/FIA-MS

The amount of 6PPD present in the dichloromethane extractables of the rubber vulcanizates was quantified using a capillary gas chromatograph equipped with a split injector and a flame ionization detector. Identification of the different peaks was done by FIA-MS using the Platform-II quadrupole ex Micromass. In positive ESI, components should give $[M + H]^+$ or $[M + Na]^+$ adducts, so m/z values of $M + 1$ or $M + 23$ are expected to be formed. Ionization was done by electrospray positive/negative (scan range 200-1500 Da; capillary voltage 3.50kV; HV lens 0.5V; skimmer 5V; Cone voltage 10/30 V/60V; source temperature 60°C). Methanol was used as a carrier solvent.

GC-conditions:

| | |
|------------------|---|
| Column | : fused silica column WCOT, 17m * 0.32 mm ID |
| Stationary phase | : Sil 5 CB, 100% polydimethylsiloxane, crosslinked |
| Film thickness | : 0.4 μ m |
| Injector | : Split, 250°C |
| Detector | : FID, 330°C |
| Temp. program | : 120°C (1 min.) $\xrightarrow{10^\circ\text{C}/\text{min.}}$ 320°C (25 min.) |

5.3 Results and discussion

The effect of the various antidegradants on the physical mechanical properties was studied making use of a typical passenger tire and truck tire sidewall compound. Compounds were tested before and after the dynamic aging test protocol, as developed in Chapter 4.¹² The following properties were determined: stress-strain properties, protection against ozone attack and resistance against fatigue. The results are described in the next two sections. The evaluation of different antidegradants is described in section 5.3.1; further study of the mechanism of PPD-C18, which appeared to be the most promising long lasting antiozonant of all the tested molecules, is described in section 5.3.2.

5.3.1 Evaluation of potential long lasting antidegradants

The effect of the antidegradants on the physical mechanical properties was studied in a typical passenger tire and truck tire sidewall compound, before and after heat aging and a dynamic aging test protocol (method 2). The compositions of the tested compounds are shown in Table 5.2 to 5.4. A comparison was made between 2.5 phr 6PPD and mixtures of 1 phr 6PPD and 1.5 phr of the newly developed antidegradants. The 6PPD was expected to provide short-term, and the other antidegradants long-term protection against ozone attack. The antidegradant PPD-C18

was also tested in its pure form, in the absence of 6PPD. The compound composition was corrected for the amount of stearic acid added when testing PPD-C18 (see compound 5). A control compound with only 1 phr 6PPD was not included in this study because we tried to develop an antidegradant package of 1 phr 6PPD and 1.5 phr of one of the newly developed antidegradants providing a proper balance between short- and long-term protection.

Curing with sulfur is a process that preferably takes place in an alkaline environment. The higher the alkalinity the lower the scorch time, the faster the cure rate and the higher the delta torque. The higher the acidity the slower the cure rate and the lower the delta torque. The cure data of the mixes are shown fig. 5.1. It is clear from these data, that the different materials behave differently with respect to delta torque as well as cure kinetics. The effect of the PPD's (paraphenylene diamines) on the scorch time can be explained by the alkalinity of these products. The lower delta torque can be explained by a lubricating effect of the PPD's. The antidegradants ADPA-B (9), DT-S-ADPA (13) and PPD-SA (19) appeared to be scorchy and could therefore give problems in processing. The antidegradants ADPA-Bred (15) and PPD-MSA (24) showed a significantly lower delta torque compared to the control compound with 6PPD (2). The lower delta torque observed for compounded PPD-MSA (24) can be explained by the low pKa value of methyl sulfonic acid (pKa = -2.00). It is known that strong acids interfere with the vulcanization mechanism leading to diminished crosslinking effects.^{13, 14}

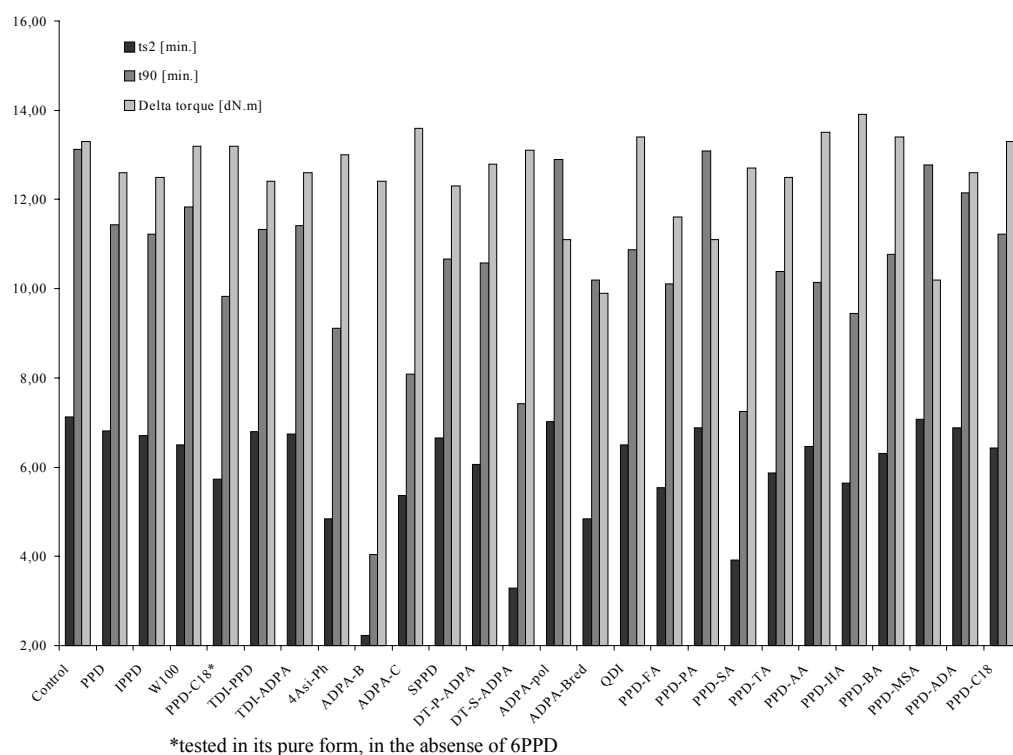
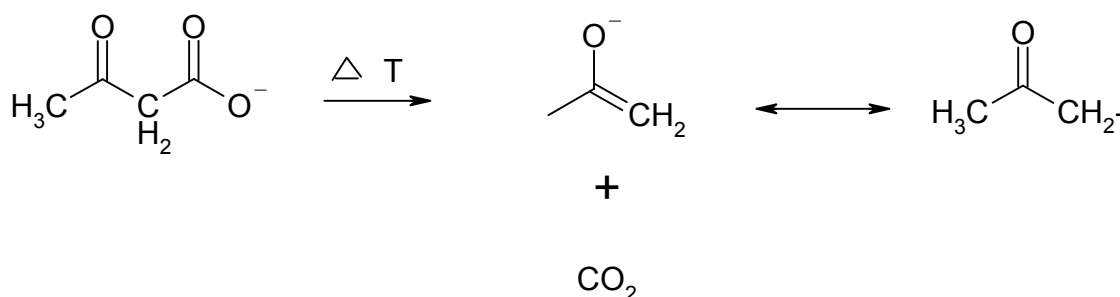


Fig. 5.1: Cure properties (ts₂ [min.], t₉₀ [min.] and Delta torque [dN.m]) determined with the MDR at 150°C/60min.

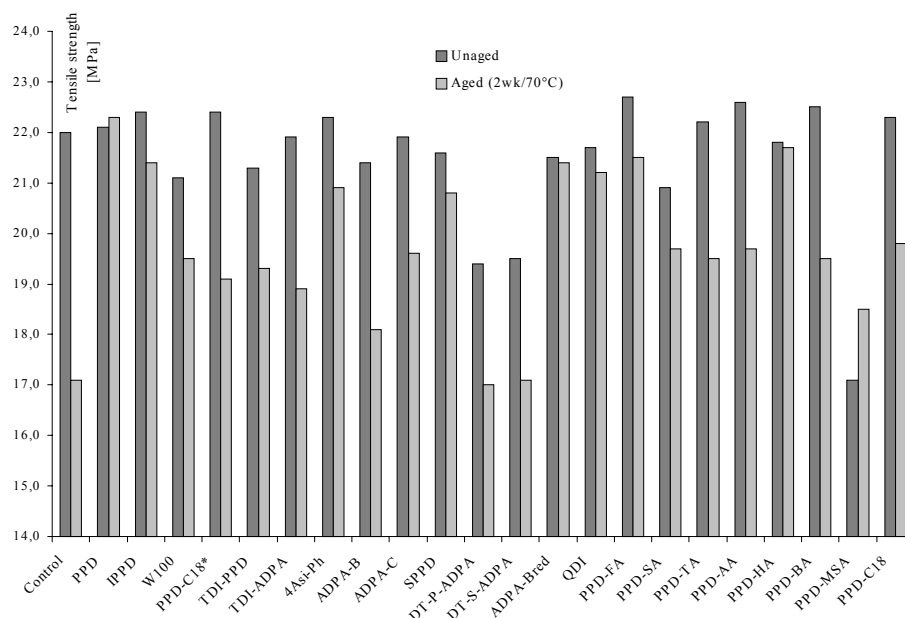
The compounds were subsequently cured to optimum cure t_{90} at 150°C. The effect of the antidegradants on the tensile strength is demonstrated in fig. 5.2. With the exception of a few, such as PPD-MSA (24), DT-P-ADPA (12) and DT-S-ADPA (13), all compounds show almost comparable tensile properties before aging. The tensile strength of the vulcanizate containing PPD-MSA (24) is very poor. This is most probably related to the relatively low delta torque of this compound.

The vulcanizates containing ADPA-pol (14), PPD-PA (18) and PPD-ADA (25) contained entrapped air and were therefore not further tested. As a possible cause, it is known that carboxylic acids like the PA and ADA contained in these antidegradants can decompose at increased temperatures, as described in scheme 5.1.¹⁵ The carbon dioxide, that is formed during this reaction is then entrapped during curing.



Scheme 5.1: Formation of carbondioxide by decomposition of carboxylic acids.

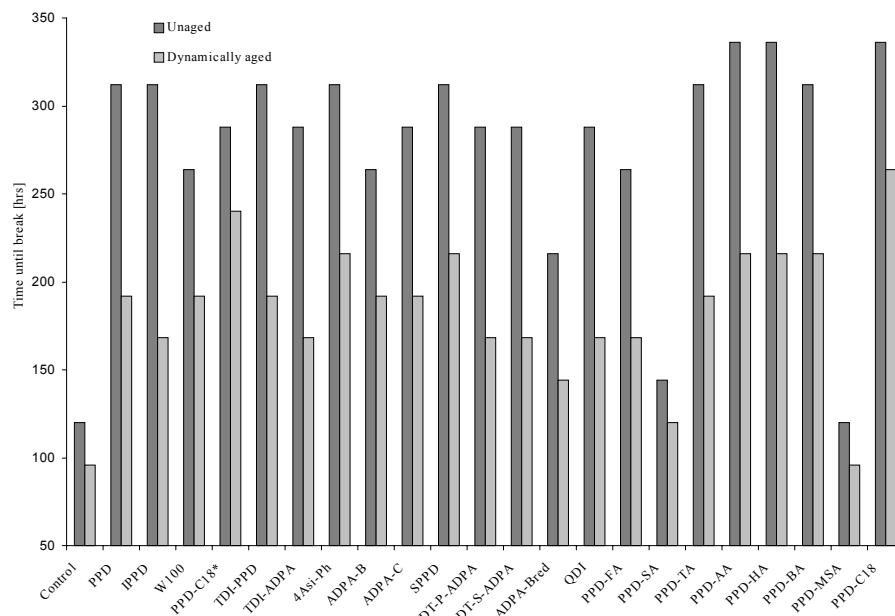
Differences in tensile properties are more pronounced after hot air aging, 2wk/70°C, as shown in fig. 5.2. The control compound with 6PPD (2) shows significantly better tensile strength compared to the control without 6PPD (1). Although none of the tested products shows improved properties compared to 6PPD (2), all of them show a better protection compared to the control without 6PPD (1). Unfortunately, the standard deviation of the tensile test is larger than the differences observed between the tested antidegradants. Therefore, no conclusions can be drawn as yet, regarding differences in antioxidant protection between the tested antidegradants. However, it is already clear that the antidegradants DT-P-ADPA and DT-S-ADPA show hardly any protection against oxygen at all.



* tested in its pure form, in the absence of 6PPD

Fig. 5.2: Tensile strength before and after heat aging (2wk/70°C).

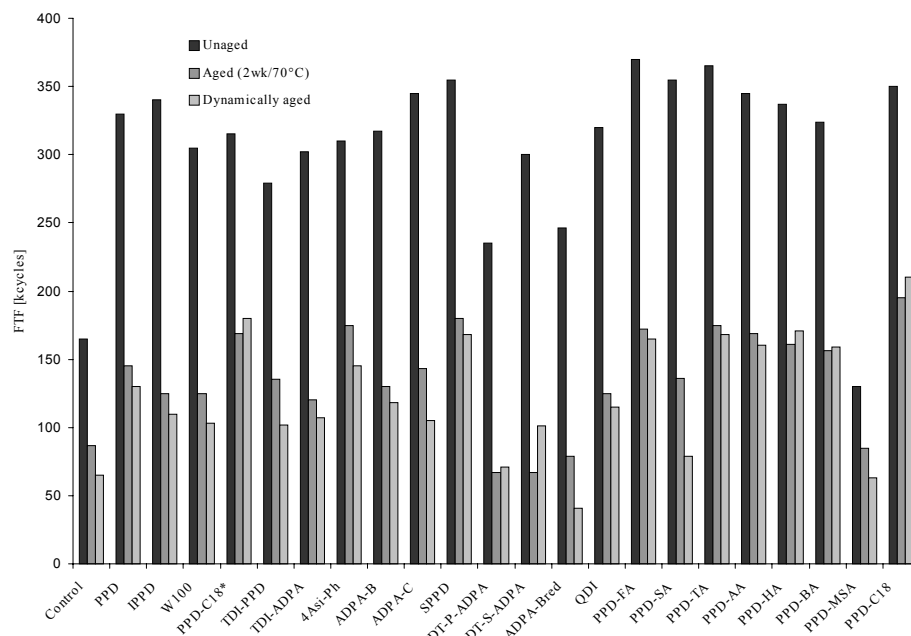
The effect of the antidegradants on the resistance against ozone is plotted in fig. 5.3. Resistance against ozone was determined before and after dynamic heat aging as described in Chapter 4. As expected, the control compound with 6PPD (2) shows much better properties compared to the control without 6PPD (1), both before and after dynamic aging. It is interesting to observe that several of the tested products now show equal or even better properties compared to the control with 6PPD (2). Especially the 6PPD-salts PPD-AA (21), PPD-HA (22), PPD-BA (23) and PPD-C18 (26) show significantly better properties compared to the control with 6PPD (2). The antidegradants SPPD (28) and 4Asi-Ph (8) also show improved protection against ozone attack after dynamic aging. PPD-C18 (5) shows inferior protection against ozone compared to PPD-C18 in the presence of 6PPD (26). This is an indication that some 6PPD is indeed necessary for the short-term protection.



* tested in its pure form, in the absence of 6PPD

Fig. 5.3: Resistance against ozone before and after dynamic heat aging (dynamic ozone test at 40°C, 50pphm ozone, 0.6m/s airflow and 25% strain).

The results of fatigue measurements are shown in fig. 5.4. The fatigue properties were determined before and after aging (hot air and dynamic heat aging). It is observed that the 6PPD-salts PPD-AA (21), PPD-HA (22), PPD-BA (23) and PPD-C18 (26), SPPD (11) and 4Asi-Ph (8), which all showed improved protection against ozone attack in fig. 5.3, now also show improved protection against fatigue. Furthermore, it is clear that the products DT-P-ADPA, DT-S-ADPA, ADPA-Bred and PPD-MSA show hardly any protection against fatigue after the applied aging conditions. A possible explanation for the improved properties of the 6PPD-salts is given in the next section.



* tested in its pure form, in the absence of 6PPD

Fig. 5.4: Resistance against fatigue to failure (FTF) before and after aging.

5.3.2 Investigations into the mechanism of PPD-C18

The mechanism of PPD-C18, shown to be the best long lasting antidegradant of all tested antidegradants, was investigated using different techniques. The compound compositions for these studies are given in Tables 5.3 and 5.4.

5.3.2.1 Migration behavior of PPD-C18

The migration behavior of PPD-C18 was determined by the migration test as described in Chapter 4.^{10,11} A comparison was made with the conventional antidegradants 6PPD and IPPD.

It is known that the types of rubber and filler influence the migration characteristics of antidegradants.¹⁶ The stronger the intermolecular interactions of antidegradants with the polymer matrices, the slower the migration rates. Therefore, the amount of filler and polymer was kept constant throughout this study. The level of antidegradants used was also maintained equal in mmoles (15 mmoles / 100phr

rubber) as can be seen in Table 5.3. The migration characteristics of 6PPD, IPPD and PPD-C18, which were determined at 40°C in a typical NR/BR passenger tire sidewall compound are shown in fig. 5.5. The weight increase of the center plate (in mmoles) is plotted against the square root of the time. The slope of the curve is directly related to the migration rate of the antiozonant. It shows that IPPD migrates faster than 6PPD, which may be explained by the lower molecular weight of IPPD compared to that of 6PPD.¹⁷ The development product PPD-C18 shows a slower migration rate compared to that of 6PPD. The diffusion coefficients for 6PPD, IPPD and PPD-C18 derived from the data in fig. 5.5, using equation 4.1 described in Chapter 4, are given in Table 5.5. Consequently the ranking with respect to increasing diffusion coefficient is: PPD-C18 < 6PPD < IPPD.

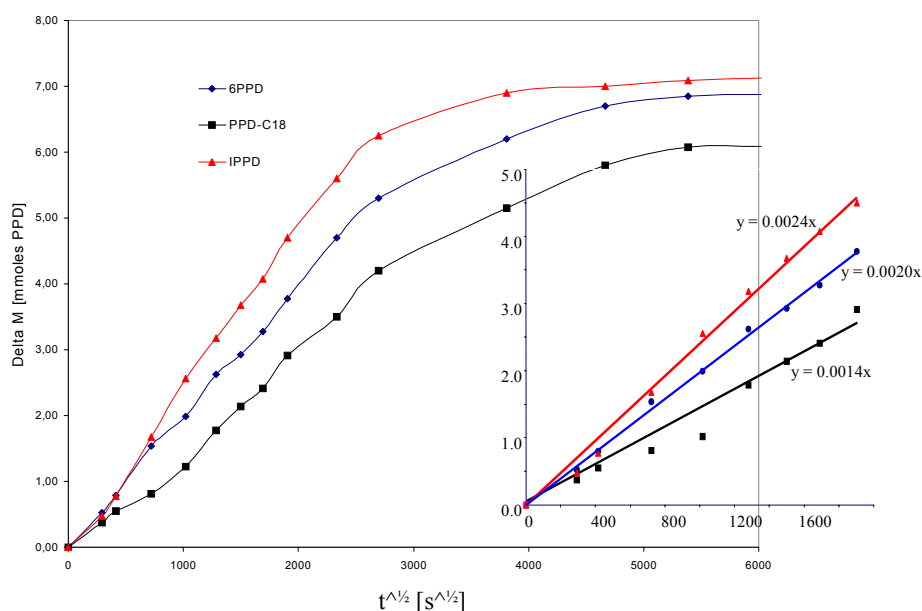


Fig. 5.5: Migration behavior of IPPD (30), 6PPD (28) and PPD-C18 (29) determined at 40°C, in a typical passenger tire sidewall compound.

Table 5.5: Diffusion coefficients of IPPD, 6PPD and PPD-C18 determined at 40°C in a typical passenger tire sidewall compound.

| Tested antiozonant | D [mm ² /sec] at 40°C |
|--------------------|----------------------------------|
| IPPD | 2.23 * 10E-6 |
| 6PPD | 1.66 * 10E-6 |
| PPD-C18 | 1.04 * 10E-6 |

The rubber plates were further analyzed by FIA-MS before and after the migration test, in order to correlate the observations. The middle plates, coded B in fig. 4.8 of Chapter 4, were extracted overnight with dichloromethane. The dichloromethane extractables were subsequently analyzed by FIA-MS for the amount of 6PPD and stearic acid. The peak area obtained by the detector of the mass spectrometer is large for products that can be easily ionized and is concentration dependent. Fig. 5.6 demonstrates, that the center plate B of the PPD-C18 sample specimen contained a lower amount of 6PPD than that of the 6PPD reference. On the other hand, similar amounts of stearic acid were found in the center plate B for all the tested antiozonants, as shown for the Control (27B), 6PPD (28B) and PPD-C18 in fig. 5.7. PPD-C18 is a complex of 6PPD and stearic acid and all the recipes contain 2.5 phr stearic acid. Fig. 5.7 shows no difference in the amount of migrated stearic acid. PPD-C18 and 6PPD were added in equimolar amounts. And, because fig. 5.6 shows that less 6PPD migrated from compounded PPD-C18 (29) than from compounded 6PPD (28), it can be concluded that PPD-C18 is a slow migrating complex. Furthermore, it can be concluded that PPD-C18 slowly releases 6PPD to the surface of the rubber vulcanizate.

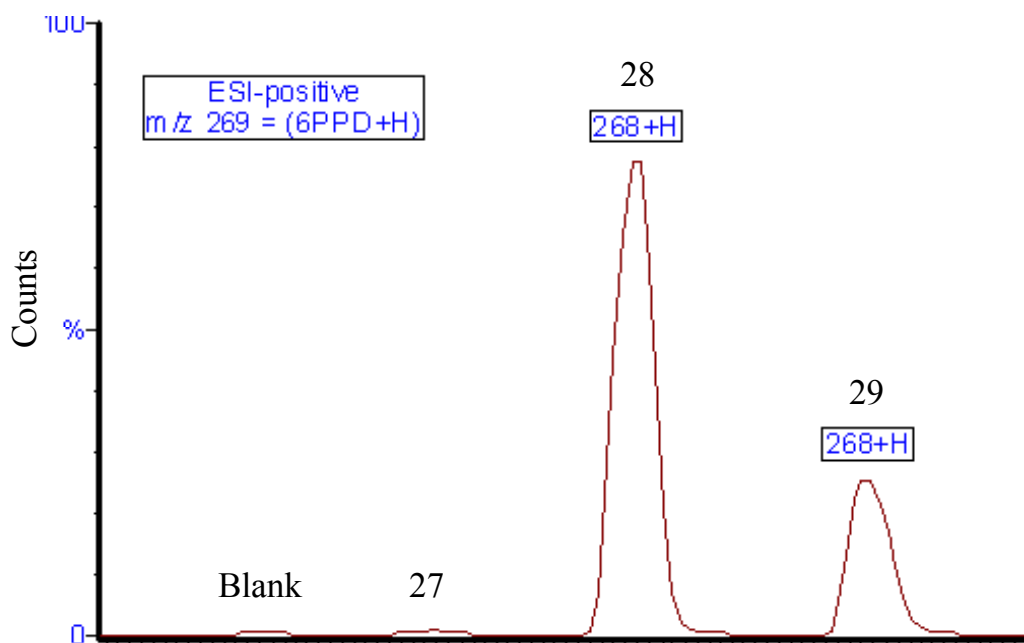


Fig. 5.6: FIA-MS (ESI-positive, 6PPD-H) of the dichloromethane extract of compound 27B (CONTROL), 28B (PPD) and 29B (PPD-C18) after the migration test protocol, at 14 days and 40°C.

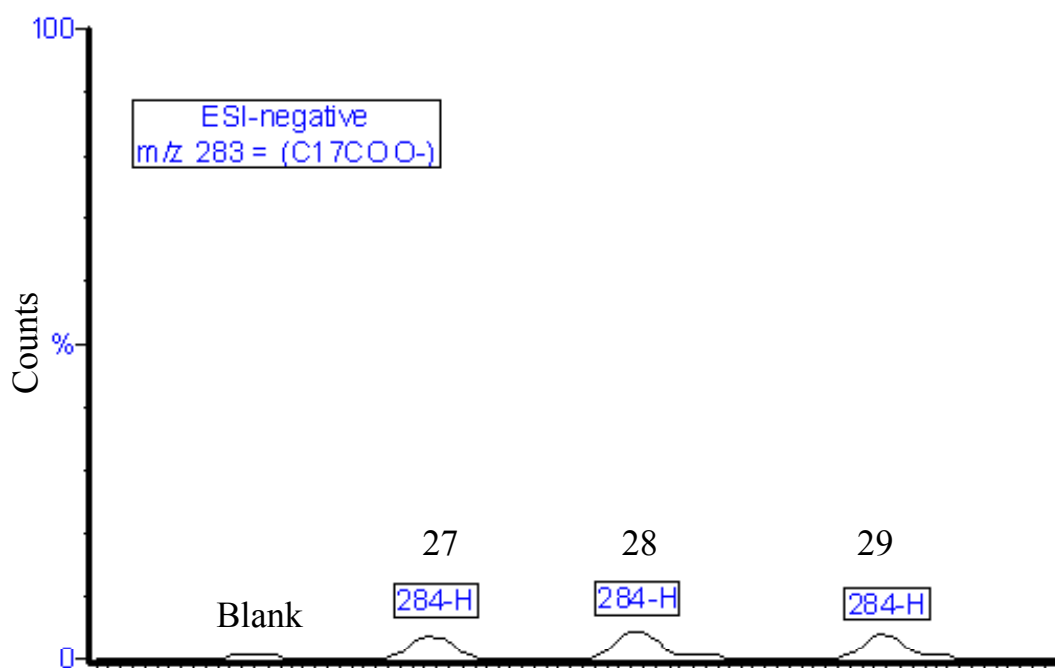


Fig. 5.7: FIA-MS (ESI-negative, C17C00) of the dichloromethane extract of compound 27B (Control), 28B (6PPD) and 29B (PPD-C18) after the migration test protocol, at 14 days and 40°C.

A slow migration rate of antiozonants should result in long-term protection when applied to tires, because they are longer available than conventional antiozonants. Ofcourse, the migration rate should not be too low, because antiozonants are also needed for short-term protection. A combination of a blended parafinic and microcrystalline wax, 6PPD and a slower migrating antiozonant like PPD-C18 is therefore expected to provide a proper combination of short-term protection as well as longer lasting and better appearance of black tire sidewalls. The better appearance was confirmed by tire tests done with tire sidewalls containing either 6PPD and wax or a combination of 6PPD / PPD-C18 and wax. The tire containing the combination 6PPD / PPD-C18 and wax showed less staining, as shown in fig. 5.8.

Tire test: Sidewall Number of kilometers driven: 3000 km

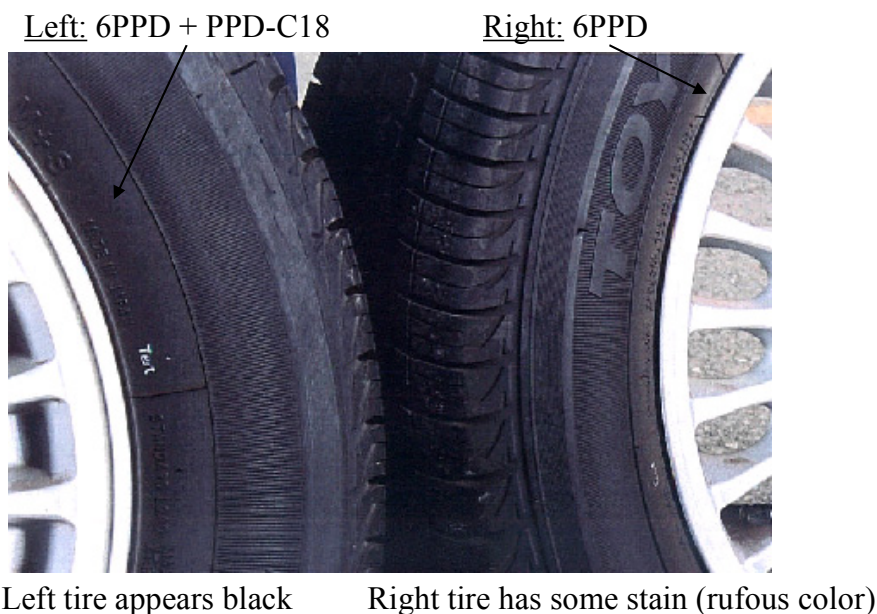


Fig. 5.8: Comparison of staining on tire sidewalls made with 6PPD (right tire) and a combination of 6PPD and PPD-C18 (left tire).

5.3.2.2 Effect of antidegradants on the physical and dynamic properties of a truck tire sidewall compound

The effect of antidegradants on the physical mechanical properties was studied in a typical truck tire sidewall compound before and after aging (static and dynamic heat aging). The compound composition is given in Table 5.4. A comparison was made between 2 phr 6PPD and a mixture of 1 phr 6PPD and 1 phr PPD-C18. The PPD-C18 was not tested in the pure form but in combination with 6PPD, because based on the results shown in § 5.3.1, 6PPD is expected to provide short-term and PPD-C18 longer-term protection against ozone attack. Compounds were mixed and cured to optimum cure t_{90} at 150°C.

As can be seen from fig. 5.9, hardly any difference in cure characteristics could be observed between the compounds with 6PPD and the mixture of 6PPD and PPD-C18. Both compounds show a marginal decrease in scorch time and Delta torque compared to the control compound. The effect of the PPD's on the scorch time can be explained by the pKa value of these products. The lower delta torque can be explained by a small lubricating effect of the PPD's.

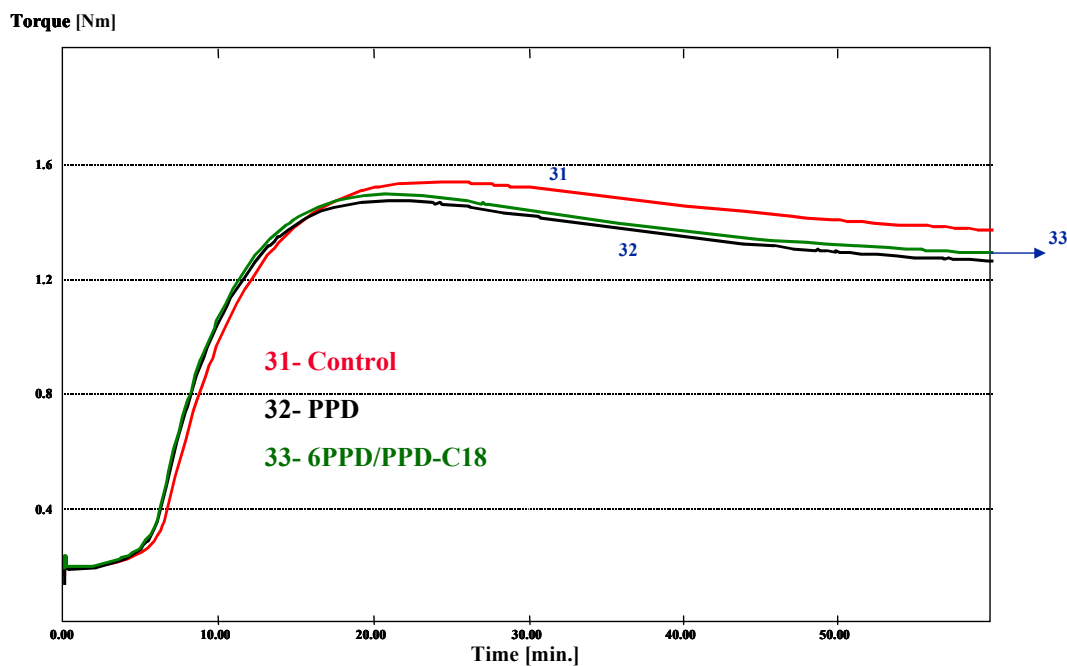


Fig. 5.9: Cure characteristics of the compounds given in Table 5.4, determined with the MDR at 150°C/60min.

The effect of the tested antiozonants in the truck tire sidewall compound on the tensile strength was determined, as shown in fig. 5.10. It is clear that in the presence of the combination 6PPD/PPD-C18 better properties are obtained than with the compound containing 6PPD only (compare mix 32 with mix 33). The difference is most pronounced after dynamic aging. Similar observations were made for the resistance against ozone: fig. 5.11, and for the fatigue properties: fig. 5.12. All in all, the combination PPD-C18 + 6PPD showed better retention of physical and dynamic properties, which is in line with the results obtained in the passenger tire sidewall compound as described in §5.3.1. Further, the surface of the compound containing 6PPD/PPD-C18, mix 33, looked better than the compound containing 6PPD only: mix 32.

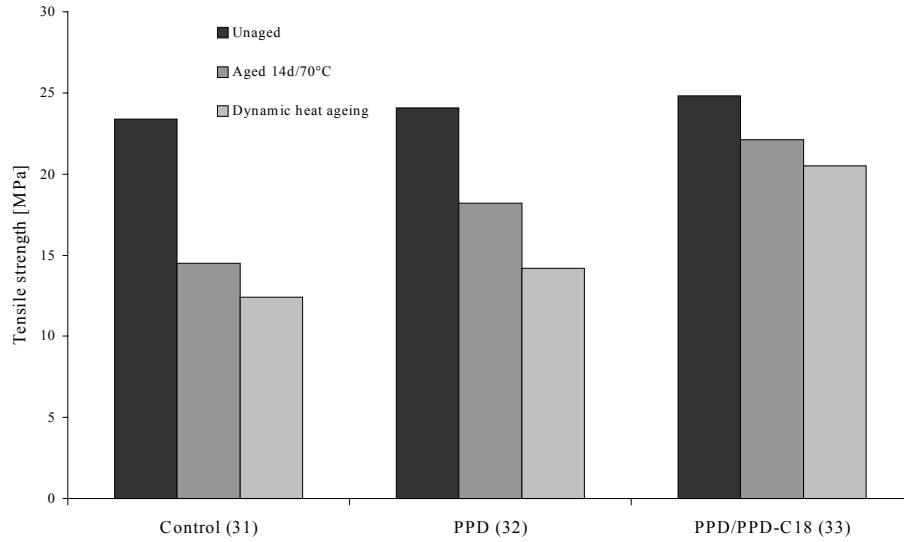


Fig. 5.10: The effect of different antiozonants on the tensile strength, in a truck tire sidewall recipe according to Table 5.4.

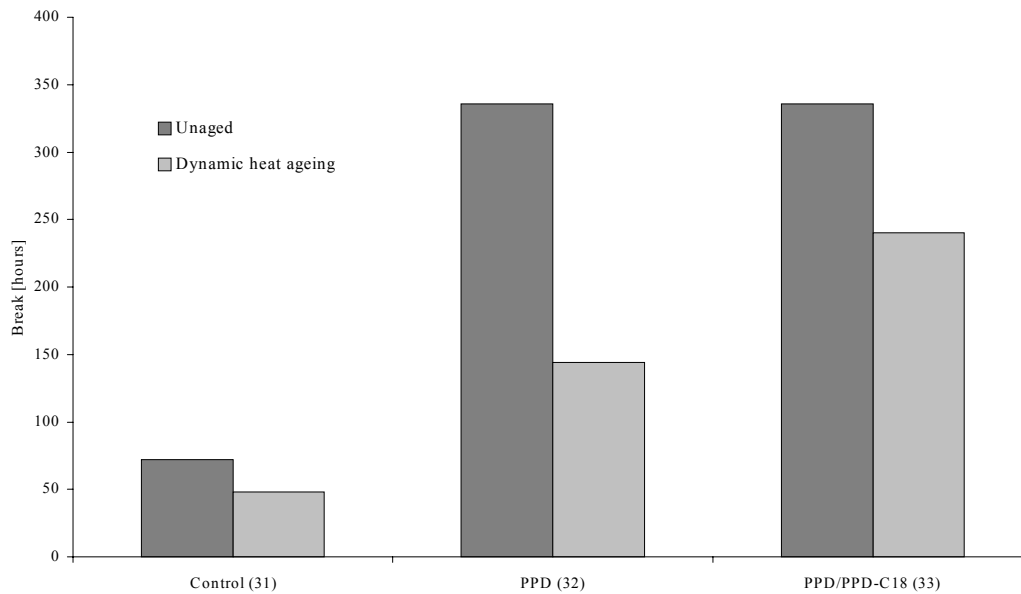


Fig. 5.11: The effect of different antiozonants on the resistance against ozone, in a truck tire sidewall recipe according to Table 5.4.

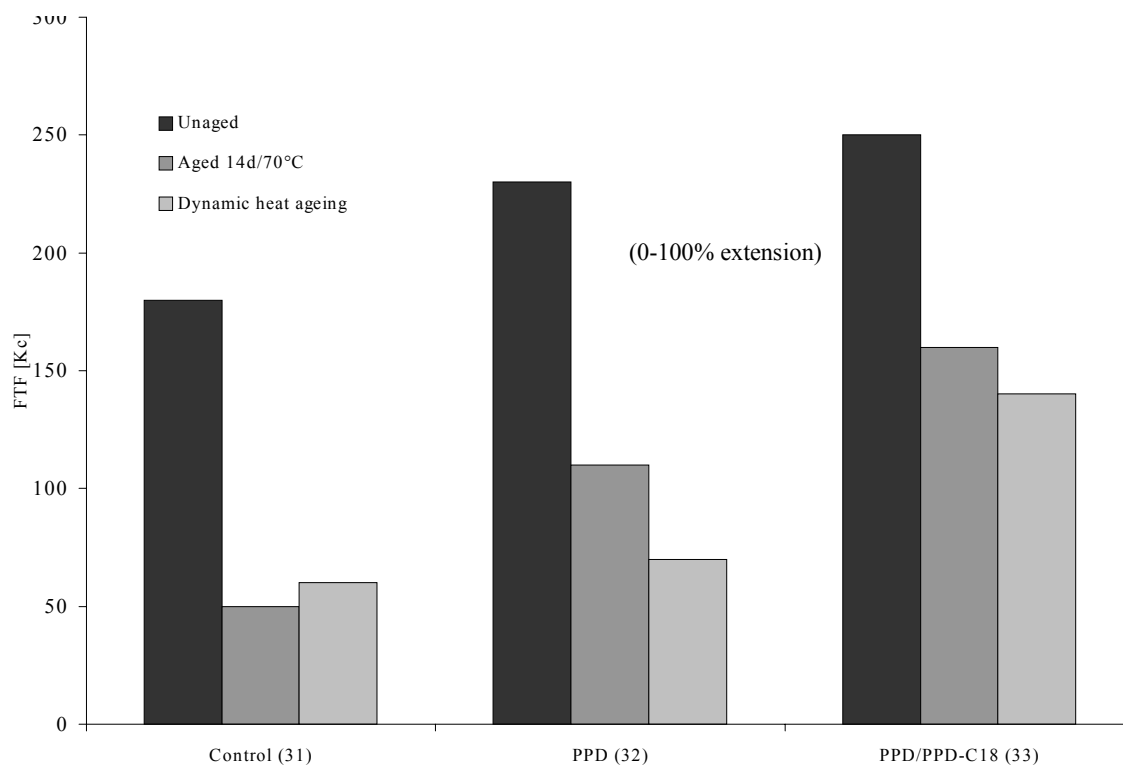


Fig. 5.12: Effect of different antiozonants on fatigue properties, in a truck tire sidewall recipe according to Table 5.4.

In order to correlate the improved physical and dynamic aging properties of the compound containing PPD-C18 with the ones containing 6PPD or the control, it is worthwhile to elucidate the fine structure of the network. Before aging, hardly any difference in crosslink density nor in the distribution of crosslink types can be observed between the vulcanizates with 6PPD and with the mixture of 6PPD and PPD-C18: see Table 5.6. Although the total crosslink density has remained the same after aging, there is a shift to shorter sulfur bridges in all three compounds. The one with the blend of 6PPD and PPD-C18 has best kept its polysulfidic nature. This higher ratio of polysulfidic/monosulfidic crosslinks can be considered to explain the better fatigue properties of this compound. Polysulfidic crosslinks are often quoted to break up under strain and to rearrange with formation of crosslinks at different sites upon removal of the load.¹⁸ The better tensile properties can also be explained by the higher amount of polysulfidic crosslinks, according to investigations done by S. Brown, et al., who postulated that crosslinks capable of lowering the stress peaks give a favorable network with respect to strength properties.¹⁹ The free mobility of chain segments of the rubber macromolecules depends on the relative distance between crosslinks, or the molecular weight between the crosslinks M_c . The larger the molecular weight between crosslinks the larger the possible polymer displacement or slipping during mechanical or thermal loading of the vulcanizate.

Table 5.6: Crosslink density and distribution of crosslink types before and after dynamic heat aging of compounds according to Table 5.4.

| Compounds / Crosslinks# | 31 Control | 32 6PPD | 33 6PPD/PPD-C18 |
|----------------------------|---------------|------------|--------------------|
| <u>Unaged</u> | | | |
| Total | 4.98 | 5.05 | 5.10 |
| Poly-S | 3.92 | 4.05 | 4.10 |
| Di-S | 0.83 | 0.74 | 0.75 |
| Mono-S | 0.23 | 0.26 | 0.25 |
| <u>Dynamic aging</u> | | | |
| Total | 4.70 | 5.20 | 5.25 |
| Poly-S | 2.51 | 2.70 | 3.62 |
| Di-S | 0.60 | 0.52 | 0.70 |
| Mono-S | 1.59 | 1.98 | 0.93 |

Crosslink density expressed in $2M_c^{-1}$ mole/gram rubber * 10^5 ; M_c is the average molecular weight between crosslinks.

5.4 Conclusions

It has been demonstrated that physical and dynamic properties of rubber vulcanizates are better retained in the presence of a combination of 6PPD and PPD-C18, compared to conventional antiozonants such as IPPD and 6PPD. It has also been shown, that a combination of antiozonants: 6PPD + PPD-C18, provides longer lasting and better appearance of tire black sidewalls. The observed differences in physical and dynamic properties can be explained by the structure of the polymer networks before and after aging. There is hardly any difference, neither in crosslink density nor in the distribution of crosslink types, between vulcanized compounds with 6PPD and with a mixture of 6PPD and PPD-C18 before aging. However, after dynamic aging the vulcanizate made with the mixture of 6PPD and PPD-C18 contained a significantly higher amount of polysulfidic and a lower amount of monosulfidic crosslinks. The better tensile and fatigue properties of this vulcanizate after aging must be due to the higher ratio of polysulfidic/monosulfidic crosslinks.

A lower migration rate for PPD-C18 was observed, as reflected in weight increase of the middle plate in the migration test, compared to the conventional antiozonants IPPD and 6PPD. This lower migration rate can be explained by the fact, that the PPD-C18 complex by itself does not or hardly not migrate, but is active as a slow release compound for 6PPD, which then migrates with the usual speed. The lower migration rate of PPD-C18 and thus the higher amount of antiozonant available after aging can explain the improved resistance against ozone observed for the vulcanizate containing the mixture of 6PPD and PPD-C18.

The 6PPD-salts PPD-AA, PPD-HA, and PPD-BA also show a significantly improved protection against ozone attack after dynamic aging, compared to conventional antiozonants like 6PPD and IPPD. The development products SPPD

and 4-Asi-Ph also show improved protection against ozone attack after dynamic aging and can therefore be considered potential long lasting antiozonants.

It has also been shown that the pKa value of the acid used for preparing the 6PPD-salts has a strong effect on the cure properties. 6PPD-salts made from strong acids, like methyl sulfonic acid hamper the cure and are therefore not suitable for the described application. Furthermore, several carboxylic acids, like phthalic acid and adipic acid can decompose upon heating, resulting in the formation of carbon dioxide. This carbon dioxide is entrapped in the rubber vulcanizate during curing. Consequently, the low modulus observed for the vulcanizates containing 6PPD-salts made from these acids, can be explained by the presence of entrapped carbon dioxide.

5.5 References

1. A. Cottin, G. Peyron, WO 200123464-A1, Michelin, (2001).
2. F. Cataldo, Polym. Degrad. Stab. **72**, (2001), 287.
3. S.D. Razumovskii, L.S. Batashova, Rubber Chem. Technol., **43**, (1970), 1340.
4. H.W. Engels, H. Hammer, D. Brück, W. Redetzky, Rubber Chem. Technol., **62**, (1989), 609
5. J. C. Ambelang, R.H. Kline, O.M. Lorenz, C.R. Parks and C. Wadelin, Rubber Chem. Technol., **36**, (1963), 1497.
6. W. Hofmann, "Rubber Technology Handbook", Hanser Publishers, (1989), 273.
7. J.C. Andries, C.K. Rhee, R.W. Smith, D.B. Ross, H.E. Diem, Rubber Chem. Technol., **52**, (1979), 823.
8. S.W. Hong, Elastomer, **34**, No. 2, (1999), 156.
9. R.N. Datta, A.G. Talma, WO 01/68761 A1, Flexsys (2001).
10. S.M. Kavun, Yu.M. Genkina, V.S. Filippov, Kauch. Rezina, **6**, (1995), 10.
11. P. Lehocky, L. Syrový, S.M. Kavun, RubberChem'01, Brussels, Paper #18 (April 3-4, 2001).
12. N.M. Huntink, R.N. Datta, A.G. Talma, paper #14A presented at the ITEC'02 in Akron, (10 September 2002).
13. F.I. Ignatz-Hoover, Rubber World, (August 1999), 24.
14. A.Y. Coran, Rubber Chemistry and Technology, **68**, (1995), 351.
15. E.J. Corey, J. Am. Chem. Soc., **74**, (1952), 5897.
16. Sung-Seen Choi, J. Appl. Polym. Sci, **81**, (2001), 237.
17. D.F. Parra, J. do Rosário Matos, Journal of Thermal Analysis and Calorimetry, **67**, (2002), 287.
18. A.V. Tobolsky, P.F. Lyons, J. Appl. Polym. Sci, **6**, (1968), 1561.
19. P.S. Brown, M. Porter and A.G. Thomas, Kautsch. Gummi Kunstst., **40**, (1987), 17.

Chapter 6

Ozonolysis of model olefins - Efficiency of antiozonants -

In this study, the efficiency of several potential long lasting antiozonants was studied by ozonolysis of model olefins. 2-methyl-2-pentene was selected as a model for natural rubber (NR) and 5-phenyl-2-hexene as a model for styrene butadiene rubber (SBR).

A comparison was made between the efficiency of conventional antiozonants like N-(1,3 dimethylbutyl)-N'-phenyl-p-phenylene diamine (6PPD), N-isopropyl- N'-phenyl-p-phenylene diamine (IPPD) and a mixture of diaryl p-phenylene diamines (Wingstay 100) and some newly synthesized antiozonants. The stearic acid salt of 6PPD (PPD-C18), 2,4,6-Tris(4-(phenylamino)phenyl)-1,3,5-triazinane (ADPAT) and 4-pyrole diphenylamine (PDPA) showed a higher efficiency compared to the conventional antiozonants in both NR as well as SBR model system.

Special attention was paid to the carboxylic acid salts of 6-PPD such as PPD-C18, which has shown good long-term protection of passenger tire sidewall compounds in Chapter 5. It was demonstrated that by varying the chain length: C7, C18 and C22, of the carboxylic acid part of the 6PPD salts, the ozone protection was not influenced under the selected test conditions. The 6PPD-salts made from strong acids like succinic acid (SA) and methyl sulfonic acid (MSA) appeared to be less efficient than PPD-C18.

It was also investigated if the reactions between ozone and the double bonds of the model rubber could be measured on-line by a spectroscopic technique. It was demonstrated that near infrared spectroscopy (NIR) is a suitable technique to study these reactions. FT-Raman looked also a promising technique due to the high response factor of double bonds. However, the addition of p-phenylene diamines (PPDA's) to the sample solution resulted in a strong discoloration (dark brown) and therefore in a high fluorescence background signal. This technique can therefore not be used for the evaluation of staining antiozonants.

6.1 Introduction

Ozone cracking is an electrophilic reaction and starts with the attack of ozone at a location with a high electron density.¹ In this respect unsaturated organic compounds like most rubbers are highly reactive with ozone. The reaction of ozone is a bimolecular reaction where one molecule of ozone reacts with one double bond of

the rubber to form a primary ozonide, as shown in Chapter 2, fig. 2.6. At room temperature, these ozonides cleave as soon as they are formed to give an aldehyde or ketone and a zwitterion. By combination of zwitterions polymeric peroxides can be formed. Due to the retractive forces in stretched rubber, the aldehyde and zwitterion fragments are separated at the molecular-relaxation rate. Therefore, the ozonides and peroxides form at sites remote from the initial cleavage, and underlying rubber chains are exposed to ozone. These unstable ozonides and polymeric peroxides cleave to a variety of oxygenated products, such as acids, esters, ketones, and aldehydes, and also expose new rubber chains to the effects of ozone. The net result is that, when rubber chains are cleaved, they retract in the direction of the stress and expose underlying unsaturation. Continuation of this process results in the formation of the characteristic ozone cracks, as demonstrated in fig. 6.1. The presence of water increases the rate of chain cleavage, which is probably related to the formation of hydroperoxides. The same chemistry occurs on ozonation of rubber, in solution and in the solid state.^{2,3}

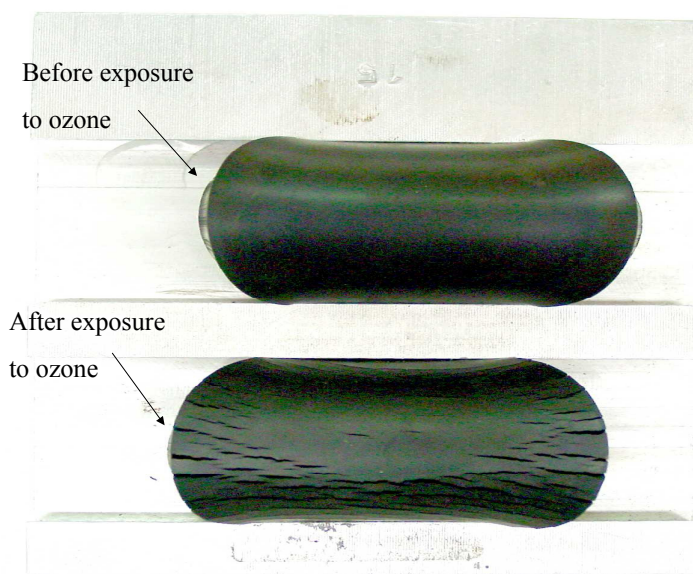


Fig. 6.1: Formation of characteristic ozone cracks after exposure to ozone.

The reaction of ozone with olefinic compounds is very fast.⁴ Substituents on the double bond that donate electrons, increase the rate of reaction while electron-withdrawing substituents slow the reaction down. Thus the rate of reaction with ozone decreases in the following order: polyisoprene > polybutadiene > polychloroprene.⁵ Rubbers can be protected against ozone by using chemical antiozonants and via several physical methods. The chemical antiozonants protect rubber under both static and dynamic conditions, whereas the physical methods are more related towards protection at static conditions.

Chemical antiozonants have been developed to protect rubber against ozone under dynamic conditions. Several mechanisms have been proposed to explain how

chemical antiozonants protect rubber. The scavenging mechanism, the protective film mechanism or a combination of both are nowadays the most accepted mechanisms, as described in Chapter 2.⁵⁻¹⁴

Because rubber, whether vulcanized or not, is generally difficult to investigate by standard analytical and spectroscopic techniques, researchers have attempted to overcome this by looking at isolated network constituents: the concept of Model-Compound Vulcanization (MCV).^{15,16} A low molecular weight model is chosen to represent the reactive unit of the polymeric rubber. This concept has also been chosen for the ozonolysis experiments in this chapter. 5-phenyl-2-hexene was selected as the model for Styrene Butadiene Rubber (SBR). 2-Methyl-2-pentene and squalene were selected as model for Natural Rubber (NR). The structure of the selected models is shown in fig. 6.2.

The choice of an appropriate model compound is determined by the specific properties of the models and by the purpose of the experiments. An elementary disadvantage of low-molecular-weight models such as 2-methyl-2-pentene or 5-phenyl-2-hexene is that they are monofunctional, i.e. they contain only one double bond. Polyfunctional models such as squalene can display reactivity for which more than one double bond is required. Unfortunately, all the double bonds in squalene are trans-configured and not cis-configured as in NR.

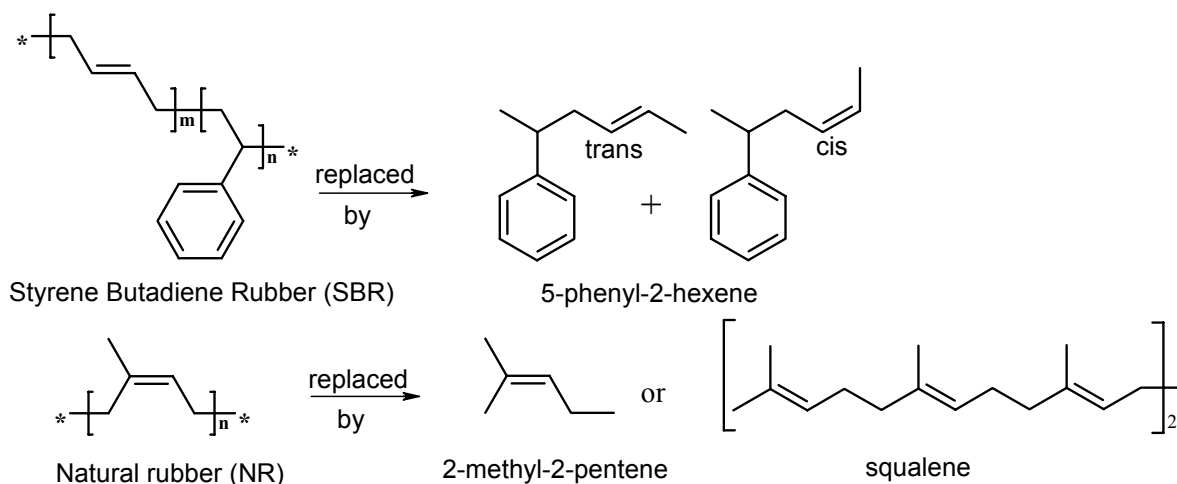


Fig. 6.2: Structure of the model compounds used for NR and SBR.

The first part of this chapter focuses on the determination of the efficiency of different antiozonants by competitive experiments in CH_2Cl_2 . 2-Methyl-2-pentene and 5-phenyl-2-hexene (cis and trans) are selected as models for NR and SBR, respectively. The efficiency of some of the newly synthesized antiozonants is determined and compared to that of conventional antiozonants like 6PPD, IPPD and Wingstay 100. Only the initial reaction of the antiozonant with ozone is rapid; the

resulting ozonized products always react much more slowly. Thus, the number of moles of ozone absorbed by a compound is not necessarily an indication of the effectiveness of the antiozonant. It is only the rate of reaction that is important. The kinetics of the reaction between ozone and the model compound is studied in the presence and the absence of those antiozonants. The kinetics are followed via determination of the concentration of antiozonant and model compound by GC-analysis, before and after treatment with ozone for several time intervals.

The loss of antiozonants, either in a chemical or physical manner, appears to be the limiting factor in providing long-term protection of rubber products. That is why for new antiozonants not only the efficiency of the antiozonants must be evaluated, but one also has to carefully investigate other properties which influence their protective functions in a different manner. For instance the antiozonant's mobility, its ability to migrate, is one of the parameters determining the efficiency of antiozonant action, as already described in Chapter 5.

It is also investigated if the reaction between ozone and the model rubber compound can be followed on-line, by a spectroscopic technique. Both FT-Raman and near infrared spectroscopy are applied for this purpose. These techniques are capable of monitoring the decrease of double bonds and can therefore probably also be used for monitoring rubbers or model rubbers, like squalene, having multiple double bonds. FT-Raman is the preferred spectroscopic technique because it is very sensitive for symmetric vibrations and is non-invasive. These results are described in the Appendix of this chapter.

6.2 Experimental

6.2.1 Materials

Materials used for ozonolysis experiments:

2-methyl-2-pentene (Janssen, assay min. 99%; CAS nr. [625-27-4]); squalene (Janssen, assay 98%; CAS nr. [111-02-4]); dichloromethane (J.T. Baker, assay min. 99.5%; CAS nr. [75-09-2]); 5-phenyl-2-hexene: synthesis see below; potassium iodide (Janssen, assay min. 99.5%; CAS nr. [7758-05-6]); sodium hydroxide (Janssen, assay min. 98%; CAS nr. [1310-73-2]); n-decane (Aldrich, assay min. 99%; CAS nr. [124-18-5]); calcium chloride (Janssen, assay min. 96%; CAS nr. [10043-52-4]).

Materials used for 5-phenyl-2-hexene (SBR model) synthesis:

Ethyl-triphenyl phosphonium bromide (Aldrich, assay min. 99%; CAS nr. [1530-32-1]); n-butyllithium (Acros, 2.5M solution in hexane; CAS nr. [109-72-8]); 3-phenylbutyraldehyde (Aldrich, assay 97%; CAS nr. [16251-77-7]); anhydrous diethylether (J.T. Baker, assay min 99%; CAS nr. [60-29-7]); magnesium sulfate, dried (Janssen, assay min. 99%; CAS nr. [7487-88-9]).

Tested antiozonants:

The chemical name, structure and abbreviation of the tested antiozonants are described in Table 5.1 of Chapter 5. The following commercial antiozonants were tested: 6PPD (Flexsys, assay 95%; CAS nr. [793-24-8]), 77PD (Flexsys, assay 93%; CAS nr. [3081-14-9]), IPPD (Flexsys, assay 95%; CAS nr. [101-72-4]), 6QDI (Flexsys, assay 90%; CAS nr. [52870-46-9]) and Wingstay 100 (Goodyear, mixture of diaryl-p-phenylene diamines; CAS nr. [68953-84-4]); The synthesis and characterization of the other tested new antiozonants was described in Chapter 3.

6.2.2 Synthesis of 5-phenyl-2-hexene (model for SBR)

The SBR-model 5-phenyl-2-hexene was synthesized in two steps via a Wittig reaction, as demonstrated in fig. 6.3.¹⁷ It is very important that the reactor and the glassware used during the synthesis do not contain any traces of water!

25g, 67.4 mmole Triphenyl phosphonium bromide is added into a 1 liter three-necked round bottom flask, which is flushed with nitrogen in order to eliminate traces of water. Then 250ml anhydrous diethylether is added, while stirring the solution. Next, 40 ml butyllithium is added dropwise via a dropping funnel in 60 minutes. The reactor is cooled with ice during the addition of butyllithium. The solution, which becomes orange colored, is stirred for 4 hours at room temperature. Then 15ml 3-phenylbutyraldehyde is added dropwise in 60 minutes. The reactor is again cooled with ice during the addition of 3-phenylbutyraldehyde. A white powder precipitates.

The reaction mixture is refluxed overnight at $T = 40^{\circ}\text{C}$. The reaction product is cooled down to room temperature, filtered, washed with anhydrous diethylether and dried on a rotavapor. The reaction product is washed three times with 100ml water and subsequently dried over magnesium sulfate. The final product is purified by vacuum Kugelrohr distillation; its boiling point is 230°C at 8 mbar. The product was identified by $^1\text{H-NMR}$, see fig. 6.4. The purity was 98%.

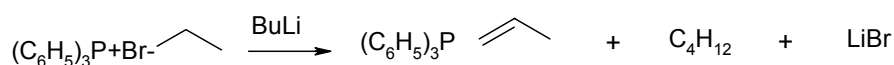
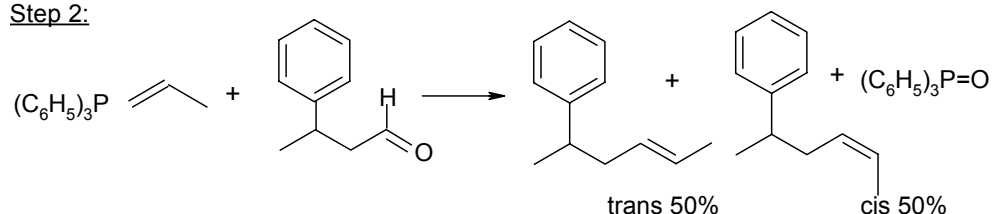
Step 1:Step 2:

Fig. 6.3: Reaction mechanism for the synthesis of 5-phenyl-2-hexene.

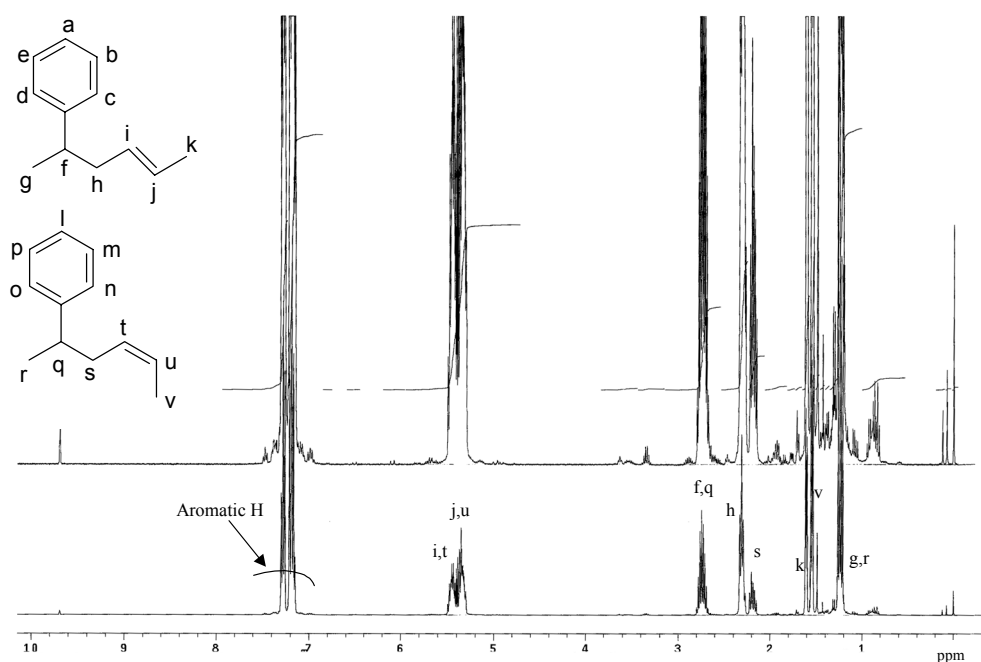


Fig. 6.4: $^1\text{H-NMR}$ spectrum of 5-phenyl-2-hexene determined in CDCl_3 .
 $(^1\text{H-NMR}: \delta 7.1-7.3 \text{ (aromatic H)}; \delta 5.3-5.5 \text{ (i,t,j,u)}; \delta 2.73 \text{ (f,q)}; \delta 2.32 \text{ (h)};$
 $\delta 2.21 \text{ (s)}; \delta 1.61 \text{ (k)}; \delta 1.55 \text{ (v)}; \delta 1.25 \text{ (g,r)}).$

6.2.3 Ozonolysis

Equipment

Experiments were done in the equipment shown in figures 6.5 and 6.6. The ozone generator was used under the conditions: oxygen flow 50 liter/hour and current 3.2 Ampere, which generate an ozone flow of 40g/1000liter oxygen. The oxygen was dried through a saturated calcium chloride solution and a molsieve in order to protect the ozone generator against corrosion.

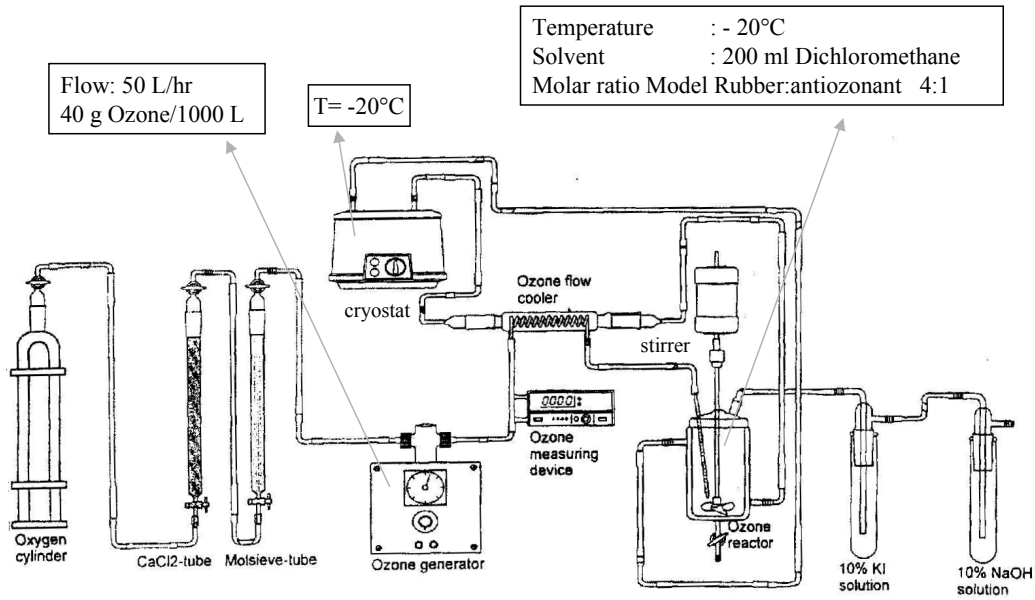


Fig. 6.5: Diagram of the ozonolysis test equipment.

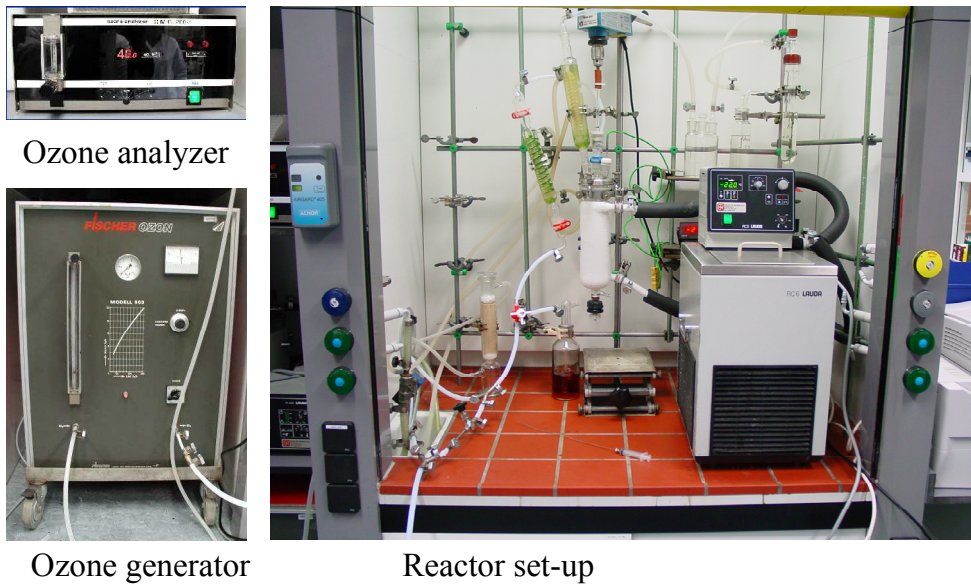


Fig. 6.6: Ozonolysis test equipment.

Procedure

200 ml Dichloromethane is poured into the reactor. The reactor temperature is stabilized at a temperature of -20°C , before starting the ozonolysis. This relatively low temperature is selected in order to prevent evaporation of the low molecular weight model rubbers. A solution of the model rubber, 4g (48 mmole) 2-methyl-pentene or 1.9g (12 mmole) 5-phenyl-2-hexene, 12 mmole antiozonant for testing of the NR-model or 3 mmole for testing of the SBR-model and 1.7g (12 mmole) n-decane for testing of the NR-model or 0.43g (3 mmole) for testing of the SBR-model is injected into the reactor.

The ozone is introduced into the reactor when the ozone flow is stabilized at 40g/l. Samples are taken at several fixed time intervals and analyzed by GC. Samples are taken with a syringe by using a rubber septum. The first sample is taken when the reaction mixture is homogenized, time $t=0$.

6.2.4 Characterization of the ozonolysis products*¹H-NMR*

The structure and purity of the ozonolysis products were characterized using ¹H-NMR spectroscopy. The products were dissolved in deuterated chloroform (Aldrich, 99.8 atom-% D; Cas nr [865-49-6]). ¹H-NMR measurements were performed on a Varian Inova – 400 MHz (Varian) model L 700 spectrometer.

GC-analysis

Samples gathered during the ozonolysis experiments were analyzed by GC in order to quantify the amount of remaining model rubber and antiozonant. n-Decane was used as an internal standard. Measurements were done under the conditions described below:

| | |
|-------------------|---------------------------------|
| Column | : Sil 5 CB |
| Column dimensions | : 17m * 0.32 mm ID |
| Film thickness | : 0.4 μm |
| Injection temp. | : Split, 325 $^{\circ}\text{C}$ |

2methyl-2-pentene:

| | |
|-----------------|--|
| Temp. program | : 35 $^{\circ}\text{C}$ (5 min.) $\xrightarrow{5^{\circ}\text{C}/\text{min.}}$ 80 $^{\circ}\text{C}$ $\xrightarrow{20^{\circ}\text{C}/\text{min.}}$ 320 $^{\circ}\text{C}$ (14 min.) |
| Detection temp. | : FID, 200 $^{\circ}\text{C}$ |

5-phenyl-2-hexene:

| | |
|-----------------|--|
| Temp. program | : 35 $^{\circ}\text{C}$ (5 min.) $\xrightarrow{20^{\circ}\text{C}/\text{min.}}$ 320 $^{\circ}\text{C}$ (21 min.) |
| Detection temp. | : FID, 375 $^{\circ}\text{C}$ |

GC/MS

Identification of the different peaks was done by FIA-MS using the Platform-II quadrupole ex Micromass. In positive ESI, components should give $[M + H]^+$ or $[M + Na]^+$ adducts. Ionization was done by electrospray positive/negative (scan range 200-1500 Da; capillary voltage 3.50kV; HV lens 0.5V; skimmer 5V; Cone voltage 10/30 V/60V; source temperature 60°C). Methanol was used as a carrier solvent.

FT-Raman spectroscopy

FT-Raman measurements were performed on a Kaiser Hololab series 5000 Raman spectrometer. Experiments were done with two different lasers: an external 30 mW HeNe laser, 632.8 nm with filtered probehead, 2.5" focal length lens and an internal 250 mW, 785 nm diode laser with filtered probehead, 1" focal length lens. Spectra were collected with Holograms V3.1 with settings: 1 accumulation, cosmic ray correction, and dark subtraction. Data were evaluated using the Galactic Grams 32 V4.04 software, including Quantbasic.

Near Infra Red spectroscopy

Near Infra Red (NIR) measurements were performed on a Bomem MB160 NIR spectrometer with 3mm-vial holder. The temperature of the vial holder was 95°C. Spectra were collected using the following settings: absorbency mode; resolution 8 cm^{-1} ; 25 scans; region from 4500-10000 cm^{-1} . Data were evaluated using the Galactic Grams 32 V4.04 software, including Quantbasic.

6.3 Results and discussion

The efficiency of several of the newly synthesized antiozonants was determined and compared to that of conventional antiozonants like 6PPD, IPPD and Wingstay 100. The antiozonants were tested in competition experiments with model rubber compounds. It was investigated how fast the tested antiozonant reacts with ozone during ozonolysis, by comparing the decrease of the amount of model rubber to that of the antiozonant. Experiments were performed at model/antiozonant ratios of 4:1. Reactions were followed by GC-analysis of samples obtained after several fixed time intervals.

Because GC-analyses are rather time consuming and because the experiments are disturbed by taking samples, it was investigated if the reactions between ozone and the double bonds of the model rubber can also be followed on-line, by a spectroscopic technique. FT-Raman and NIR spectroscopy were investigated for this purpose.

6.3.1 Optimization of test conditions

Before testing the efficiency of different antiozonants, test conditions had to be optimized. Four experiments were done in order to find out which 2-methyl-2-pentene/6PPD ratio: 4:0, 4:0.5, 4:1 or 4:2, is the most suitable for testing the antiozonant efficiency. The results for 60 min. ozonolysis are shown in Table 6.1. As can be seen from these results, a good protection of the model rubber was obtained in the presence of 6PPD. A much lower amount of 2-methyl-2-pentene did react with ozone when 6PPD was present. Testing at the ratios 4:1 and 4:2 resulted in approximately the same protection of the model rubber, indicating that the 4:1 ratio is close to an optimum. This ratio was therefore selected to test the different antiozonants.

Table 6.1: Remaining amount of 2-methyl-2-pentene (model for NR) and 6PPD antiozonant after 60 minutes ozonolysis.

| Molar ratio 2-methyl-2-pentene / 6PPD [mole / mole] | Remaining 2-methyl-2-pentene [%] | Remaining 6PPD [%] |
|---|--|--------------------------|
| 4 : 0 | 25 | - |
| 4 : 0.5 | 42 | 16 |
| 4 : 1 | 75 | 31 |
| 4 : 2 | 76 | 47 |

6.3.2 Rate of ozonolysis of model rubbers in absence of antiozonants

The SBR-model 5-phenyl-2-hexene was tested at a four times lower concentration compared to the NR-model 2-methyl-2-pentene, because the SBR-model is not commercially available and because the synthesis of this product was rather time consuming. This explains the approximately four times faster disappearance of the SBR-model compared to that of the NR-model, as can be seen from figures 6.7 and 6.8. For this reason, samples were taken every 20 minutes during the 2-methyl-2-pentene experiments and every 5 minutes during the 5-phenyl-2-hexene experiments.

Reaction rates between 2-methyl-2-pentene and 5-phenyl-2-hexene with ozone can be concluded to be the same, when tested in the absence of antiozonants, because there is no competition and because all the ozone that is passed into the reactor does react. The latter can be derived from the fact that no discoloration of the KI-solution behind the ozone reactor was observed during the ozonolysis experiments.

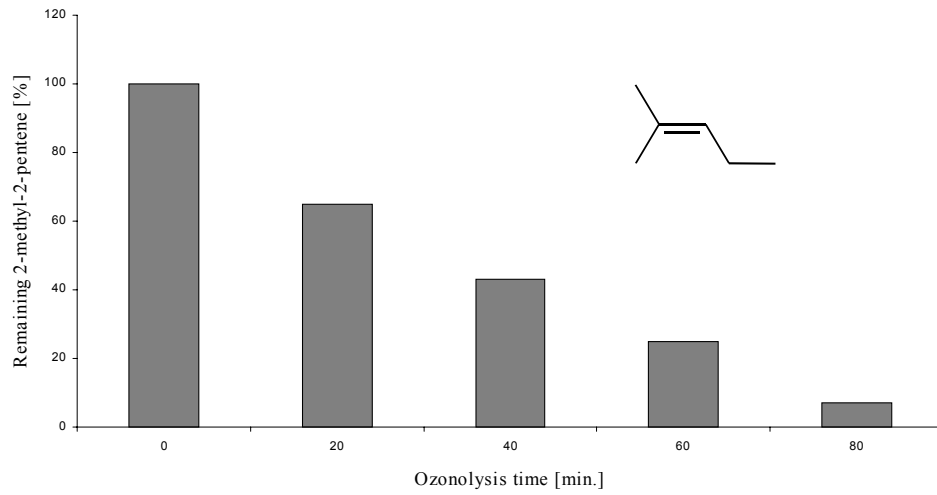


Fig. 6.7: Ozonolysis of the NR-model 2-methyl-2-pentene in absence of antiozonant (40g ozone/1000liter, flow 50 liter/hour).

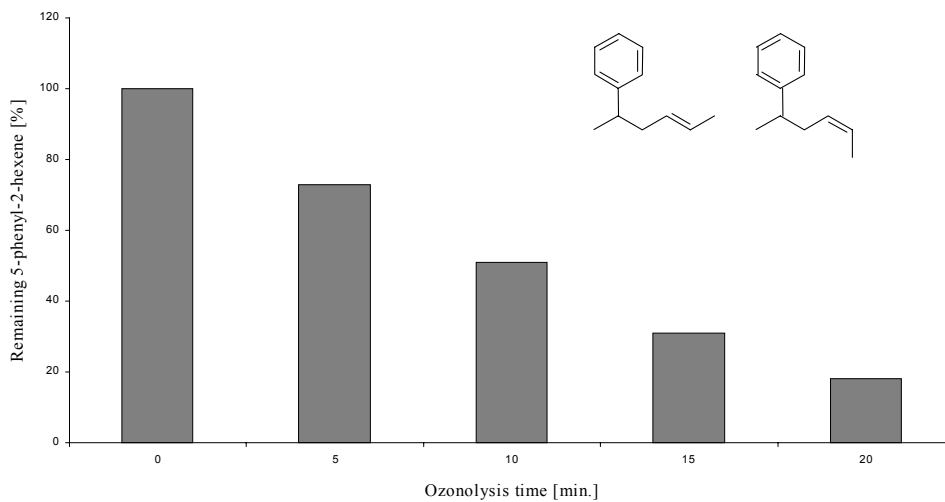


Fig. 6.8: Ozonolysis of the SBR-model 5-phenyl-2-hexene in absence of antiozonant (40g ozone/1000liter, flow 50 liter/hour).

Ozonolysis of 5-phenyl-2-hexene showed, that there is a small difference between reactivity of the cis- and the trans-form. The cis-form appeared to be slightly more reactive. The trans-form is supposed to be more reactive according to Baily.¹⁸ However, Huisgen showed that the cis-form can also be more reactive, when tested in the liquid form.¹⁹ No conclusion could be drawn to explain these differences. No differences between reactivity of the cis- and the trans-form were made during the ozonolysis experiments described in this chapter. The sum of both the cis- and the trans-form is reported as the estimated amount of 5-phenyl-2-hexene.

Measurements were performed at low temperatures (-20°C) in order to minimize evaporation of the model rubbers during ozonolysis, especially for the low boiling NR-model: the boiling point of 2-methyl-2-pentene is 67°C. However, even at this low temperature, approximately 7% of the NR-model evaporated during 80 min. of ozonolysis. This was estimated by passing oxygen into the reactor instead of ozone, at the same flow as used during the ozonolysis experiments. All results tabulated in this chapter are therefore corrected for this value. The SBR-model did not evaporate during the experiment with oxygen.

Several experiments were performed in duplicate in order to estimate the reproducibility of the test. Differences found between duplicate values were approximately 3% for the NR-model and 4% for the SBR-model. The reaction products formed by ozonolysis of the model rubbers were characterized by GC/MS. The products that were formed are shown in fig. 6.9.

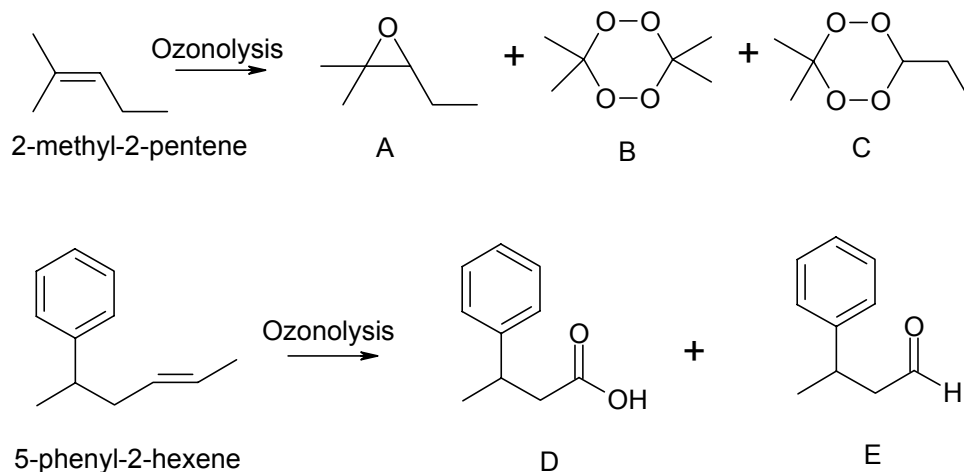


Fig. 6.9: Reaction products formed by ozonolysis of 2-methyl-2-pentene and 5-phenyl-2-hexene: (A) 3-ethyl-2,2-dimethyloxirane; (B) 3,3,6,6-tetramethyl-1,2,4,5-tetroxane; (C) 3,3-dimethyl-6-ethyl-1,2,4,5-tetroxane; (D) 3-methyl-3-phenyl propanoic acid; (E) 3-methyl-3-phenyl propanal.

6.3.3 Rate of ozonolysis of model rubbers in presence of antiozonants

It is known that antiozonants like 6PPD also have antioxidant activity. Therefore, it was first investigated if 6PPD does react with oxygen under the applied ozonolysis test conditions. A mixture of 2-methyl-2-pentene and 6PPD (4:1) was tested by passing oxygen instead of ozone through the reactor. The reaction was stopped after 80 minutes and the reaction products were analyzed by GC. It showed that disappearance of 6PPD was negligible during this test, indicating that the reaction between antiozonant and oxygen is very slow at the applied test temperature (-20°C), and can therefore be neglected during the ozonolysis experiments.

Several conventional and new antiozonants were tested in the presence of 2-methyl-2-pentene and 5-phenyl-2-hexene model rubbers. The amount of remaining antiozonant and model rubber is reported after 60 minutes reaction for 2-methyl-2-pentene and after 15 minutes reaction for 5-phenyl-2-hexene, in order to make a comparison between both systems and between the different antiozonants possible. The results are reported in Table 6.2 for both models and the various antiozonants tested. The results obtained for 6PPD tested in the presence of the 2-methyl-2-pentene are shown in fig. 6.10, as an example.

Table 6.2: Remaining amount of model rubber and antiozonant obtained after 60 minutes ozonolysis of 2-methyl-2-pentene and 15 minutes of 5-phenyl-2-hexene. The ratio model:6PPD = 4:1.

| Tested product | 2-methyl-2-pentene (NR-model) | | 5-phenyl-2-hexene (SBR-model) | |
|----------------|-------------------------------|--------------------|-------------------------------|--------------------|
| | Remaining amount | | Remaining amount | |
| | Model [%] | Antiozonant [%] | Model [%] | Antiozonant [%] |
| Control | 25 | - | 27 | - |
| 6PPD | 75 | 31 | 82 | 42 |
| IPPD | 72 | 33 | 80 | 39 |
| 77PD | 75 | 27 | 84 | 42 |
| Wingstay 100 | 69 | 36 | 77 | 31 |
| 6QDI | 49 | 75 | 58 | 64 |
| PPD-C18 | 83 | 30 | 89 | 40 |
| PPD-C7 | 81 | 13 | N.D. | N.D. |
| PPD-C22 | 81 | 38 | N.D. | N.D. |
| PPD-SA | 63 | 30 | N.D. | N.D. |
| PPD-MSA | 61 | 16 | N.D. | N.D. |
| ADPA-DTBF | 66 | ? | N.D. | N.D. |
| ADPAT | 87 | 79 | 93 | 71 |
| PDPA | 81 | 37 | 85 | 48 |

Notes: - ADPA-DTBF could not be analyzed by GC
 - The concentration of 5-phenyl-2-hexene and the corresponding amount of antiozonant are four times lower than that of 2-methyl-2-pentene.

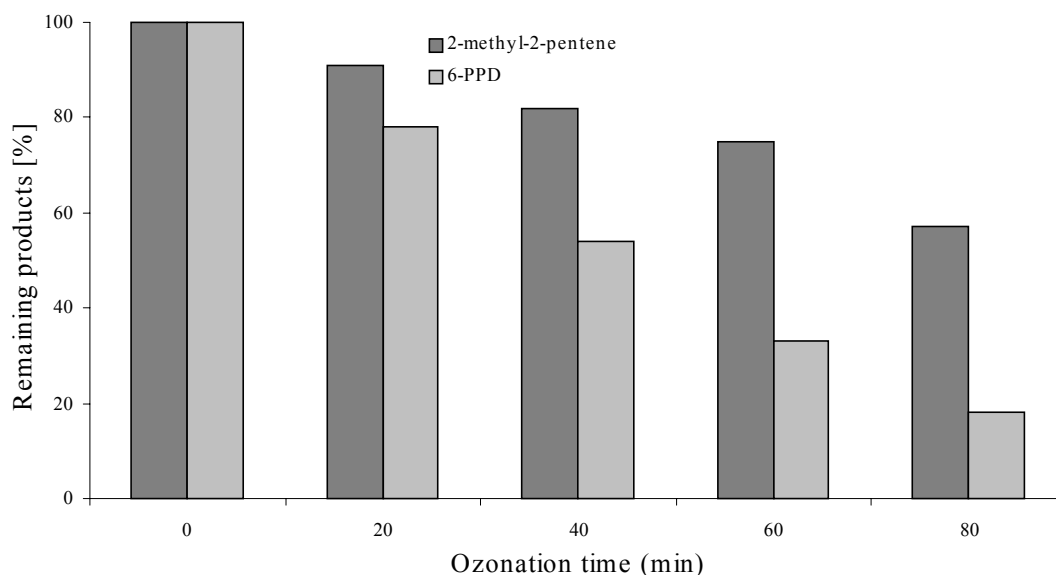


Fig. 6.10: Results obtained for the ozonolysis of 2-methyl-2-pentene in the presence of 6PPD; ratio model:6PPD = 4:1.

It is clear from these results that 2-methyl-2-pentene is slightly more reactive than 5-phenyl-2-hexene, which can be explained by a higher electron density of the double bond of 2-methyl-2-pentene compared to the double bond of 5-phenyl-2-hexene. The latter is di-substituted instead of the tri-substituted 2-methyl-2-pentene. Both the methyl- and the phenyl group are electron donating groups. However, the phenyl group in 5-phenyl-2-hexene is further away from the double bond compared to the methyl group in 2-methyl-2-pentene and therefore has less influence on the electron density of the double bond.

The product 6QDI shows a worse efficiency compared to 6PPD. This can be explained by the fact that it is one of the reaction products formed by ozonolysis of 6PPD, as shown in fig. 6.11, and therefore has lost part of its reactivity already.

From all the tested new antiozonants, the products PPD-C18, ADPAT and PDPA show improved efficiency compared to the conventional antiozonants 6PPD and IPPD. The improved efficiency observed for ADPAT can be explained by a high amine functionality of this molecule. The improved efficiency observed for PPD-C18 and PDPA corresponds with the improved antiozonant properties in a typical passenger tire sidewall compound, as described in Chapter 5. It is most likely related to the higher reactivity of one of the nitrogen atoms in these molecules and/or due to a better solubility compared to 6PPD. Unfortunately, many reaction products are

formed during the ozonolysis experiments, which makes it very difficult and time consuming to draw conclusions based on the individual products.

Based on performance, the stearic acid salt of 6PPD (PPD-C18) seems to be one of the most attractive products to be developed as long lasting antiozonant. It shows, besides a decreased migration rate (see Chapter 5), also improved antiozonant efficiency compared to 6PPD. The 6PPD-salts of other organic acids were therefore studied in some more detail. A comparison was made between 6PPD-salts prepared from different carboxylic acids, having various alkyl chain lengths C7, C18 and C22 and different pKa values: stearic acid with pKa = 5, succinic acid with pKa = 4.16 – 5.61 and methyl sulfonic acid with pKa = -2. The results are given in Table 6.2. It is clear from these results, that the alkyl chain length hardly shows any effect on the remaining amount of model rubber. However, it seems that the efficiency of 6PPD-salts prepared from strong acids like succinic acid (SA) and methyl sulfonic acid (MSA) is lower. This may be related to a lower solubility of these products in dichloromethane, but was not further investigated.

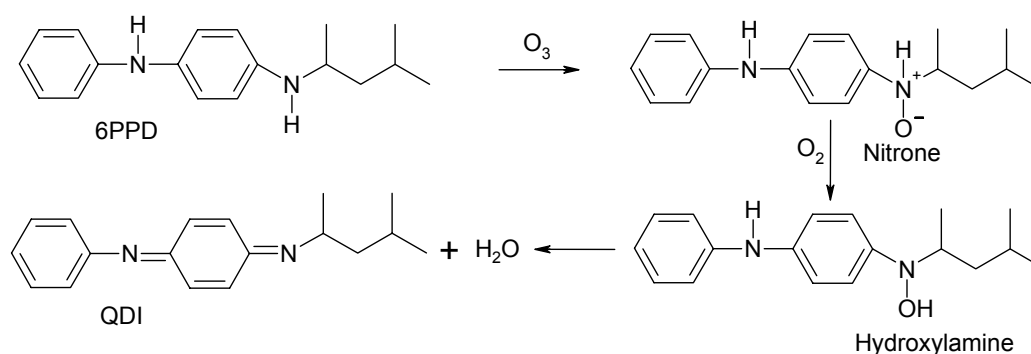


Fig. 6.11: Reaction mechanism for the formation of 6QDI by ozonolysis of 6PPD.

6.4 Conclusions

The efficiency of several potential long lasting antiozonants was studied by ozonolysis of model rubbers in the presence and absence of those products. 2-Methyl-2-pentene was used as model for natural rubber and 5-phenyl-2-hexene was used as model for styrene-butadiene-rubber. The NR-model appeared to be slightly more reactive than the SBR-model due to a higher electron density of the double bonds in the NR-model.

ADPAT, PDPA and the carboxylic acid salts of 6PPD (PPD-C7, PPD-C18 and PPD-C22) showed increased reactivity with ozone compared to the conventional antiozonants like 6PPD and IPPD. The increased reactivity of ADPAT can be explained by the relatively high amount of amine units in one molecule. The increased efficiency observed for PDPA and the carboxylic acid salts of 6PPD is most likely

related to an enhanced reactivity of one of the nitrogen atoms present in these molecules or due to a better solubility in dichloromethane.

The alkyl chain length of the carboxylic acid: C7, C18 and C22, used to prepare the 6PPD-salts has hardly any effect on the antiozonant efficiency. The pKa value of the carboxylic acids used to prepare the 6PPD-salts seemed to be more important. 6PPD-salts prepared from strong acids (SA, MSA) appeared to be less efficient than PPD-C18.

It can be concluded from the results described in the Appendix that, NIR-spectroscopy is a suitable technique for online detection of the ozonolysis. A linear calibration curve was obtained for the concentration of squalene plotted against the absorption at 5277 cm^{-1} .

Although FT-Raman spectroscopy showed a higher sensitivity for double bonds compared to NIR-spectroscopy, this technique was not suitable to analyze samples containing staining antiozonants like 6PPD and IPPD. A high fluorescence background signal was observed in the presence of those products. Replacement of the excitation source (632.6 nm) by a laser having a higher excitation wavelength (785 nm) resulted in a reduced fluorescence background signal but it was still too high to detect double bonds under the applied concentration levels used for the ozonolysis experiments.

Appendix 6.1: Online detection of ozonolysis by spectroscopic techniques.

FT-Raman spectroscopy and NIR-spectroscopy were applied as spectroscopic techniques for online detection of the ozonolysis. These techniques are capable of monitoring the decrease of double bonds and can probably also be used for monitoring rubbers or model rubbers, like squalene, having multiple double bonds.

The first technique investigated was FT-Raman spectroscopy, because this technique is very sensitive for symmetric vibrations and is non-invasive. Figure 6.12 shows the Raman spectra of 5-phenyl-2-hexene, 2-methyl-2-pentene and squalene recorded with a Raman system equipped with a HeNe laser. Unfortunately, this technique appeared to be not sensitive enough to detect C=C double bonds in the concentration level as used during the ozonolysis experiments: 2 m/m% 2-methyl-2-pentene in CH₂Cl₂. Increasing the concentration of 2-methyl-2-pentene in order to raise the detection limit was not possible, because of the limited availability of the 2-methyl-2-pentene. The extinction coefficient for the double bond of 5-phenyl-2-hexene was even lower due to the presence of the aromatic ring in this molecule. Squalene has a much higher response factor compared to 2-methyl-2-pentene and 5-phenyl-2-hexene due to the multiplicity of the double bonds: 6 double bonds in one molecule. As can be seen from fig. 6.13, a concentration of 1% can easily be detected. The vibration signals obtained from dichloromethane do not interfere with the signal of the double bonds of squalene. However, as can be seen from fig. 6.14, a high fluorescence background signal is observed when 6PPD is present in the system. Addition of 6PPD resulted in a strong discoloration (black to brown) of the reaction mixture. It is known that FT-Raman spectroscopy is difficult to apply for the analysis of dark colored products. It was further investigated if the amount of fluorescence could be reduced by replacing the excitation source (632.6 nm) by a laser having a higher excitation wavelength (785 nm). However, as can be seen from the results plotted in fig. 6.14, the fluorescence background is reduced but still too high to detect the double bonds of squalene. It must be concluded from these results that FT-Raman spectroscopy is not a suitable spectroscopic technique to monitor decrease of double bonds of model compounds for online detection of ozonolysis in the presence of staining colored antiozonants.

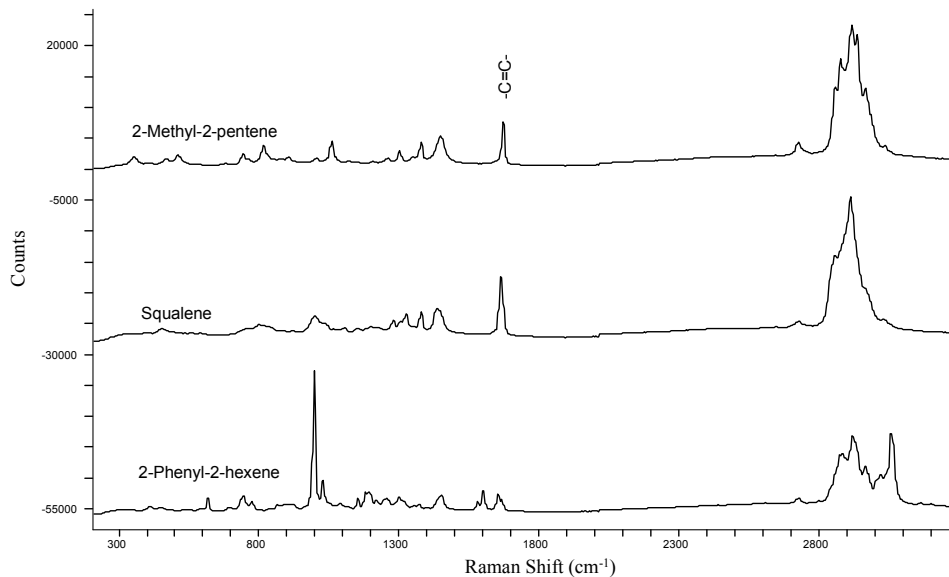


Fig. 6.12: FT-Raman spectra of pure 2-methyl-2-pentene, 5-phenyl-2-hexene and squalene.

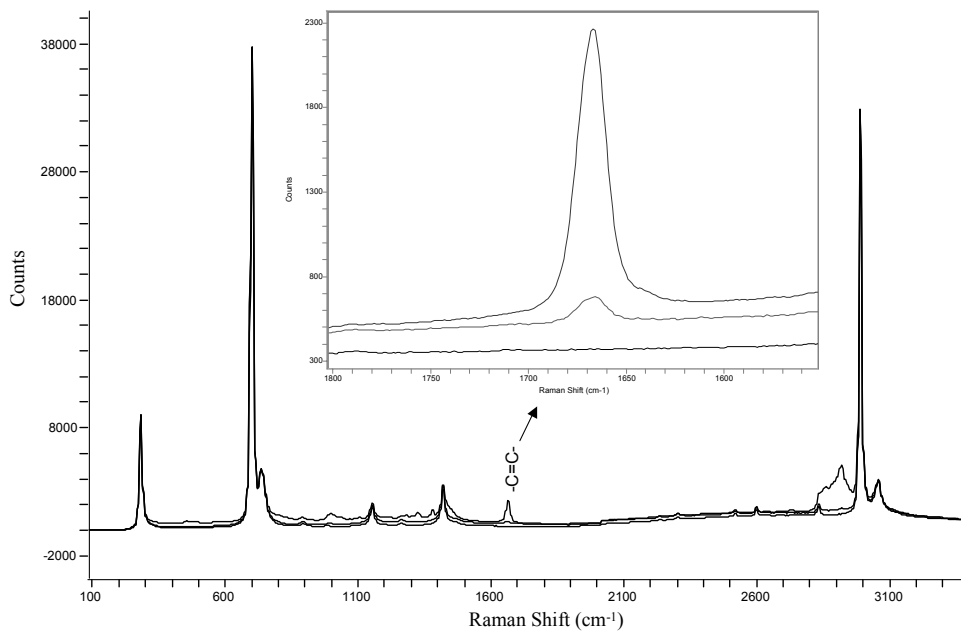


Fig. 6.13: FT-Raman spectra of squalene: 0, 1 and 10 m/m% in dichloromethane.

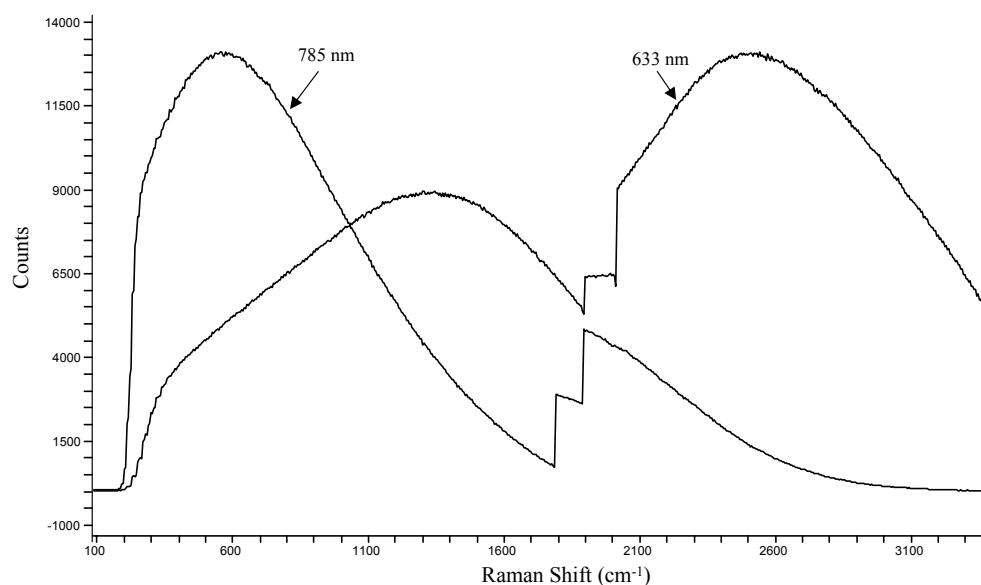


Fig. 6.14: FT-Raman spectra of 2 m/m% squalene and 0.5 m/m% 6PPD in dichloromethane.

Subsequently, the application of NIR-spectroscopy as online detection method for ozonolysis was evaluated for squalene in the presence of 6PPD. Although much weaker as with FT-Raman spectroscopy, the C=C double bonds are supposed to vibrate also in the near infrared. An example of a NIR spectrum of one of these experiments is shown in fig. 6.15. Unfortunately, no specific C=C absorption band could be observed in the NIR spectrum. However, a good linear relation was found between the absorption band at 5277cm^{-1} and the concentration of the remaining amount of squalene: see fig. 6.16. The absorption band at 5277cm^{-1} is most probably related to a reaction product of the double bonds of squalene with ozone but was not further investigated. This technique seems therefore to be most suitable for on-line detection of ozonolysis. Unfortunately, this route could not be applied for screening different antiozonants, because of time limitation and no longer availability of the test equipment. Results were included in this chapter for future reference.

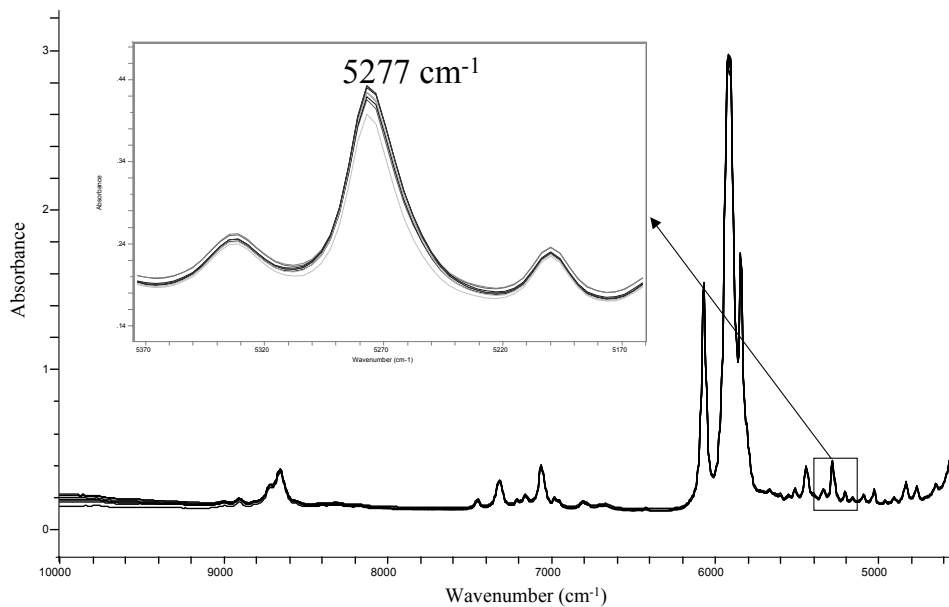


Fig. 6.15: NIR spectra of 2 m/m% squalene and 0.5 m/m% 6PPD in dichloromethane after ozonolysis.

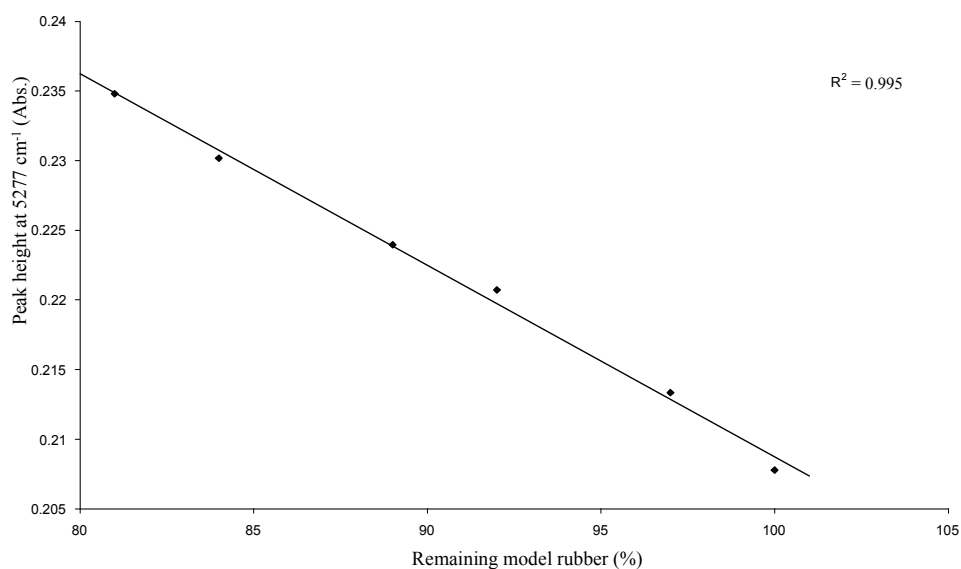


Fig. 6.16: Calibration curve for quantification of squalene by NIR-spectroscopy.

6.5 References

1. Y. Saito, *Int. Polym. Sci. Technol.*, **22**, (1995), 47.
2. D. Bruck, H. Konigshofen, and L. Ruetz, *Rubber Chem. Technol.*, **58**, (1985), 728.
3. P.S. Bailey, "Ozonation in organic chemistry", Volume 39.1, (1978), 25.
4. S.D. Razumovskii, L.S. Batashova, *Rubber Chem. Technol.*, **43**, (1970), 1340.
5. S.D. Razumovskii, V.V. Podmasteriev, G.E. Zaikov, *Polym. Degrad. Stab.*, **20**, (1988), 37.
6. M. Braden, *J. Appl. Polym. Sci.*, **6**, (1962), 86.
7. H.W. Engels, H. Hammer, D. Brück, W. Redetzky, *Rubber Chem. Technol.*, **62**, (1989), 609.
8. J. C. Ambelang, R.H. Kline, O.M. Lorenz, C.R. Parks and C. Wadelin, *Rubber Chem. Technol.*, **36**, (1963), 1497.
9. W. Hofmann, "Rubber Technology Handbook", Hanser Publishers, (1989), 273.
10. J.C. Andries, C.K. Rhee, R.W. Smith, D.B. Ross, H.E. Diem, *Rubber Chem. Technol.*, **52**, (1979), 823.
11. R.P. Latimer, E.R. Hooser, R.W. Layer, C.K. Rhee, *Rubber Chem. Technol.*, **53**, (1980), 1170.
12. R.P. Latimer, E.R. Hooser, R.W. Layer, C.K. Rhee, *Rubber Chem. Technol.*, **56**, (1983), 431.
13. S.W. Hong, C-Y. Lin, *Rubber World*, (August 2000), 36.
14. S.W. Hong, P.K. Greene, C-Y. Lin, ACS Rubber Division 155th Conference, Chicago, IL, Paper No. 65 (April 13-16, 1999).
15. J. Hahn, M. Runk, M. Schollmeyer, U. Theimer and E. Walter, *Kautschuk Gummi Kunststoffe*, **51**, (March 1998), 206.
16. P.J. Nieuwenhuizen, J.G. Haasnoot and J. Reedijk, *Kautschuk Gummi Kunststoffe*, **53**, (2000), 144.
17. H.E. Baumgarten, *Organic Syntheses*, **5**, (1973), 751
18. P.S. Baily, "Ozonation in Organic Chemistry", Vol. 39-I and II (1978).
19. R. Huisgen, *Angewandte Chemie Internat. Edit.*, **2**, nr. 11, (1963), 633.

Quinonediimine as bound antioxidant in silica compounds with the possibility to reduce the level of silane coupling agent[#]

The effect of N-(1,3-dimethyl)-N'-phenyl quinonediimine (6QDI) has been investigated in silica containing "green tire" compounds. By adding 6QDI it is possible to reduce the level of silane coupling agent, bis-(3-triethoxysilylpropyl) tetrasulfide (TESPT), to provide either equivalent or better performance characteristics such as increased cure rate, improved abrasion resistance etc. The polymer-filler and filler-filler interaction parameters are significantly improved indicating better reinforcement characteristics. Network studies suggest better protection of the polysulfidic network following aging, demonstrating improved antioxidant characteristics of the compounds containing 6QDI.

NMR, LC-MS studies suggest that there is no reaction of TESPT either with 6PPD or 6QDI. The interaction between 6QDI and the rubber model compound squalene was studied by spectroscopic analysis. It demonstrated that 6QDI reacts with squalene in the presence of accelerator/sulfur and forms squalene-S_x-PPD adducts; 6QDI is converted to 6PPD during this reaction. Based on this, it is postulated that either an ENE reaction or the double sulfur addition of 6QDI are causing grafting of 6QDI to the polymer, accounting for the improved antioxidant characteristics in this system.

7.1 Introduction

Silica is being used extensively in the tire industry as reinforcing filler to provide improved tear resistance and decreased rolling resistance.¹⁻⁸ Compounders face problems in mixing silica because of the presence of strong interactions between silanol groups on the surface of the silica. Bifunctional organosilane coupling agents are commonly used to chemically modify the surface of the silica to enhance interaction with hydrocarbon rubbers. Remarkable improvements in the mechanical properties of the silica-reinforced rubber vulcanizates are obtained by using

[#] Parts of the work described in this chapter have been published and/or accepted for publication: N.M. Huntink, S. Datta, R.N. Datta, accepted for publication in *Kautschuk Gummi Kunstst.*; R.N. Datta, N.M. Huntink, A.G. Talma, PCT WO 02150180 A1 June 27, 2002.

bifunctional organosilane coupling agents, such as improvements in tensile strength, elongation at break, low tangent delta at 60°C and consequently low heat build up in the tire.^{9,10}

The organosilane coupling agents which are most widely used in silica applications are bis-3-(triethoxysilylpropyl) tetrasulfide (TESPT) and bis-3-(triethoxysilylpropyl) disulfide (TESPD), and to a lesser extent, γ - mercaptopropyl triethoxy silane (MPTES).^{11,12} The structure of TESPT is shown in fig. 7.1. However, the use of TESPT and TESPD poses problems to the environment, while generating volatile alcohol's by the reaction of ethoxy silyl groups of the coupling agent with the silanol groups of the silica.^{13,14} In addition, a reduction of the amount of silica coupling agent is desired, since its use in conventional amounts of 1:10 relative to the silica adds to the costs of the rubber vulcanizate.

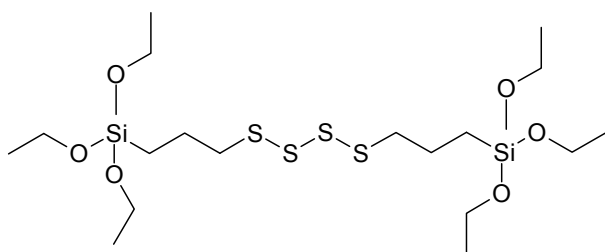


Fig. 7.1: Structure of bis-3-(triethoxysilylpropyl) tetrasulfide (TESPT).

Recently, N-(1,3-dimethyl)-N'-phenyl quinonediimine (6QDI), figure 7.2, has been introduced providing improved processing benefits as well as bound antioxidant characteristics.¹⁵⁻¹⁸ In this chapter, the effect of 6QDI will be dealt with in a typical "green tire" passenger tread formulation.¹⁹ The objective of this study is to develop formulations with a lower amount of organosilane coupling agents and thus a reduced amount of volatile alcohols, with either equal or enhanced performance, by replacing a part of TESPT by the potential long lasting antidegradant 6QDI. The results are described in the first part of this chapter. The second part of this chapter focuses on the mechanism of the reaction between 6QDI and the polymer. In order to elucidate the mechanism of 6QDI in the rubber matrix, the reaction of 6QDI was carried out in squalene as a model for diene rubbers.

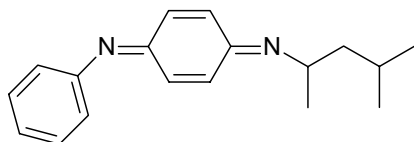


Fig. 7.2: Structure of N-(1,3-dimethyl)-N'-phenyl quinonediimine (6QDI).

7.2 Experimental

7.2.1 Materials used

The mixes for the experiments contained: solution SBR (Buna VSL 5025 HM; Bayer) composed of 75% butadiene with 50% vinyl content, and 25% styrene, extended with 37.5 phr aromatic oil, with a Mooney viscosity ML (1+4) 100°C of 65; BR Buna CB 10 (butadiene rubber with a cis-content of 95% and a vinyl content of 1%, Buna Werk Huels); Silica KS 408 gr (Akzo PQ); Bis(triethoxysilylpropyl) tetrasulfide (TESPT; Silquest A-1289, OSI Specialties Group / Crompton Corporation); Aromatic oil (Enerflex 75, BP Oil Europe); ZnO (Harzsiegel standard); stearic acid (J.T. Baker); Santoflex 6PPD (Flexsys); Wax PEG 4000 (polyethylene glycol, Clariant GMBH); Santocure TBBS (Flexsys); Santocure CBS (Flexsys); Perkacit DPG (Flexsys); sulfur (J.T. Baker); Santoflex 6QDI (Flexsys); Squalene (Janssen, assay 98%); Zinc stearate (Merck).

7.2.2 Formulations, mixing and curing

Formulations

Formulations are shown in Table 7.1. The “green tire tread” compounds were taken from patent literature.¹⁹

Table 7.1: Formulations (optimization of the level of TESPT in the “green tire tread formulation”).

| Ingredients/Mixes | 1 | 2 | 3 | 4 | 5 |
|-------------------|--------|--------|--------|--------|--------|
| SBR Buna 5025-1 | 103.13 | 103.13 | 103.13 | 103.13 | 103.13 |
| BR Buna CB10 | 25.0 | 25.0 | 25.0 | 25.0 | 25.0 |
| Silica KS 408 gr | 80.0 | 80.0 | 80.0 | 80.0 | 80.0 |
| TESPT | 6.7 | 5.4 | 5.4 | 4.5 | 4.5 |
| Aromatic oil | 8.0 | 8.0 | 8.0 | 8.0 | 8.0 |
| Zinc oxide | 3.0 | 3.0 | 3.0 | 3.0 | 3.0 |
| Stearic acid | 2.0 | 2.0 | 2.0 | 2.0 | 2.0 |
| Santoflex 6PPD | 2.0 | 2.0 | 2.0 | 2.0 | 2.0 |
| 6QDI | 0 | 0 | 1 | 0 | 1 |
| Wax PEG 4000 | 3.1 | 3.1 | 3.1 | 3.1 | 3.1 |
| Santocure TBBS | 1.7 | 1.7 | 1.7 | 1.7 | 1.7 |
| Perkacit DPG | 2.0 | 2.0 | 2.0 | 2.0 | 2.0 |
| Sulfur | 1.5 | 1.5 | 1.5 | 1.5 | 1.5 |

Mixing

The compounds were mixed in three stages. 6QDI was added in the first stage. The first two stages were effected in a Werner & Pfleider mixer: volume 5.0 liter; load factor 70%; preheating at 50°C and rotor speed 30 rpm. After every mixing step the compound was sheeted out on a Schwabenthan Polymix 150L two-roll mill. The second mixing stage was applied to homogenize the compound. The mixing procedures employed are described below:

- Stage 1. Start temperature: 50°C; the cooling on the mixer was activated when the compound reached a temperature of 90°C.

Time [min.]

| | |
|----------|--------------------------|
| t=0 min. | Addition of S-SBR and BR |
| t=1 min. | ½ silica+silane |
| t=2 min. | ½ silica +oil +6QDI+rest |
| t=4 min. | Sweep |
| t=6 min. | Dump |

- Stage 2. The cooled mix from stage 1 was transferred into the mixer and the rotor speed increased to 144 rpm, such that the temperature reached 125°C. The rotor speed was then reduced to 72 rpm and the temperature of the mixer kept constant for 5 minutes by lifting the ram. The temperature of the batches varied from 155-157°C.

- Stage 3. The third mixing step was carried out on a Schwabenthan Polymix 150L two-roll mill with friction ratio set to 1:1.22 and temperature 50 – 70°C. The accelerators and sulfur were added during this step in approximately 10 minutes, as mentioned earlier.¹⁸

Curing

Cure characteristics were determined using a MDR 2000EA rheometer. Delta torque or extent of crosslinking is the maximum torque (M_H) minus the minimum torque (M_L). Scorch safety (t_{s2}) is the time needed to reach 2 dNm above minimum torque (M_L); optimum cure time (t_{90}) is the time required to reach 90% of the delta torque above minimum. Sheets and test specimens were vulcanized by compression molding in a Fontyne TP-400 press at 170°C for the defined periods as indicated in the respective tables.

7.2.3 Aging

Test pieces were aged in an air circulation oven for 3 days at 100°C. Samples were kept for 24 hours at room temperature before final measurements.

7.2.4 Testing

Physical-mechanical properties:

Tensile stress-strain properties were determined according to ISO 37, tear as per ISO 34/1, and DIN abrasion according to ISO 4649. Aging of the test specimens was carried out in a ventilated oven in the presence of air at 100°C for 3 days (ISO 188). Heat buildup after dynamic loading was determined using a Goodrich Flexometer (Load 11 Kg; stroke 0.445 cm, frequency 30Hz, start temperature 100°C, running time 1h) according to ISO 4666/3. Dynamic mechanical analyses were carried out using a Rheometrics RDA-700 viscoanalyzer (prestrain 0.75%, frequency 15Hz at 60°C and 1% double strain amplitude (DSA), ASTM D 2231). Storage modulus (E'), loss modulus (E'') and the loss tangent ($\tan \delta$) were measured.

Network structure:

The network structure was determined by equilibrium swelling in toluene using the method reported by Ellis and Welding.²⁰ The rubber volume fraction (V_r) obtained was converted into the Mooney-Rivlin elastic constant (C_1) and finally into the concentration of chemical crosslinks by using the Flory-Rehner equations as described in literature.^{21,22} The proportions of mono-, di-, and polysulfidic crosslinks in the vulcanizates were determined by equilibrium swelling in toluene before and after treatment with thiol amine chemical probes.²³ Details of the procedure have been reported by Datta et al.²⁴⁻²⁶

Filler-polymer and filler-filler interaction:

The measurement of filler-polymer interaction is difficult, because of the problem to isolate this parameter from other physical and chemical phenomena, e.g., the polymer crosslink network, filler microdispersion and polymer occluded within the black/silica structure.²⁷ The filler-polymer interaction σ is nowadays measured as the ratio of the 300% and 100% modulus: M_{300}/M_{100} .¹⁹ The M_{300}/M_{100} ratio is basically related to the shape of the tensile curve. The greater the tendency of the stress to grow with elongation, the higher the M_{300}/M_{100} ratio and the stronger the polymer-filler interaction.¹ The M_{300}/M_{100} ratio has been found to be a better indicator of the polymer filler interaction than modulus values itself.

The filler-filler interaction η (Payne effect), is calculated from the difference of the dynamic elastic modulus, E' , between 1% and 25% double strain amplitude. These measurements were done with the RPA 2000 process analyzer at 100°C and a frequency of 0.33 Hz. The lower the filler-filler interaction the better the dispersibility of silica in the rubber matrix.

7.2.5 Interaction of 6PPD or 6QDI with TESPT-silica chemistry

The reaction between 6PPD or 6QDI with TESPT was investigated in order to find out whether these antidegradants interfere with the silane chemistry. 0.1 mole, 0.27g 6PPD or 6QDI and 0.5 mole, 2.53g TESPT were mixed in a NMR tube, using deuterated tetrachloroethane as a solvent, and subsequently heated at 130°C. The reaction mixtures were analyzed by ¹H-NMR and by HPLC-MS after 0, 15, 30, 45, 60 and 90 minutes heating. The ¹H-NMR and HPLC-MS conditions used to characterize the reaction products are described in § 7.2.7.

7.2.6 Model Vulcanization

In order to elucidate the mechanism of the reaction between 6QDI and the rubber matrix, the reaction of 6QDI was carried out in squalene as a model for diene rubbers. To minimize the analytical complexity, simple gum stock formulations were used for model compound vulcanization. The formulations are shown in Table 7.2.

Table 7.2: Model compound formulations.

| Ingredients | 6 | 7 | 8 | 9 |
|----------------|-----|-----|-----|-----|
| Squalene | 100 | 100 | 100 | 100 |
| Zinc stearate | 2 | 2 | 2 | 2 |
| Santocure CBS | 0.6 | 0.6 | 0.6 | 0.6 |
| Santoflex 6PPD | 5 | - | 2 | - |
| 6QDI | - | 5 | - | 2 |
| Sulfur | - | - | 2.5 | 2.5 |

Prior to the reaction, reagents are homogenized by stirring the mixtures in a 25ml Erlenmeyer flask while heating for 5 minutes in an oil bath at 75°C. The reaction is started by placing the flask in an oil bath at 150°C. The samples are stirred during the reaction. Periodically, 50 µl samples are taken to monitor the progress of the reaction. The reaction is typically stopped after 1hour by removing the flask from the oil bath and allowing it to cool down at room temperature. The ¹H-NMR and HPLC-MS conditions used to characterize the reaction products are described in § 7.2.7

7.2.7 Characterization of the reaction products described in § 7.2.5 and § 7.2.6

¹H-NMR:

¹H-NMR measurements were performed on a Varian Inova – 400 MHz (Varian) model L 700 spectrometer equipped with a high temperature NMR probe, using trimethyl silane (TMS) as a reference. Measurements at 130°C in the high

temperature probe were performed in deuterated tetrachloroethane. The $^1\text{H-NMR}$ chemical shifts δ (ppm) of all sample solutions were measured against blank solutions of the individual starting raw materials.

HPLC-MS:

HPLC-MS was performed introducing the samples directly into the spectrometer and after separation of the components by HPLC or HP-SEC. Details of the HPLC and MS conditions are summarized below:

HPLC conditions:

Guard column : Reversed phase packing
Analytical column : Lichrospher 100 RP-18, 125 * 4 mm, 5 μm
Mobile phase : A: 75 Volume % of 0.01M ammonium acetate in water
and 25 volume % methanol with 0.1% acetic acid
B: Methanol with 0.1% acetic acid
Filtered and degassed
Gradient : 95% A 60 min. \rightarrow 0% A (10 min.) 1 min. \rightarrow 95%A (4 min.)
Flow rate : 1 ml/min.
Oven : 25°C (selected temperature constant within 0.2°C)
Injection volume : 10 μl
Detection : UV at 280 nm

HP-SEC conditions:

Guard column : HP-SEC packing
Analytical column : PL-gel; 100Å; 600X7.5 mm ID; dp = 5 μ
Mobile phase : Tetrahydrofuran (THF), stabilized with
0.025% BHT, filtered and degassed
Flow rate : 1.0 ml/min
Temperature : Ambient
Detector : 34°C
Injection volume : 50 μl
Detection : Refractive Index
Sample conc. : ca. 100mg/10ml THF

MS-conditions:

Instrument : Platform-II quadrupole ex Micromass
Ionization : Electro spray positive
Carrier solvent : Methanol
Flow : 20 $\mu\text{l}/\text{min}$.
Injection volume : 10 μl
Scan range : 200-1500 Da
Capillary voltage : 3.5 kV
HV lens : 0.5 V
Skimmer : 5 V

Cone voltage : 30 V / 60 V

Source temperature : 60°C

Multiplier : 650

(In positive electro spray ionization (ESI), component should give $[M + H]^+$ adducts, so m/z values of $M + 1$ are expected).

7.3 Results and discussion

7.3.1 Partial replacement of TESPT by 6QDI in green tire passenger tread formulations

The development of green tire passenger tread formulations with a lower amount of organosilane coupling agents like TESPT and thus a reduced amount of volatile alcohols, with either equal or enhanced performance, is described in the current chapter. It was investigated if TESPT can be partially replaced by the antidegradant 6QDI. The compound composition of the tested compounds is shown in Table 7.1.

The cure data of the tested compounds are described in Table 7.3. It is clear from these data that, when the amount of silica coupling agent, TESPT is decreased from 6.7 to 5.4 phr, scorch time t_{s2} or scorch safety is decreased as well: compare compound 1 versus compound 2. Incorporation of a quinonediimine (6QDI) improves the scorch safety and results in a shortened cure time t_{90} and an increased cure rate $t_{90}-t_{s2}$: compare the data of compound 2 with that of compound 3. Further reduction of the amount of TESPT from 5.4 to 4.5 phr resulted in a slightly increased scorch time and a reduced cure time t_{90} : compare compound 2 with that of compound 4. Incorporation of QDI to the compound with 4.5 phr TESPT resulted in a slightly reduced scorch time t_{s2} and the cure rate $t_{90}-t_{s2}$: compare compound 4 versus 5.

Table 7.3: Cure data of the compounds obtained at 170°C.

| Properties/Mixes | 1 | 2 | 3 | 4 | 5 |
|-----------------------|------|------|------|------|------|
| Delta torque, Nm | 2.29 | 2.31 | 2.10 | 2.16 | 2.17 |
| M_L , Nm | 0.32 | 0.31 | 0.27 | 0.36 | 0.30 |
| t_{s2} , min | 1.19 | 0.87 | 1.26 | 1.03 | 0.96 |
| t_{90} , min | 21.3 | 19.6 | 13.7 | 17.7 | 16.5 |
| $t_{90}-t_{s2}$, min | 20.1 | 18.7 | 12.4 | 16.7 | 15.5 |

The compounds 1, 2, and 3 were selected for further studies. The data presented in Table 7.4 show that the effects of reducing silane coupling agent, e.g. decreased tensile modulus and tensile strength, increased heat build up and increased abrasion loss, can largely be compensated by the addition of 1.0 phr 6QDI. The aging data after 3 days at 100°C are also presented in Table 7.4. It is clear, that the mix containing 6QDI retains a considerable portion of strength properties, e.g. tensile and tear strength following aging. This is in line with earlier observations for black filled compounds.¹⁶

Table 7.4: Properties of the rubber vulcanizates.

| Properties/mixes | 1 | 2 | 3 |
|---|----------------|----------------|----------------|
| Cure temp./time | 170°C/20' | 170°C/20' | 170°C/15' |
| Modulus, M_{100} , MPa | 4.0 (5.1) | 3.7 (5.2) | 3.8 (5.4) |
| Modulus, M_{300} , MPa | 14.6 (-) | 13.9 (-) | 14.2 (-) |
| Tensile strength, MPa | 16.5 (14.1) | 14.2 (10.2) | 17.1 (16.2) |
| Elongation at break, % | 315 (240) | 370 (210) | 350 (250) |
| Tear strength, kN/m | 60 (30) | 50 (25) | 60 (45) |
| Heat build up at 100°C, ΔT , °C | 34 | 39 | 36 |
| Abrasion loss, mm ³ | 102 | 120 | 96 |

* Data within the parentheses are those for the vulcanizates after aging at 100°C for 3days

The viscoelastic properties of the vulcanizates are given in Table 7.5. It is seen from these data that the use of 6QDI results in compensation of the hysteresis loss, tangent delta, seen when the amount of silane coupling agent in the rubber composition is reduced.

Table 7.5: Viscoelastic properties of the rubber vulcanizates.

| Properties/mixes | 1 | 2 | 3 |
|------------------------------------|-----------|-----------|-----------|
| Cure temp./time | 170°C/20' | 170°C/20' | 170°C/15' |
| Storage modulus, E' , MPa | 7.41 | 7.01 | 7.20 |
| Loss modulus, E'' , MPa | 0.815 | 0.862 | 0.756 |
| Tangent delta, 60°C | 0.110 | 0.123 | 0.105 |
| Loss compliance, MPa ⁻¹ | 0.0148 | 0.0175 | 0.0146 |

The loss compliance, a measure of energy loss at constant stress, is also matched by addition of 6QDI into the compound. Tangent delta as well as loss compliance indicate that the rolling resistance of tires based on these recipes is not negatively affected by reducing the dosage of TESPT and balancing the effect by incorporating 6QDI.

7.3.2 Interaction of 6PPD or 6QDI with TESPT-silica chemistry

In general, the silane-coupling agent TESPT is reactive towards most rubber ingredients such as zinc oxide, accelerators, etc.⁵ This leads to an overall lower yield of silane-bridges between the silica particles and the rubber polymers. The beneficial effect of 6QDI, as seen in the previous paragraph, could therefore be due to many reasons, of which a few ones are:

- a synergistic activation of TESPT by 6QDI and 6PPD
- suppression of radical reactions occurring with TESPT at high mixing temperatures, leading to premature scorch and afterwards lower efficiency as coupler.^{4,5}
- positive interference in detrimental side-reactions between TESPT and curing agents, which otherwise decrease the efficiency of TESPT.

In that perspective, it was of interest to investigate direct reactions between antidegradants such as 6PPD and 6QDI with TESPT, to see whether these antidegradants interfere with the silane chemistry.

The reaction of TESPT with 6PPD or 6QDI was studied by ¹H-NMR (using the high temperature NMR probe) and HPLC-MS techniques. The obtained results are shown in figures 7.3-7.7. It is obvious from the ¹H-NMR spectra shown in figures 7.3 and 7.4 that both 6PPD and 6QDI do not react with TESPT under the applied reaction conditions. Even 90 minutes heating at 130°C does not result in the formation of any chemical reaction products. The only observation which can be made is peak broadening upon increased heating times, which is clearly demonstrated in figures 7.3 and 7.4 for the peaks of respectively 6PPD and 6QDI between 6.5 and 7.5 ppm. The peak broadening is related to molecular dynamics, which are changing during the reaction due to small changes in the matrix. Although no chemical reaction between the PPD's and TESPT seems to take place, a very small amount of solids is formed in time, having a large effect on the line width of the NMR spectra.

The reaction mixtures were also analyzed by HPLC-MS, a technique that has a lower detection limit than ¹H-NMR. However, as can be seen in figures 7.5 and 7.6, besides 6PPD, 6QDI and the oligomers of TESPT, no additional peaks are detectable. The peak at 42 minutes was identified by mass spectrometry as 6PPD: see figure 7.7A, and the peak at 46 minutes as 6QDI: see figure 7.7B. The tested 6PPD sample contains approximately 5% 6QDI and the tested 6QDI sample 5% 6PPD impurities. The 6PPD/6QDI ratio does also hardly change upon reaction with TESPT. The relatively sharp peaks having a retention time between 58 and 68 minutes were identified as oligomers of TESPT, having an increased amount of sulfur atoms

between the silane groups. The peak having a retention time of 59 minutes was identified as the oligomer bis-3-(triethoxysilylpropyl) disulfide (TESPD). The structure and the mass spectrum of this peak are plotted in figure 7.7C.

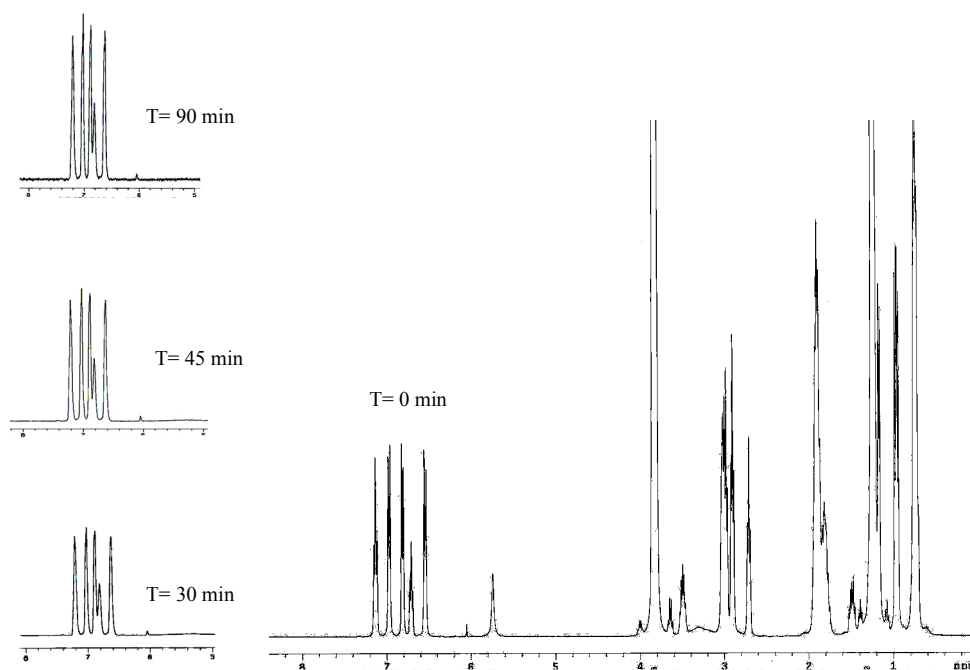


Figure 7.3: ¹H-NMR spectrum of 6PPD + TESPT heated at 130°C for different time intervals.

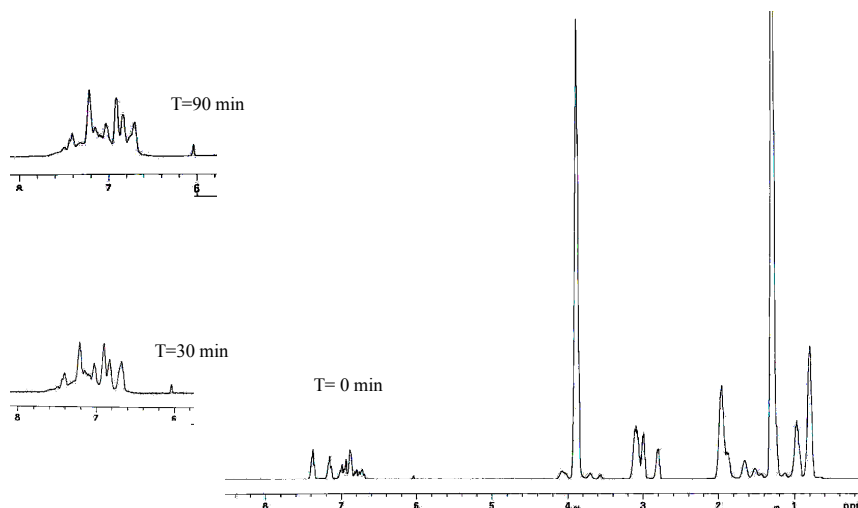


Figure 7.4: ^1H -NMR spectrum of 6QDI + TESPT heated at 130°C for different time intervals.

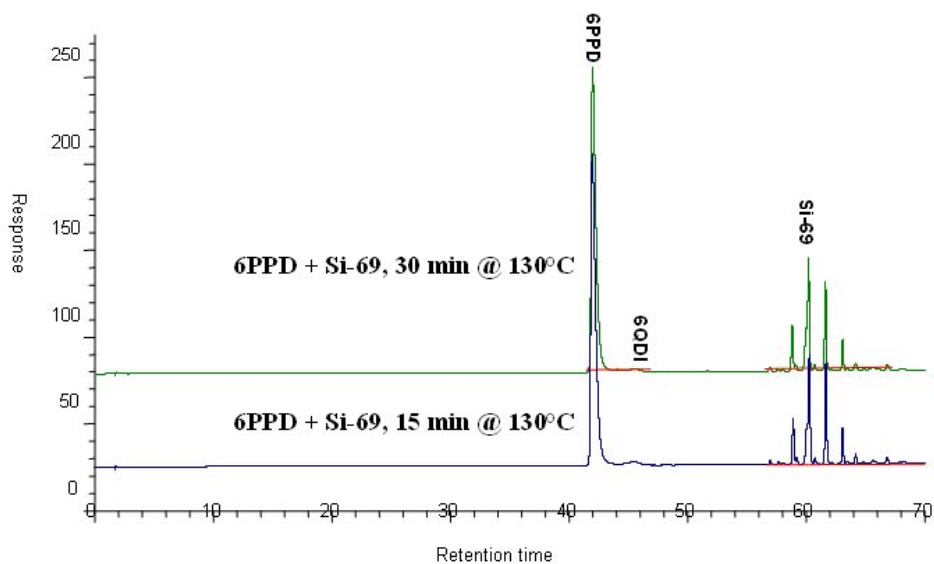


Figure 7.5: Gradient HPLC of TESPT + 6PPD heated at 130°C for different time intervals.

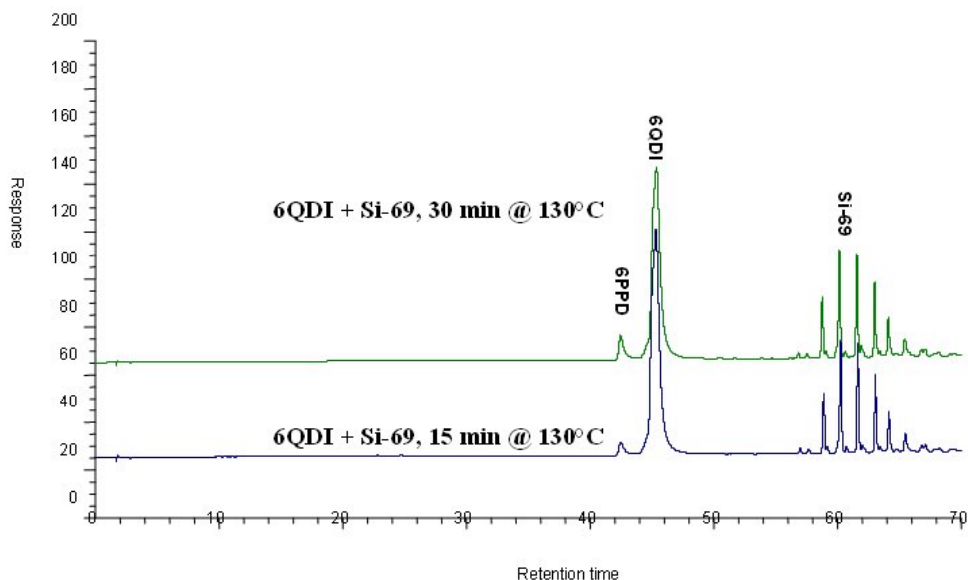


Figure 7.6: Gradient HPLC of TESPT + 6QDI heated at 130°C for different time intervals.

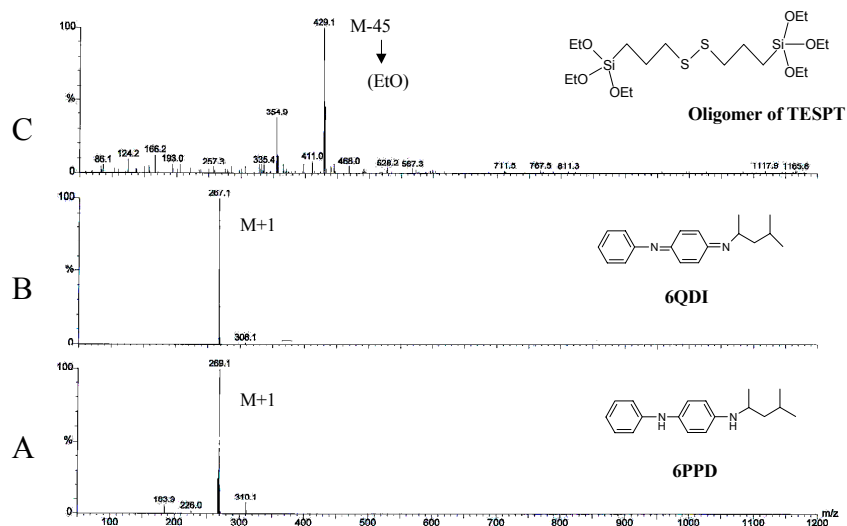


Figure 7.7: Gradient HPLC-MS spectra of several peaks selected from figures 7.5 and 7.6: Retention time of 42min. (A), 46 min. (B) and 59 min. (C).

It can be concluded from the figures 7.3-7.7, that both 6PPD and 6QDI undergo little or no reaction with TESPT and hence do not interfere directly with the silane chemistry.

7.3.3 The effect of 6QDI/TESPT on filler reinforcement

Studies on reinforcement have generally demonstrated, that the surface interaction between fillers and rubber molecules or network segments involves a range of bond energies from relatively weak to very strong. In all cases, physical adsorption undoubtedly occurs to varying degrees depending on the particular surface and molecular segments. When a rubber is filled with reinforcing fillers, above a critical filler concentration filler-filler interaction takes effect. It is determined both by the physical or chemical surface interaction and the distance between filler aggregates in the rubber compound. It can be measured in the range of small deformations.^{4,5,29,30}

The elastic modulus of a filled rubber is experimentally strongly dependent on the deformation and decreases substantially at higher strains. This phenomenon is known as the Payne effect and is attributed to the presence and breakdown of the filler network during dynamic deformation. The use of a silane coupling agent like TESPT minimizes the Payne effect in silica reinforced rubber compounds. On the other hand, it hydrophobizes the silica surface, thereby enhancing physical interaction with the predominantly hydrophobic rubber, and minimizing mutual hydrophilic interactions between the silica particles. On the other hand, it is also creating a chemical bridge between rubber polymer and silica, thereby chemically grafting the rubber to the silica surface. It is clear from the results shown in Table 7.6 that partial replacement of TESPT by QDI results in an improved Payne effect: decreased filler-filler interaction: $\eta = E_{(1\%strain)} - E_{(25\%strain)}$. It can also be seen that partial replacement of TESPT by QDI show no loss in polymer-filler interaction: $\sigma = M_{300}/M_{100}$.

Table 7.6: Payne effect and polymer-filler interaction.

| Properties | M_{300}/M_{100} (σ) | $E_{(1\%strain)} - E_{(25\%strain)}$ (η) |
|------------|-----------------------------------|--|
| Mixes | | |
| 1 | 3.7 | 0.92 |
| 3 | 3.8 | 0.37 |

Note: see Table 7.1 for compound composition

7.3.4 The effect of 6QDI/TESPT on the distribution of crosslink types

The crosslink density and distribution of crosslink types was determined for several compounds (mixes 1, 2, and 3) in order to correlate the vulcanizate properties with the network characteristics. The data are given in Table 7.7. The compounds were cured to optimum cure t_{90} . It is clear from these data that use of 6QDI results in an improved retention of polysulfidic crosslinks, i.e. poly-S, following aging at reduced amount of silane coupling agent and shorter cure time. This better protection of poly-S network is likely to be due to bound antioxidant behavior of the compounds containing 6QDI, as will be described in next paragraph.³¹

Table 7.7: Crosslink density* and crosslink types.

| Mixes | 1 | 2 | 3 |
|------------------|----------------|----------------|----------------|
| Cure temp./time | 170°C/20' | 170°C/20' | 170°C/15' |
| Total crosslinks | 5.01 (5.41) | 4.81 (5.02) | 4.90 (5.23) |
| Poly-S | 2.65 (1.01) | 2.10 (0.82) | 2.57 (1.41) |
| Di-S | 0.67 (0.50) | 0.51 (0.40) | 0.58 (0.45) |
| Mono-S | 1.69 (3.90) | 2.20 (3.80) | 1.75 (3.37) |

* Crosslink density expressed in grammole/gram rubber hydrocarbon $\times 10^{-5}$

♣ Data in the parentheses are those for the vulcanizates aged for 3 days at 100°C

7.3.5 Proposed reaction mechanism between rubber and silica via 6QDI and bound antioxidant properties of 6PPD and 6QDI

The restored tensile modulus and hysteresis upon inclusion of 6QDI in the rubber composition, as shown in Table 7.5, are an indication of chemical coupling of silica with rubber via 6QDI, similar to the chemical coupling via TESPT.¹⁻⁵ A proposed mechanism is depicted in fig. 7.8. It is assumed in this mechanism that 6QDI reacts with the rubber in the presence of accelerator/sulfur and forms rubber-S_x-PPD adducts; 6QDI is converted to 6PPD during this reaction: see later. The aryl alkyl-substituted NH group reacts with oxygen producing a nitron. This nitron reacts further with water producing a hydroxylamine, which subsequently reacts with the silanol group of the silica particles, resulting in a chemical coupling of silica and rubber.

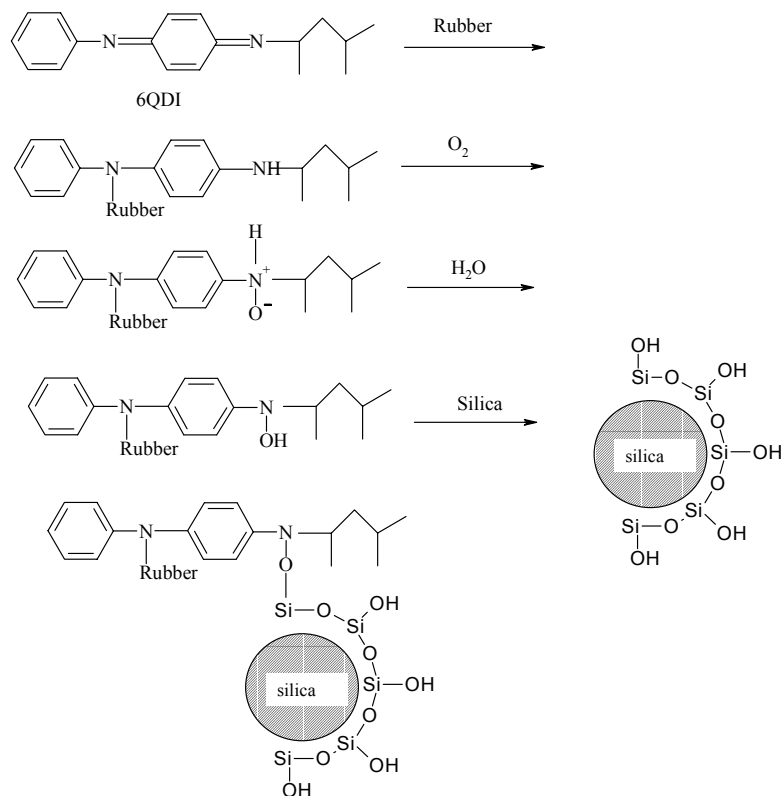


Fig. 7.8: Reaction of rubber and silica via 6QDI.

It has been postulated before that 6QDI reacts with diene rubbers thereby getting attached to the polymer backbone providing persistent antioxidant properties.³¹ In order to further elucidate the mechanism behind the positive effects of addition of 6QDI, as seen in the previous paragraphs, model experiments were done according to the procedure described in § 7.2.5. Squalene was taken as the model for diene rubbers because of practical reasons: it has a low volatility and is easy to analyze. The reaction kinetics between 6PPD or 6QDI with different diene rubbers like NR, BR and SBR will be different but the mechanism is expected to be similar.

In the model reaction of squalene with 6PPD or 6QDI it was possible to distinguish the course and differences of the reaction of 6PPD and 6QDI. Mixture 6 of Table 7.2, analyzed via HP-SEC showed no significant level of adduct: “Squa + 6PPD” figure 7.9, whereas in the presence of 6QDI (mix. 7 of Table 7.2), a third component can be identified, which is represented as “Squa + 6QDI” in figure 7.10. The mass spectrum of this peak shows a mass of 677.4 (M+1) which corresponds to the structure shown in fig. 7.11. On the contrary, in the presence of 6PPD, no mass equivalent to the adduct of “Squa+6PPD” could be identified: figure 7.12.

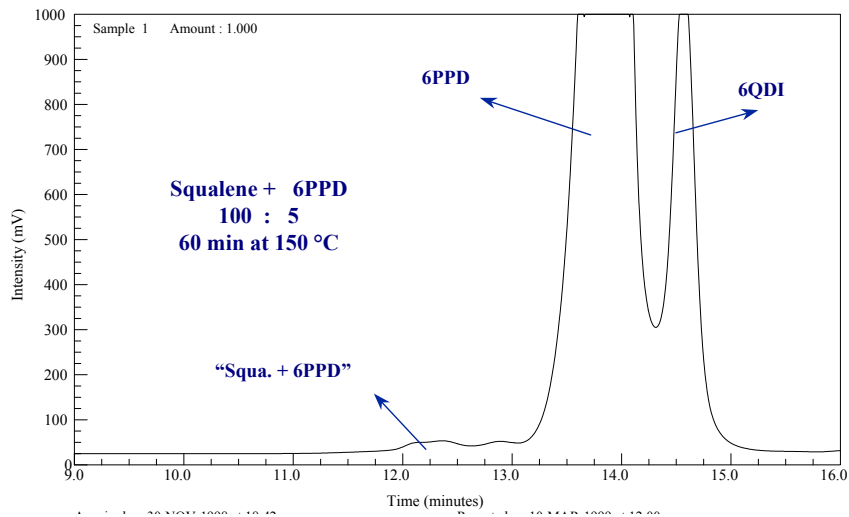


Figure 7.9: HP-SEC analysis of mixture of 6PPD and Squalene heated to 150°C for 60 minutes.

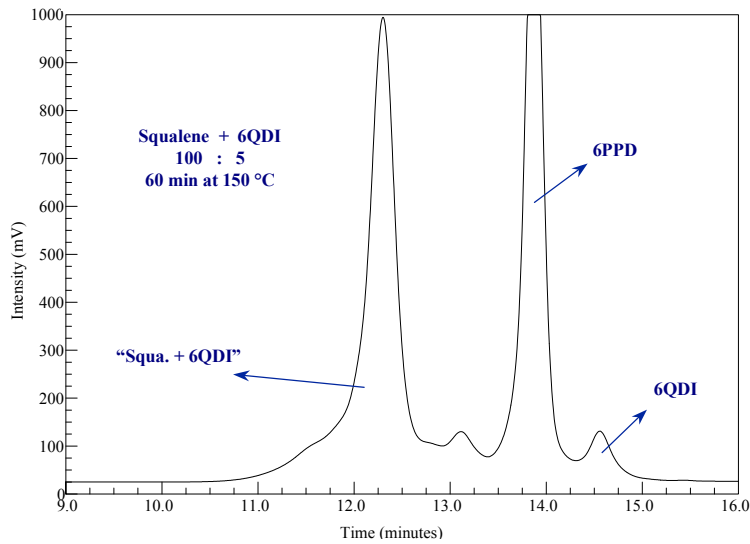


Figure 7.10: HP-SEC analysis of a mixture of 6QDI and squalene heated to 150°C For 60 minutes.

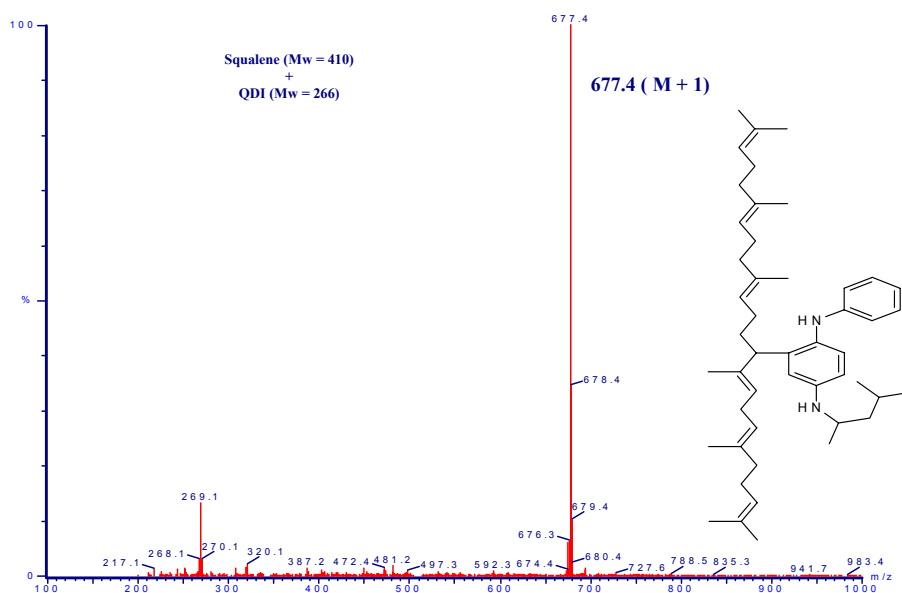


Figure 7.11: Mass spectrum of Squa + 6QDI adduct.

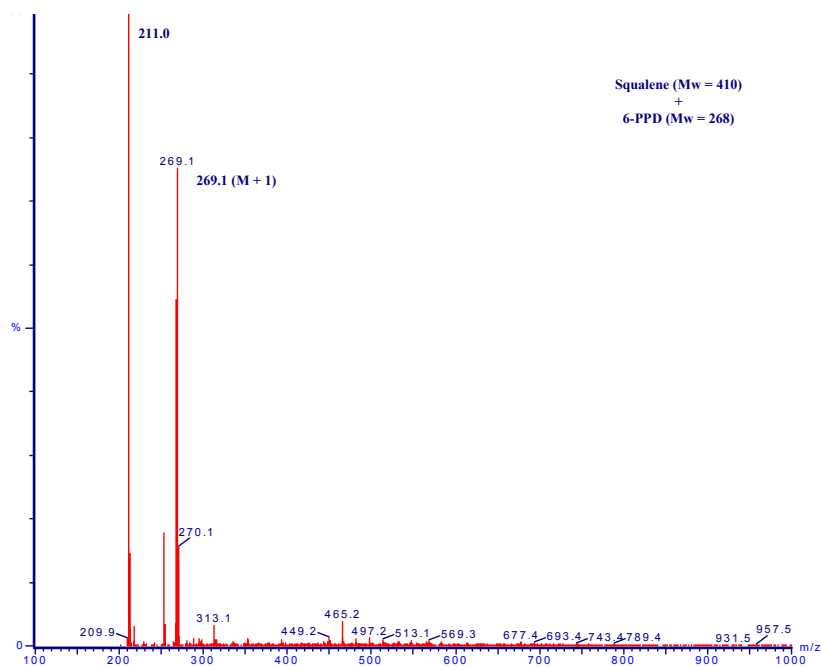


Figure 7.12: Mass spectrum of the high MW fraction of the reaction squalene + 6PPD.

When the mixtures containing sulfur as well: mixes 8 and 9 of Table 7.2, were analyzed, the HP-SEC analyses do not show much difference in the chromatograms while using the refractive index (RI) detector. However, analysis of the different MW fractions by FIA-MS showed a clear difference between the mixes containing 6PPD and 6QDI, as shown in figures 7.13 and 7.14 respectively. In the mass spectrum of mix 9 containing 6QDI, squalene-Sx-6PPD like adducts (x=0-4) are found. These type of adducts are not found in mix 8 containing 6PPD.

The above findings demonstrate, that in the presence of 6QDI, squalene is modified with 6PPD units attached to its backbone. The same is expected to happen in the rubber matrix of diene type rubbers, where 6PPD units are grafted to the polymer backbone, providing better as well as long term protection against oxidation.

It is also known that 6QDI provides a reinforcing effect, an increase in modulus in typical diene rubber formulations. This is another indication that 6QDI can react with rubber chains with the aid of double sulfur addition, figure 7.14, as well as via ene-type reaction as demonstrated in figure 7.15.

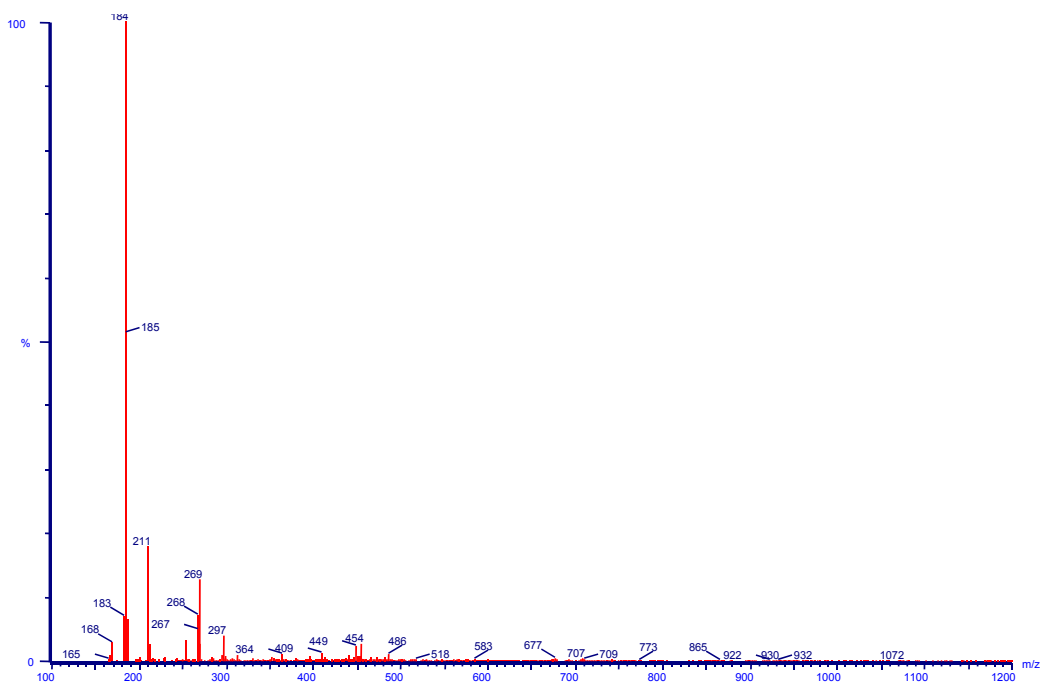


Figure 7.13: FIA-MS spectrum of a particular high MW fraction of mix 8, Table 7.2: Squalene+6PPD+CBS+S+zinc stearate.

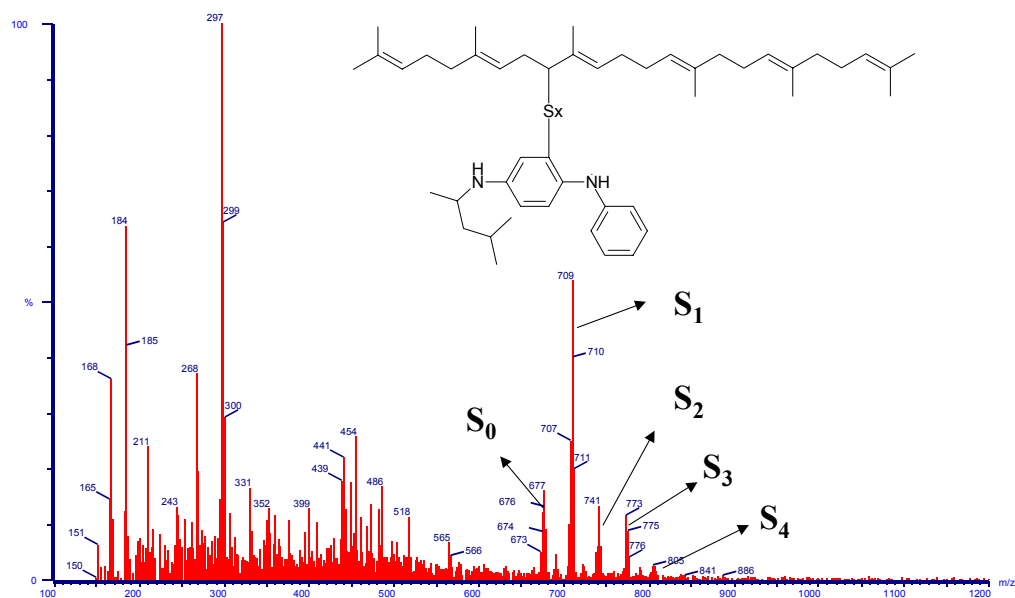


Figure 7.14: FIA-MS spectrum of a particular high MW fraction of mix 9, Table 7.2: Squalene+6QDI+CBS+S+zinc stearate.

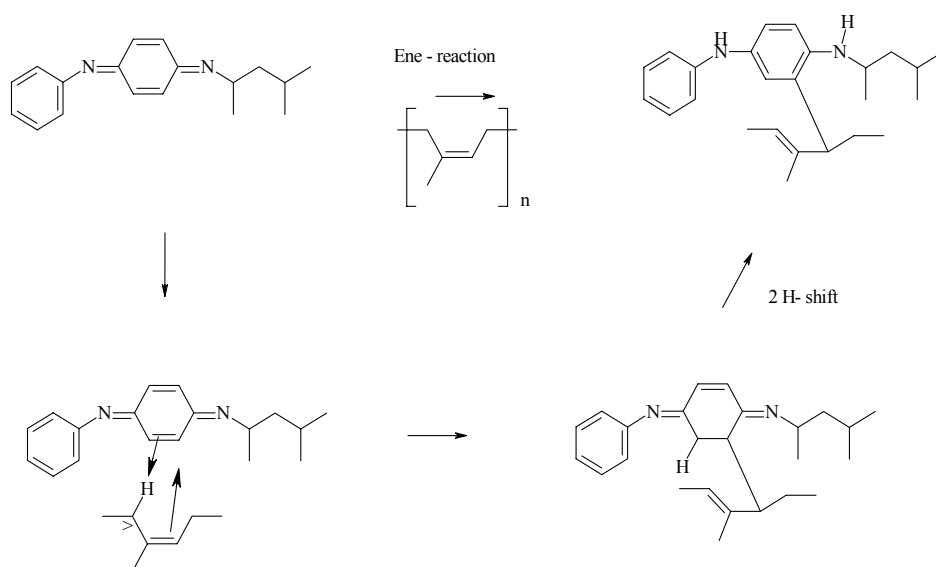


Figure 7.15: Possible ENE-reaction between 6QDI and polyisoprene.

7.4 Conclusions

The partial replacement of the silane-coupling agent TESPT by 6QDI in silica-reinforced “green tire” compounds has been studied. It was demonstrated that reducing the level of TESPT has negative consequences on the properties such as stress-strain, tear strength and hysteresis. However, incorporating 6QDI into the compounds containing a reduced level of TESPT compensates the negative effects providing equal or even better performance. A reaction mechanism between silica, 6QDI and rubber has been proposed to explain the improvement in Payne effect. Network density data indicate that 6QDI provides improved antioxidant protection as reflected in the retention of a polysulfidic network following aging. Above all, the data indicate that it is possible to optimize the level of TESPT with no detrimental effect on product performance.

The interaction between 6QDI and the rubber model compound squalene was studied by spectroscopic analysis of the adducts formed. It could be concluded that bound antioxidant properties of 6QDI are related to the fact, that 6QDI reacts with squalene in the presence of accelerator/sulfur and forms squalene-S_x-PPD adducts; 6QDI is converted to 6PPD during the reaction. Further, it is suggested that either an ENE reaction or the double sulfur addition of 6QDI and squalene are causing the grafting of 6QDI to the polymer.

7.5 References

1. J.W. ten Brinke, L.A.E.M. Reuvekamp, P.J. van Swaaij, J.W.M. Noordermeer, *Kautsch. Gummi Kunstst.*, **55**, (2002), 244.
2. L.A.E.M. Reuvekamp, J.W. ten Brinke, P.J. van Swaaij, J.W.M. Noordermeer, *Rubber Chem. Technol.*, **75**, (2002), 187.
3. L.A.E.M. Reuvekamp, J.W. ten Brinke, P.J. van Swaaij, J.W.M. Noordermeer, *Kautsch. Gummi Kunstst.*, **55**, (2002), 41.
4. J.W. ten Brinke, “Silica Reinforced Tyre Rubbers”, Twente University Press, ISBN 90 365 17583.
5. L.A.E.M. Reuvekamp, “Reactive mixing of silica and rubber for tyres and engine mounts”, Twente University Press, ISBN 90 365 1856 3.
6. S. Wolff, *Tire Sci. Technol.*, **15**, (1987), 276.
7. M.P. Wagner, *Rubber Chem. Technol.*, **49**, (1976) 703.
8. E.M. Dannenberg, *Rubber Chem. Technol.*, **55**, (1982) 862.
9. E.M. Dannenberg, *Rubber Chem. Technol.*, **48**, (1975) 410.
10. Y.Bomal, S. Touzet, R. Barruel, P. Cochet and D. Dejean, *Kautschuk Gummi Kunstst.*, **50**, (1997) 434.
11. B.T. Poh and C. C. Ng, *Eur. Poly. J.*, **24**, (1998), 975.
12. S. Wolff, *Kautschuk Gummi Kunstst.*, **30**, (1977), 516.

13. U. Gorl and J. Muenzenberg, paper no. 38, ACS, Rubber Division, Anaheim, California, (May 6-9, 1997).
14. A. Hunche, U. Gorl, H. G. Koban and T. Lehmann, *Kautschuk Gummi Kunstst.*, **51**, (1998), 525.
15. F. Ignatz-Hoover and R. N. Datta, *Rubber World*, **5**, (2000), 43.
16. R.N. Datta, P. Ebell and F. Ignatz-Hoover, *Gummi Fasern Kunststoffe*, **53**, (2000), 457.
17. R.N. Datta and F. Ignatz-Hoover, ACS, Rubber Division, Orlando, (September 21-24, 1999).
18. R.N. Datta, N.M. Huntink, and A.G. Talma, PCT WO 02150180 A1, (June 27, 2002).
19. R. Rauline, EP 0501227A1, (September 2, 1992).
20. B. Ellis and G. N. Welding, *Rubber Chem. Technol.*, **37**, (1964), 571.
21. P.J. Flory and J. Rehner, *J. Chem. Phys.*, **11**, (1943), 521.
22. B. Saville and A. A. Watson, *Rubber Chem. Technol.*, **40**, (1967), 100.
23. M. L. Selker and A.R. Kemp, *Ind. Eng. Chem.*, **36**, (1944), 20.
24. R.N. Datta and J.C. Wagenmakers, *J. Polym. Mat.*, **15**, (1998), 370.
25. R.N. Datta and F.A.A. Ingham, *Kautschuk Gummi Kunstst*, **52**, (1999), 758.
26. A.H.M. Schotman, P.J. C. van Haeren, A.J.M. Weber, F.G.H. van Wijk, J.W. Hofstraat, A.G. Talma, A. Steenbergen and R.N. Datta, *Rubber Chem. Technol.* **69**, (1996), 727.
27. J.A. Ayala, W.M. Hess, A.O. Dotson, and G.A. Joyce, *Rubber Chem. Technol.* **63**, (1990), 747.
28. R.N. Datta, S. Datta and N.M. Huntink, unpublished results
29. A.R. Payne, *Rubber Chem. Technol.* **39**, (1966), 365.
30. A.Y. Coran and J.B. Donnet, *Rubber Chem. Technol.* **65**, (1992), 1016.
31. R.N. Datta, S. Datta, N.M. Huntink and A.G. Talma, accepted for publication in *Kautschuk Gummi Kunstst*.
32. I.R. Gelling, G.T. Knight, "Plastics and Rubber Processing", (1977), 83.

Chapter 8

Ranking of several antidegradants for their effectiveness to protect rubber against oxidation using differential scanning calorimetry and by accelerated aging of steelcord skim compounds

The oxidation characteristics of several new types of potentially long-lasting antioxidants have been examined using differential scanning calorimetry (DSC). Oxidation induction times (OIT) were determined for polyisoprene that contains 0.5% of the experimental antioxidants. The antioxidants N-phenyl-3-(4-(phenylamino)phenylamino)propanoate (PPPP), 2-phenoxyethyl-3-(4-(phenylamino)phenylamino)propanoate (PEPPP) and the stearic acid salt of N-(1,3-dimethylbutyl)-N'-phenyl-p-phenylenediamine (PPD-C18) showed improved antioxidant efficiency compared to conventional antioxidants like polymerized 2,2,4-trimethyl-1,2-dihydroquinoline (TMQ) and N-(1,3-dimethylbutyl)-N'-phenyl-p-phenylenediamine (6PPD). Wingstay 100, a mixture of diaryl p-phenylene diamines, showed the best antioxidant efficiency in the OIT-test.

The efficiency of these antioxidants was also investigated in skim compounds during oxidative aging. Application of PPPP, PEPPP and PPD-C18 resulted indeed in improved network stabilization. The migration characteristics of the tested antioxidants were also investigated. Improved network stability obtained in the presence of PPPP, PEPPP and PPD-C18 could be explained by a combination of both increased OIT and decreased migration rates. PPPP seems to be the best antioxidant, because the product does not migrate under the applied test conditions and shows the highest antioxidant efficiency of all the tested antioxidants.

8.1 Introduction

The effectiveness of stabilizers is an important feature in the protection of rubber formulations used in the tire industry and other industrial rubber products. The stabilizers improve the rubber properties either during vulcanization or during service life. The stabilizers play a vital role when products are exposed to environments rich in oxygen and/or ozone, to thermal aging and other hostile service conditions. The characteristics of the rubber formulation will improve the performance of the product with the help of the applied stabilizer.¹

The oxidation of polymers is most commonly described in terms of the kinetic scheme developed by Bolland and coworkers.² The scheme is summarized in Chapter 2, figure 2.1. The key to the process is the initial formation of a free-radical species. At high temperatures and at large shear forces, it is likely that free radical formation takes place by cleavage of carbon-carbon and carbon-hydrogen bonds.

Many elastomers are already observed to oxidize at moderate temperatures below 60°C, where the energetics do not favor cleavage of carbon-carbon and carbon-hydrogen bonds. Therefore, several studies have been conducted to determine whether trace impurities present in the polymer systems account for the relative ease of oxidation. In two studies the conclusion was drawn that traces of peroxide were present in the polymer and that initiation occurred at low temperatures due to the relatively easy homolysis of these peroxides into free radicals.^{3,4} Due to the high reactivity of free radicals, only trace amounts of these peroxides need to be present to provide initiation of the oxidative chain process. On the other hand, mechanical shear during processing and bale compaction, and localized heat during the drying and packaging of the raw polymer are the most important causes of carbon-carbon and carbon-hydrogen bond cleavage. The resulting free radicals react with oxygen to form the peroxides responsible for degradation.

The oxidation of hydrocarbon polymers resembles the oxidation of low molecular weight hydrocarbons, with the polymer having its own internal source of peroxide initiators present. By making the assumption that peroxides are present in even the most carefully produced raw rubber, the ease of oxidation of rubber at low to moderate temperatures can be understood. Therefore, it is important to compound rubber for extended oxidation resistance by the use of protective additives and to be aware of pro-oxidant impurities present in the rubber or the rubber compound.

Complete inhibition of oxidation is seldomly obtained in elastomers by addition of antioxidants or stabilizers. What is usually observed is an extended period of retarded oxidation in the presence of the antioxidant. It has been demonstrated that during this period the rate of oxidation decreases with inhibitor concentration until the optimum concentration is reached and then increases again. The rate of the retarded reaction is affected by changes in oxygen concentration,⁵ in contrast to the uninhibited reaction, which proceeds at the same rate in oxygen or in air. These and other differences observed in the presence of oxidation inhibitors reflect significant changes in initiation and propagation, as well as in termination reactions.

The most common test used to study the oxidation resistance of rubber compounds involves accelerated aging of tensile dumbbell samples in an oxygen containing atmospheres. The resistance of a compound to oxidation is then measured by the percentage change in various physical properties, e.g. tensile strength, elongation at break, hardness and modulus. For an elastomer which reacts with oxygen resulting in crosslinking, generally butadiene-based elastomers such as BR, SBR, NBR, the accelerated tests result in increases in tensile modulus and hardness with a corresponding decrease in ultimate elongation. For an elastomer which reacts with oxygen resulting in chain scission, generally isoprene-based elastomers such as NR and IR, the accelerated aging tests result in decreases in tensile modulus and

hardness with either increasing or decreasing ultimate elongation, depending on the extent of degradation.⁶ The most effective antioxidant package for a given elastomer compound gives the smallest changes in physical properties during an accelerated aging test.

Thermoanalytical techniques such as DSC and TGA have widely been used to study rubber oxidation.⁷⁻¹⁰ The thermal stability of rubbers and the effectiveness of various antioxidants can be studied by thermal analysis. The oxidation induction time (OIT) has been proved to be a useful diagnostic tool in assessing the extent of degradation in polymeric materials. OIT is measured using DSC in isothermal mode and is calculated as the time from heating in O₂ atmosphere until the onset of rapid oxidation reaction. Rapid oxidation occurs after the antioxidant of the sample has been exhausted. Thus, OIT is related to the amount and type of antioxidant in the sample, and is a measure of its consumption during aging.

The aim of this chapter is to evaluate some new synthesized antidegradants as persistent, long-lasting antioxidants. A comparison will be made with regard to OIT values of the new products versus some commonly used antidegradants, such as TMQ, 6PPD and Wingstay 100. Finally, rubber tests are performed to correlate the findings of OIT ranking with network stability.

8.2 Experimental

8.2.1 Materials used

Compound ingredients:

Ingredients used for evaluation in rubber: NR SMR L (natural rubber, Wurfain & Co B.V.); carbon black N-326 (Cabot B.V.); Paraffinic oil (Sunpar 2280, Sun Petroleum Products Co.); ZnO (Harzsiegel standard); stearic acid (J.T. Baker); N-tert-butyl-di(2-benzothiazolesulfen)imide (Santocure TBSI, Flexsys); Crystex OT 20 (polymeric sulfur coated with 20% naphthenic oil, Flexsys); Tackifier SP-1068 (Alkyl phenol formaldehyde resin, Schenectady Europe); Bonding agent NAPCO 105 (Cobalt naphthenate containing 10.5% Cobalt, Shepard Chem).

Tested antidegradants:

Flectol TMQ (Flexsys); Santoflex 6PPD (Flexsys); Wingstay 100 (Goodyear); Q-Flex QDI (Flexsys); Stearic acid salt of 6PPD (PPD-C18, prepared as described in Chapter 3); N-Phenyl-3-(4-(phenylamino)phenylamino)-propanamide (PPPP, prepared as described in Chapter 3); 2-Phenoxyethyl 3-(4-(phenylamino)phenylamino)propanoate (PEPPP, prepared as described in Chapter 3). The structure of the tested antidegradants is shown in Table 8.1.

Table 8.1: Abbreviation, chemical name and structure of the tested antidegradants

| Abbrev. | Chemical name | Structure |
|--------------|---|-----------|
| 6PPD | N-(1,3-dimethylbutyl)-N'-phenyl-p-phenylenediamine | |
| 6QDI | Benzamine, N-(4-(1,3-dimethylbutyl)imino)-2,5-cyclohexadiene-1-ylidene) | |
| TMQ | 2,2,4-Trimethyl-1,2-dihydroquinoline, polymerized | |
| Wingstay 100 | mixture of diaryl p-phenylene diamines | |
| PPD-C18 | Stearic acid salt of 6PPD | |
| PPPP | N-Phenyl-3-(4-(phenylamino)phenylamino)propanoate | |
| PEPPP | 2-Phenoxyethyl-3-(4-(phenylamino)phenylamino)propanoate | |

8.2.2 Differential scanning calorimetry (DSC)

Materials:

cis-Polyisoprene (Aldrich, MW approximately 40.000; CAS nr. [43-126-5]); chlorobenzene (Aldrich, assay min. 99%; CAS nr. [108-90-7]).

Procedure:

DSC was used to determine the oxidation induction time (OIT). A sample of 0.5 weight % antioxidant in polymer was used for DSC oxidation induction time analysis. The polymer was dissolved in ten parts by weight of chlorobenzene. The antioxidant to be tested was weighed on a microbalance to a hundredth of a milligram. The polymer in chlorobenzene was weighed into the sample bottle containing the weighed antioxidant, and the sample bottle was covered with a septum lid and sonicated for 15 minutes to dissolve the antioxidant. Two microliters of this solution were added to an inverted Perkin-Elmer lid (part# 0219-0062) and the solvent was allowed to evaporate (10 min) before being placed in the DSC. The sample was run on a TA Instruments 2910 differential scanning calorimeter equipped with nitrogen delivery at 30 ml/min and 100% oxygen delivery at 70 ml/min. An isothermal program was used at 160°C under oxygen. The sample was first equilibrated at 160°C

under nitrogen. Oxygen was then turned on when the isothermal step of the program starts. The oxidation induction time was measured from the point when oxygen was turned on to the onset of the oxidation exotherm.

Cautions to be taken for OIT measurements:

- Cover with nitrogen after each time the polymer sample bottle is opened. OIT becomes shorter as the polymer ages.
- The isothermal temperature can be adjusted for an antioxidant/polymer system to give an exotherm, which occurs between about 15 min. to one hour.
- The amount of solution calculated to give a 0.5% AO in polymer is added to the weighed amount of AO. Once dissolved, the AO in polymer should be used immediately. If allowed to stand overnight, the OIT is shorter.
- If more sample or a different sample configuration is used, the OIT increases with sample thickness. Therefore, experiments have to be done under exactly the same conditions in order to make a reliable comparison possible between different antioxidants.

Comments:

The isothermal DSC technique involves subjecting a polymer sample to an isothermal temperature under an oxidizing atmosphere until an oxidative exotherm occurs. At this point, one calculates the time to onset of oxidation and uses this “onset time” as an indication of the polymer’s resistance to oxidation or the effectiveness of an antidegradant package. Several aspects of this procedure and analysis need further discussion.

Since most samples start at room temperature and need some time to be heated to the isothermal temperature, there is an initial period where the scan is not isothermal.¹¹ The effect of this period has to be taken care of by keeping the atmosphere inert during this period and then, once isothermal conditions are reached, by changing the atmosphere to the oxidizing condition to start the test.

The selection of the “onset time” is not completely straightforward. Extrapolation of the baseline slope to the tangent of the inflection point of the curve is the usual technique for calculating the “extrapolated onset time”. However, in slow oxidizing systems, the difference between this extrapolated onset and the actual time of departure of the curve from the baseline can be significant, as demonstrated in fig. 8.2. Much discussion has taken place in the literature over this point and this problem has still not been completely resolved, although the current extrapolation technique is still used extensively.⁷ This technique was also applied in this study.

Extrapolation of onset times from one temperature (used for testing) to another temperature (actual use) can lead to problems. These problems arise from changes in the nature of the materials, like polymers and additives, over the range of temperatures involved. For instance, the evaluation of an antidegradant at 100°C for extrapolation to use at room temperature can be problematic. The antidegradant may be a crystalline solid with limited solubility in the polymer at room temperature, but a liquid with substantial solubility at 100°C. These difficulties often lead to improper

conclusions when extrapolating high temperature results to lower temperature use conditions. It should be noted, however, that this problem is not limited to this thermal technique or procedure. This is the case with any experimentation that requires a different temperature to allow predictive testing in time frames shorter than the actual application.

Finally, the sample configuration (surface area, sample weight) has a large influence on the obtained results, as shown in fig. 8.3. From a practical standpoint, the isothermal technique can be very time consuming if no attempts are made to find a proper isothermal temperature range within which to operate. It is desirable to have the induction time for these oxidations to range between 15 minutes and one hour.

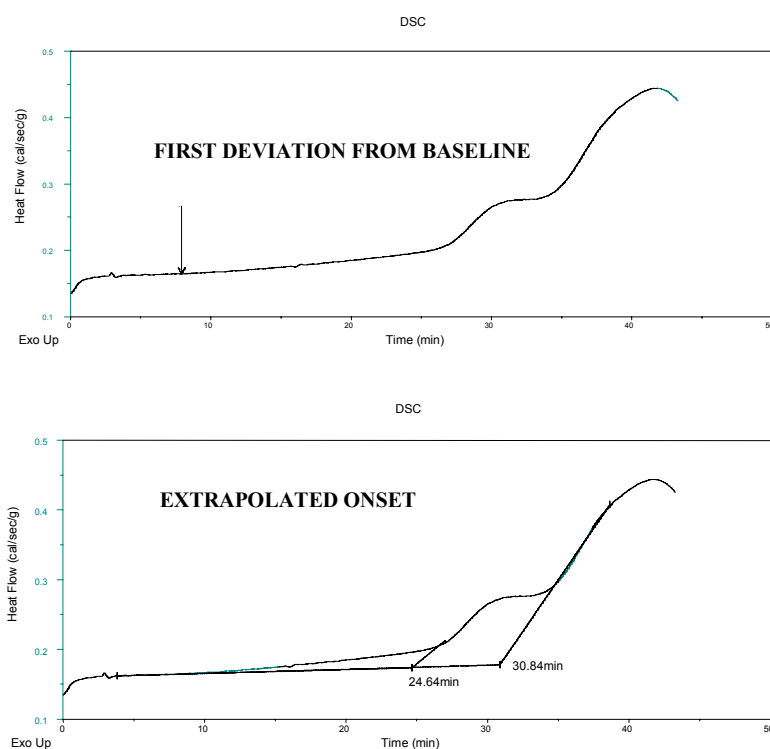


Fig. 8.2: Determination of the “extrapolated onset time”

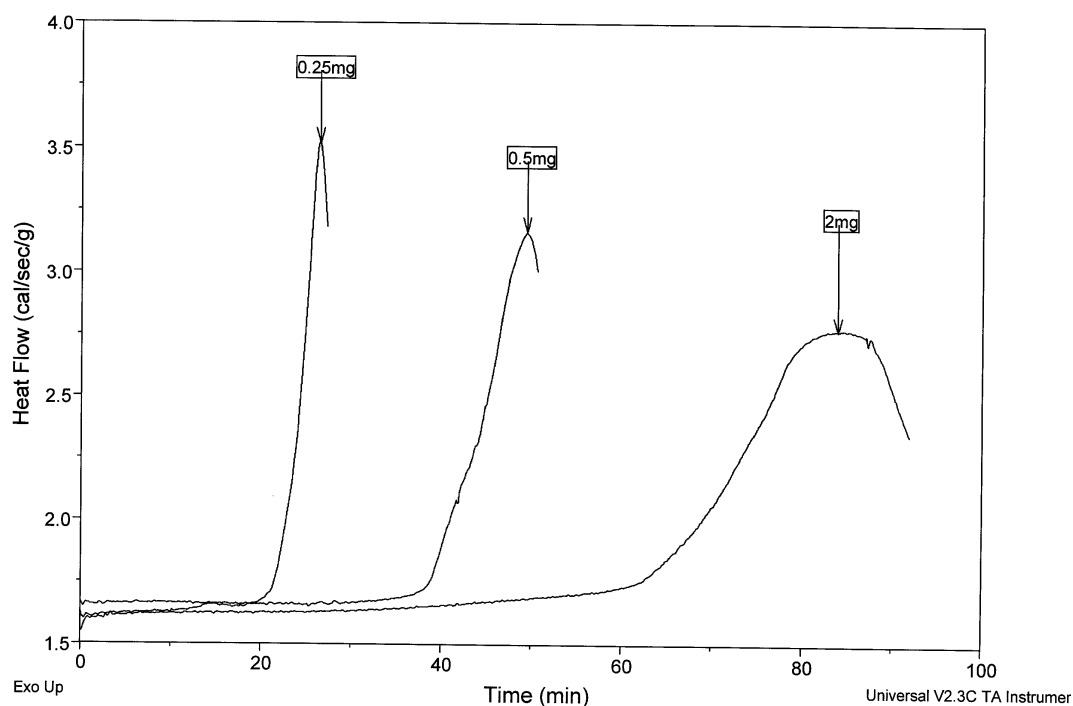


Fig. 8.3: The effect of the sample size on OIT determined by DSC-measurements (0.5 m/m% Wingstay 100 in polyisoprene at 160°C).

8.2.3 Formulations, mixing and curing

The compound formulations are shown in Table 8.2. All the ingredients except sulfur and accelerators were mixed in a 1.6L internal mixer. Sulfur and accelerator were subsequently added on a two-roll mill at 50-65°C according to standard laboratory mixing conditions.

Cure characteristics were determined using an MDR 2000EA rheometer. Delta torque or extent of crosslinking is the maximum torque (M_H) minus the minimum torque (M_L). Scorch safety (t_{s2}) is the time needed to reach 2 dNm above minimum torque (M_L); optimum cure time (t_{90}) is the time needed to reach 90% of the delta torque above minimum. Sheets and test specimens were cured to optimum cure by compression molding in a Fontyne TP-400 press at 150°C / $t_{90}+10$ minutes.

Table 8.2: Formulations (skim compound).

| Ingredient/mix | 1 | 2 | 3 | 4 | 5 | 6 | 7 | 8 |
|----------------------|--------|--------|--------|--------|--------|--------|--------|--------|
| NR SMR L | 100.00 | 100.00 | 100.00 | 100.00 | 100.00 | 100.00 | 100.00 | 100.00 |
| Carbon black N-326 | 60.00 | 60.00 | 60.00 | 60.00 | 60.00 | 60.00 | 60.00 | 60.00 |
| Par. Oil Sunpar 2280 | 2.00 | 2.00 | 2.00 | 2.00 | 2.00 | 2.00 | 2.00 | 2.00 |
| Tackifier SP-1068 | 2.00 | 2.00 | 2.00 | 2.00 | 2.00 | 2.00 | 2.00 | 2.00 |
| Bond.ag. NAPCO 105 | 1.10 | 1.10 | 1.10 | 1.10 | 1.10 | 1.10 | 1.10 | 1.10 |
| ZnO Harzsiegel st. | 5.00 | 5.00 | 5.00 | 5.00 | 5.00 | 5.00 | 5.00 | 5.00 |
| Ctx OT 20 | 5.00 | 5.00 | 5.00 | 5.00 | 5.00 | 5.00 | 5.00 | 5.00 |
| Santocure TBSI | 0.90 | 0.90 | 0.90 | 0.90 | 0.90 | 0.90 | 0.90 | 0.90 |
| Stearic acid | 2.00 | 2.00 | 2.00 | 2.00 | 2.00 | 2.00 | 2.00 | 2.00 |
| Santoflex 6PPD | - | 2.00 | - | - | - | - | - | - |
| Wingstay 100 | - | - | 2.00 | - | - | - | - | - |
| Flexitol TMQ | - | - | - | 2.00 | - | - | - | - |
| Santoflex 6QDI | - | - | - | - | 2.00 | - | - | - |
| PPPP | - | - | - | - | - | 2.00 | - | - |
| PEPPP | - | - | - | - | - | - | 2.00 | - |
| Santoflex PPD-C18 | - | - | - | - | - | - | - | 4.00 |

8.2.4 Testing

Stress-strain properties:

Tensile stress-strain properties were determined according to ISO 37. Aging of the test specimens was carried out in a ventilated oven in the presence of air at 100°C for 1 day according to ISO 188.

Network structure:

The network structure was determined by equilibrium swelling in toluene using the method reported by Ellis and Welding.¹² The volume fraction (V_r) obtained was converted into the Mooney-Rivlin elastic constant (C_1) and finally into the concentration of chemical crosslinks by using equations described in the literature.^{13,14} The proportions of mono-, di-, and polysulfidic crosslinks in the vulcanizates were determined by equilibrium swelling in toluene before and after thiol amine chemical probe treatment.¹⁵ Details of the procedure have been reported by Datta et al.¹⁶⁻¹⁸

Migration characteristics:

The migration characteristics of the antidegradants shown in Table 8.1 were determined by diffusion experiments according to the method described in Chapter 4. The amount of antioxidant present in the toluene and dichloromethane extractables of the rubber vulcanizates was quantified by GC/FIA-MS, as described in § 8.2.5.

8.2.5 Characterization of the rubber vulcanizates by GC/FIA-MS

The amount of antioxidant present in the toluene and dichloromethane extractables of the rubber vulcanizates was quantified using a capillary gas chromatograph equipped with a split injector and a flame ionization detector. Identification of the different peaks was done by FIA-MS using the Platform-II quadrupole ex Micromass. In positive ESI, components should give $[M + H]^+$ or $[M + Na]^+$ adducts, so m/z values of $M + 1$ or $M + 23$ are expected to be formed. Ionization was done by electrospray positive/negative: scan range 200-1500 Da; capillary voltage 3.50kV; HV lens 0.5V; skimmer 5V; Cone voltage 10/30 V/60V; source temperature 60°C. Methanol was used as a carrier solvent.

GC-conditions:

| | |
|------------------|---|
| Column | : fused silica column WCOT, 17m * 0.32 mm ID |
| Stationary phase | : Sil 5 CB, 100% polydimethylsiloxane, crosslinked |
| Film thickness | : 0.4 μ m |
| Injector | : Split, 250°C |
| Detector | : FID, 330°C |
| Temp. program | : 120°C (1 min.) $\xrightarrow{10^\circ\text{C}/\text{min.}}$ 320°C (25 min.) |

8.3 Results and discussion

The oxidation characteristics of several new types of expected long-lasting antioxidants were examined making use of differential scanning calorimetry (DSC). Oxidation induction times (OIT) were determined for polyisoprene containing 0.5% antioxidant. The obtained results are described in the first part of this paragraph. The results obtained with OIT were compared with actual compounds, by determination of the network stability in skim compounds containing these antioxidants. These results are described in the second part of this paragraph. The migration characteristics of the tested antioxidants were also investigated and summarized at the end of this paragraph.

8.3.1 OIT measurements

The described isothermal DSC approach was used to determine the effectiveness of several potential long-lasting antioxidants, while considering all the concerns indicated earlier. The antioxidants were tested in polyisoprene at 160°C. The obtained results are shown in Table 8.3 and fig. 8.4. The new products PPD-C18, PPPP and PEPPP show improved antioxidant protection compared to the conventional antioxidants like 6PPD and TMQ, as demonstrated by significantly larger induction periods. Wingstay 100 shows the largest induction period and thus the best antioxidant protection. TMQ shows a low antioxidant activity, which is rather

unexpected because it is widely used as an antioxidant. The latter is most probably related to the relatively low cost of TMQ compared to products like 6PPD. It is possible, that there is a synergistic effect between 6PPD and TMQ, as discussed by Parra et al. for mixtures of diamines and ADPA.¹⁹ This means that the combined effect of both antioxidants is greater than the sum of the individual effects. 6QDI shows a worse antioxidant protection compared to 6PPD, which can be explained by the fact that 6QDI is one of the reaction products formed by oxidation of 6PPD and therefore has less antioxidant functionality left. The ranking in increasing antioxidant protection or increasing OIT is: TMQ < 6QDI < 6PPD < PPD-C18 < PEPPP < PPPP < Wingstay 100.

Table 8.3: OIT determined by DSC-measurements for different antioxidants: 0.5 m/m% in polyisoprene at 160°C.

| Antidegradant | OIT [min.] |
|---------------|------------|
| Control | 0.1 |
| 6PPD | 15.8 |
| Wingstay 100 | 58.1 |
| TMQ | 3.9 |
| 6QDI | 10.6 |
| PPPP | 49.8 |
| PEPPP | 42.3 |
| PPD-C18 | 25.0 |

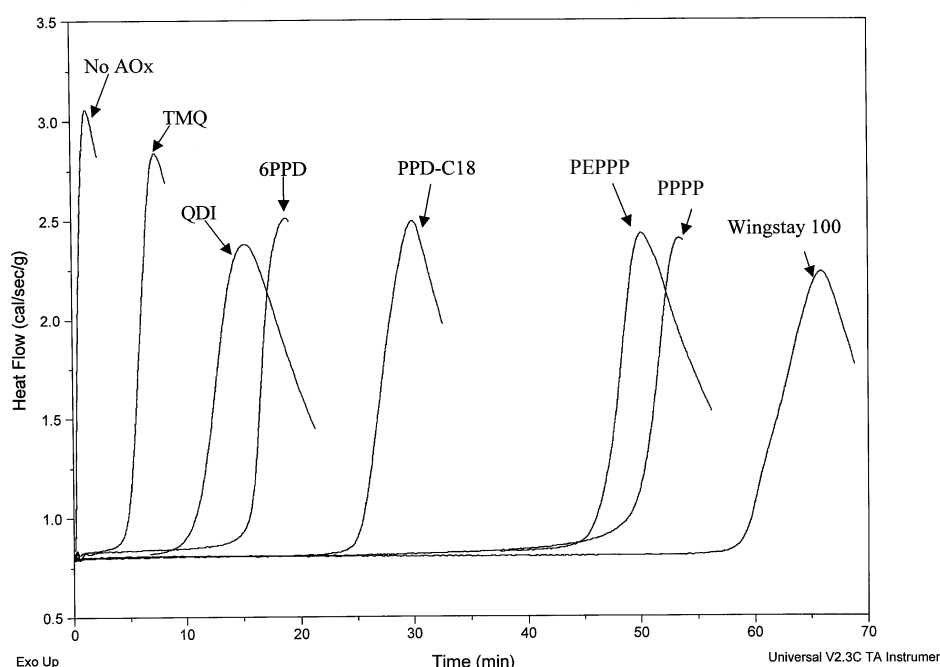


Fig. 8.4: OIT determined by DSC measurements for different antioxidants: 0.5m/m% in polyisoprene at 160°C.

8.3.2 Network protection during oxidative aging of skim compounds

The factors, such as volatility (molecular weight), solubility in polyisoprene, molecular shape and melting point are believed to be contributing factors to the oxidation induction times, as measured by DSC. It is therefore necessary to check the effect of these antidegradants as observed with the OIT in actual rubber compounds. We tested the antioxidants in a typical steelcord adhesion skim compound and monitored the effectiveness by the stress-strain properties before and during oxidative aging. The compositions of the tested compounds are shown in Table 8.2. The relatively high sulfur loading, 5phr insoluble sulfur, is necessary to obtain good steelcord adhesion properties.²⁰

The cure data of the tested compounds are described in Table 8.4. It is clear from these data that incorporation of 6QDI improves the processing behavior of the skim compound by lowering the viscosity as reflected in lower M_L .²¹ Incorporation of all the tested antioxidants results in decreased scorch times as reflected in t_{s2} or scorch safety. Incorporation of N-Phenyl-3-(4-(phenylamino)phenylamino)propanoate (PPPP) results in the lowest scorch safety, the shortest cure time t_{90} and the fastest cure rate t_{90} - t_{s2} of all the tested products.

Table 8.4: Cure data of the compounds obtained at 150°C.

| Properties/mixes | 1 Contr. | 2 6PPD | 3 W100 | 4 TMQ | 5 6QDI | 6 PPPP | 7 PEPPP | 8 PPD-C18 |
|---|-------------|-----------|-----------|----------|-----------|-----------|------------|--------------|
| Extent of crosslinking, R_∞ , Nm | 2.28 | 2.10 | 2.16 | 2.06 | 2.23 | 2.27 | 2.11 | 2.28 |
| M_L , Nm | 0.23 | 0.22 | 0.24 | 0.24 | 0.20 | 0.25 | 0.25 | 0.23 |
| T_{s2} , min | 3.00 | 2.82 | 2.63 | 2.97 | 2.69 | 1.87 | 2.49 | 2.42 |
| T_{90} , min | 13.56 | 11.60 | 11.58 | 12.06 | 13.13 | 9.75 | 11.22 | 11.02 |
| T_{90} - t_{s2} , min | 10.56 | 8.88 | 8.95 | 9.02 | 10.44 | 7.88 | 8.73 | 8.60 |

Stress-strain properties were determined before and after hot air aging: 1 day at 100°C. The results are given in Table 8.5. Differences before aging are small and within the standard deviation of the test method. The results obtained after aging show some clear differences. Better retention of tensile strength and elongation at break is obtained for compounds containing PPPP (6), PEPPP (7) or PPD-C18 (8) as compared to other compounds. It needs to be mentioned that compounds containing 6QDI are slightly better compared to that of the conventional antioxidants 6PPD, Wingstay 100 and TMQ but inferior compared to PPPP (6), PEPPP (7) and PPD-C18 (8).

Table 8.5: Stress-strain properties determined by tensile measurements, cured @ 150°C/t₉₀+10min.

| Properties/mix | 1 | 2 | 3 | 4 | 5 | 6 | 7 | 8 |
|------------------------|----------------|----------------|----------------|----------------|----------------|----------------|----------------|----------------|
| | Contr. | 6PPD | W100 | TMQ | 6QDI | PPPP | PEPPP | PPD-C18 |
| Modulus, M100, MPa | 3.9 (6.8) | 3.8 (6.8) | 4.0 (7.1) | 3.7 (6.7) | 4.2 (7.6) | 3.7 (6.8) | 3.9 (6.6) | 4.2 (7.2) |
| Modulus, M300, MPa | 16.5 (-) | 15.7 (-) | 15.6 (-) | 15.2 (6.7) | 16.8 (-) | 14.6 (-) | 15.6 (-) | 16.3 (-) |
| Tensile strength, MPa | 26.3 (18.2) | 26.4 (19.7) | 26.4 (18.6) | 25.0 (20.1) | 24.9 (20.6) | 25.1 (21.5) | 26.1 (21.4) | 25.1 (21.5) |
| Elongation at break, % | 461 (230) | 484 (246) | 479 (238) | 473 (265) | 448 (270) | 477 (291) | 471 (282) | 464 (285) |

* Data within parentheses are those for the vulcanizates after aging at 100°C for 1day

The crosslink density and distribution of crosslink types was determined in order to correlate the vulcanizate properties with the network characteristics. The data are presented in Table 8.6. The increased crosslink density following aging can be explained by the formation of new crosslinks from residual sulfur still present in the compound after vulcanization: i.e. free sulfur, pendent groups, cyclic sulfur or polysulfidic crosslinks.²²

It is clear from these data that use of 6QDI, PPPP, PEPPP and PPD-C18 results in improved retention of polysulfidic crosslinks, poly-S, following aging: a higher amount of polysulfidic and a lower amount of monosulfidic crosslinks is obtained for these compounds after aging. This better protection of poly-S network can be explained by the bound antioxidant behavior of 6QDI, as described in Chapter 7, and by a decreased migration rate of PPPP, PEPPP and PPD-C18 compared to that of 6PPD and Wingstay 100, as shown in fig. 8.4. The stabilization of network obtained in the presence of PPPP, PEPPP and PPD-C18 can be explained by a combination of both increased antioxidant efficiency (increased OIT) and decreased migration rates. The antioxidant PPPP seems to be the best antioxidant, because this product does not migrate under the applied test conditions and shows the highest antioxidant efficiency of all the tested antioxidants.

The lower migration rate observed for TMQ can be explained by the fact that only the lower molecular weight oligomers are migrating. This type of antioxidant was therefore also expected to be a long-lasting antioxidant. However, incorporation of TMQ did not result in improved stress-strain properties following aging compared to 6PPD, which is in line with the worse antioxidant activity of TMQ estimated by isothermal DSC measurements.

Wingstay 100 is, based on the OIT measurements, expected to give good antioxidant protection in rubber compounds. However, as can be seen from the relatively low tensile strength and low amount of polysulfidic crosslinks after aging, its effectiveness is similar to that of 6PPD and worse compared to 6QDI, PPD-C18, PEPPP and PPPP. This is most probably related to the relatively large migration coefficient of Wingstay 100: see fig. 8.4. Based on stress-strain properties and network analyses, the ranking in increasing antioxidant protection is: Wingstay 100 < TMQ < 6PPD < 6QDI < PPD-C18 \approx PEPPP \approx PPPP.

Table 8.6: Crosslink density* and crosslink types of skim compounds, cured @ 150°C/t₉₀+10min.

| Properties/mix | 1 Contr. | 2 6PPD | 3 W100 | 4 TMQ | 5 6QDI | 6 PPPP | 7 PEPPP | 8 PPD-C18 |
|------------------|--------------|--------------|--------------|--------------|--------------|--------------|--------------|--------------|
| Total crosslinks | 5.5 (6.5) | 5.2 (6.9) | 5.2 (6.9) | 5.1 (6.7) | 5.6 (7.3) | 5.1 (6.7) | 5.2 (6.7) | 5.4 (7.4) |
| Poly-S | 4.1 (4.2) | 3.5 (4.1) | 3.5 (4.4) | 3.6 (4.2) | 4.0 (4.7) | 3.6 (4.8) | 3.6 (4.6) | 3.7 (4.8) |
| Di-S | 0.2 (0.3) | 0.7 (1.2) | 0.5 (0.7) | 0.4 (0.8) | 0.6 (1.3) | 0.6 (0.7) | 0.7 (0.8) | 0.8 (1.0) |
| Mono-S | 1.2 (2.0) | 1.0 (1.7) | 1.2 (1.9) | 1.1 (1.7) | 1.0 (1.3) | 0.9 (1.2) | 0.9 (1.3) | 1.1 (1.6) |

* Crosslink density expressed in grammole/gram rubber hydrocarbon $\times 10^{-5}$

♣ Data within parentheses are those for the vulcanizates aged for 1 day at 100°C

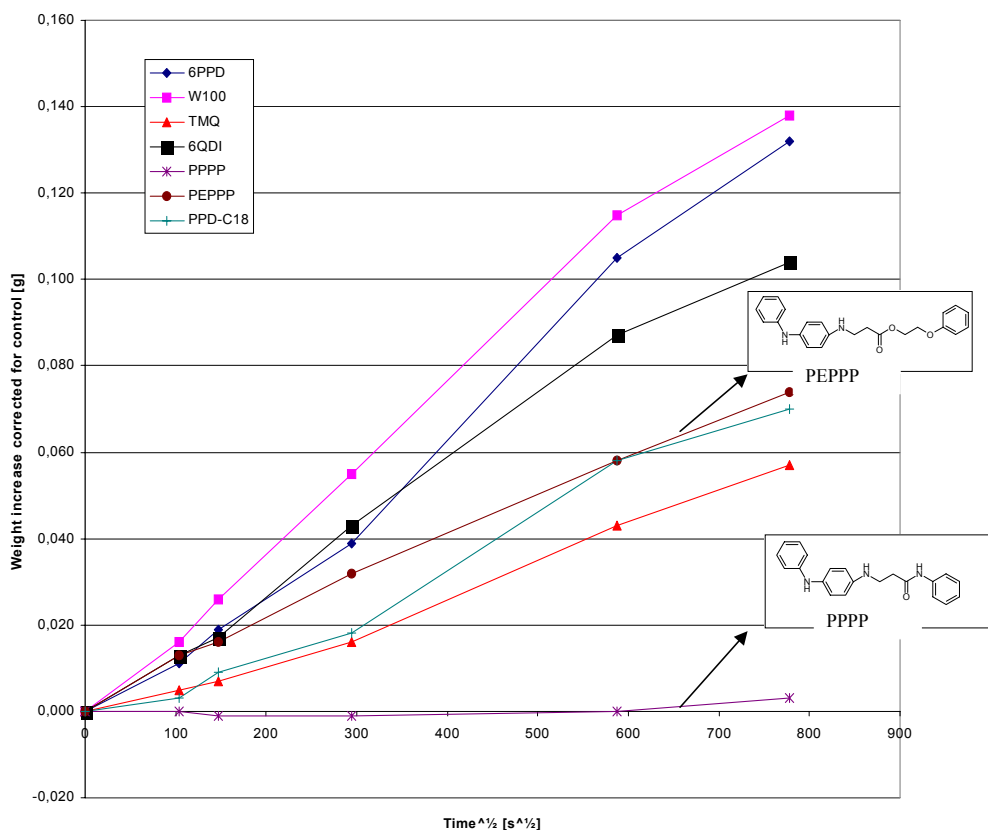


Fig. 8.4: Migration behavior of different antidegradants determined at 40°C, cured @ 150°C/ t_{90} +10min.

8.4 Conclusions

The oxidation characteristics of several new types of potentially long-lasting antioxidants have been examined using differential scanning calorimetry (DSC). Oxidation induction times (OIT) were determined from polyisoprene containing 0.5 m/m% antioxidants. The antioxidants PPPP, PEPPP and PPD-C18 showed improved antioxidant efficiency compared to conventional antioxidants like TMQ and 6PPD. Wingstay 100 showed the best antioxidant efficiency.

The efficiency of these antioxidants was also investigated by determination of the network stability in skim compounds. Incorporation of 6QDI, PPPP, PEPPP and PPD-C18 resulted in improved network stabilization. The improved network stabilization observed in the presence of 6QDI could be explained by its bound antioxidant properties. The stabilization of network obtained in the presence of PPPP, PEPPP and PPD-C18 could be explained by a combination of both increased antioxidant efficiency (increased OIT) and decreased migration rates. The antioxidant PPPP seems to be the best antioxidant, because this product does not migrate under

the applied test conditions and shows the highest antioxidant efficiency of all the tested antioxidants.

TMQ showed a decreased migration rate, but still poor antioxidant efficiency compared to 6PPD: decreased OIT. The relatively poor network stabilization observed after incorporation of TMQ can be explained by the low antioxidant efficiency of this product. Consequently the ranking in increasing antioxidant protection is: TMQ < 6PPD < Wingstay 100 < 6QDI < PPD-C18 < PEPPP < PPPP.

8.5 References

1. A.D. Roberts, Natural Rubber Science and Technology, Oxford University Press, Oxford, (1988), 650.
2. J.L. Bolland, Quart. Rev., Chem. Soc., **3**, (1949), 1.
3. J.R. Shelton and D.N. Vincent, J. Am. Chem. Soc., **85**, (1963), 2433.
4. L. Bateman, M. Cain, T. Colclough, and J.I. Cunneen, J. Chem. Soc., (1962), 3570.
5. J.R. Shelton, Rubber Chem. Technol., **30**, (1957), 1270.
6. A.N. Gent, J. Appl. Polym. Sci., **6**, (1962), 497.
7. D.J. Burlett, Rubber Chem. Technol., **72**, (1999), 165.
8. N.C. Billingham, D.C. Bott and A.S. Manke, Applied Science Publishers, London, chap. 3 (1981).
9. D.I. Marshall, E. George, J.M. Turnipseed and J.L. Glenn, Polym. Eng. Sci., **13**, (1973), 415.
10. H.E. Bair, Polym. Eng. Sci., **13**, (1973), 435.
11. S.M. Marcus, R.L. Blaine, ASTM Spec. Tech. Publ., **1326**, (1996).
12. B. Ellis and G.N. Welding, Rubber Chem. Technol., **37**, (1964), 571.
13. P.J. Flory and J. Rehner, J. Chem. Phys., **11**, (1943), 521.
14. B. Saville and A.A. Watson, Rubber Chem. Technol., **40**, (1967), 100.
15. L. Selker and A.R. Kemp, Ind. Eng. Chem., **36**, (1944), 20.
16. R.N. Datta and J.C. Wagenmakers, J. Polym. Mat., **15**, (1998), 370.
17. R.N. Datta and F.A.A. Ingham, Kautschuk Gummi Kunstst, **52**, (1999), 758.
18. A.H.M. Schotman, P.J.C. van Haeren, A.J.M. Weber, F.G.H. van Wijk, J.W. Hofstraat, A.G. Talma, A. Steenbergen and R.N. Datta, Rubber Chem. Technol., **69**, (1996), 727.
19. D.F. Parra, J.R. Matos, Journal of Thermal Analysis and Calorimetry, **67**, (2002), 287.
20. J.M. Swarts, Rubber World, (February 2002), 26.
21. R.N. Datta, P. Ebell, F. Ignatz-Hoover, Kautschukchemikalien, GAK 7/2000, **53**, (2000), 457.
22. R.N. Datta, N.M. Huntink, KGK Kautschuk Gummi Kunststoffe, **55**, (2002), 350.

Chapter 9

The interaction of antidegradants with sulfur vulcanization agents

The interaction between antidegradants and other rubber chemicals is an important feature, especially when they are used in critical parts like compounds reinforced with steelcord. These compounds consist of a relatively high concentration insoluble sulfur, which is a metastable product that can revert to soluble sulfur. Reversion takes place at elevated temperatures and it depends on the thermal stability of insoluble sulfur. The presence of impurities and other rubber chemicals (i.e. antidegradants) can affect the thermal stability of insoluble sulfur.

The effect of several antidegradants on the thermal stability of insoluble sulfur, versus its reversion to soluble sulfur has been examined with blooming experiments, bin scorch measurements, a thermal stability test in a transparent butadiene rubber and a thermal stability test in mineral oil (HTS-test).

Benzamine, N-(4-(1,3-dimethylbutyl)imino)-2,5-cyclohexadiene-1-ylidene) (6QDI) has a negative effect on the thermal stability of insoluble sulfur as demonstrated by the HTS-test as well as the transparent BR-test, compared to the corresponding amine antidegradant N-(1,3-dimethylbutyl)-N'-phenyl-p-phenylenediamine (6PPD).

Polymerized 2,2,4-trimethyl-1,2-dihydroquinoline (TMQ) also has a negative effect on the thermal stability of insoluble sulfur due to the presence of low molecular weight amine impurities, like aniline. The purified product (Antigene FR) and the reaction product of TMQ and maleic anhydride (Naugard Q extra) showed negligible effect on the thermal stability of insoluble sulfur.

FT-Raman spectroscopy was applied to study the thermal stability of insoluble sulfur in the presence of different antidegradants. Unfortunately, this technique could not be used to study compounds containing 6QDI, due to a high fluorescence background signal caused by the dark color of these compounds. The S_{01} polymeric sulfur allotrope has a better thermal stability than the S_{02} allotrope. In the presence of 6PPD however no difference in thermal stability was found between both insoluble sulfur allotropes.

9.1 Introduction

The interaction between antidegradants and rubber chemicals is an important feature especially when they are used in critical parts like compounds reinforced with steelcord. Improving the network stability of steelcord adhesion skim compounds is one of the main research topics at tire manufactures. These compounds consist of a relatively high concentration of insoluble sulfur, which is a metastable product that can revert to soluble sulfur. Reversion takes place at elevated temperatures and depends on the thermal stability of the insoluble sulfur. The presence of impurities and other rubber chemicals like antidegradants can affect the thermal stability of insoluble sulfur. One way to improve the network and insoluble sulfur stability could be replacement of conventional antidegradants like 6PPD and TMQ by longer-lasting antidegradants. The bound antioxidant properties of 6QDI, as shown in Chapter 7 for silica reinforced green tire compounds and in Chapter 8 for steelcord adhesion skim compounds, could help to provide improved network stability. From an application point of view it is important to know the effect of these antidegradants on the thermal stability of insoluble sulfur. This chapter focuses on the interaction between antidegradants and insoluble sulfur.

Insoluble sulfur is used as a vulcanizing agent in critical compounds where high sulfur loadings, concentrations higher than the solubility limit of soluble sulfur (SS), are needed. Unlike rhombic soluble sulfur, insoluble sulfur (IS) is not soluble in uncured rubber, as the name implies. The solubility of rhombic soluble sulfur varies with temperature: the higher the temperature, the better is the solubility in the rubber matrix. However, at room temperature some rhombic soluble sulfur (RMS), consisting of S8 rings, will migrate to the surface of a rubber article and crystallize when it is used as a vulcanizing agent at concentrations above the solubility limit. This phenomenon is referred to as sulfur blooming. No blooming can occur when insoluble sulfur is used, since it can not freely migrate throughout the material. The critical property of insoluble sulfur is its thermal stability over a wide temperature range. Chemical decomposition should occur in the neighborhood of the crosslinking temperature, as shown in fig. 9.1. In other words, the temperature at which insoluble sulfur decomposes into low MW sulfur species should be as high as possible. Although it is known to a certain extent how to influence the thermal stability of insoluble sulfur during its production, the factors that determine the thermal stability are not exactly known. In the past, some evidence was obtained, that physical/chemical properties such as purity, molecular weight, particle size, porosity, crystalline structure, crystalline perfection, etc. are responsible for the thermal stability.¹⁻³

Insoluble sulfur consists of three different polymeric sulfur allotropes, denoted by $S_{\omega 1}$, $S_{\omega 2}$ and S_{ψ} .¹ The crystal structures of the three allotropes are remarkably similar. All three consist of polymeric sulfur helices; the stacking order of these helices is however different as shown in fig. 9.2.

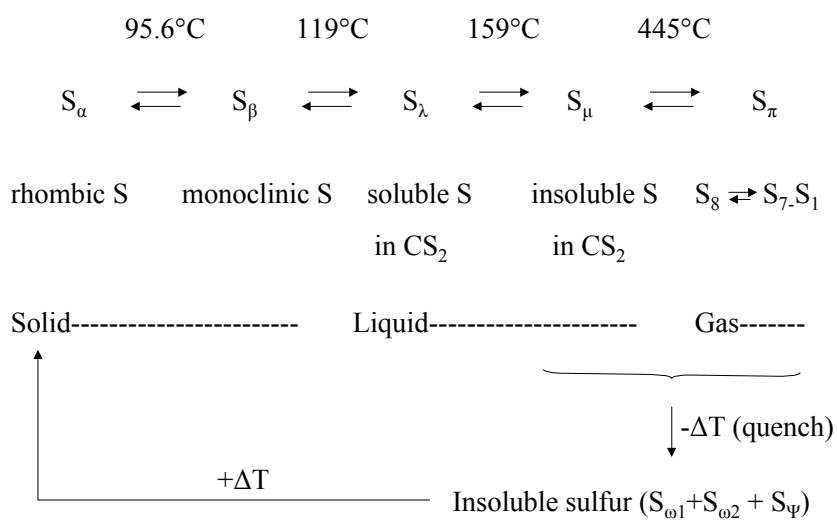


Fig. 9.1: Physical form of sulfur at different temperatures.⁴

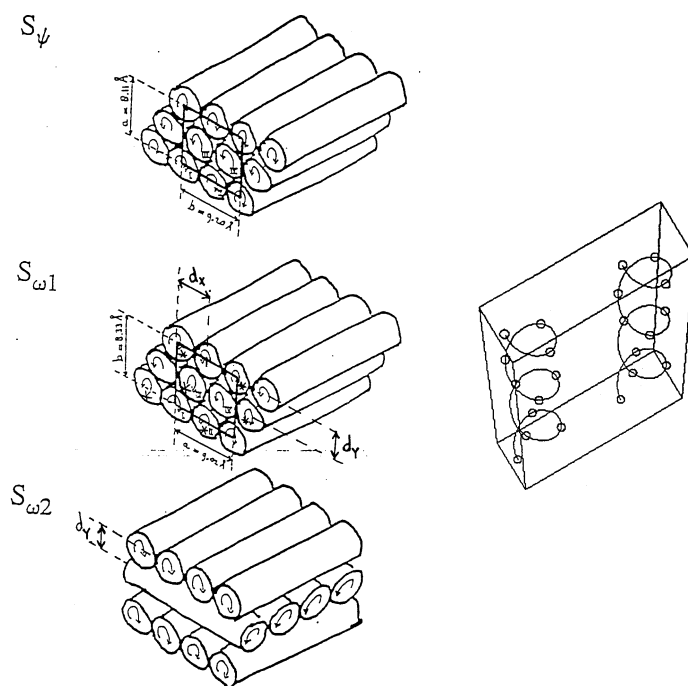


Fig. 9.2: Schematic view of polymeric sulfur allotropes $S_{\omega 1}$, $S_{\omega 2}$ and S_ψ , calculated by application of molecular modeling based on the force field published by Stillinger et al.⁵

The stability of each allotrope is related to its structure. Recently, we have prepared relatively pure samples of the $S_{\omega 1}$ and $S_{\omega 2}$ allotropes. Characterization of these allotropes was done by Differential Scanning Calorimetry (DSC), X-ray diffraction (XRD) and FT-Raman analysis.⁶ It was demonstrated by these methods, that in the solid state the $S_{\omega 2}$ allotrope has a much higher thermal stability than the $S_{\omega 1}$ allotrope. This is in contradiction however with results obtained from a thermal stability test of insoluble sulfur dispersed in a mineral oil (HTS-measurements). The carbon disulfide insoluble part after high temperature treatment: HTS, compared with that before high temperature treatment: IS, is a measure for the thermal stability of insoluble sulfur in oil: HTS/IS. The HTS-measurements showed a higher thermal stability, increased HTS/IS ratio, for insoluble sulfur having an increased $S_{\omega 1}/S_{\omega 2}$ ratio, suggesting that $S_{\omega 1}$ is the more stable allotrope. It was demonstrated by XRD-measurements of samples having different thermal stabilities that the crystalline perfection is more important than the type of polymeric sulfur allotrope, as shown in figures 9.3 and 9.4. An example of a XRD spectrum of insoluble sulfur is shown in fig. 9.5.

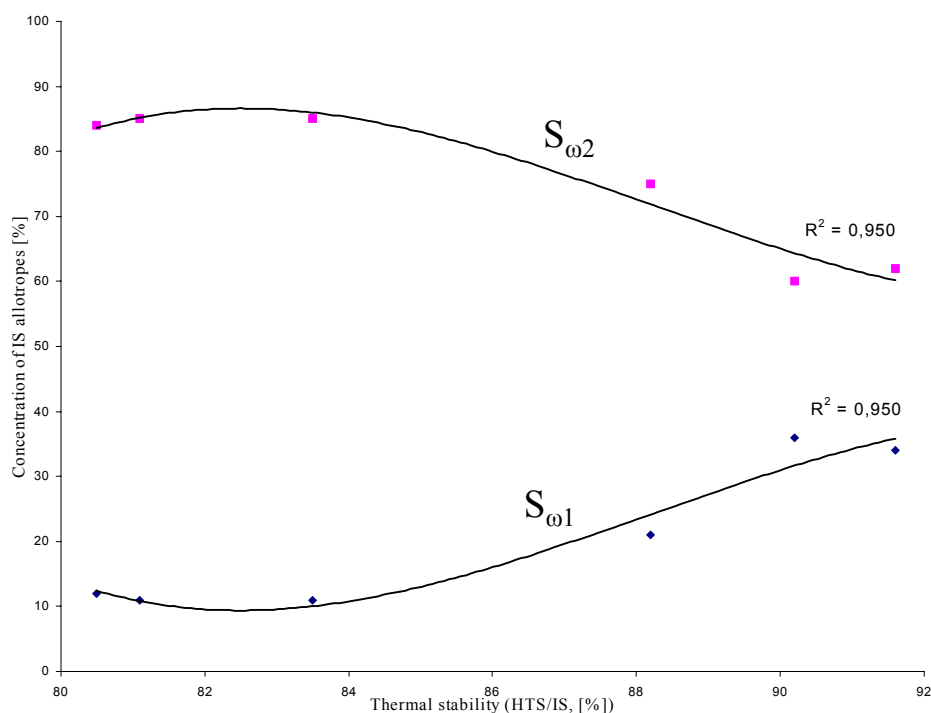


Fig. 9.3: Correlation between thermal stability of insoluble sulfur and the $S_{\omega 1}/S_{\omega 2}$ ratio.

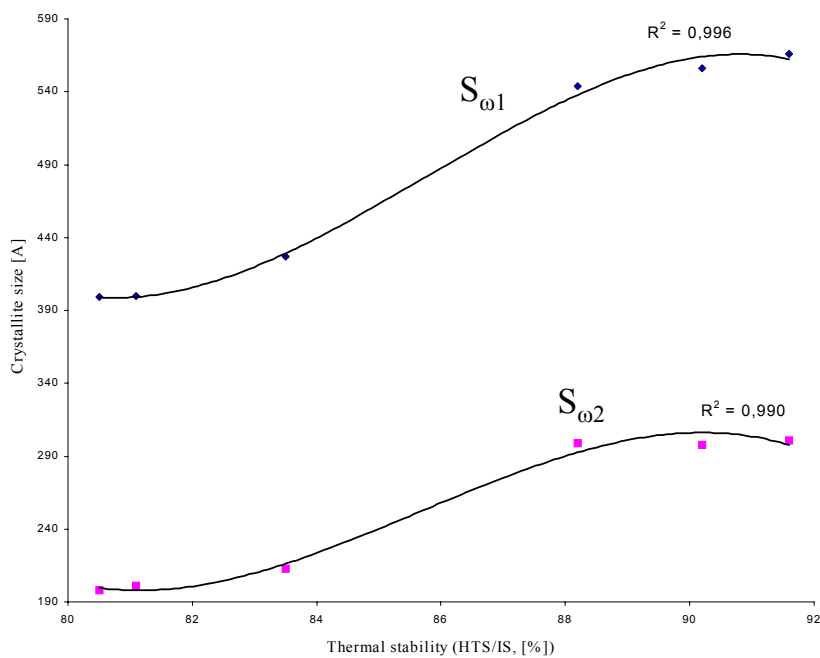


Fig. 9.4: Correlation between thermal stability of insoluble sulfur and crystallite size of the polymeric allotropes.

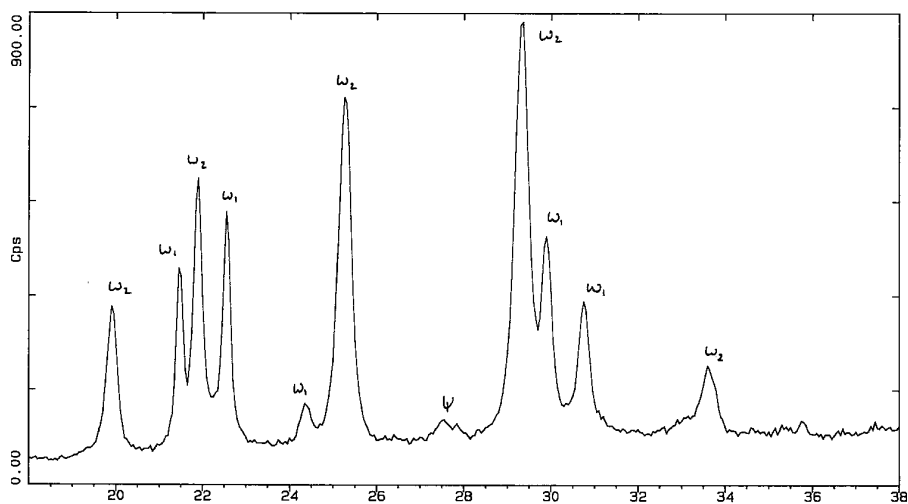


Fig. 9.5: X-ray diffraction diagram of insoluble sulfur, consisting of three insoluble sulfur allotropes: S_{ω1}, S_{ω2} and S_ψ.

As to the antidegradants, conventional TMQ grades are polymeric materials, condensation products of aniline and acetone, with a substantial amount of amine impurities. It is known that these impurities have a negative effect on the thermal stability of insoluble sulfur.⁷ Therefore, producers of rubber chemicals tried to develop new products to overcome this problem. A purified TMQ grade, Antigene FR, was recently introduced on the market.⁷ This purified grade predominantly contains the dimer of conventional TMQ, together with only minor amounts of impurities. Apart from an improved antidegradant performance, the new product is claimed to have less effect on the reversion of insoluble sulfur to soluble sulfur and, consequently, will show less sulfur blooming.

Uniroyal issued a patent on a new quality of TMQ, Naugard Q extra.⁸ The patent suggests that the new product is a reaction product of conventional TMQ and an acid anhydride, e.g. maleic anhydride, resulting in a product having a lower alkalinity and thus less effect on the reversion of insoluble sulfur. This leads to less sulfur blooming than when conventional TMQ products are used.

In the present study, the effect of 6PPD, 6QDI, TMQ and modified TMQ grades on the thermal stability of insoluble sulfur are examined as an example, with results obtained from blooming experiments, bin scorch (scorch at storage conditions) measurements, a thermal stability test in a transparent butadiene rubber (BR) and a thermal stability test in a mineral oil. FT-Raman and XRD-measurements are performed in order to find out if there is a difference in interaction between antidegradants with the S_{01} or the S_{02} polymeric sulfur allotrope.

9.2 Experimental

9.2.1 Materials used

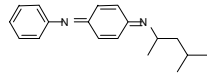
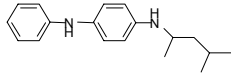
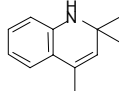
Compound ingredients:

The compounds for the experiments contained: NR SMR CV 60 (Standard Malaysian Natural Rubber with a constant viscosity ML(1+4) 100°C of 60±5, Wurfain & Co B.V.); BR Cariflex 1220 (butadiene rubber with a Cis-content of 90%, Shell); carbon black N-330 (Cabot); ZnO (Harzsiegel standard); stearic acid (J.T. Baker); Santocure CBS (Flexsys); Mucron OT 20 (insoluble sulfur coated with 20% naphthenic oil, Shikoku); RMS (soluble sulfur, J.T. Baker).

Tested antidegradants:

Santoflex 6PPD (Flexsys); Q-Flex QDI (Flexsys); Flectol TMQ (Flexsys); Naugard Q (TMQ, Uniroyal Chemical); Naugard Q extra: reaction product of TMQ and maleic anhydride (Uniroyal Chemical); Anox HPG: TMQ (Great Lakes); Antigene FR: purified TMQ (Sumitomo). The abbreviation, chemical name and structure of the tested materials are shown in Table 9.1.

Table 9.1: Abbreviation, chemical name and structure of the tested antidegradants.

| Abbrev. | Chemical name | Structure |
|---------|--|---|
| 6QDI | Benzamine, N-(4-(1,3-dimethylbutyl)imino)-2,5-cyclohexadien-1-ylidene) |  |
| 6PPD | N-(1,3-dimethylbutyl)-N'-phenyl-p-phenylenediamine |  |
| TMQ | Polymerized 2,2,4-trimethyl-1,2-dihydroquinoline |  |

Materials used for the HTS-test:

Blandol (paraffinic oil, Witco B.V.); Carbon disulfide (Janssen Chimica, assay min. 99.9%; CAS nr. [75-15-0]).

9.2.2 Compound formulations

Table 9.2: Formulations used for the transparent BR-test to compare 6PPD with 6QDI.

| Ingredient / mix | 1 | 2 | 3 | 4 |
|---------------------|------|------|------|------|
| BR Cariflex 1220 | 100 | 100 | 100 | 100 |
| Insol. Sulfur OT 20 | 3.75 | 3.75 | 3.75 | - |
| 6PPD | - | 1.00 | - | - |
| 6QDI | - | - | 1.00 | - |
| RMS | - | - | - | 3.00 |

Table 9.3: Formulations used for the transparent BR-test to compare different TMQ grades.

| Ingredient / mix | 5 | 6 | 7 | 8 | 9 | 10 | 11 |
|---------------------|------|------|------|------|------|------|------|
| BR Cariflex 1220 | 100 | 100 | 100 | 100 | 100 | 100 | 100 |
| Insol. Sulfur OT 20 | 3.75 | 3.75 | 3.75 | 3.75 | 3.75 | 3.75 | - |
| Flectol TMQ | - | 1.00 | - | - | - | - | - |
| Anox HPG | - | - | 1.00 | - | - | - | - |
| Naugard Q | - | - | - | 1.00 | - | - | - |
| Naugard Q extra | - | - | - | - | 1.00 | - | - |
| Antigene FR | - | - | - | - | - | 1.00 | - |
| RMS | - | - | - | - | - | - | 3.00 |

Table 9.4: Formulations used for the blooming and bin scorch tests to compare 6PPD with 6QDI.

| Ingredient / mix | 12 | 13 | 14 | 15 | 16 | 17 |
|---------------------|--------|--------|--------|--------|--------|--------|
| NR SMR CV | 100.00 | 100.00 | 100.00 | 100.00 | 100.00 | 100.00 |
| Carbon black N-330 | 50.00 | 50.00 | 50.00 | 50.00 | 50.00 | 50.00 |
| ZnO | 5.00 | 5.00 | 5.00 | 5.00 | 5.00 | 5.00 |
| Stearic acid | 2.00 | 2.00 | 2.00 | 2.00 | 2.00 | 2.00 |
| 6PPD | - | 1.00 | - | - | 1.00 | - |
| 6QDI | - | - | 1.00 | - | - | 1.00 |
| CBS | 1.00 | 1.00 | 1.00 | 1.00 | 1.00 | 1.00 |
| RMS | 7.00 | 7.00 | 7.00 | - | - | - |
| Insol. Sulfur OT 20 | - | - | - | 8.75 | 8.75 | 8.75 |

Table 9.5: Formulations used for the blooming and bin scorch tests to compare different TMQ grades.

| Ingredient / mix | 18 | 19 | 20 | 21 | 22 | 23 | 24 | 25 |
|---------------------|--------|--------|--------|--------|--------|--------|--------|--------|
| NR SMR CV | 100.00 | 100.00 | 100.00 | 100.00 | 100.00 | 100.00 | 100.00 | 100.00 |
| Carbon black N-330 | 50.00 | 50.00 | 50.00 | 50.00 | 50.00 | 50.00 | 50.00 | 50.00 |
| ZnO | 5.00 | 5.00 | 5.00 | 5.00 | 5.00 | 5.00 | 5.00 | 5.00 |
| Stearic acid | 2.00 | 2.00 | 2.00 | 2.00 | 2.00 | 2.00 | 2.00 | 2.00 |
| CBS | 1.00 | 1.00 | 1.00 | 1.00 | 1.00 | 1.00 | 1.00 | 1.00 |
| Soluble sulfur | 7.00 | 7.00 | 7.00 | 7.00 | - | - | - | - |
| Flectol TMQ | - | 1.00 | - | - | - | 1.00 | - | - |
| Naugard Q | - | - | 1.00 | - | - | - | 1.00 | - |
| Naugard Q extra | - | - | - | 1.00 | - | - | - | 1.00 |
| Insol. Sulfur OT 20 | - | - | - | - | 8.75 | 8.75 | 8.75 | 8.75 |

9.2.3 Characterization of the tested TMQ grades

Alkalinity index of TMQ:

The alkalinity index was determined by a non-aqueous titration in acetone with perchloric acid.

Aniline content of TMQ:

TMQ is a condensation product of aniline and acetone. The remaining amount of aniline was determined by HPLC, using the following conditions:

- Equipment : Varian Star Liquid Chromatographic System
- Pump : Varian 9010 Ternary Chromatographic
- Autosampler : Varian 9100
- Detector : Varian 9065 Diode Array detector
- Wave length range : 190 – 367 nm (254nm used to detect aniline)
- Column : Zorbax Eclipse XDB-C8
- Column dimensions : 4.6 mm I.D. * 250 mm L, 5 µm particle diameter
- Eluent A : 80% Water / 20% Acetonitrile
- Eluent B : 100% Acetonitrile
- Gradient : 50%B $\xrightarrow{10'}$ 60%B $\xrightarrow{20'}$ 90%B $\xrightarrow{10'}$ 100%B (20')
- Flow rate : 1.4 ml/min.
- Injection volume : 10µl
- Concentration : 125mg in 25ml Acetonitrile

9.2.4 Characterization of insoluble sulfur

X-ray diffraction spectroscopy (XRD):

The insoluble sulfur allotrope composition and the crystalline perfection were determined by XRD. Diffraction patterns were recorded on a Philips PW1050 reflection diffractometer, with Cu-K α radiation.

- Generator settings : 40kV, 40mA
- Slits : 0.5°, 0.2mm 0.5°
- Measuring conditions : 2 θ = 4 – 50°, step size 0.02°, time per step 20 sec.

HTS-test:

1.25g Insoluble sulfur is suspended in 20ml paraffinic oil, with or without 400mg dissolved antidegradant, and heated at 105°C during 15 minutes. After cooling down, the part insoluble in carbon disulfide is filtered, dried and weighed. The carbon disulfide insoluble part: HTS, compared with that before high temperature treatment: IS, is a measure for the thermal stability of the product: HTS/IS.

9.2.5 Testing of insoluble sulfur in rubber compounds

Thermal stability in a transparent butadiene rubber:

The compound formulations are shown in Tables 9.2 and 9.3. Butadiene rubber (BR) is masticated for 3 minutes in a 1.6L internal mixer according to standard laboratory mixing conditions. 200g Of the masticated BR, 6g insoluble sulfur and 2g of the antidegradant are mixed on a two-roll mill at low temperatures of approximately 50°C. The mixed compounds are heated in a press between Mylar foil, for 1 hour at the following temperatures: 70, 80, 90, 100, 105 and 110°C. All the compounds can be heated in one single mold, thus enabling a good comparison between the compounds. The obtained products are then subjected to observation of color and transparency. A change in color from opaque yellow to transparent yellow indicates that the insoluble sulfur has reverted to soluble sulfur and subsequently dissolved into the rubber compound. A higher temperature for the change in color corresponds with an increased thermal stability of the sulfur.

FT-Raman spectroscopy:

The rubber compounds are also analyzed by FT-Raman spectroscopy in order to quantify the amount of reverted soluble sulfur and to determine the $S_{\omega_1}/S_{\omega_2}$ ratio, before and after the temperature treatment. FT-Raman spectra are recorded with a Bruker RFS100 spectrometer equipped with a 1064nm Nd:YAG (Adlas model DPY 421N). Spectra are taken with a resolution of 1 cm^{-1} using a laser power of 500mW. Typically, 256 interferograms are collected for each spectrum. The laser spot has a diameter of approximately $100\mu\text{m}$ at the sample position. Quantification of insoluble sulfur content is done by comparison of the insoluble sulfur signals before and after temperature treatment.

Blooming test:

The compound formulations are shown in Tables 9.4 and 9.5. All the ingredients except sulfur, accelerator and antidegradants are mixed in a 5.0L internal mixer. Sulfur, accelerator and antidegradants are mixed on a two-roll mill at 50-65°C according to standard laboratory mixing conditions. The obtained rubber compounds are then heated in a press between Mylar polyester foil for 60 minutes at 105°C. The compounds are heated in a mold of 6mm thickness and 65mm diameter, in which 9 samples can be heated at once. The Mylar foil is released from one side of the vulcanizate immediately after opening of the mold. The vulcanizates are then stored at room temperature and observed for bloom at several fixed time intervals.

| | | |
|-------------------------|-------|-------------------------------------|
| <u>Rating of bloom:</u> | 0 | : no bloom |
| | X | : bloom on some part of the surface |
| | XX | : bloom on 25% of the surface |
| | XXX | : bloom on 50% of the surface |
| | XXXX | : bloom on 75% of the surface |
| | XXXXX | : bloom on total surface |

Bin scorch test:

The compound formulations are shown in Tables 9.4 and 9.5. A rubber masterbatch of all the ingredients except sulfur, accelerators and antidegradants is made in a 5.0L internal mixer. 4g CBS, 4g antidegradant and 28g insoluble sulfur are mixed into 628g of the masterbatch on a two-roll mill, at 50-65°C according to standard laboratory mixing conditions. A part of this mixture, 100g, is then mixed with 606mg, 1 phr, of the antidegradant on a two-roll mill. The thermal stability and the effect of antidegradants on the thermal stability of insoluble sulfur are determined by determination of the cure characteristics at different temperatures using an MDR 2000EA rheometer. Delta torque or extent of crosslinking is the maximum torque M_H minus the minimum torque M_L . Scorch safety t_{s2} is the time to reach 2 dNm above minimum torque; optimum cure time t_{90} is the time to reach 90% of the delta torque above minimum. Bin scorch behavior, premature vulcanization at storage condition, can be predicted by extrapolation of the plot of estimated scorch times t_{s2} against temperature to lower temperatures, i.e. room temperature.⁹ A comparison is made between antidegradants in the presence of soluble sulfur, in order to find out if differences in scorch behavior are related to: differences in thermal stability of the insoluble sulfur, a stabilizing or destabilizing effect of the antidegradants on the thermal stability of insoluble sulfur, or an effect of the antidegradants on the vulcanization rate.

9.3 Results and discussion

The effect of several antidegradants on the thermal stability of insoluble sulfur has been examined using results obtained from blooming experiments, bin scorch measurements, a thermal stability test in a transparent butadiene rubber (BR) and a thermal stability test in mineral oil: HTS-test. A comparison will be made between conventional and some recently developed antidegradants. The first section describes the differences observed between 6PPD and 6QDI. The second section describes the differences observed between TMQ and modified TMQ grades.

9.3.1 The effect of 6PPD and 6QDI on the thermal stability of insoluble sulfur in various media

As demonstrated in Chapter 8, the network stability of steelcord adhesion skim compounds can be improved by incorporation of 6QDI. However, before tire manufacturers decide to change the composition of critical compounds, like steelcord adhesion skim compounds, they have to be sure that other important features like tackiness and scorch are not negatively affected. The effect of other ingredients on the thermal stability of insoluble sulfur is very important for skim compounds because this affects their tackiness and migration characteristics of sulfur.¹⁰ Therefore, we

decided to study the effect of 6QDI on the thermal stability of insoluble sulfur and made a comparison with 6PPD.

The low value of HTS/IS shown in Table 9.6 for the sulfur + 6QDI combination, demonstrates that 6QDI has a negative effect on the thermal stability of insoluble sulfur in mineral oil. On the other hand, 6PPD seems to have a negligible effect on the decomposition of insoluble sulfur relative to a blank without any stabilizer. The difference observed between 6QDI and 6PPD is most probably related to Michael addition reactions between 6QDI and sulfur, which are not possible for 6PPD, as demonstrated in Chapter 7.¹¹

Table 9.6: Thermal stability of insoluble sulfur determined with the HTS-test at 105°C.

| Sample | HTS / IS [%] |
|---------------|-----------------|
| ISOT20 | 87.1 – 88.8 |
| ISOT20 + 6PPD | 86.0 – 85.5 |
| ISOT20 + 6QDI | 19.9 – 19.3 |

The decreased thermal stability of insoluble sulfur in the presence of 6QDI was confirmed by the transparent BR-test, as shown in fig. 9.6. It is clear from this figure, that the test specimen containing insoluble sulfur is transparent when 6QDI is incorporated, indicating that all insoluble sulfur has reverted to soluble sulfur and subsequently dissolved into the rubber matrix, and opaque when 6PPD is incorporated into the compound.

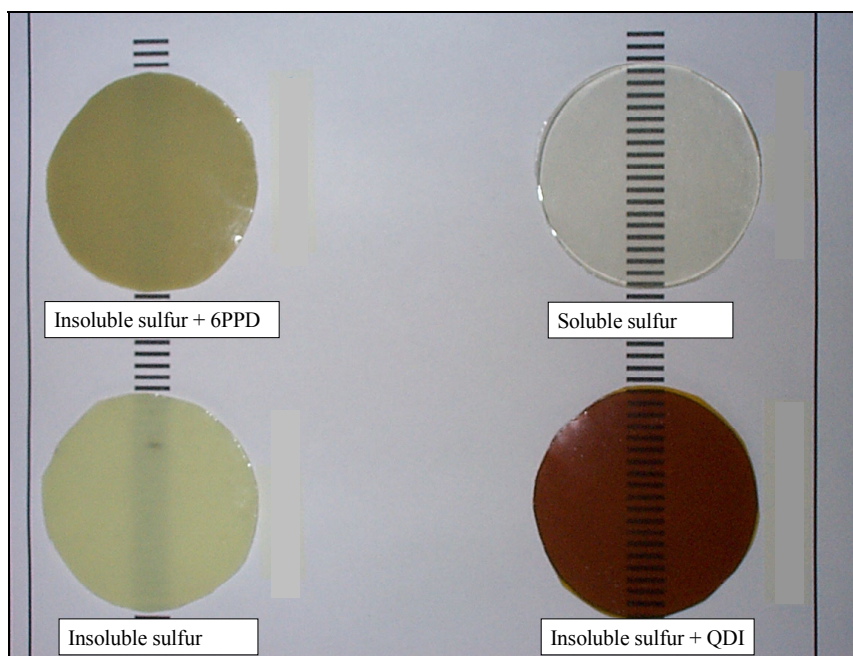


Fig. 9.6: Results of the transparent BR-test at 110°C.

A more sophisticated evaluation of the stability of insoluble sulfur can be achieved using FT-Raman spectroscopy. With this technique, it is possible to quantify the insoluble sulfur allotropes ($S_{\omega 1}$, $S_{\omega 2}$ and, S_{ψ}) as well as the soluble sulfur part. This technique was applied to analyze the rubber vulcanizates described in Table 9.2 and 9.3, after heating at 90, 100 and 110°C for one hour. No sample pretreatment was necessary. Because of the high scattering cross section, the sulfur allotropes could be detected even at the low concentrations of sulfur present in these compounds.¹² Figure 9.7 shows the spectra of the control compound, mix 1 of Table 9.2, after different temperature treatments and after normalizing on the rubber absorption band at 1652 cm^{-1} . In these spectra, absorption bands are observed from the different insoluble sulfur allotropes ($S_{\omega 1}$ at 423 and 261 cm^{-1} , $S_{\omega 2}$ at 417 and 272 cm^{-1} and $S_{\omega 1} + S_{\omega 2}$ at 456 cm^{-1}). Furthermore, bands are found from soluble sulfur, S_{α} , with absorption at 472, 217 and 152 cm^{-1} . It can be seen, that the higher the temperature, the more insoluble sulfur decomposes to S_{α} . Note that the peaks of S_{α} normally would have been much higher, regarding the degradation of insoluble sulfur and the fact that the Raman scattering cross section of S_{α} is a factor 5 higher than that of insoluble sulfur. Apparently, a part of S_{α} dissolves into the rubber matrix, resulting in a lower response factor. Furthermore, it can be seen that $S_{\omega 2}$ decomposes more easily than $S_{\omega 1}$ as evidenced by the faster decrease of the 417 and 272 cm^{-1} bands in contrast to the 423 and 261 cm^{-1} bands. The increased thermal stability of the $S_{\omega 1}$ allotrope compared to the $S_{\omega 2}$ allotrope is most probably related to the difference in crystallite size between both allotropes. As shown in fig. 9.4, the $S_{\omega 1}$ allotrope has a larger crystallite size than the $S_{\omega 2}$ allotrope. Figure 9.8 shows the spectra of the insoluble sulfur / rubber mixtures with 6PPD addition, mix 2 of Table 9.2, after different temperature treatments and after normalizing on the rubber absorption band at 1652 cm^{-1} . Again, it can be seen that the higher the temperature the more insoluble sulfur decomposes to S_{α} but, in contrast to the control without 6PPD, $S_{\omega 2}$ and $S_{\omega 1}$ seem to decompose to the same extent. This difference could not be explained. Furthermore, the stability of insoluble sulfur in the presence of 6PPD is slightly better compared to the control. After 1 hour heating at 110°C still 55% insoluble sulfur remains instead of 40% for the control. Finally, in fig. 9.9 the spectra of the insoluble sulfur / rubber mixtures with 6QDI, mix 3 of Table 9.2, are shown after different temperature treatments and after normalizing on the rubber absorption band at 1652 cm^{-1} . Unfortunately, the spectra are superimposed on a high fluorescence background caused by 6QDI. Some rubber absorption bands around 3000 and 1600 cm^{-1} are still present but no sulfur peaks are detected. The same problem was also faced in Chapter 6, where FT-Raman spectroscopy could not be applied to study the ozonolysis of model rubbers, in the presence of staining antiozonants, because of a high fluorescence background signal.

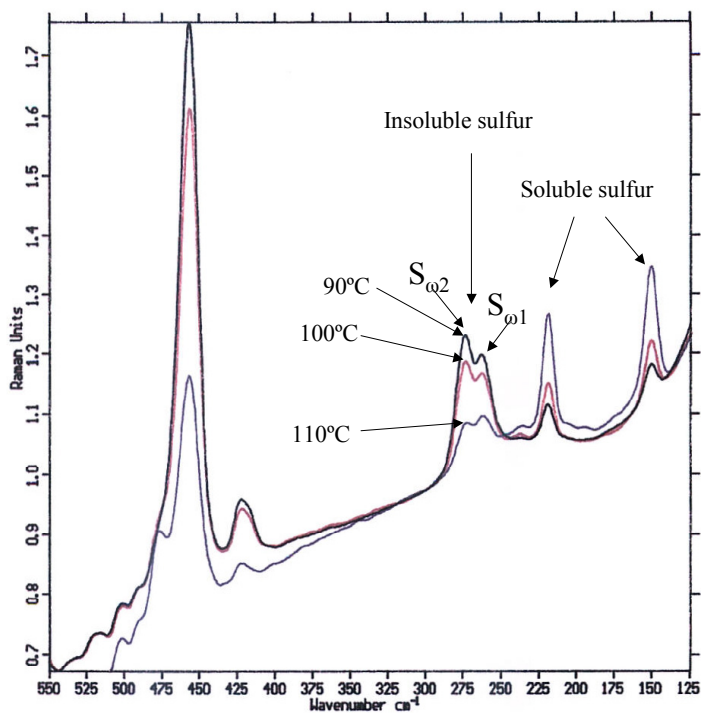


Fig. 9.7: FT-Raman spectra of 3.75 phr Insol. Sulfur OT 20 in BR, mix 1 of Table 9.2, after heating for 60 min. at 90, 100 and 110°C.

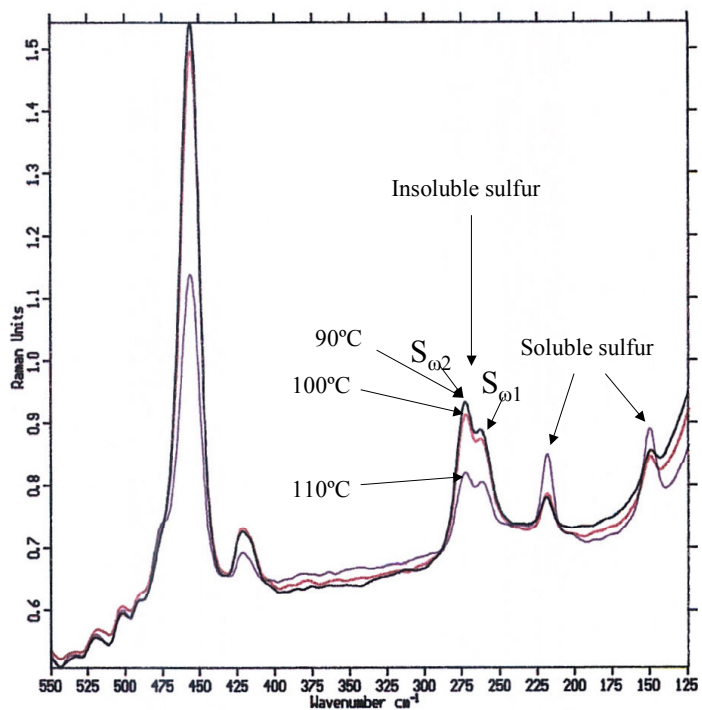


Fig. 9.8: FT-Raman spectra of 3.75 phr Insol. Sulfur OT 20 and 1phr 6PPD in BR, mix 2 of Table 9.2, after heating for 60 min. at 90, 100 and 110°C.

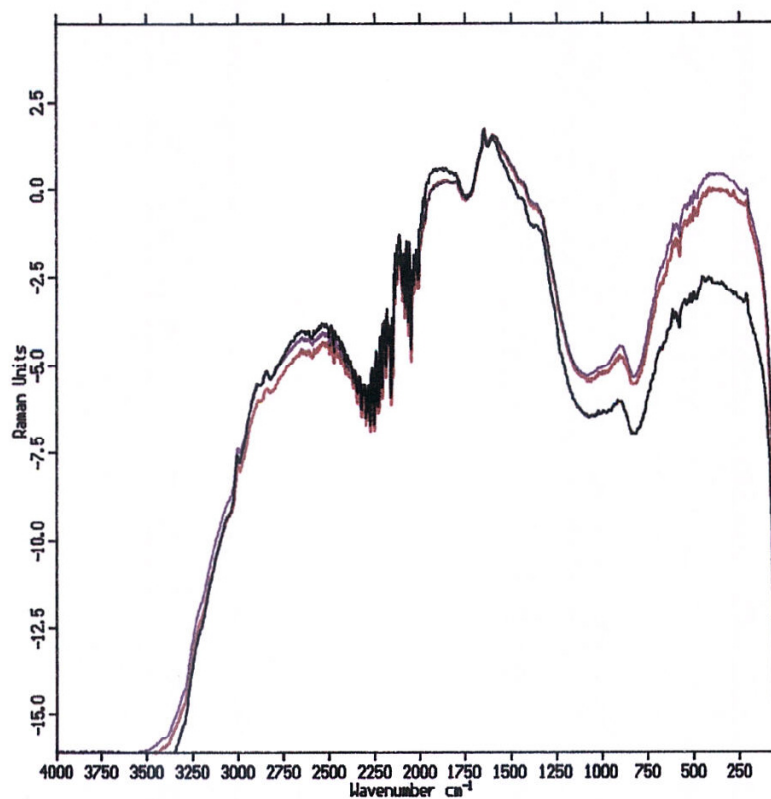


Fig. 9.9: FT-Raman spectra of 3.75 phr Insol. Sulfur OT 20 and 1phr 6QDI in BR, mix 3 of Table 9.2, after heating for 60 min. at 90, 100 and 110°C.

The effect of 6QDI and 6PPD on the thermal stability of insoluble sulfur was further examined by blooming and bin scorch measurements. The compound compositions of the tested compounds are shown in Table 9.3. A comparison was made with soluble sulfur. The results of the blooming test are shown in Table 9.7 and the results of the bin scorch measurements in Table 9.8. It is clear from these results that the blooming properties of compounded insoluble sulfur improve significantly when 6QDI is incorporated: compare compound 15 and 17. This could be the result of a better thermal stability of the insoluble sulfur due to stabilization of the reversion mechanism by 6QDI. However, because 6QDI also induces an decreased blooming behavior for soluble sulfur: compare compound 12 and 14, it is more likely that 6QDI reacts with sulfur and is subsequently grafted to the polymer backbone. In this way, sulfur is immobilized and not available for bloom anymore. Model experiments with squalene have demonstrated that sulfur indeed reacts with 6QDI and is grafted to squalene by 1 to 4 sulfur atoms, as shown in Chapter 7. These reactions were not observed for 6PPD. This explains the difference in blooming behavior observed between incorporated 6QDI and 6PPD.

Table 9.7: Blooming properties obtained after heating for 60 min. at 105°C.

| Time / mix | 12 | 13 | 14 | 15 | 16 | 17 |
|---------------|-------|------|----|----|-----|----|
| 5 min. | 0 | 0 | 0 | 0 | 0 | 0 |
| 15 min. | 0 | 0 | 0 | 0 | 0 | 0 |
| 60 min. | X | 0 | 0 | 0 | 0 | 0 |
| 4 hrs. | XX | X | 0 | X | X | 0 |
| 24 hrs. | XXX | XX | X | X | X | X |
| 48 hrs. | XXXX | XXX | X | X | X | X |
| 1 week | XXXXX | XXXX | X | XX | XXX | X |

The results in Table 9.8 show, that the scorch safety at low temperatures of compounded insoluble sulfur is better than that of soluble sulfur: compare compound 12 and 15. This can be explained by the fact that insoluble sulfur first has to revert to soluble sulfur, or to low molecular weight sulfur species, before being available for cure. However, reversion is fast at cure temperatures and soluble sulfur seems to have an increased scorch safety at these temperatures $\geq 140^\circ\text{C}$. The latter must be related to a higher reactivity of reverted insoluble sulfur ($S_1 - S_7$) compared to that of soluble sulfur (S_8). Scorch safety improved significantly by the presence of 6QDI: compare compound 15 and 17. A slightly inferior scorch safety was observed in the presence of 6PPD: compare compound 15 and 16, which can be explained by the alkalinity of 6PPD. In general, all bases (i.e. 6PPD) have an accelerating influence, and acids a retarding one on the cure reaction.¹³

Table 9.8: Scorch time t_{s2} [min.] determined with the MDR at different temperatures.

| t_{s2} / mix | 12 | 13 | 14 | 15 | 16 | 17 |
|-------------------|------|------|------|-------|-------|-------|
| 100°C | 98.2 | n.d. | n.d. | 117.5 | 107.1 | 154.7 |
| 110°C | 45.6 | n.d. | n.d. | 49.4 | 46.4 | 66.7 |
| 120°C | 20.8 | n.d. | n.d. | 21.3 | 20.6 | 31.2 |
| 150°C | 2.5 | n.d. | n.d. | 2.4 | 2.4 | 3.55 |

9.3.2 The effect of TMQ on the thermal stability of insoluble sulfur

The effect of different TMQ grades on the thermal stability of insoluble sulfur was first investigated by HTS measurements in oil. The results of these measurements are shown in Table 9.9. The low HTS/IS values observed when the conventional TMQ grades Flectol TMQ and Anox HPG are used indicate, that they have a negative effect on the thermal stability of insoluble sulfur. The worst thermal stability is observed in the presence of Flectol TMQ, whereas Anox HPG shows the least effect on the thermal stability of insoluble sulfur. Anox HPG shows even less effect on the thermal stability of insoluble sulfur than the purified TMQ grade. The reaction product of TMQ and maleic anhydride, shows a negligible effect on the thermal

stability of insoluble sulfur. The latter can be explained by the lower alkalinity index of the reaction product of TMQ and maleic anhydride due to the presence of less basic impurities like aniline, as shown in Table 9.10.

Table 9.9: Thermal stability of IS determined with the HTS-test at 105°C.

| Sample | HTS / IS [%] |
|----------------------------|-----------------|
| ISOT20 | 87.1 – 88.8 |
| ISOT20 + air | 87.0 – 87.6 |
| ISOT20 + Flectol TMQ | 8.1 – 9.1 |
| ISOT20 + Flectol TMQ + air | 7.9 – 9.3 |
| ISOT20 + Antigene FR | 76.1 – 76.9 |
| ISOT20 + Antigene FR + air | 76.3 – 77.4 |
| ISOT20 + Naugard Q | 10.4 – 10.9 |
| ISOT20 + Naugard Q extra | 87.0 – 87.4 |
| ISOT20 + Anox HPG | 67.1 – 67.3 |

Table 9.10: Alkalinity index and aniline content determined for several TMQ grades.

| Tested products | Alkalinity index [mg HClO ₄ /g] | Aniline content [%] |
|-----------------|---|------------------------|
| Flectol TMQ | 545 | 0.030 |
| Naugard Q | 541 | 0.022 |
| Naugard Q extra | 436 | <0.01 |

The effect of the different TMQ grades on the thermal stability of insoluble sulfur was also investigated by the transparent BR test. The formulations of the tested compounds are shown in Table 9.3. Before heating, all the compounds showed an opaque yellow color due to the presence of undissolved sulfur. After heating at 70, 80 and 90°C, all the compounds made with insoluble sulfur still were opaque. However, the compound made with RMS was transparent yellow, indicating that all the sulfur had dissolved into the rubber matrix. Differences between the tested compounds could only be observed after heating at 100°C. At this temperature, the reference compound made with insoluble sulfur and no TMQ was still opaque yellow, whereas the compound made with RMS was completely transparent. The other compounds ranged from opaque yellow to transparent yellow in the following order:

Insoluble sulfur and no TMQ ≈ Naugard Q extra > Antigene FR ≈
Anox HPG > Flectol TMQ >> RMS.

The order of transparency and thus the order of thermal stability correlates well with the thermal stability of insoluble sulfur determined by the HTS-measurements. When tested at 110°C, only mix 5: no TMQ, and mix 9: IS + the reaction product of TMQ and maleic anhydride, were still opaque, indicating that

insoluble sulfur is still present after this temperature treatment. This means that the conventional and the purified TMQ grades all promoted complete reversion of insoluble sulfur to soluble sulfur.

The thermal stability of insoluble sulfur in the presence of the reaction product of TMQ and maleic anhydride was also examined by bin scorch measurements. A comparison was made with the conventional TMQ grades. The formulations of the tested compounds are shown in Table 9.5. The effect of the antidegradants on the bin scorch behavior was tested both for soluble and insoluble sulfur. The results are shown in Table 9.11 and fig. 9.10. It can be seen from these results that all the tested TMQ grades showed a positive effect on the bin scorch behavior of both soluble and insoluble sulfur. The latter indicates a positive effect on the thermal stability of insoluble sulfur, which is in contradiction with the HTS-measurements in oil. Furthermore, it can be seen that the increase in scorch time in the presence of TMQ is larger for insoluble sulfur than for RMS, which is most probably a result of a stabilizing effect of TMQ on the reversion of insoluble sulfur. The reaction product of TMQ and maleic anhydride: mix 25, showed the best stabilizing effect on the reversion of insoluble sulfur.

It is known that TMQ shows only antidegradant action in an oxidative environment by formation of the corresponding nitroso compound, which is able to inhibit radical degradation reactions: see e.g. fig. 2.3 in Chapter 2, where a similar mechanism is shown for a HALS stabilizer. The fact that air has no influence on the stability of insoluble sulfur, see Tab. 9.9, could lead to the conclusion that degradation of insoluble sulfur induced by TMQ in oil is not a radical process, but an ionic process catalyzed by the amine-containing impurities as suggested by Inui et al.⁷ It might very well be possible that the degradation mechanism of insoluble sulfur in rubber is a radical process and that TMQ now can act as a stabilizer by its radical scavenging properties (assuming that sufficient oxygen is present in the rubber matrix). If these considerations are correct it must be concluded that degradation mechanisms of insoluble sulfur in oil and in rubber are completely different (ionic versus radical mechanism).

Table 9.11: Scorch time t_{s2} [min.] determined with the MDR at 100, 110, 120 and 150°C.

| t_{s2} / temp. | 18 [min.] | 19 [min.] | 20 [min.] | 21 [min.] | 22 [min.] | 23 [min.] | 24 [min.] | 25 [min.] |
|---------------------|--------------|--------------|--------------|--------------|--------------|--------------|--------------|--------------|
| 100°C | 102.59 | 106.25 | 107.33 | 107.90 | 128.80 | 133.33 | 139.07 | 141.52 |
| 110°C | 45.93 | 46.95 | 47.69 | 47.84 | 53.29 | 54.87 | 56.62 | 57.53 |
| 120°C | 21.54 | 21.71 | 21.94 | 22.19 | 22.49 | 22.86 | 23.63 | 23.84 |
| 150°C | 2.58 | 2.60 | 2.58 | 2.63 | 2.40 | 2.37 | 2.40 | 2.46 |

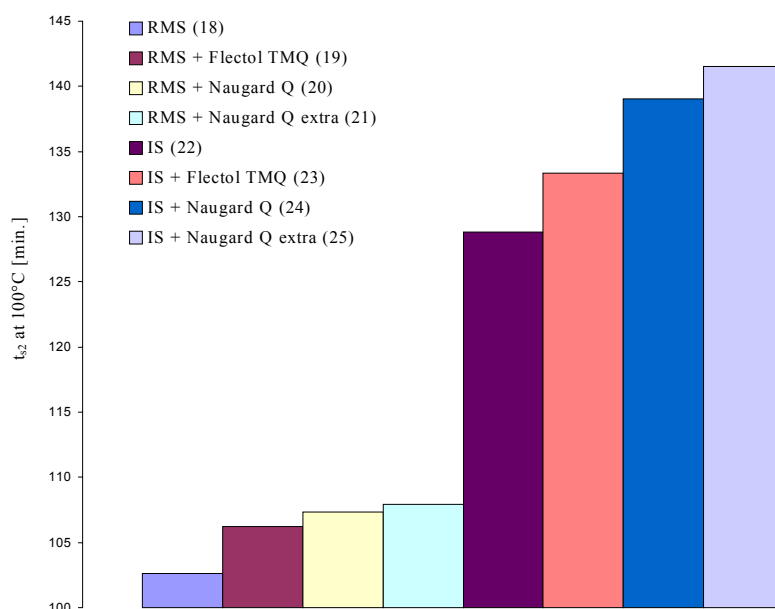


Fig. 9.10: Scorch time t_{s2} determined with the MDR at 100°C.

9.4 Conclusions

The effect of several antidegradants on the thermal stability of insoluble sulfur versus its reversion to soluble sulfur has been examined with blooming experiments, bin scorch measurements, a thermal stability test in a transparent butadiene rubber and a thermal stability test in mineral oil: HTS-test.

Benzamine, N-(4-(1,3-dimethylbutyl)imino)-2,5-cyclohexadiene-1-ylidene) (6QDI) has a negative effect on the thermal stability of insoluble sulfur, according to HTS-measurements and the transparent BR-test, compared to the corresponding amine antidegradant N-(1,3-dimethylbutyl)-N'-phenyl-p-phenylenediamine (6PPD).

Polymerized 2,2,4-trimethyl-1,2-dihydroquinoline (TMQ) also has a negative effect on the thermal stability of insoluble sulfur due to the presence of low molecular weight amine impurities, like aniline. The purified product (Antigene FR) and the reaction product of TMQ and maleic anhydride (Naugard Q extra) showed negligible effect on the thermal stability of insoluble sulfur. It is most likely that the degradation mechanism of insoluble sulfur in rubber in the presence of TMQ is a radical process, where TMQ can act as a stabilizer by its radical scavenger properties. On the other hand, in paraffinic oil it seems to be an ionic process catalyzed by amine impurities.

FT-Raman spectroscopy was applied to study the thermal stability of insoluble sulfur in the presence of different antidegradants. Unfortunately, this technique could not be used to study compounds containing 6QDI, due to a high fluorescence background signal caused by the dark color of these compounds. The S_{01} polymeric sulfur allotrope has a better thermal stability than the S_{02} allotrope in the absence of antidegradants. In the presence of 6PPD however no difference in thermal stability was found between both insoluble sulfur allotropes.

9.5 References

1. F. Tuinstra, *Acta Cryst.*, **20**, (1966), 341.
2. F. Tuinstra, *Physica*, **34**, (1967), 113.
3. J. Schenk, thesis at TU Delft, (1956).
4. H. Bratzsch, *Kautschuk Gummi Kunstst.*, **41**, (1988), 455.
5. F.H. Stillinger, T.A. Weber, *J. Chem. Phys.*, **85**, No. 11, (1986), 6460.
6. N.M. Huntink, H. Hofstraat, R. van Puijenbroek, M. Janssen-Mulders, unpublished results.
7. N. Inui, H. Nagasaki, T. Yamaguchi, *Kautschuk Gummi Kunstst.*, **47**, (1994), 248.
8. R.J. Cornell, D.H. Roberts, W.R. True, (to Uniroyal Chemical Company Inc.), WO 95/21214, (January 25, 1995).
9. Z. R. Haifa, H.G. Burhin, *Kautschuk Gummi Kunstst.*, **47**, (1994), 268.
10. B.H. To, F. Ignatz-Hoover, G. Anthoine, paper #56, ACS Rubber Div. Meeting, Providence, Rhode Island, (April 24-27, 2001).
11. R. N. Datta, S. Datta, N. M. Huntink and A. G. Talma, accepted for publication in *Kautschuk Gummi Kunstst.*
12. N.M. Huntink, W.J.H. Janssen-Mulders, unpublished results.
13. W. Hofman, "Rubber Technology Handbook", Hanser Publishers, (1994), 23.

Main symbols and abbreviations

| | | |
|---------------------|--|----------------------|
| δ | chemical shift | [ppm] |
| η | filler-filler interaction (Payne effect) | [-] |
| σ | ratio of the 300% and 100% modulus: M_{300}/M_{100} | [-] |
| C1 | Mooney-Rivlin elastic constant | [-] |
| D | diffusion coefficient | [mm ² /s] |
| E' | storage modulus | [MPa] |
| E'' | loss modulus | [MPa] |
| l | vulcanizate plate thickness | [mm] |
| M_L | minimum torque | [Nm] |
| M_H | maximum torque | [Nm] |
| t_{90} | time to optimum cure | [min.] |
| $\tan \delta$ | loss tangent | [-] |
| t_{s2} | scorch time | [min.] |
| V_f | volume fraction | [-] |
| M_c | molecular weight between crosslinks | [g/mole] |
| AA | acetic acid | |
| ACM | acrylic rubber | |
| ADA | adipic acid | |
| ADPA | acetone/diphenylamine condensation product | |
| ADPA-B | N, N phenyl benzoyl-N-phenyl paraphenylenediamine | |
| ADPA-Bred | 1,2-diphenyl-2-(4-(phenylamino)phenylamino)ethanol | |
| ADPA-C | N, N phenyl methylene benzoyl-N-phenyl paraphenylenediamine | |
| ADPA-DTBF | 2,6-di-tert-butyl-4-(4-(phenylamino)phenyliminomethyl)phenol | |
| ADPA-pol | 3-(4-(phenylamino)phenylamino)butanoic acid | |
| ADPAT | 2,4,6-tris(4-(phenylamino)phenyl)-1,3,5-triazine | |
| AFS | bis-(1,2,3,6-tetrahydrobenzaldehyde)-pentaerythrityl acetal | |
| AFD | 4-(benzyloxymethylene)cyclohexene | |
| AOx | antioxidant | |
| AOz | antiozonant | |
| 4Asi-Ph | 1-phenyl-3-(4-(phenylamino)phenylamino)pyrrolidine-2,5-dione | |
| ATR | attenuated total reflection | |
| BA | benzoic acid | |
| BD | benzofurane derivative | |
| BHT | butylated hydroxy toluene | |
| BuLi | butyl lithium | |
| BR | butadiene rubber | |
| CBA | chain braking electron acceptors | |
| CDCl ₃ | deuterated chloroform | |
| CH ₂ O | formaldehyde | |
| CM | chlorinated polyethylene | |
| ¹³ C-NMR | carbon nuclear magnetic resonance spectroscopy | |

| | |
|---------------------|---|
| CO | polychloromethyloxiran |
| CR | chloroprene rubber |
| CSM | chlorosulfonated polyethylene |
| DABCO | 1,4-diazabicyclo[2,2,2]octane |
| DIDP | diphenyl isodecyl phosphite |
| DIOP | diphenyl isooctyl phosphite |
| DLTDP | dilauryl thiodipropionate |
| DMF | dimethylformamide |
| DMSO | dimethyl sulfoxide |
| D _n OPPD | N,N'-di-n-octyl-PPDA |
| DNPD | N,N'-di-β-naphtyl-p-phenylenediamine |
| DOSY | diffusion ordered spectroscopy |
| DPDP | distearyl pentaerythritol diphosphite |
| DPPD | N,N'-diphenyl-p-phenylenediamine |
| DSA | double strain amplitude |
| DSC | differential scanning calorimetry |
| DTBH | 3-(3,5-di-tert-butyl-4-hydroxyphenyl)propionic acid |
| DT-P-ADPA | 3,3'-dithiobis((4-phenylaminophenyl)propanamide |
| DTPD | N,N'-ditolyl-p-phenylenediamine |
| DT-S-ADPA | 2,2'-dithiobis((phenylaminophenyl)benzamide |
| EAM | ethylene-ethyl acrylate copolymer |
| ECO | epichlorohydrin rubber |
| EDTA | ethylene diamine tetra acetic acid |
| ENB | ethylidene norbornene |
| EPDM | ethylene propylene diene rubber |
| EPM | ethylene propylene rubber |
| ESI | electro spray ionization |
| ETMQ | 6-ethoxy-2,2,4-trimethyl-1,2-dihydroquinoline |
| EtOH | ethanol |
| EVM | ethylene-vinylacetate copolymer |
| FA | fumaric acid |
| FDA | US food and drug administration |
| FIA-MS | flow injection analysis mass spectroscopy |
| FID | flame ionization detector |
| FKM | fluor rubbers |
| FTF | fatigue to failure |
| FTIR | Fourier transform infra-red spectroscopy |
| GC | gas chromatography |
| HA | heptanoic acid |
| HALS | hindered amine light stabilizer |
| ¹ H-NMR | proton nuclear magnetic resonance spectroscopy |
| HPPD | N-phenyl-N'-(1,3-dimethylbutyl)-p-phenylenediamine |
| HP-SEC | high performance size exclusion chromatography |
| HQ | hydroquinone |
| HTS | high thermal stability |
| HTT | hexahydro-1,3,5-triphenyl-1,3,5-triazine |
| IIR | butyl rubber |
| IPPD | N-isopropyl-N'-phenyl-p-phenylenediamine |

| | |
|--|--|
| IR | polyisoprene rubber |
| IS | insoluble sulfur |
| Kc | kilo cycles |
| KI | potassium iodide |
| MCV | model-compound vulcanization |
| MDR | moving dye rheometer |
| MeOH | methanol |
| MMBI | methyl-2-mercaptobenzimidazole |
| MPTES | γ - mercaptopropyl triethoxy silane |
| MS | mass spectroscopy |
| MSA | methyl sulfonic acid |
| MW | molecular weight |
| NaBH ₄ | sodium borohydride |
| NBR | nitrile butadiene rubber |
| NiDMC | nickel dimethyldithiocarbamate |
| NIR | near infrared spectroscopy |
| NR | natural rubber |
| O ₂ | oxygen |
| O ₃ | ozone |
| ODPA | octylated diphenylamine |
| OIT | oxidation induction time |
| OT | oil treated |
| PA | phthalic acid |
| PAN | phenyl- α -naphthylamine |
| PBN | phenyl- β -naphthylamine |
| PCD | polycarbodiimide |
| P(C ₆ H ₅) ₃ | triphenyl phosphonium bromide |
| PCl ₃ | tris-nonylphenol phosphates |
| 44PD | N,N'-di-sec-butyl-p-phenylenediamine |
| 77PD | N,N'-bis(1,4-dimethylpentyl)-p-phenylenediamine |
| PDPA | 4-pyrrolle-diphenylamine |
| PEPPP | 2-phenoxyethyl-3-(4-phenylamino)phenylamino)propanoate |
| phr | parts per hundred parts of rubber |
| 6PPD | N-(1,3-dimethylbutyl)-N'-phenyl-p-phenylenediamine |
| PPD-C18 | stearic acid salt of 6PPD |
| PPD's | paraphenylene diamines |
| pphm | parts per hundred million |
| PPPA | 3-((4-phenylamino)phenylamino) propanoic acid |
| PPPP | N-phenyl-3-(4-(phenylamino)phenylamino)propanoate |
| Q | silicone rubber |
| 6QDI | N-(1,3-dimethyl)-N'-phenyl quinonediimine |
| RI | refractive index |
| RPA | rubber process analyzer |
| S | sulfur |
| S _{α} | rhombic sulfur |
| S _{ω1} , S _{ω2} , S _{ψ} | polymeric sulfur allotropes |
| SA | succinic acid |
| SAPH | styrenated and alkylated phenol |

| | |
|----------|--|
| SBR | styrene-butadiene-rubber |
| SDPA | styrenated diphenylamine |
| SEM | scanning electron microscopy |
| SPH | styrenated phenol |
| SPPD | N-phenyl-N'-(1-phenylethyl)-1,4-benzenediamine |
| SS | soluble sulfur |
| TA | tartaric acid |
| TAHQ | 2,5-di(tert-amyl)hydroquinone |
| TAPTD | 2,4,6-tris-(N-1,4-dimethylpentyl-para-phenylenediamino)-1,3,5-triazine |
| TBHQ | 2,5-di-t-butyl hydroquinone |
| TBMC | 4,4'-thiobis-6-(t-butyl-m-cresol) |
| TBTT | tetrahydro-1,3,5-tri-(n)-butyl-(S)-triazinethione |
| TDI | toluenediisocyanate |
| TDI-ADPA | 2,4-bis(4-phenylamino)phenylureido)toluene |
| TDI-PPD | 2,4-bis((N-4-phenylamino)phenyl)-N-(1,3-dimethylbutyl)ureido)toluene |
| TEA | triethanol amine |
| TESPD | bis-3-(triethoxysilylpropyl) disulfide |
| TESPT | bis-(3-triethoxysilylpropyl) tetrasulfide |
| TGA | thermal graphical analysis |
| THQ | toluhydroquinone |
| TMTD | tetramethyl thiuram disulfide |
| TMQ | 2,2,4-trimethyl-1,2-dihydroquinoline, polymerized |
| TMS | trimethyl silane |
| TNPP | tris(mixed mono- and di-nonylphenyl)phosphite |
| ZMBI | zinc-2-mercaptobenzimidazole |
| ZMMBI | zinc-2-methylmercaptoimidazole |

Summary

Today, it is recognized that most of the degradation encountered with natural and synthetic rubbers is due either to oxygen or to ozone. Although the latter is present only in tiny quantities in ambient air, about 10 parts per thousand million, its effects are devastating, particularly for dynamically loaded rubbers. The result is early appearance of cracks across the direction of stress. The rate of crack growth increases with tension and varies from one kind of rubber to another. In every case, the rate of crack growth is fast enough to render the rubber useless. Some synthetic rubbers containing few or no unsaturated carbon-carbon bonds are resistant to ozone. However, by far most rubbers need special protection against ozone attack.

Although a lot of research has already been done to improve the lifetime of rubber articles, there is a need for antidegradants that last longer in rubber compounds and provide longer-term protection. Nowadays, truck tires need improved protection of the sidewall, because they are retreaded more and more times. And in Japan for example, recently a requirement was defined for modulus (hardness) stabilization of passenger tire tread compounds, in order to keep their road grip performance constant upon aging.

The objective of the investigations presented in this thesis is to develop new long-lasting antidegradants and to gain a better insight in the protection mechanism of these products. A better understanding of the mechanism can help to pave the way for new developments, providing longer-term protection of rubber compounds. Long-lasting antioxidants are expected to remain longer active in rubber compounds compared to conventional antioxidants, both during processing and service. Developments in this field are based on high molecular weight and polymer bound antioxidants. Long-lasting antiozonants are meant to migrate slower to the surface of rubber compounds compared to conventional antiozonants. Developments in this field are based on high molecular weight products.

An overview of available antidegradants and their mechanistic aspects is presented in **Chapter 2**. Most developments, with emphasis on long-term antioxidant as well as antiozonant protection are summarized. Conventional antidegradants such as N-isopropyl-N'-phenyl-p-phenylenediamine (IPPD) and N-(1,3-dimethylbutyl)-N'-phenyl-p-phenylenediamine (6PPD) are still the most widely used antidegradants in rubber, but there is a trend and demand for longer-lasting and non-staining products. The relatively low molecular weight (MW) antioxidants have undergone an evolutionary change towards higher molecular weight products, to achieve permanence in the rubber polymer without loss of antioxidant activity. In the last two decades, several approaches have been evaluated in order to achieve this: attachment of hydrocarbon chains to conventional antioxidants in order to increase the MW and compatibility with the rubber matrix; oligomeric or polymeric antioxidants; and polymer bound or covulcanizable antioxidants. The disadvantage of polymer bound antioxidants was overcome by grafting antioxidants on low MW polysiloxanes, which

are compatible with many polymers. New developments on antiozonants have focused on non-staining and slow-migrating products, which last longer in rubber compounds. Several new types of non-staining antiozonants have been developed, but none of them appeared to be as efficient as the chemically substituted p-phenylenediamines. The most prevalent method to achieve non-staining ozone protection of diene rubbers, is to blend them with inherently ozone-resistant, saturated backbone polymers. The disadvantage of this approach however, is the complicated mixing procedure needed to ensure that the required small polymer domain size is achieved.

The outline of the synthesis of several potential long lasting antidegradants is described in **Chapter 3**. Slow-diffusion (high molecular weight) antidegradants were prepared by addition of 4-amino-diphenylamine (4-ADPA) and/or 6PPD onto different chemical groups by exploiting various kinds of chemistry: salt formation, Michael addition, Mannich reactions, nucleophilic substitution, amide formation and formation of disubstituted ureas. The syntheses appeared to be straightforward. However, purification of the final products was complicated. Purification by distillation was not possible due to the relatively high molecular weight of the antidegradants. While purifying by washing, a relatively large amount of the synthesized antidegradants was lost due to the small difference in polarity between that of the raw materials and final product. No attempts were made to optimize the syntheses because only small amounts of sample were needed for evaluation in the context of this thesis. The structures and purities of the products synthesized were confirmed by $^1\text{H-NMR}$ and $^{13}\text{C-NMR}$. Special attention was paid to the characterization of PPD-C18, the most promising antidegradant according to the results described later in Chapter 5. It was demonstrated by DOSY $^1\text{H-NMR}$ (diffusion ordered spectroscopy) that the salt prepared from 6PPD and stearic acid appeared to be a complex, when analyzed in the melt. However, the salt seemed to be a rather weak complex, that decomposes into a mixture of 6PPD and stearic acid, when analyzed in a solvent.

The development of test protocols for screening conventional and the newly synthesized potential slow-migrating antidegradants, providing slow-diffusion antiozonant protection, is described in **Chapter 4**. A good correlation was found between outdoor aging and dynamic heat aging as developed in this chapter. Although both dynamic strain and temperature showed a large effect on the depletion of 6PPD, the effect of temperature appeared to be most pronounced.

The effect of a variety of potential long-lasting antidegradants on the dynamic and mechanical properties of rubber vulcanizates is described in **Chapter 5**. The working mechanism of PPD-C18 was investigated. A comparison was made with regard to migration and protection against heat, ozone and flexing of antidegradants such as 6PPD, IPPD and 18 newly synthesized products in typical passenger tire sidewall compounds, using the test protocols developed in Chapter 4. The combination of 6PPD and the stearic acid salt of 6PPD (PPD-C18) provided longer lasting and better appearance of tire black sidewalls. Physical and dynamic properties were better retained in the presence of this newly developed antidegradant. PPD-C18 acts as a slow-release compound for 6PPD, having a slower migration rate compared

to 6PPD and IPPD. The corresponding protection mechanism against ozone of this antiozonant is therefore similar to that of 6PPD.

A study into the efficiency of several potential long-lasting antiozonants by ozonolysis of model olefins, is described **Chapter 6**. 2-methyl-2-pentene was selected as a model for natural rubber (NR) and 5-phenyl-2-hexene as a model for styrene butadiene rubber (SBR). A comparison was made between the efficiency of conventional antiozonants like 6PPD, IPPD and a mixture of diaryl p-phenylene diamines (Wingstay 100) and some newly synthesized antiozonants. The stearic acid salt of 6PPD (PPD-C18), 2,4,6-tris(4-(phenylamino)phenyl)-1,3,5-triazinane (ADPAT) and 4-pyrrole diphenylamine (PDPA) showed a higher efficiency compared to the conventional antiozonants 6PPD and IPPD in both NR as well as in SBR model systems. Special attention was paid to the carboxylic acid salts of 6PPD such as PPD-C18. It was demonstrated that by varying the chain length: C7, C18 and C22, of the carboxylic acid part of the 6PPD salts, the ozone protection was not influenced under the selected test conditions. The 6PPD-salts made from strong acids like succinic acid (SA) and methyl sulfonic acid (MSA) appeared to be less efficient than PPD-C18.

Chapter 7 described an investigation into the effect of N-1,3-dimethylbutyl-N'-phenyl quinonediimine (6QDI) as polymer bound antioxidant in silica-reinforced "green tire" compounds. It was shown, that by adding 6QDI, it was possible to reduce the level of silane coupling agent: bis-(3-triethoxysilylpropyl) tetrasulfide (TESPT), to provide either equivalent or better performance characteristics such as increased cure rate, improved abrasion resistance etc. The polymer-filler and filler-filler interaction parameters were significantly improved indicating better reinforcement characteristics. Network studies suggested better protection of the polysulfidic network following aging, demonstrating improved antioxidant characteristics of the compounds containing 6QDI. NMR, LC-MS studies showed that there is no reaction of TESPT either with 6PPD or 6QDI. Interaction between 6QDI and the rubber model compound squalene was studied by spectroscopic analysis. 6QDI was demonstrated to react with squalene in the presence of accelerator/sulfur to form squalene-S_x-PPD adducts; 6QDI is converted to 6PPD during this reaction. Based on this, it was postulated that either an ENE reaction or the double sulfur addition of 6QDI are causing grafting of 6QDI to the rubber polymer, accounting for the improved antioxidant characteristics in this system.

An examination of the oxidation characteristics of several new types of potentially long-lasting antioxidants is described in **Chapter 8**. Use is made of differential scanning calorimetry (DSC). Oxidation induction times (OIT) were determined for polyisoprene that contains 0.5% of the experimental antioxidants. The antioxidants N-phenyl-3-(4-(phenylamino)phenylamino)propanoate (PPPP), 2-phenoxyethyl-3-(4-(phenylamino)phenylamino)propanoate (PEPPP) and PPD-C18 showed improved antioxidant efficiency compared to conventional antioxidants like 6PPD and polymerized 2,2,4-trimethyl-1,2-dihydroquinoline (TMQ). Wingstay 100, a mixture of diaryl p-phenylene diamines, showed the best antioxidant efficiency in the OIT-test. The efficiency of these antioxidants was also investigated in skim compounds during oxidative aging. Application of PPPP, PEPPP and PPD-C18

resulted in improved network stabilization. The migration characteristics of the tested antioxidants were also investigated. Improved network stability obtained in the presence of PPPP, PEPPP and PPD-C18 could be explained by a combination of both increased OIT and decreased migration rates. PPPP seems to be the best antioxidant, because the product does not migrate under the applied test conditions and shows the highest antioxidant efficiency of all the tested antioxidants.

The interaction of several antidegradants with sulfur vulcanizing agent is the subject of the study described in **Chapter 9**. This is of particular importance for critical rubber parts, like steelcord adhesion skim compounds for tires. These compounds consist of a relatively high concentration of insoluble sulfur, a metastable product that can revert to soluble sulfur. Soluble sulfur will bloom out of the compound and in this way negatively influence the network stability. The thermal stability of insoluble sulfur was examined considering results obtained from blooming experiments, bin-scorch measurements, a thermal stability test in a transparent butadiene rubber (BR) and a thermal stability test in a mineral oil (HTS-test). 6QDI showed a negative effect on the thermal stability of insoluble sulfur as demonstrated by the HTS-test as well as the transparent BR-test, compared to the corresponding amine antidegradant 6PPD. TMQ showed also a negative effect on the thermal stability of insoluble sulfur due to the presence of low molecular weight amine impurities, like aniline. A purified TMQ grade and the reaction product of TMQ and maleic anhydride showed negligible effects on the thermal stability of insoluble sulfur. FT-Raman spectroscopy proved to be a suitable technique to quantify the amount of soluble and insoluble sulfur in rubber compounds. This technique was successfully applied for the determination of the thermal stability of insoluble sulfur in the presence of different antidegradants. Unfortunately, this technique could not be used to study rubber compounds containing 6QDI, due to a high fluorescence background signal caused by the dark color of these compounds. The $S_{\omega 1}$ polymeric sulfur allotrope showed a better thermal stability than the $S_{\omega 2}$ allotrope. In the presence of 6PPD however no difference in thermal stability was found between both insoluble sulfur allotropes.

Samenvatting

Degradatie van natuurrubber en synthetische onverzadigde rubbers, veroorzaakt door zuurstof of ozon, is tegenwoordig een bekend fenomeen. Hoewel ozon slechts in kleine hoeveelheden aanwezig is in de omgevingslucht, ongeveer 10 delen per duizend miljoen, is het effect ervan desastreus. Dit geldt vooral voor rubbers die dynamisch worden belast, met name zijvlakken van autobanden. Het resultaat van ozondegradatie is snelle vorming van scheurtjes, loodrecht op de richting van de aangebrachte spanning. De snelheid van de scheurvorming wordt groter bij verhoging van de spanning en varieert van rubber tot rubber. In alle gevallen is de snelheid van scheurvorming groot genoeg om het rubber onherstelbaar te beschadigen. Sommige synthetische rubbers bevatten geen of slechts weinig onverzadigde bindingen en zijn resistent tegen ozon. De meeste onverzadigde rubbers moeten echter beschermd worden tegen invloed van ozon.

Hoewel er reeds veel onderzoek is gedaan aan het verlengen van de levensduur van rubbers, is er nog steeds behoefte aan antidegradanten die langer werkzaam blijven in rubbermengsels en bescherming bieden op de langere termijn. Tegenwoordig heeft het zijvlak van een vrachtautoband verbeterde bescherming, omdat het loopvlak van de band meerdere malen wordt vernieuwd en dus het karkas en met name het zijvlak langer moet meegaan. Verder is er bijvoorbeeld in Japan nieuwe wetgeving van kracht geworden op het gebied van modulus (hardheid) stabilisatie voor het loopvlak van personenautobanden, om te zorgen dat de gripeigenschappen constant blijven tijdens het verouderingsproces.

Het doel van het onderzoek beschreven in dit proefschrift, is het ontwikkelen van nieuwe antidegradanten die bescherming bieden op de langetermijn en het verkrijgen van een beter inzicht in het beschermingsmechanisme van deze producten. Een beter inzicht in het mechanisme kan helpen de weg vrij te maken voor nieuwe ontwikkelingen, om rubbermengsels voor langere tijd te beschermen. Van persistente antioxidanten wordt verwacht dat ze langer actief zijn in rubbermengsels dan conventionele antioxidanten, zowel tijdens de verwerking als in het gebruik. Ontwikkelingen op dit gebied zijn gebaseerd op hoogmoleculaire en polymeer gebonden antioxidanten. Van persistente antiozonanten wordt verwacht dat ze langzamer migreren naar het oppervlak van het rubberartikel (b.v. autoband), in vergelijking tot conventionele antiozonanten. Ontwikkelingen op dit gebied zijn gebaseerd op hoog moleculaire producten.

Een overzicht van de beschikbare antidegradanten en hun mechanistische aspecten wordt beschreven in **Hoofdstuk 2**. De meeste ontwikkelingen, met de nadruk op persistente antioxidant en persistente antiozonant bescherming, zijn er samengevat. Conventionele antiozonanten zoals N-isopropyl-N'-phenyl-p-phenyleendiamine (IPPD) en N-(1,3-dimethylbutyl)-N'-phenyl-p-phenyleendiamine (6PPD) zijn nog steeds de meest gebruikte antidegradanten, maar er is een trend en grote vraag naar persistente antioxidanten en niet-verkleurende antioxidanten. De

antioxidanten met een relatief laag molgewicht (MW) hebben een evolutionaire verandering ondergaan in de richting van producten met een hoog molgewicht, die langer in rubbermengsels verblijven zonder dat daarbij hun werking minder wordt. In de laatste twee decennia zijn er verschillende methodes van aanpak geëvalueerd om langetermijn bescherming van rubber artikelen te bereiken: het koppelen van koolwaterstoffen aan conventionele antioxidant om het molgewicht te verhogen en de compatibiliteit met de rubbermatrix te verbeteren, oligomere of polymere antioxidant en polymeergebonden of co-vulkanizeerbare antioxidant. Het nadeel van polymeergebonden antioxidant (ze zijn alleen lokaal werkzaam) is opgelost door het koppelen van antioxidant aan laagmoleculaire polysiloxanen, die compatibel zijn met veel polymeren. Nieuwe ontwikkelingen op het gebied van antiozonanten zijn gericht op het gebied van niet-verkleurende en langzaam migrerende producten, die langer in het rubberartikel beschikbaar zijn/blijven. Er zijn verschillende nieuwe types niet-verkleurende antiozonanten ontwikkeld, echter geen van deze producten bleek zo efficiënt te zijn als de chemisch gesubstitueerde p-phenylenediamines. De beste methode om dieenrubber te beschermen tegen ozon zonder dat er verkleuring optreedt, lijkt het mengen van deze rubbers met als zodanig ozonresistente polymeren die geen onverzadigheden in de hoofdketen bevatten. Het nadeel van deze aanpak is echter de gecompliceerde mengmethode, die noodzakelijk is om er zeker van te zijn dat er een zeer kleine polymeer domeingrootte van het ene polymeer in het andere wordt bereikt.

In **Hoofdstuk 3** wordt de synthese beschreven van een aantal persistente antidegradanten. Langzaam-migrerende antidegradanten (hoog molecuul gewicht) zijn bereid door additie van 4-amino-diphenylamine (4-ADPA) en/of 6PPD op verschillende functionele groepen. Hiervoor werden de volgende typen reacties gebruikt: zoutvorming, Michael additiereacties, Mannich reacties, nucleofiele substitutiereacties, amidevorming en vorming van di-gesubstitueerde ureas. De syntheses verliepen zonder noemenswaardige problemen. Het zuiveren van de eindproducten was echter vaak wel gecompliceerd. Zuiveren d.m.v. destillatie was niet mogelijk door de relatief hoge molecuulgewichten van de antidegradanten en de overeenkomstig hoge kookpunten. Tijdens zuivering door uitwassing waren de opbrengstverliezen vaak groot door het geringe verschil in polariteit tussen de grondstoffen en het eindproduct. Er werden geen pogingen ondernomen de syntheses te optimaliseren, omdat er slechts kleine hoeveelheden nodig waren voor de evaluatie in de context van dit poefschrift. De structuren en zuiverheden van de gesynthetiseerde producten werden bepaald m.b.v. $^1\text{H-NMR}$ en $^{13}\text{C-NMR}$. Speciale aandacht is er besteed aan de karakterisering van PPD-C18, de meest veelbelovende antidegradant volgens de resultaten die later beschreven worden in Hoofdstuk 5. Door middel van DOSY $^1\text{H-NMR}$ ("Diffusion Ordered Spectroscopy") werd aangetoond dat het zout bereid uit 6PPD en stearinezuur zich gedraagt als een complex, indien het wordt geanalyseerd in gesmolten toestand. Het zout bleek echter een relatief zwak complex te zijn, dat dissocieert in een mengsel van 6PPD en stearinezuur wanneer het wordt geanalyseerd in een oplosmiddel.

De ontwikkeling van testmethoden voor het screenen van de conventionele en de nieuw gesynthetiseerde potentiële langzaam-migrerende antidegradanten, die “slow-diffusion” antiozoantbescherming bieden, staat beschreven in **Hoofdstuk 4**. Er werd een goede correlatie gevonden tussen verouderingsexperimenten uitgevoerd in de openlucht en een dynamische veroudering bij verhoogde temperatuur (= versnelde veroudering) zoals ontwikkeld in dit hoofdstuk. Hoewel zowel de dynamische uitrekking als de temperatuur een groot effect vertoonden op het verdwijnen van 6PPD, bleek de temperatuur het meeste effect te hebben.

Het effect van een groot aantal potentiële persistente antidegradanten op de dynamische en mechanische eigenschappen van rubbervulkanizaten is beschreven in **Hoofdstuk 5**. Het werkingsmechanisme van PPD-C18 werd onderzocht. Er werd een vergelijking gemaakt op basis van migratie en bescherming tegen hitte, ozon en uitrekking tussen antidegradanten zoals 6PPD, IPPD en 18 nieuw gesynthetiseerde producten in typische zijvlakmengsels van personenautobanden, door gebruik te maken van de testprotocollen ontwikkeld in Hoofdstuk 4. Toepassing van een combinatie van 6PPD en het zout van stearinezuur en 6PPD (PPD-C18) resulteerde in een langere levensduur en een beter uiterlijk van zwarte zijvlakmengsels. Fysische en dynamische eigenschappen bleven beter behouden in de aanwezigheid van deze nieuw ontwikkelde antidegradant. PPD-C18 migreert niet of slecht maar werkt als een “slow-release agent” voor 6PPD, waardoor 6PPD ogenschijnlijk een lagere migratiesnelheid heeft dan 6PPD en IPPD. Het overeenkomende beschermingsmechanisme tegen ozon van PPD-C18 is daarom identiek aan dat van 6PPD.

Een studie naar de effectiviteit van verschillende potentiële persistente antiozonanten, door middel van ozonolyse van modelrubbers, is beschreven in **Hoofdstuk 6**. 2-Methyl-2-penteen werd geselecteerd als model voor natuurrubber (NR) en 5-phenyl-2-hexeen als model voor styreen-butadiëenrubber (SBR). Er werd een vergelijking gemaakt tussen de effectiviteit van conventionele antiozonanten zoals 6PPD, IPPD en een mengsel van diaryl-p-phenyleen diamines (Wingstay 100) en een aantal nieuw gesynthetiseerde antiozonanten. Het zout van stearinezuur en 6PPD (PPD-C18), 2,4,6-tris(4-(phenylamino)phenyl)-1,3,5-triazine (ADPAT) en 4-pyrol diphenylamine (PDPA) bleken een grotere effectiviteit te hebben dan de conventionele antiozonanten 6PPD en IPPD, zowel in het NR- als het SBR-modelsysteem. Speciale aandacht werd besteed aan de carbonzure zouten van 6PPD, zoals PPD-C18. Er werd aangetoond dat door het variëren van de ketenlengte: C7, C18 en C22 van het carbonzure gedeelte van de PPD-zouten, de bescherming tegen ozon niet werd beïnvloed onder de geselecteerde testcondities. De 6PPD-zouten van de sterkere zuren barnsteen zuur (SA) en methylsulfonylzuur (MSA) bleken minder effectief te zijn dan PPD-C18.

Hoofdstuk 7 beschrijft een onderzoek naar het effect van N-1,3-dimethylbutyl-N'-phenyl quinondiimine (6QDI) als polymeergebonden antioxidant in met silica versterkte ‘groene-band’ formuleringen. Er werd aangetoond dat het mogelijk is, door toevoeging van 6QDI, de hoeveelheid silaan “coupling agent”: bis-(3-triethoxysilylpropyl)tetrasulfide (TESPT) te verlagen en daarbij vergelijkbare of betere eigenschappen te verkrijgen zoals een grotere vulkanisatiesnelheid en

verbeterde slijtageweerstand. De polymeer-vulstof en vulstof-vulstof interactieparameters werden significant verbeterd, hetgeen duidt op betere versterkende eigenschappen. Netwerkstudies suggereren een betere bescherming van het polysulfidenetwerk tijdens veroudering, hetgeen een teken is voor verbeterde antioxidanteigenschappen van rubbermengsels die 6QDI bevatten. ^1H - ^{13}C -NMR, LC-MS studies toonden aan dat er geen reactie plaats vindt tussen TESPT met 6PPD noch met 6QDI. De interactie tussen 6QDI en het rubbermodel squaleen werd onderzocht met behulp van spectroscopische analysetechnieken. Er werd aangetoond dat 6QDI met squalene reageert in de aanwezigheid van versneller en zwavel door vorming van squalene- S_x -PPD. Tijdens deze reactie wordt 6QDI omgezet in 6PPD. Hierop gebaseerd, werd verondersteld dat een 'ENE reactie' of de 'dubbele zwaveladditie aan 6QDI' zorg draagt voor de covalente binding van 6QDI aan het rubberpolymeer en daarbij verantwoordelijk is voor de verbeterde antioxidant-eigenschappen in dit systeem.

Een onderzoek naar de oxidatie-eigenschappen van verschillende nieuwe types potentiële persistente antioxidanten is beschreven in **Hoofdstuk 8**. Er is gebruik gemaakt van "differential scanning calorimetry" (DSC). Oxidatie-inductietijden (OIT) werden bepaald voor polyisopreen dat 0.5% van de experimentele antioxidanten bevat. De antioxidanten N-phenyl-3-(4-(phenylamino)phenylamino)propanoaat (PPPP), 2-phenoxyethyl-3-(4-(phenylamino)phenylamino)propanoaat (PEPPP) en PPD-C18 lieten een grotere antioxidant-effectiviteit zien in vergelijking tot conventionele antioxidanten zoals 6PPD en gepolymeriseerd 2,2,4-trimethyl-1,2-dihydroquinoline (TMQ). Wingstay 100, een mengsel van diaryl p-phenyleen diamines, gaf de beste antioxidant-effectiviteit te zien in de OIT-test. De effectiviteit van deze antioxidanten werd ook onderzocht in rubbermengsels, die gebruikt worden voor staalkoordhechting, tijdens veroudering in lucht. Toepassing van PPPP, PEPPEP en PPD-C18 resulteerde in verbeterde netwerkstabilisatie. De migratie-eigenschappen van de geteste antioxidanten werden ook onderzocht. De verbeterde netwerkstabilisatie verkregen in de aanwezigheid van PPPP, PEPPEP en PPD-C18 kon verklaard worden door een combinatie van een grotere OIT en een lagere migratiesnelheid. PPPP lijkt de beste antioxidant te zijn omdat dit product niet migreert onder de toegepaste testcondities en tevens de beste antioxidant-effectiviteit toonde van alle geteste antioxidanten.

De interactie van verschillende antidegradanten met het vulkanisatiemiddel zwavel is het onderwerp van de studie beschreven in **Hoofdstuk 9**. Dit is vooral belangrijk voor kritische rubberonderdelen, zoals rubbermengsels die gebruikt worden voor hechting aan staalkoord in autobanden. Deze mengsels bevatten een relatief hoge concentratie aan onoplosbaar zwavel, een metastabiel product dat kan reverteren naar oplosbaar zwavel. Oplosbaar zwavel 'bloemt' uit het rubbermengsel en beïnvloedt de stabiliteit van het netwerk op een negatieve manier. De thermische stabiliteit van onoplosbaar zwavel werd onderzocht op basis van resultaten verkregen uit 'bloem' experimenten, "bin-scorch" metingen, een thermische stabiliteitstest in een transparante butadiëenrubber (BR) en een thermische stabiliteitstest in een minerale olie (HTS-test). 6QDI toonde een negatief effect op de thermische stabiliteit van

onoplosbaar zwavel in zowel de HTS-test als de transparante BR-test, in vergelijking met het overeenkomstige amine antidegradant 6PPD. TMQ toonde ook een negatief effect op de thermische stabiliteit van onoplosbaar zwavel door de aanwezigheid van laagmoleculaire amineachtige verontreinigingen, zoals aniline. Een gezuiverde TMQ en het reactieproduct van TMQ en maleinezuuranhydride toonden verwaarloosbare effecten op de thermische stabiliteit van onoplosbaar zwavel. FT-Raman spectroscopie bleek een geschikte techniek te zijn om de hoeveelheid oplosbaar en onoplosbaar zwavel in rubbermengsels te kwantificeren. Deze analysetechniek werd succesvol toegepast voor de bepaling van de thermische stabiliteit van onoplosbaar zwavel in de aanwezigheid van verschillende antidegradanten. Helaas kon deze techniek niet worden toegepast voor rubbermengsels met 6QDI, omdat de donkere kleur van deze rubbermengsels een groot fluorescentie achtergrondsignaal veroorzaakt. De S_{01} polymeer zwavelallotroop gaf een betere thermische stabiliteit te zien dan de S_{02} allotroop. Echter, in de aanwezigheid van 6PPD kon er geen verschil worden aangetoond tussen de stabiliteit van beide onoplosbaar zwavelallotropen.